UNIVERSITY OF SOUTHAMPTON

FACULTY OF ENGINEERING AND APPLIED SCIENCE
INSTITUTE OF SOUND AND VIBRATION RESEARCH

ACTIVE CONTROL OF HIGH FREQUENCY ENCLOSED SOUND FIELDS

by

Phillip Frederick Joseph

A thesis submitted for the award of
Doctor of Philosophy

April 1990

Acknowledgements

The author believes that he could not have produced this thesis without the assistance of his supervisors, Drs Stephen Elliott and Philip Nelson, to whom he would like to offer his most sincere appreciation and thanks. It is only due to their generous supervision and encouragement that ideas which began as "Loony Wheezes" have developed into the "Good Schemes" which have made this thesis possible. Furthermore, the author believes that £50 per hour supervision time represents extremely good value.

The author would also like to express his thanks to Ian Stothers for taking the time to build, in less than a day, the fully automated computer controlled "Lego Train Set" which has enabled the experiments described in Chapter 6 to be performed.

Thanks must also go to the many friends I have made during the last three years in the Signal Processing and Control Group within the I.S.V.R for making this time so extremely enjoyable and special.

Lastly, the author would like to thank his fiancé, Karen, for her patience and understanding through the long period during which this thesis was written.

To my Mother,

for her love and support over the years.

ACTIVE CONTROL OF HIGH FREQUENCY ENCLOSED SOUND FIELDS

CONTENTS

CHAPTER 1

AN INTRODUCTION TO THE ACTIVE CONTROL OF SOUND IN ENCLOSED SPACES

1.0. Introduction

It is a surprising but fortunate fact of nature that sounds which are perceived as loud are in reality very small perturbations of the steady state pressure. It is generally well known that in air, acoustic disturbances representing sound pressure levels up to about 120 dB combine linearly which in subjective terms represent very large, damaging sensations of loudness at the ear. This linear behaviour of sound waves leads to the fundamental property of linear superposition which is the underlying physical principle behind active noise control.

Almost without exception, every paper published to date concerned with active noise control deals primarily with low frequency sound, because it is at long wavelengths where active control has been shown to be most successful. Herein lies the appeal of active techniques, since it is precisely at low frequencies where conventional passive methods are least effective. It is generally accepted that in an enclosed space, the performance of active noise control degrades with increasing frequency. The reasons are two fold. The first and certainly the most significant is due to the changing acoustic response of the enclosure, generally becoming more spatially complicated as the number of acoustic modes excited increases. The second is an artefact of the technology, usually arising from limitations in the transducers and primarily constraints imposed by computing speed. As time progresses, increasingly sophisticated hardware will be developed to the extent that transducers and computing technology will eventually cease to be the limiting factor. The limitations arising from the physical acoustics however, are fundamental to the problem under consideration and are therefore insurmountable. It is these reasons which provide the stimulus for the work in this thesis whose aim is to identify the limitations of active noise control at high frequencies in enclosures and reveal the factors which influence these limitations.

It is perhaps not unreasonable to suggest that in the last ten years, hardware technology and the necessary software in the form of fast and efficient control algorithms have developed at a much faster rate than has the understanding of the underlying principles by which two complex sound fields can be made to destructively interfere which is of

course the objective of active noise control. While digital computer technology has advanced at an astonishing rate, even today workers are still developing the simple fundamental theories which define the limits governing the extent by which active control is able to suppress a sound field of known spatial and temporal characteristics. The development of active noise control has evolved steadily leading to its modern day sophistication but can still considered to be an immature science. This is manifest by the fact that there are still only a few commercial applications in operation today. This will undoubtedly change over the next few years as more and more companies and universities begin to take a commercial stake in its research and development.

1.1. A brief review of the relevant literature

1933 marks the serious beginning of active noise control in the form of a patent filed by Paul Lueg in Germany called 'The process of silencing sound oscillations'[1]. The patent deals with the active control of duct borne noise which is still the classic problem most frequently studied today. Unfortunately, as revealed in a historical review by Swanson[2], apart from this patent no other records of this work exists despite extensive investigations by Guicking. Paul Lueg clearly didn't receive the appropriate recognition for this work because active noise control remained un-researched for a further twenty years (although part of this period was interupted by the war) until the publication of a classic paper published in 1953 by Harry Olson and Everett May[3]. Olson's work is considered in more detail in the next section. This paper is significant because in addition to describing the design of a successful device, Olson is credited as the first person to possess the foresight to realise the wide range of problems for which active noise control may be suitable. Active noise control in head sets, automobiles and aeroplanes are all cited by Olson as possible applications which as we realise today, thirty years later, are precisely the situations proving to be the most successful[4]. Following on from Olson is a patent filed in 1966 by Jessel *et-al*[5] re-addressing the problem of controlling noise in air conditioning ducts. This is probably the first work to demonstrate experimentally the active absorption of sound. Since this early history, the interest in active techniques in the context of noise control has increased at an ever growing rate, so much so that Guicking has compiled a comprehensive bibliography (now in its 3rd edition) containing all the work published to early 1988, a total of 1708 references[6]. It is therefore sensible to consider only those which have made a significant contribution to the development of active noise control in enclosed spaces.

In the last twenty years, more effort has been directed towards the active control of noise in ducts than in any other type of acoustic field. The reason is of course due to the

simplicity of the sound field which is variable depending upon the excitation frequency relative to the various cut off frequencies in the duct. However, most work concerned with duct noise appears to be concentrated at frequencies below the first cut off frequency for which the sound field is limited to plane wave propagation. The work of Jessel[7], Swinbanks[8] and Leventhall[9] have all contributed greatly in this area. These papers describe an array of strategically placed secondary sources in various ingenious arrangements to avoid reflections of the incident primary field. A good survey of the various mechanisms of control in the one dimensional sound field is presented by Curtis[10] although the work was primarily intended to illustrate the principles associated with the active control of acoustic resonances. A celebrated commercial example of controlling the sound radiated from the end of a gas turbine exhaust stack which supports a one dimensional sound field in turbulent air flow is described by Swinbanks[11]. Results are given for the reduction of noise at the lowest audible octave (22 - 55 Hz) emitted from the 12 m high, 3.3 m diameter gas turbine exhaust stack. This large scale experiment, started in 1980, includes the use of 72, 15 " bass loudspeakers requiring a total of 12 KW of amplification. In its final form, the system was able to produce an overall broadband reduction of around 7.5 dB and a 13 dB reduction from the largest spectral peak. The system is still in use today.

Attempts to control the more general three dimensional sound field have met with varying degrees of success. Bullmore *et-al*[12] have undertaken an extensive, systematic computer based study of pure tone low modal density sound fields using the quadratic minimisation theory set out by Nelson *et-al*[13]. These results are shown to be in close agreement with experiments performed by Elliott *et-al*[14]. Considerable global reductions of the total acoustic potential energy are reported using only a small number of error sensors and secondary loudspeakers. The possibilities for complete global quiet obtained through active methods remains one of the ultimate objectives of active control. Central to this concept is the principle that the sound field produced by a source and the source of sound itself are not uniquely related from which one can postulate the non-uniqueness of sources. An attempt to verify this fundamental principle was undertaken by Kempton[15] who was able to approximately synthesise the far field produced by a free field point monopole source located at the origin of coordinates using a multi-pole source expansion centred on a point away from the origin. The goodness of fit between the real far field and the synthesised far field was shown to increasingly improve as the order of the highest ordered source included in the source array was increased. However, the notion of source ambiguity has been recognised for some time and has been previously described by, for example, Ffowcs Williams[16].

Recognising the practical and physical difficulties associated with trying to impose global quiet in more complicated sound fields, many workers have sought to adopt a local control strategy which will tend to confine the benefits of quiet to some pre-defined region. One approach which has been tried by Keith and Scholaert[17] involves using the feedback control system suggested by Olson in order to create a zone of quiet around the head of a pilot in an aircraft cabin. A good level of noise reduction is reported over a frequency band of more than 500 Hz at the control microphone reaching a maximum reduction of more than 30 dB at around 100 Hz. However, the reduction in the sound pressure level was observed to diminish very quickly with increasing distance from the control point where at a distance of 15 cm, the level of attenuation was found to fall to between 1 and 2 dB. Unfortunately, no details relating to the cabin dimensions are reported. A similar experiment has also been undertaken by Berge[18] in a small van who describes an experiment which uses an 18" loudspeaker to drive the pressure to zero at a microphone located 50 cm from the loudspeaker. Berge reports that the level of attenuation was found to be insensitive to the exact measurement position within an area of about 0.5 m^2 centred around the driver's head position. Furthermore, a total sound power reduction of 14.5 dB is observed in the frequency band 0 - 200 Hz. These findings are almost certainly due to the spatial simplicity of the pressure field in the cabin since only the 'breathing' (0,0,0) mode of the enclosure is present below 110 Hz for which the sound field may be regarded as spatially homogeneous. Similar findings are reported by Brewer *et-al*[19] obtained from a series of computer simulations.

The work of Chaplin *et-al* is also worthy of mention[20]. Chaplin's experimental arrangement involves the use of two loudspeakers mounted close to the floor of a tractor whose noise is radiated into the cabin as a series of harmonically related tones. The loudspeakers are driven by signals derived from the tractor engine, which are adjusted in order to minimise the pressure at a microphone mounted close to the driver's head position. This arrangement is therefore different from those described above because of the remoteness of the loudspeaker from the region of local control. Another fundamental difference is that this control scheme is an example of feedforward control which uses some control signal to predict the response of the sound field at some future time. Between 10 and 20 dB of attenuation at each discrete frequency are reported. It is also acknowledged that the level of attenuation diminishes with increasing distance from the control point although satisfactory reductions were measured in all of the normal head positions. However, no data is given relating to the effect on the sound field globally. Similar feedfoward methods using multiple secondary sources to minimise the sound field at multiple error microphones have more recently been found to be very effective in actively controlling the low frequency, engine boom in cars[21].

The last five years have seen a significantly raised interest in active noise control. Many workers are now beginning to perform expensive, large scale experiments in order to test the feasibility of active methods in, for example, propeller aircraft. In particular, for suppressing the noise radiated by the rotating propeller into the fuselage of the new range of turbo-propeller aircraft. This problem is ideally suited to the new technology because of the periodic, low frequency tonal nature of the sound field which predominates in the fuselage. The fundamental frequency which is directly related to the blade passage frequency is typically between 80 and 150 Hz, well within the capability of the current technologies. Correspondingly, the sound field to be controlled is of low modal density where global strategies have been shown to be most effective[22].

Recently, Elliott *et-al*[23] and Dorling *et-al*[24] have published concurrent papers reporting the results of multi-channel active control of propeller induced cabin noise during flight trials of a British Aerospace BAe 748, 48 seater twin turboprop aircraft. Elliott's arrangement utilises an array of 16 loudspeakers to minimise the sum of the square pressures at an array of 32 microphones located at the head height plane. The blade passage frequency for this aircraft is 88 Hz for which an average sound pressure level reduction of between 14 and 10 decibels over all control microphones are reported. The spatial complexity of the sound field increases considerably at the first harmonic frequency of 176 Hz for which an average level of reduction of between 6 dB at the port side, falling to less than 4 dB at the starboard side of the aircraft. Similarly, Dorling's data for the same aircraft flying under identical conditions reveal similar results for an array of 24 loudspeakers driven to minimise the pressures at a total 32 control microphones. At the fundamental frequency, their results indicate an average reduction of between 11 and 8 decibels. The average reduction at the first harmonic of 176 Hz increases to 13 dB at the port side of the aircraft to 9 dB at the start board side.

Further large scale work has been carried out for the Douglas aircraft company by an American - British partnership M. A. Simpson *et - al*[25] in the aft cabin of a full size DC - 9 aircraft inside a large anechoic test facility. This series of tests were confined to the ground necessitating the need to simulate the primary excitation that would be observed in-flight. This was provided by an array of primary loudspeakers external to the fuselage and a series of shakers attached to each engine pylon. The control system is reported to use an array of 16 'optimally' positioned secondary loudspeakers driven by a controller according to the error signals from 30 microphones located at the back rest of the seats. Good global reductions of between 5 and 15 dB are reported for a range of tones excited by the loudspeakers and shakers simultaneously in the frequency range between 100 and 200 Hz.

Above these frequencies however, the level of reductions were found to be reduced but still useful nevertheless; 5 dB being typical. It is fair to suggest that these measured figures are slightly optimistic estimates since they refer to reductions at the control microphones and under laboratory conditions. The actual performance of the control system under flight conditions remains to be demonstrated.

The last piece of work which will be cited here is that undertaken by M. Salikuddin and K. K. Ahuja[26] who describe an innovative application of active noise control aimed at reducing sonic fatigue of the fuselage skin together with the added benefits of reducing the interior cabin noise. The idea involves applying local control to a number of points inside the aircraft fuselage using the Olson type monopole configuration for which the pressure is driven to zero at a microphone close to the loudspeaker. The loudspeakers are located on the outer side of the aircraft's skin while the error microphones are situated immediately adjacent, but on the interior side of the fuselage skin. The advantage of this arrangement is that each loudspeaker unit is said to be sufficiently well coupled to the pressure at its adjacent microphone that each control unit may be adjusted independently. The authors argue that acoustic fatigue is reduced by creating points of null pressure and therefore zones of pressure reduction on the surface of the outer skin which will tend to lessen the damaging acoustic forces thereby reducing acoustic fatigue. The authors also maintain that since each point on the pressure waveform impacting with the outer skin is itself an elementary source of sound radiating into the aircraft cabin (Huygen's principle), the cancellation of the pressure at points placed at closely spaced periodic intervals will remove these contribution thereby causing global suppression of the cabin interior noise field.

The proposed control scheme was investigated experimentally using four Olson type units mounted flush to a 2 mm thick plate enclosed within an anechoic chamber. The loudspeakers were fixed to the plate, but on the same side as the primary loudspeakers used to simulate the exterior noise field. Their respective control microphones were mounted on the opposite side from the primary loudspeaker. More than 20 dB of attenuation of the primary wavefield are recorded across the plate on which the pressure is being controlled at a pure tone of 400 Hz. This level of reduction was shown to gradually diminish across increasingly distant parallel planes to the plate. In reality the presence of structural modes of the outer skin will degrade the performance of this technique as will the high level of reverberation inside the aircraft cabin also neglected in this experiment. The density of control units required at high frequencies for good global pressure reductions was not not discussed in this paper neither was a discussion of the performance of loudspeakers travelling at 600 miles per hour.

This short survey of the active noise control literature is clearly not exhaustive but is meant to convey the diversity of the field and the nature of the important work undertaken in this interesting area of acoustics. For a more complete review of the physical principles and related literature of active noise control, one is refered to good review papers by Ffowcs Williams[27], Warnaka[28], and Swanson[2] of which the paper by Ffowcs Williams is particularly good and an extensive review of the earlier work by Lindqvist[29].

1.2. The work of Olson and May

Special attention to the work of Olson and May is justified not only for its historical importance (since this work is among the most commonly cited in the active noise control literature), but because it is the first published work to propose the concept of localised regions of quiet or 'quiet zones' in enclosed sound fields. It is therefore the most closely related work to this thesis. This work appears in two papers; the first published in 1953[3] entitled 'Electronic sound absorber' and a later paper providing more description of the control arrangement and suggesting more applications published in 1956[30] entitled 'Electronic control of noise, vibration and reverberation'. In these two companion papers, Olson gives a discussion on the active control of acoustic fields which show considerable insight into the mechanisms of active control. Ideas are suggested in these papers which even to the present day have still not been satisfactorily resolved and explored to maximum benefit.

A schematic diagram revealing the essence of the proposed single channel control scheme is indicated in figure 1.1 which is taken from Olson's original 1953 paper. The experimental arrangement consists simply of a single control microphone located close to, and on-axis of a secondary loudspeaker via a power amplifier and gain controls.

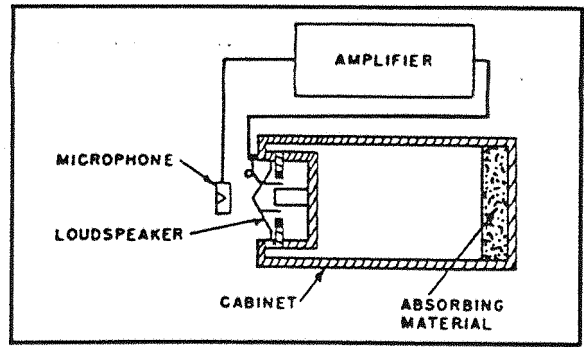

Figure 1.1. A schematic diagram of the 'sound pressure absorber' proposed by Olson and May in 1953 taken from their original paper.

The underlying principle governing Olson's 'Sound pressure reducer' is in principle very straightforward. On sensing the *total* sound pressure p at the control microphone, the signal generated by the microphone is fed back via a power amplifier with a gain -A to the neighbouring secondary loudspeaker to produce a volume velocity $q = -Ap / Z$ where Z is the transfer impedance from the secondary source to the microphone. The total pressure p at the control microphone is formed from the sum of the primary acoustic pressure p_p and the acoustic pressure from the secondary source to give the total pressure $p = p_p - Ap$. One can therefore show that the ratio of the total pressure p at the control microphone to the primary pressure p_p is given by $(p/p_p) = (1 + A)^{-1}$. The gain of the inverting power amplifier is therefore set as high as possible with which to drive the secondary loudspeaker, but not so high as to make the system unstable. The result is to form a pressure at the control microphone which is as close as possible to zero over a broad band of frequencies thereby creating a zone of quiet in the vicinity of the microphone. The difficulties associated with trying to accurately control the phase change around the feedback loop is dealt with by ensuring linearity in the electronics and by locating the control microphone as close as possible to the loudspeaker. The proximity of the control microphone to the loudspeaker appears to be principal design consideration in order to ensure that the phase shift around the feedback loop is equal to the phase characteristics of the amplifier. Cancelling the pressure at the surface of the source is sometimes known as the acoustical virtual earth[10] of which Olson's device is an approximation.

Olson suggests that this arrangement may be employed in two distinct configurations. The first is as a 'Sound power absorber' and the second is a 'Sound pressure reducer'. On the basis of the paper title, one could reasonably suppose that it is as an absorber of sound power that the arrangement shown in figure 1.1 is most successful. While probably the first to suggest that a loudspeaker could be employed in these two possible modes of operation, it is intriguing to observe that no details are reported relating to how one might use this arrangement for sound power absorption or even whether this is a desirable objective. It transpires that in some cases, this mode of operation can adversely influence the total sound power output radiated into an enclosure[12]. Apart from a few remarks regarding sound power absorption, much of the paper is dedicated to reducing the sound pressure around the control microphone. In a later chapter of this thesis it is shown that driving a loudspeaker in order to reduce the sound pressure level in the way Olson describes can, in general, only produce an increase in the sound power output of the secondary source and consequently does not cause sound power absorption. To call the device a sound power absorber is therefore very much a misnomer and it is with a 'Sound pressure reducer' that these papers are primarily concerned.

One way in which Olson's sound pressure reducer could be configured as an absorber of sound is to place a sheet of porous sound absorbent material located within the point of null pressure and the loudspeaker cone itself. The large pressure gradient created in the intervening space will tend to accelerate the particle velocity through the material thereby causing an increase in its absorption efficiency. While this strategy will undoubtedly work, it is questionable as to whether the amount of sound power absorbed resulting from acoustic dissipation in the absorbent material is sufficiently great as to make this scheme economically viable.

As a technological achievement, the work of Olson and May is broadly regarded as outstanding given the technological limitations of the day. However, much of the underlying physics is vaguely reported. For example, no details regarding the distance of the microphone to the loudspeaker is reported, and the diameter of the loudspeaker is only reported by implication which appears to suggest a value equal to 3". The control arrangement is an example of feedback control which consequently does not require any details of the sound field being controlled. In contrast, more sophisticated feedfoward control schemes by necessity require accurate knowledge of the transmission paths of the primary and secondary sound field which therefore tend to be more effective but more difficult to implement[31]. The perfect cancellation of the pressure at a point therefore naturally lends itself to feedback control in this tightly coupled configuration. However, precisely how a sound field which impinges upon a secondary loudspeaker can be absorbed through a simple feedback of some control signal remains to be explained.

One of the most appealing features of this feedback control arrangement which uses control microphones located close to the loudspeaker, which to the author's knowledge has never been publicly recognised, is that the problems associated with causality when dealing with broadband noise radiated into a reverberant space are to a large degree overcome. This is of course due to the close proximity of the control microphone to the secondary loudspeaker so that the pressure field radiated by the secondary loudspeaker appears almost instantaneously at the control microphone. It is therefore possible, in principle, to drive the pressure at a point to zero which is close to the secondary source regardless of the level of 'randomness' of the primary sound field.

Recent attempts to duplicate this experiment by Ross[32] has suffered from severe stability problems. This is exemplified by Ross who remarks "The task of producing this device proved to be more difficult than was originally believed". However, his experiment has been shown to afford broadband control over more than two octaves with a maximum attenuation of 20 dB. Ross partly attributes the success of his modern version of Olson's

device to digital filtering techniques which were of course not available to Olson. However, despite the increased sophistication of modern methods, Ross reports the usual problem of instability causing the system to 'howl' whenever a system transfer function is slightly altered. As Ffowcs Williams observes[27], "This occurs whenever a human head is inserted into the quiet zone to hear the benefit of the device!" Clearly this is because the transmission path of high frequency sound from the loudspeaker to the microphone may incur a phase shift greater than 180° which will turn negative feedback of the control signal into positive feedback thereby causing the system to oscillate.

1.3. The structure and original contribution of this thesis

The ultimate task of active noise control in enclosures is the reduction of broadband noise at high frequencies, factory noise is an important example. While the temporal characteristics of random noise introduces its own difficulties from the point of view of analysis, the reverberant nature of the enclosure presents further complications by producing reflections at the boundary walls. If the number of reflections is large or if there is a substantial level of scattering of the sound field by objects in the room, the interference of a large number of 'elementary' waves may cause the sound field to take on the characteristics of a random process from point to point in the enclosure. It is easy to understand why a sound field which is both random in time and space is extremely difficult to control actively to any useful degree.

The work undertaken in the last three years has attempted to address this problem. The task of trying to develop a theory which embodies both the spatial and temporal random elements of the general problem is clearly formidable, therefore the two facets of the problem are considered independently. This is not to say that the spatial and temporal characteristics of the sound field may be treated independently in this way since they are inter-dependent. Nevertheless, this approach helps to isolate the problems associated with each type of random fluctuation and furthermore, helps to considerably simplify the analysis.

Most of the work presented in this thesis is the result of original research undertaken over a three year period by the author in close collaboration with his supervisors, Drs S. J. Elliott and P. A. Nelson. However, important parts of this thesis is the contribution of the supervisor's own work for which appropriate recognition is due.

The theory developed in Chapter 2 is essentially an extension of the free field sound power minimisation problem for stationary random signals investigated by Dr P. A.

Nelson. The author's own contribution to this problem has been to provide an interpretation of the principles underlying free field sound power minimisation in terms of the power spectral density. More importantly, the author has extended this single channel theory to include reflections from a single reflecting surface. This study has highlighted the recursive structure of the impulse response function of the optimal secondary source strength. Steady state levels of sound power reduction obtained for the causally constrained and unconstrained controller, which are pertinent to white noise signals and harmonic signals respectively, are derived and compared. This chapter considers the minimum sound power output of, and the interaction between two white noise sources radiating into a semi-infinite duct assuming plane wave propagation. This model problem was chosen because of the spatial simplicity of the sound field by virtue of being one dimensional. Reverberation is simply introduced by way of a single termination at one end of the duct where dissipation is introduced by means of a real, frequency independent reflection coefficient.

In chapter 3, the converse problem is contemplated whereby the sound field has a simple variation in time but whose spatial variation appears random. In all of the diffuse field work described in this thesis, the controller will be assumed to be feedforward in operation so that the only restrictions on the level of reductions obtainable in principle are imposed by the physical characteristics of the primary and secondary pressure fields themselves. In this work the temporal characteristics of the noise source is kept deliberately simple by considering only harmonic sources of sound at a frequency above the Schröder frequency. Above this critical frequency, the number of normal modes making a significant contribution to the total pressure response is sufficiently large that the spatially sampled sound field to all practical purposes may be regarded as a random variable. Specifically, the minimum sound power output of two closely spaced point monopole sources in an enclosed sound field above this critical frequency is determined for which the first and second order statistics are derived.

In developing the analysis in chapter 3, the author recognises the contribution of Dr S. J. Elliott for providing the correct interpretation of the physical mechanisms of sound power minimisation in a diffuse field environment. In particular, for showing that the sound power output of a point secondary source driven to minimise the combined sound power outputs from itself and a point primary source in a reverberant space is exactly zero. The author would also like to acknowledge Dr Elliott for his help in recognising the relationship between the normalised variance of the diffuse field reverberant pressure contributions and the modal overlap factor.

Recognising that this contrived model geometry is a special case and unrealistic of the type of problem encountered in reality, the more practically orientated problem of local control in the diffuse field is considered in chapter 4. The problem of cancelling the pressure to zero at a point which is remote from all sources is investigated. Elementary statistical methods are employed in order to derive expressions for the spatial extent of the so called quiet zone, the secondary source strength requirements and the increase in the potential energy well away from the point of cancellation. The derivation of the expression for the space averaged diffuse field quiet zone is also attributed to Dr Elliott, although a slightly modified version of his analysis is presented in this thesis. Despite the apparent simplicity of this single channel control strategy, the results obtained turn out to be surprisingly subtle. However, it is demonstrated that the size of the zone of quiet formed in this high frequency enclosed sound field between successive experiments is extremely large making it impossible to talk in terms of average values with any meaning. Moreover, the increase in the potential energy formed by this process is shown to be sufficiently large that the average value over all source and cancellation positions is infinite. The statistical ill-conditioning of this unconstrained control scheme is the motivation for the work presented in chapter 5.

Chapter 5 deals with the results of constrained diffuse field active control. In particular, the effects of 'hard limiting' is examined. This quite severe constraint attempts to mimic the behaviour of a real control system which will obviously impose some upper value on the maximum secondary source strength it can deliver. Multi-channel control schemes are also studied, both from an analytic view point and from the results obtained from a systematic series of Monte-Carlo simulations which have yielded some enlightening empirical results. As a special case, the zone of quiet formed around two diffuse field points, which are close compared to the acoustic wavelength, has been studied using computer simulations for which the sum of the squares of pressures has been minimised.

Undoubtedly, the most successful control strategy investigated so far in this thesis for dealing with high frequency enclosed sound fields is that originally suggested by Olson; namely the cancellation of the pressure at a point close to the secondary loudspeaker i.e., the 'Sound pressure reducer'. This is the subject of chapter 6. The size and shape of the zone of quiet around a control microphone in this configuration is shown to be predominantly governed by the free space, near field characteristics of the source whereas previously, for the case discussed in chapter 4, the size of the quiet zone was shown to be a sole function of the spatial cross correlation function of the diffuse sound field. The principal advantage of this near field arrangement, compared with cancelling the pressure at a point which is remote from the influence of directly transmitted sound, is that the energy

radiated to the 'far field' of the secondary source is now significantly reduced. For example, an increase in the overall sound pressure level of more than 10 dB was found to be typical using a remote secondary source, whereas in this tightly coupled configuration, the increase in sound pressure level well away from the point of cancellation is restricted, in many cases to only a small fraction of 1 dB. In both cases however, the size of the quiet zone within which the pressure has been reduced by 10 dB with respect to the primary field, is shown to be about one tenth of a wavelength.

The theory developed in chapter 6 for the square pressure variation in the vicinity of a point of null pressure in the loudspeaker's near field is supported by experimental results presented in the same chapter. Measurements of the sound pressure level was made by a single microphone which traversed along the axis of the secondary loudspeaker in the direction of its motion through the point of cancellation. The electronics enabling the experimentation to implemented automatically was designed and built by Mr Ian Stothers, who is gratefully acknowledged.

CHAPTER 2

CAUSALLY CONSTRAINED MINIMUM SOUND POWER OUTPUT IN THE PRESENCE OF REFLECTIONS

2.0. Introduction

This chapter is intended to provide a brief introduction to the active control of broadband stationary random sound fields. Particular emphasis is given to the effects of reverberation. The characteristic feature of this type of sound field is that at any point in space, the acoustic pressure possesses a waveform which is time varying in a fashion which is generally not wholly deterministic. Moreover the difficulty from the point of view of analysis and control is compounded by an infinite succession of reflections by the enclosure walls. The investigation reported here is motivated by the need to establish the feasibility of active noise control in reverberant spaces when the primary sound field varies randomly in time. The critical constraint on the controller when seeking to reduce this sound field according to some prescribed criterion is that it must act causally with respect to the action of the primary source. The appropriate condition on the optimal secondary source $q_{so}(t)$ is that

$$q_{so}(t) = 0 \quad \text{for} \quad t < 0 \qquad \text{provided } q_p(t) = 0 \text{ for } t < 0 \tag{2.1}$$

where the origin of time $t = 0$ is taken from the first action of the primary source. Depending on the statistics of the primary source output signal and the relative source positions, this fundamental constraint may have a significant bearing on the levels of reduction that ultimately may be achieved.

Surprisingly little work has been undertaken in this area. This is most probably due to the difficulty of time domain analyses, where the causality of the controller may be monitored directly, over corresponding frequency domain analyses where the causality of the controller cannot be immediately verified. This is perhaps surprising since time domain optimisation techniques form a large part of modern signal processing particularly since the pioneering work of Wiener[33] in the 1940's and later work by Kalman[34] in the 1950's. To the author's knowledge, the first person to apply classical time domain methods to the realm of active noise control was Nelson[35] who has used the theories developed by Wiener to study a number of model problems in the active control of sound. One example is the deduction of the causally constrained minimum sound power output of two closely spaced point monopole sources in free field. Also derived are analogous results in matrix form for

the multi-channel problem enabling causal constraints to be imposed on the optimal secondary source strength seeking to minimise the total potential energy of the randomly excited sound field in rooms. Each acoustic mode excited in the room is considered as an independent source of variation so that the sound field in the room may be regarded as a multi - degree of freedom system.

Inevitably, the solution for the optimal causal controller requires the inversion of a large matrix whose size is determined by the number of acoustic modes considered to be necessary to adequately represent the sound field. This may be hundreds of thousands of modes in some cases, particularly when the acoustic damping and the excitation bandwidth are simultaneously large. As a first approximation, Joplin[36] has carried a numerical investigation using this theory which incorporates just eight modes. However, the exercise was performed more as an illustration of the governing physical principles than a serious attempt to model the behaviour of a real system.

In this chapter, the causally constrained free field minimum sound power output of two idealised plane sources radiating plane waves into an infinite hard walled duct is investigated. This problem is considered from the point of view of the sound power spectral density of each of the sources which quantifies the sound power output per unit frequency bandwidth (this is not to be confused with power spectral density which is defined for arbitrary signals of different physical origins which in general do not have the units of Watts per unit frequency). The mutual interaction between the primary source and secondary source is investigated by considering the power spectral density of each of the sources in turn. Previous work has only considered the total time averaged sound power output. Frequency decomposition of the power outputs of the sources offers a clearer picture of broadband sound power minimisation and is valuable in being able to reveal the subtle interaction between the source pair. The idea of predictability, which is central to the active control of random noise, is investigated more closely and a qualitative, empirical relationship between the 'predictability' bandwidth of the primary source signal and its frequency bandwidth is proposed.

The equations are developed further to determine the optimal causal secondary source strength which minimises the sound power radiated into a hard walled duct terminated at one end. Dissipation is introduced by way of a real, frequency independent reflection coefficient at the duct termination. The governing equations are shown to possess an exact solution for the important limiting cases where the primary signal is either Gaussian white noise or a harmonically varying pure tone. The two cases are considered separately and compared.

2.1 The unconstrained minimum sound power output in the free field

While this thesis is predominantly concerned with the active control of pure tone reverberant sound fields, this section is given to a discussion concerned with the active control of broadband noise radiated into free space. This is because the presence of reflected sound profoundly complicates the analysis so that for the one dimensional problem under consideration here, reflections from boundaries such as those from the walls of rooms will initially be disregarded. A free field analysis is not entirely irrelevant to the control of enclosed sound fields. In many cases, particularly at high frequencies, the levels of sound power reduction which are physically achievable in free field are closely related to the levels of sound power reduction which are possible in an enclosed space. This is particularly true in three dimensional enclosed sound fields with large room absorption at high frequencies where the level of reflected sound is, on average, much less than the level of directly radiated sound. This is problem is addressed in detail in chapter 3.

As an example of a one dimensional free field problem, consider an infinite, hard walled duct in which there are situated two idealised plane sources $q_s(t)$ and $q_p(t)$

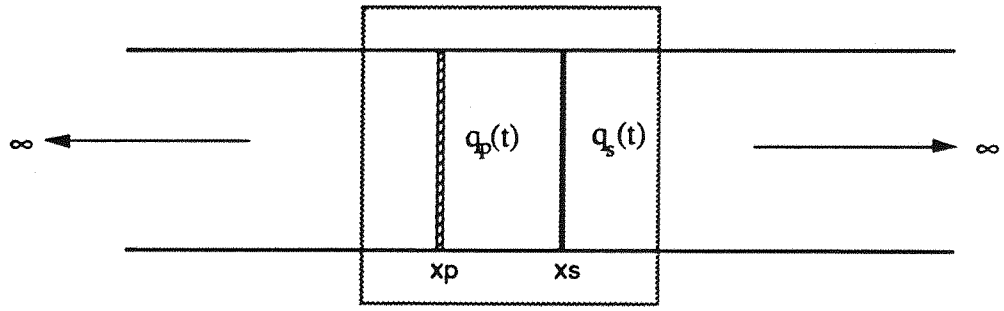

Figure 2.1. An infinite hard walled duct containing a primary and secondary plane source

The acoustic pressure p(t,x) radiated by the volume velocity $q(t,x_q)$ which is located at some point x_q are related via the inhomogeneous wave equation[37]

$$\left(\nabla^2 - \frac{1}{c_0^2} \frac{\partial^2}{\partial t^2} \right) p(t,x) = -\rho \frac{\partial q(t,x_q)}{\partial t} \qquad (2.2)$$

where ∇^2 is the Laplacian operator, c_0 and ρ symbolise the sound speed and the ambient density in the medium respective and where $q(t,x_q)$ represents the volume velocity density in the volume acting to accelerate the fluid which therefore behaves as a source of sound. The primary and secondary sources indicated in the figure above are intended to represent

idealised plane sources whose source strength densities are concentrated in a plane normal to the length of the duct according to

$$q(t,x_q) = q(t)\,\delta(x - x_q) \tag{2.3}$$

where δ symbolises a Dirac delta function which is only meaningful within the context of integration. In an infinite one dimensional duct, assuming only plane waves are allowed to propagate, the D'Alembert retarded time solution is given by

$$p(t,x) = Z_p\, q\left(t - \frac{|x - x_q|}{c_0}\right) \tag{2.4}$$

where Z_p is the plane wave impedance for the duct $\rho c_0/2S$. For a single tone at a frequency ω, $q(t) = q(\omega)e^{j\omega t}$ so that the complex pressure may be obtained from equation (2.4) to give

$$p(\omega,x) = Z_p q(\omega)e^{-jk|x - x_q|} \tag{2.5}$$

where k is the wavenumber ω/c_0.

We will now derive the minimum sound power output from the source pair indicated in figure 2.1. For the elementary source types described by equation (2.3), the total sound power output W from the two sources radiating simultaneously is given by[38]

$$W = \tfrac{1}{2}\Re\,\{q_s^* p(x_s) + q_p^* p(x_p)\} \tag{2.6}$$

where $\Re$ denotes the process of taking the real part.
The volume velocity dependence on frequency and source position have been dropped for brevity. The total acoustic pressure resulting from both sources p(x) assuming linear superposition is given by

$$p(x) = q_s Z(x_s|x) + q_p Z(x_p|x) \tag{2.7}$$

where $Z(x_s|x)$ and $Z(x_p|x)$ represent the complex acoustic transfer impedances relating the secondary source at x_s and the primary source at x_p to the complex pressure at some point x respectively. Substitution of the total pressure p(x) into equation (2.6) for the total sound power output yields a quadratic function of the complex secondary source strength q_s of the general form

$$W = q_s A q_s^* + b q_s^* + b^* q_s + c \tag{2.8}$$

whose coefficients may be identified in terms of the transfer impedances thus

$$A = \tfrac{1}{2}\Re\{Z(x_s|x_s)\},\ b = \tfrac{1}{2}q_p\Re\{Z(x_p|x_s)\},\ c = \tfrac{1}{2}|q_p|^2\,\Re\{Z(x_p|x_p)\} \qquad (2.9)$$

The properties of the general quadratic form given by equation (2.8) have been extensively investigated with optimisation problems of this type[13,39]. A three dimensional plot of W against the real part of the complex secondary source strength $\Re\{q_s\}$ and the imaginary part $\Im\{q_s\}$ produces a bowl shape function whose minimum value is uniquely defined by the bottom of the bowl. The existence of a well defined minimum solution follows from the positive definiteness of the constant 'A' which is guaranteed since the source on its own is unable to absorb sound power in the absence of any external sound field[40]. The value of $q_s = q_{so}$ which identifies the minimum of this quadratic function must simultaneously satisfy

$$\frac{\partial W}{\partial \Re\{q_s\}} = 0 \quad \text{and} \quad \frac{\partial W}{\partial \Im\{q_s\}} = 0 \qquad (2.10)$$

The solution to this equation has been derived[40] and may be shown to be given by

$$q_{so} = -A^{-1}b \qquad (2.11)$$

For the current example, using equation (2.5) and (2.9) one can show that, $A = \frac{1}{2}Z_p$ and $b = \frac{1}{2}q_pZ_p \cos k|x_s - x_p|$ such that from equation (2.11), one obtains the solution

$$q_{so} = -\,q_p \cos k|x_s - x_p| \qquad (2.12)$$

In its present frequency domain representation, the optimal secondary source strength q_{so} given above says very little about how the secondary source achieves optimal reductions in total sound power output. The mechanism of control is revealed more clearly in the time domain. The multiplicative term $-\cos k|x_s - x_p|$ may be regarded as a transfer function relating the optimal secondary source strength to the primary source strength according to $q_{so} = -\,q_pH_o(\omega)$. The corresponding impulse response function $h_o(t)$ may be obtained from $H_o(\omega)$ via the inverse Fourier transform given by

$$h_o(t) = \frac{1}{2\pi}\int_{-\infty}^{\infty} H_o(\omega)e^{j\omega t}\,d\omega \qquad (2.13)$$

Given that $H_o(\omega) = -\cos k|x_s - x_p|$, then taking the inverse Fourier transform gives

$$h_o(t) = -\tfrac{1}{2}[\,\delta(t-\mu) + \delta(t+\mu)\,] \qquad (2.14)$$

where μ is simply the propagation time between the two sources $|x_s - x_p|/c_0$.
In this form, the optimal secondary source strength as a function of time is derived from the primary source time history $q_p(t)$ via a convolution with the impulse response function according to

$$q_{so}(t) = \int_{-\infty}^{\infty} h_o(\tau)\, q_p(t - \tau)\, d\tau \qquad (2.15)$$

Using equations (2.14) and (2.15), the secondary source strength time history $q_{so}(t)$ is simply

$$q_{so}(t) = -\frac{1}{2}[\, q_p(t - \mu) + q_p(t + \mu)\,] \qquad (2.16)$$

which has previously been derived in reference [41]. Equation (2.16) embodies two of the most fundamental mechanisms of active noise control; sound power absorption and primary source loading. It is important at the outset to understand the underlying physical processes associated with free space sound power minimisation before considering the more complicated effects of reverberation. This may be considerably assisted by using the graphical representation shown in figure 2.2 of the evolution of acoustic pressures in the duct due to the secondary source in response to a primary source signal consisting simply of a unit pressure pulse at t = 0

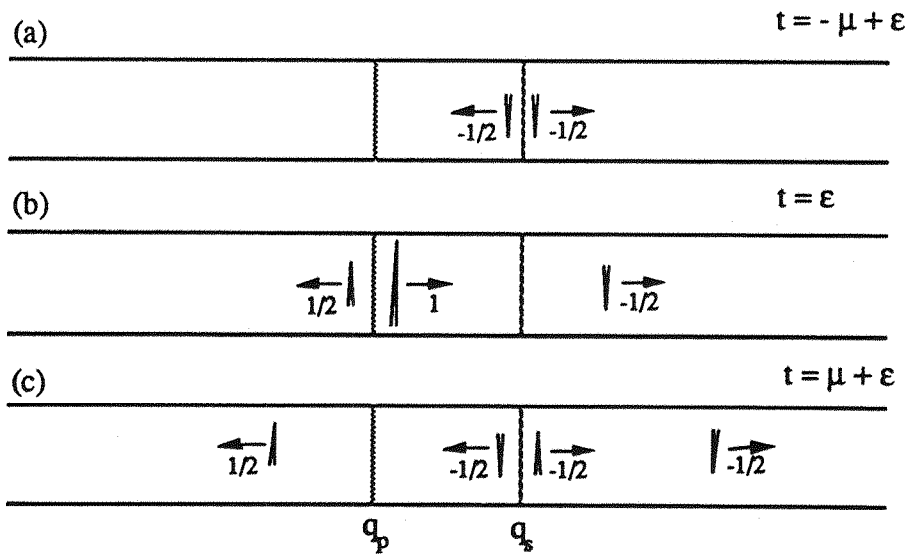

Figure 2.2. A pulse diagram indicating the evolution of the pressure in response to a primary source pulse of unit amplitude.

where ε is used to denote a 'short time later'. This pulse interpretation of the mechanism of sound power minimisation is due to Curtis[10].

As indicated in figure 2.2a, the secondary source starts by anticipating the action of the primary source by a time μ which then radiates an inverted replica of the primary source pressure waveform, but one half its magnitude so as to arrive at the primary source just in time to meet the pressure only just radiated at $t = 0$. This will have the effect of halving the downstream radiation impedance of the primary source such that only half of the original pressure is radiated for the same volume velocity in the absence of control as suggested by figure 2.2b. The rôle of this component of the solution is to provide a *prediction* of the primary signal for the purpose of *loading* the primary source.

The remaining term $-1/2\, q_p(t - \mu)$ of the optimal secondary source strength is responsible for *absorbing* half of the primary source pressure radiated towards the secondary source whose upstream radiation impedance is unaltered by the previous action. The absorption of the incident primary source energy is indicated in figure 2.2c. The square pressure amplitude in the absence of the secondary source is simply 1^2 (which for plane waves is proportional to the radiated energy). Figure 2.2c indicates that the total energy radiated by the source pair as result of active control is now equal to $(1/2)^2 + (1/2)^2 + (1/2)^2 + (1/2)^2$ which is exactly one half the original energy radiated by the primary source. This combination of sound power absorption and primary source loading is therefore able to offer a reduction in the total sound power output exactly equal to one half of the original primary source sound power output. It is emphasised that this level of sound power reduction represents an average reduction over all frequencies since the system response to a unit pulse may be considered to be the average harmonic system response taken over all frequencies. This is because a pulse of infinitesimal duration possesses a 'flat' spectrum where all frequencies are represented to the same degree. For pure tone sources, the actual level of reduction is very dependent on its frequency. Substituting equation (2.11) for the optimal secondary source strength into the general quadratic form of equation (2.8) yields the minimum value W_{min} which is given by

$$W_{min} = c - bA^{-1}b^* \tag{2.17}$$

Substituting the values of A, b and c given in equation (2.9) gives

$$W_{min} = \tfrac{1}{2} Z_p |q_p|^2 [\, 1 - \cos^2 k\mu \,] \tag{2.18}$$

Constructing the primary source sound power output W_p radiated in the absence of the secondary source according to the formulation given in equation (2.6), one can show that

$$W_p = \tfrac{1}{2} Z_p |q_p|^2 \tag{2.19}$$

According to equation (2.18) and (2.19), the minimum total sound power output in terms of the primary source sound power output is given by

$$W_{min} = W_p [\, 1 - \cos^2 k\mu]$$ (2.20)

By inspection, the average reduction in sound power output taken over all frequencies is exactly one half the original primary sound power output which is consistent with the time domain interpretation described by figure 2.2. The level of reduction at any single frequency can therefore be seen to be highly dependent on the phase difference $k\mu$ of the tone between the two source positions. Equation (2.20) indicates that complete suppression of the total sound power output is possible for source separation distances exactly equal to an integer number of half wavelengths. Conversely, the total sound power output remains unaltered for source separation distances exactly equal to an odd number of quarter wavelengths.

The most significant property of the optimal secondary source strength time history $q_{so}(t)$ given by equation (2.16) is that it contains at least one term $q_p(t + \mu)$ which requires an *apriori* knowledge of the primary signal at an advanced time μ. For most primary signals therefore, this filter cannot be realised in practice. One can now immediately see that this formulation of the minimum sound power output is, in general, only appropriate for harmonic signals which are infinitely repetitive and is therefore not relevant for random primary signals. The difficulty lies in the nature of frequency domain analysis which clearly does not recognise negative time as a violation of physical laws. Since no distinction is made between positive and negative time in the frequency domain, causality cannot be readily incorporated into the solution and one must resort to time domain techniques where the causality of the solution can be imposed directly.

2.2. Causally constrained minimum sound power output in the free field

Now follows an exactly analogous formulation of the total sound power output in the time domain using an approach suggested by Nelson[35]. The total time averaged sound power radiated from the source pair may be written as

$$W = \lim_{T\to\infty} \frac{1}{2T} \int_{-T}^{T} [\, q_s(t)p(x_s,t) + q_p(t)p(x_p,t) \,]\, dt$$ (2.21)

The total pressure p(x,t) resulting from primary and secondary source contributions is given by

$$p(x,t) = Z_p \left[q_p\left(t - \frac{|x_p - x|}{c_0}\right) + q_s\left(t - \frac{|x_s - x|}{c_0}\right) \right] \tag{2.22}$$

Substitution of this equation into equation (2.21) yields

$$W = Z_p \lim_{T\to\infty} \frac{1}{2T} \int_{-T}^{T} \left\{ q_s(t)\left[q_p\left(t - \frac{|x_p - x_s|}{c_0}\right) + q_s(t)\right] + q_p(t)\left[q_p(t) + q_s\left(t - \frac{|x_s - x_p|}{c_0}\right)\right] \right\} dt \tag{2.23}$$

We now assume that $q_s(t)$ and $q_p(t)$ are linearly dependent and related by a *causal* impulse response function $h(\tau)$ according to the relation

$$q_s(t) = \int_0^{\infty} h(\tau)\, q_p(t - \tau)\, d\tau \tag{2.24}$$

It is important to recognise that causality is introduced by setting the lower limit of the integral to zero which ensures that

$$q_s(t) = 0 \quad \text{for} \quad t < 0 \quad \text{provided} \; q_p(t) = 0 \; \text{for} \; t < 0 \tag{2.1}$$

Substituting $q_s(t)$ into equation (2.23) produces an expression for the total sound power output W solely in terms of the impulse response function $h(\tau)$ and the primary source signal $q_p(t)$ of the form

$$W = Z_p \lim_{T\to\infty} \frac{1}{2T} \int_{-T}^{T} \left\{ \int_0^{\infty} h(\tau_1) q_p(t - \tau_1)\, d\tau_1 \int_0^{\infty} h(\tau) q_p(t - \tau)\, d\tau + q_p(t - \mu) \int_0^{\infty} h(\tau) q_p(t - \tau)\, d\tau + q_p(t) \int_0^{\infty} h(\tau) q_p(t - \mu - \tau)\, d\tau + q_p^2(t) \right\} dt \tag{2.25}$$

where $\mu = |x_s - x_p|/c_0$ as before.

Despite the apparent complexity of this expression, one can make considerable simplifications by noting that the orders of integration may be re-arranged and terms which subsequently appear such as

$$\lim_{T\to\infty} \frac{1}{2T} \int_{-T}^{T} q_p(t) q_p(t + \tau)\, dt = \rho_{pp}(\tau) \tag{2.26}$$

are definitions of the primary signal temporal correlation function $\rho_{pp}(\tau)$ evaluated at the appropriate time delay (or advance) τ. This simplification is clearly only valid for *stationary* random signals. Performing this sequence of operations yields

$$W = Z_p \left[\int_0^\infty \int_0^\infty h(\tau)h(\tau_1)\rho_{pp}(\tau - \tau_1)\, d\tau\, d\tau_1 + \int_0^\infty h(\tau)\, \rho_{pp}(\tau - \mu)\, d\tau \right.$$
$$\left. + \int_0^\infty h(\tau)\rho_{pp}(\tau + \mu)\, d\tau \right] + W_p \qquad (2.27)$$

The term $W_p = Z_p\rho_{pp}(0)$ is the primary source sound power output radiated in the absence of the secondary source. Using standard variational techniques[42], it is left to Appendix 2.1 to show that this function is minimised for an optimal causal impulse response function $h_o(\tau)$ which must satisfy the following relationship

$$2\int_0^\infty h_o(\tau_1)\rho_{pp}(\tau - \tau_1)\, d\tau_1 + \rho_{pp}(\tau + \mu) + \rho_{pp}(\tau - \mu) = 0 \quad \text{for } \tau > 0 \qquad (2.28)$$

The inhomogeneous integral equation given above is a form of the well known Wiener - Hopf equation whose solution, in this case, gives the optimal impulse response function for determining the causally constrained minimum sound power output radiated by the source pair. Some confidence regarding the correctness of this equation is derived if one sets the lower limit of this integral to $-\infty$ and the Fourier transform is taken. This series of operations recovers the original unconstrained optimal solution $H_o = -\cos k\mu$ derived earlier in the frequency domain.

Following Nelson *et-al*[35] the solution to equation (2.28) may be obtained partly by inspection and partly with recourse to classical techniques in linear estimation theory. By direct analogy with the optimal impulse response function obtained for the unconstrained problem in equation (2.14), assume a solution $h_o(\tau_1)$ of the form

$$h_o(\tau_1) = -\frac{1}{2}\left(\delta(\tau_1 - \mu) + u_o(\tau_1) \right) \qquad (2.29)$$

The two terms are respectively a component for the absorption of the incident sound wave as indicated before, plus an additional term $u_o(\tau_1)$ which is now substituted in place of the anticipatory term $\delta(\tau_1 + \mu)$ appearing in equation (2.14) for the unconstrained case signifying an advance in time. Substitution of the assumed form of the solution of equation (2.29) into the Wiener - Hopf equation yields the following condition on the term $u_o(\tau_1)$

$$\int_0^\infty u_o(\tau_1)\rho_{pp}(\tau - \tau_1)\, d\tau_1 = \rho_{pp}(\tau + \mu) \qquad (2.30)$$

This equation has straightforward interpretation: Given a knowledge of all *past* values of the time history $q_p(t)$, the filter $u_o(\tau_1)$ is required which affords the optimal estimate of the primary signal at some future time $q_p(t + \mu)$. The form of this equation is appropriately called the Wiener pure predictor equation whose solution is given in many standard texts on linear estimation theory and signal processing[43,44] but will only be cited here.

Assume that the primary source signal $q_p(t)$ may be represented by some shaping filter $X_p(s)$ driven by white noise, where s is the Laplace variable, whose impulse response function is x(t). This choice of model is clearly only valid for stationary random signals. The optimal predictor $U_o(s)$ which is the solution of equation (2.30) is given by

$$U_o(s) = \frac{X_{p+}(s)}{X_p(s)} \qquad (2.31)$$

where $X_{p+}(s)$ is the one sided Laplace transform of the impulse response function of the shaping filter advanced by the appropriate propagation time μ, namely $x_p(t + \mu)$. Thus

$$x_p(t) = \frac{1}{2\pi}\int_0^\infty X_p(s)\, e^{st}\, ds \quad \text{and} \quad X_{p+}(s) = \int_0^\infty x_p(t + \mu)\, e^{-st}\, dt \qquad (2.32)$$

The process described above is discussed in many texts on time series analysis, see for example Papoulis[44]. The solution to this equation for an important representative example is now discussed. Consider the case where the primary source strength $q_p(t)$ is closely represented by the output from a filter with the well known characteristic second order frequency response described by equation (2.33) driven by unit amplitude white noise. The Laplace transform of the shaping filter is given by[45]

$$X_p(s) = \frac{\omega_n^2}{s^2 + 2\zeta\omega_n s + \omega_n^2} \quad \text{for } \zeta < 1 \qquad (2.33)$$

where ζ and ω_n are the filter damping and the undamped natural frequency of the filter respectively. Equation (2.33) provides a good model of the frequency characteristics for many commonly occurring noise spectra which exhibit this typical 2nd order type response described above. Tyre noise, for example, radiated into a car body will be distributed in frequency roughly according to equation (2.33) since the excitation of the rough ground will

be approximately of the same level at all frequencies. Transmission of sound through the tyre will therefore tend to filter the noise radiated into the car interior by virtue of its associated mass, stiffness and damping. The impulse response function x(t) of this filter is also well known[45] and is given below

$$x_p(t) = \frac{\omega_n^2}{\omega_0} e^{-\zeta\omega_n t} \sin \omega_0 t \qquad (2.34)$$

where ω_0 is the frequency at which peak response occurs, $\omega_0 = \omega_n\sqrt{1 - \zeta^2}$. Employing equations (2.31) - (2.34), the optimal predictor $U_o(s)$ may be solved to give

$$U_o(s) = \frac{e^{-\zeta\omega_n\mu}}{\omega_0} [\, \omega_0 \cos \omega_0\mu + (s + \zeta\omega_n) \sin \omega_0\mu \,] \quad \text{for } \zeta < 1 \qquad (2.35)$$

where the required Laplace transforms are standard results given in many texts[45]. Putting $s = j\omega$ for the optimal predictor $U_o(\omega)$ and substituting into the frequency response function $H_o(\omega)$ relating $q_{so}(\omega)$ and $q_p(\omega)$ yields the result

$$H_o(\omega) = -\frac{1}{2} [\, e^{-j\omega\mu} + \frac{e^{-\zeta\omega_n\mu}}{\omega_0} [\, \omega_0 \cos \omega_0\mu + (j\omega + \zeta\omega_n) \sin \omega_0\mu \,] \qquad (2.36)$$

The quantities under consideration are now written as function of frequency ω to indicate that spectral decomposition has taken place. The causality of this optimal secondary source strength $q_{so}(t)$ as governed by $H_o(\omega)$ is readily verified by inverse Fourier transforming and convolving with $q_p(t)$ to give

$$q_{so}(t) = -\frac{1}{2} [\, q_p(t - \mu) + \frac{e^{-\zeta\omega_n\mu}}{\omega_0} \{\, (\omega_0 \cos \omega_0\mu + \zeta\omega_n \sin \omega_0\mu)\, q_p(t) + \sin \omega_0\mu\, \dot{q}_p(t) \} \,] \qquad (2.37)$$

which is only dependent on past and present values of the primary source strength time history $q_p(t)$. It is interesting to observe that the optimal predictor also depends on the derivative of the primary signal with respect to time $\dot{q}_p(t)$. For the sake of consistency with the previous frequency domain analysis, $q_{so}(t)$ must tend to the unconstrained result given in equation (2.16) as the damping of the shaping filter becomes increasingly narrower eventually tending to zero. In this limit, the output of the shaping filter is a single tone possessing a frequency equal to its centre frequency ω_n. The consistency of the time and frequency domain analyses are immediately verified by letting $\zeta \rightarrow 0$ so that $\omega_0 \rightarrow \omega_n$, to give

$$q_{so}(t) \rightarrow -\frac{1}{2} [\, q_p(t - \mu) + \cos\omega_n\mu\, q_p(t) + \frac{\sin\omega_n\mu}{\omega_n} \dot{q}_p(t) \,] \qquad (2.38)$$

For $\zeta = 0$, $q_{so}(t)$ is harmonically varying at a frequency ω equal to ω_n which leads to $\dot{q}_p(t) = j\omega q_p(t)$. In the limit of zero filter damping therefore, the optimal secondary source time history converges to

$$\lim_{\zeta \to 0} q_{so}(\omega) = -\frac{1}{2}\left[e^{-j\omega\mu} + e^{j\omega\mu} \right] \tag{2.39}$$

where in the time domain

$$\lim_{\zeta \to 0} q_{so}(t) = -\frac{1}{2}\left[q_p(t - \mu) + q_p(t + \mu) \right] \tag{2.16}$$

which is equivalent to the unconstrained frequency domain result derived earlier in equation (2.16). Consider first the sound power radiated by the secondary source W_{so} when seeking to minimise the total sound power output of the primary - secondary source pair. This may be expressed as

$$W_{so} = \lim_{T \to \infty} \frac{1}{2T} \int_{-T}^{T} \left[q_{so}(t) p(x_s,t) \right] dt \tag{2.40}$$

Given that the time histories of optimal secondary source strength $q_{so}(t)$ and the total acoustic pressure $p(x_s,t)$ are now known from equations (2.37) and (2.22) respectively, it is left to Appendix 2.2 to show that

$$W_{so} = \frac{W_p}{4}\left[\frac{e^{-2\zeta\omega_n\mu}}{\omega_0^2} \left(\omega_0^2 \cos^2\omega_0\mu + \zeta\omega_n\omega_0 \sin 2\omega_0\mu + \omega_n^2(1 + \zeta^2)\sin^2\omega_0\mu \right) - 1 \right]$$

where as demonstrated in Appendix 2.2 (2.41)

$$W_p = Z_p\omega_n / 8\zeta \tag{2.42}$$

Similarly, the primary source sound power output W_{po} in the presence of $q_{so}(t)$ is also derived in Appendix 2.2 to give

$$W_{po} = W_p\left[1 - \frac{e^{-2\zeta\omega_n\mu}}{\omega_0^2} \left(\omega_0^2 \cos^2\omega_0\mu + \zeta^2 \sin^2\omega_0\mu + \zeta\omega_n\omega_0 \sin 2\omega_0\mu \right) \right] \tag{2.43}$$

Before considering the behaviour of these functions for arbitrary values of the filter damping ζ, it is informative to consider the limiting case where ζ tends to zero at which the filter output is a single tone whose frequency is equal to the filter's centre frequency. The primary sound field along the infinite duct therefore reduces to a single frequency plane wave of frequency ω_n. From equations (2.41) and (2.43), as $\zeta \to 0$, one obtains the asymptotic expressions

$$W_{so} \to 0 \tag{2.44}$$

and

$$W_{po} \to W_p\left(1 - \cos^2\omega_n\mu \right) \tag{2.45}$$

In the limit of zero filter damping, the total source sound power output W therefore varies as (1 - $\cos^2\omega_n\mu$), a result already deduced according to a frequency domain analysis in equation (2.20). For perfectly predictable signals therefore, all of the sound power reduction is due entirely to the suppression of sound from the primary source since the time averaged secondary source sound power output is zero as indicated by the form of the asymptotic result in equation (2.44). From this result one can infer that the energy expended by the secondary source through loading and absorption of the primary source radiation are *exactly* equal and opposite. However, for bandlimited signals, this equilibrium condition is destroyed and the net time averaged sound power output from the secondary source will be negative. This is because the ability of the secondary source to load the primary source is a sole function of the signal predictability. This contrasts the amount of sound power absorbed by the secondary source which is entirely independent of the primary signal predictability. The functions given by equations (2.41) and (2.43) for the total primary source and secondary source sound power output are plotted overleaf in figure 2.3 for the representative values of the filter damping ζ of 0.999, 0.5, 0.1 and 0.

In the first two examples, figures 2.3a and 2.3b, for which the filter damping is set to 0.999 and 0.5 respectively, a good level of sound power reduction can be observed for source spacings up to about one half of a wavelength of the filter's centre frequency. Above this separation distance however, the primary sound power output appears to remain unchanged while the secondary source sound power is minus one quarter the primary source sound power output. The total sound power reduction is therefore only one minus one quarter of the original sound power level corresponding to a reduction of only - 1.25 dB. As the filter bandwidth becomes narrower, for $\zeta = 0.1$ in figure 2.3c, an oscillatory variation with source separation distance begins to appear owing to the onset of phase interference associated with the strong tonal component at the centre frequency of the shaping filter. As anticipated, the results derived in this section are fully consistent with earlier findings since setting the filter damping to zero in figure 2.3d recovers the variation established in the previous section for deterministic signals. These series of figures indicate that no loading of the primary source is possible for source separation distances equal to integer multiples of half wavelengths regardless of the signal bandwidth.

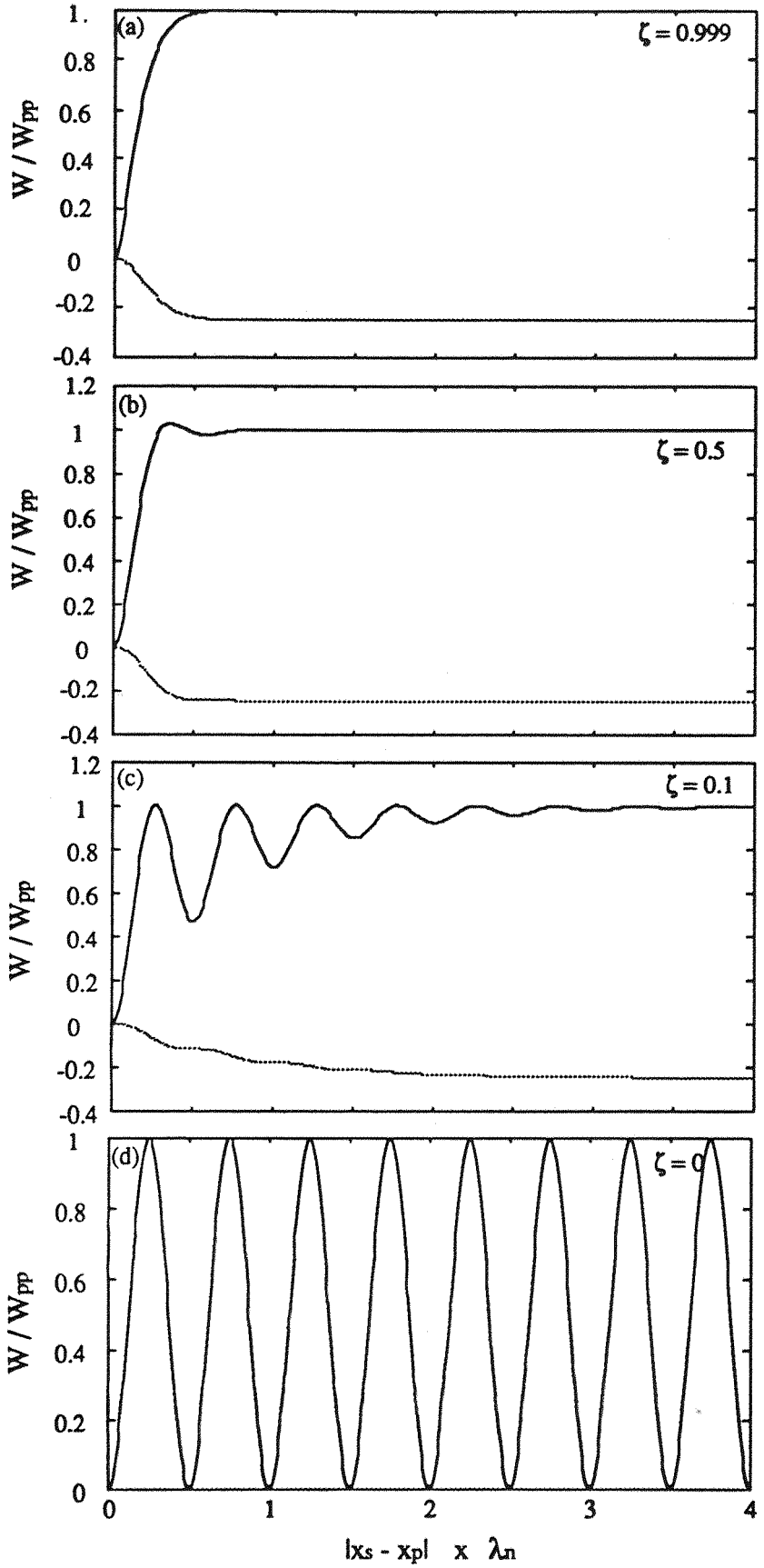

Figure 2.3. A comparison of the total sound power output from the primary (solid line) and secondary source (dashed line) versus separation distance for various values of the shaping filter damping.

2.3. Interpretation of the minimum sound power output in terms of power spectral density

In this section the sound power outputs of the primary source and the secondary source derived in the previous section are decomposed into their spectral components in order to deduce their sound power spectral densities. This exercise facilitates deeper understanding of the complex interaction which necessarily occurs between the primary and secondary sound fields in order to maximally reduce their combined radiated acoustic energies.

From equation (2.21), the time averaged secondary source sound power output W_s is determined from

$$W_s = \lim_{T\to\infty} \frac{1}{2T} \int_{-T}^{T} [\, q_s(t)p(x_s,t) \,]\, dt \;=\; \rho_{qp}(0) \tag{2.46}$$

where $\rho_{qp}(0)$ is the temporal cross correlation function between the secondary source strength and the total pressure at the secondary source point evaluated for zero time lag. The distribution in frequency of this source strength - pressure product may be determined from the Fourier transform of the cross correlation function $\rho_{qp}(\tau)$ which is defined by

$$\rho_{qp}(\tau) = \lim_{T\to\infty} \frac{1}{2T} \int_{-T}^{T} [\, q_s(t)p(x_s,t+\tau) \,]\, dt \tag{2.47}$$

Taking the Fourier transform yields the cross spectral density $S_{qp}(\omega)$ according to[44]

$$S_{qp}(\omega) = \frac{1}{2\pi} \int_{-\infty}^{\infty} \rho_{qp}(\tau)\, e^{-j\omega\tau}\, d\tau \tag{2.48}$$

Taking the the inverse Fourier transform recovers the cross correlation function, namely

$$\rho_{qp}(\tau) = \int_{-\infty}^{\infty} S_{qp}(\omega)\, e^{j\omega\tau}\, d\omega \tag{2.49}$$

Equations (2.47) and (2.49) constitute a form of the Wiener - Kinchine equations[44]. The total sound power output which has been shown to be given by $\rho_{qp}(0)$ is now represented by equation (2.49) for $\tau = 0$ to give

$$\rho_{qp}(0) = \int_{-\infty}^{\infty} S_{qp}(\omega)\, d\omega \tag{2.50}$$

From this equation one can infer that $S_{qp}(\omega)$ represents the frequency distribution of the sound power output over *all* frequencies. For convenience (since FFT analysers do not recognise negative frequencies) it is useful to formulate the sound power spectral density in terms of the *one - sided* cross spectral density function $G_{qp}(\omega)$ defined from

$$G_{qp}(\omega) = 2S_{qp}(\omega) \quad \text{for} \quad \omega > 0 \tag{2.51}$$
$$G_{qp}(0) = S_{qp}(0) \quad \text{for} \quad \omega = 0 \tag{2.52}$$
$$G_{qp}(\omega) = 0 \quad \text{for} \quad \omega < 0 \tag{2.53}$$

Recalling the following even and odd properties for cross spectra[44]

$$\Re\{S_{qp}(\omega)\} = \Re\{S_{qp}(-\omega)\} \tag{2.54}$$
$$\Im\{S_{qp}(\omega)\} = -\Im\{S_{qp}(-\omega)\} \tag{2.55}$$

so that the frequency distribution of sound power output may be written as

$$W_s(\omega) = [S_{qp}(\omega) + S_{qp}(-\omega)] = 2\,\Re\{S_{qp}(\omega)\} \tag{2.56}$$

$$W_s(\omega) = \Re\{G_{qp}(\omega)\} \tag{2.57}$$

A fuller discussion of the steps leading to these equations connected with a frequency domain analysis of sound intensity is presented by Fahy[46]. Recall that the total pressure at the secondary source point is given by $q_{so}(\omega)Z(x_s|x_s) + q_p(\omega)Z(x_p|x_s)$. The secondary source sound power spectral density $W_{so}(\omega)$ may thus be derived from

$$W_{so}(\omega) = Z(x_s|x_s)\,\Re\{G_{q_sq_s}(\omega)\} + Z(x_p|x_s)\,\Re\{G_{q_pq_s}(\omega)\} \tag{2.58}$$

where $G_{q_sq_s}(\omega)$ and $G_{q_pq_s}(\omega)$ are respectively the one sided auto power spectral density of the secondary source strength and the one sided cross power spectral density between the secondary source and the primary source strength. Alternative but equivalent definitions also exist in the form of[44]

$$G_{q_sq_s}(\omega) = \lim_{T\to\infty} \frac{E[|q_{Tso}(\omega)|^2]}{T} \quad \text{and} \quad G_{q_pq_s}(\omega) = \lim_{T\to\infty} \frac{E[q_{Tp}(\omega)q^*_{Tso}(\omega)]}{T} \tag{2.59}$$

where $q_{Tso}(\omega)$ are Fourier transforms of $q_{so}(t)$ of finite duration T and E denotes expectation with respect to time. Putting $Z(x_p|x_s) = Z_p e^{-j\omega\mu}$ and $Z(x_s|x_s) = Z_p$ for this case, the secondary source sound power spectral density reduces to

$$W_{so}(\omega) = Z_p [\Re\{G_{qsqs}(\omega) + e^{-j\omega\mu} G_{qpqs}(\omega) \}] \qquad (2.60)$$

The spectral densities given above may be re-written in terms of the primary source signal by employing the following well known input - output relations for linear, time invariant systems[44]

$$G_{qsqs}(\omega) = |H_o(\omega)|^2 G_{qpqp}(\omega) \quad \text{and} \quad G_{qpqs}(\omega) = H_o^*(\omega) G_{qpqp}(\omega) \qquad (2.61)$$

The secondary source sound power spectral density may now be written in the simpler form of

$$W_{so}(\omega) = Z_p \Re\{ |H_o(\omega)|^2 + H_o^*(\omega) e^{-j\omega\mu} \} G_{qpqp}(\omega) \qquad (2.62)$$

Recalling that in this case $H_o(\omega) = -\frac{1}{2} [e^{-j\omega\mu} + U_o(\omega)]$ which upon substitution into equation (2.62) yields the simpler expression

$$W_{so}(\omega) = -\frac{1}{4} Z_p [1 - |U_o(\omega)|^2] G_{qpqp}(\omega) \qquad (2.63)$$

where $Z_p G_{qpqp}(\omega)$ is the original primary source sound power spectral density $W_p(\omega)$ so that

$$\frac{W_{so}(\omega)}{W_p(\omega)} = -\frac{1}{4} [1 - |U_o(\omega)|^2] \qquad (2.64)$$

Equation (2.64) explicitly reveals the significance of the optimal prediction filter $U_o(\omega)$ which appears simply as a frequency dependent weighting function on the primary source power spectral density $G_{qpqp}(\omega)$. The secondary source sound power output is therefore determined by its own ability to predict the output signal of the primary source. One can see that for any given frequency the minimum value of equation (2.64) is -1/4 while the maximum value is zero. In terms of the two defining parameters of the shaping filter, ζ and ω_n, using equation (2.35) and (2.64) one can show that

$$\frac{W_{so}(\omega)}{W_p(\omega)} = -\frac{1}{4} [1 - \frac{e^{-2\zeta\omega_n\mu}}{\omega_0^2} (\omega_0^2 \cos^2\omega_0\mu + \zeta\omega_n\omega_0 \sin 2\omega_0\mu + \zeta^2\omega_n^2 \sin^2\omega_0\mu + \omega^2 \sin^2\omega_0\mu)] \qquad (2.65)$$

Following an identical procedure for the primary source sound power output $W_{po}(\omega)$ *after* control yields the relationship

$$W_{po}(\omega) = Z(x_s|x_p) \Re\{G_{qsqp}(\omega)\} + Z(x_p|x_p) \Re\{G_{qpqp}(\omega)\} \qquad (2.66)$$

Putting $Z(x_p|x_p) = Z_p$, $Z(x_s|x_p) = Z_p e^{-j\omega\mu}$, $G_{qsqp}(\omega) = H_o(\omega)G_{qpqp}(\omega)$ and substituting for $H_o(\omega)$, gives

$$W_{po}(\omega) = Z_p \Re\{ [1 - \tfrac{1}{2} e^{-2j\omega\mu} - \tfrac{1}{2} U_o(\omega) e^{-j\omega\mu}] \} G_{qpqp}(\omega) \qquad (2.67)$$

Now substituting for $U_o(\omega)$ and noting that $Z_p G_{qpqp}(\omega)$ is the primary source power spectral density function *before* control $W_p(\omega)$, gives the modified primary source sound power output resulting from acoustic interaction with the secondary source pressure. This gives

$$\frac{W_{po}(\omega)}{W_p(\omega)} = 1 - \frac{1}{2}\cos 2\omega\mu - \frac{1}{2}\frac{e^{-\zeta\omega_n\mu}}{\omega_0}(\omega_0 \cos\omega_0\mu\cos\omega\mu + \zeta\omega_n \sin\omega_0\mu\cos\omega\mu + \omega \sin\omega_0\mu\sin\omega\mu) \qquad (2.68)$$

Consider the asymptotic behaviour of W_{so} and W_{po} as the time μ over which the secondary source is required to predict primary source output tends to infinity. In this limit most signals, however narrow the frequency bandwidth, are unpredictable (except for ζ equal to zero where the primary source signals are pure tones). Letting the travel time for sound to propagate between the two sources tend to infinity i.e., $\mu \rightarrow \infty$ shows that the predictor component of the solution tends to zero, $U_o(\omega) \rightarrow 0$, from which the sound power spectral density of each of the sources can be seen to converge to the considerably simpler expressions

$$W_{so}(\omega) \rightarrow -\tfrac{1}{4} W_p(\omega) \qquad (2.69)$$

and

$$W_{po}(\omega) \rightarrow W_p(\omega)[\tfrac{3}{2} - \cos^2\omega\mu] \qquad (2.70)$$

One can now evaluate, by inspection, the total sound power reduction for this limiting geometry. The total secondary source sound power output taken at frequencies is minus one quarter that of the primary source. Far more interesting however, is the behaviour of $W_{po}(\omega)$ which is simply related to its original primary source power spectrum $W_p(\omega)$ via the frequency dependent modulation factor $(1.5 - \cos^2\omega\mu)$. This phenomenon follows directly from the shifting property of the Fourier transform[44] namely

$$\rho_{xx}(\tau - \mu) \leftrightarrow e^{-j\omega\mu} S_{xx}(\omega) \qquad (2.71)$$

Consider again the important example where the primary source sound power output is Gaussian white noise. One can immediately see from equation (2.70) that the presence of the secondary source in the duct effectively 'colours' the previously white primary source sound power spectrum. This finding arises because the transfer function describing the passage of sound leaving the primary source to the secondary source and then back again possesses memory by virtue of the finite time for the sound to make the round trip.

These asymptotic expressions describe the response of the secondary source and the primary source power spectral densities to sound power absorption by the secondary source. This is because primary source loading is not possible owing to the poor predictability of the primary signal over the time interval required for sound to propagate between the two sources at these separation distances. Assuming that the primary source power spectral density varies much slowly with frequency than $\cos^2\omega\mu$ (for example a white noise spectrum does not change at all with frequency), the total primary sound power output W_p is unchanged since this function oscillates about unity so that

$$\frac{3}{2} - \overline{\cos^2\omega\mu} = 1 \qquad (2.72)$$

where the over-bar denotes expectation representing the average value over all frequencies. At large source separation distances, the total sound power reduction from the source pair is due solely to absorption by the secondary source which is approximately one quarter the primary source sound power output with the secondary source turned off.

Some examples of the primary source and secondary source sound power spectral densities are shown in figure 2.4 for various values of the filter damping ζ and the source separation distance $(x_s - x_p)$. In the first set of figures 2.4a - 2.4d, the filter damping is set to 0.1 while the source separation distance is systematically set at 0.1, 0.5, 1 and 5 wavelengths λ_n $(= 2\pi c_0/\omega_n)$ of the centre frequency of the filter ω_n. In the second example, figures 2.4e - 2.4h, the damping of the shaping filter is set equal to 0.99 which is very close to critically damped, consequently the sound power spectral density of the primary source on its own appears to behave as a low pass filter and therefore exhibits no resonance characteristics.

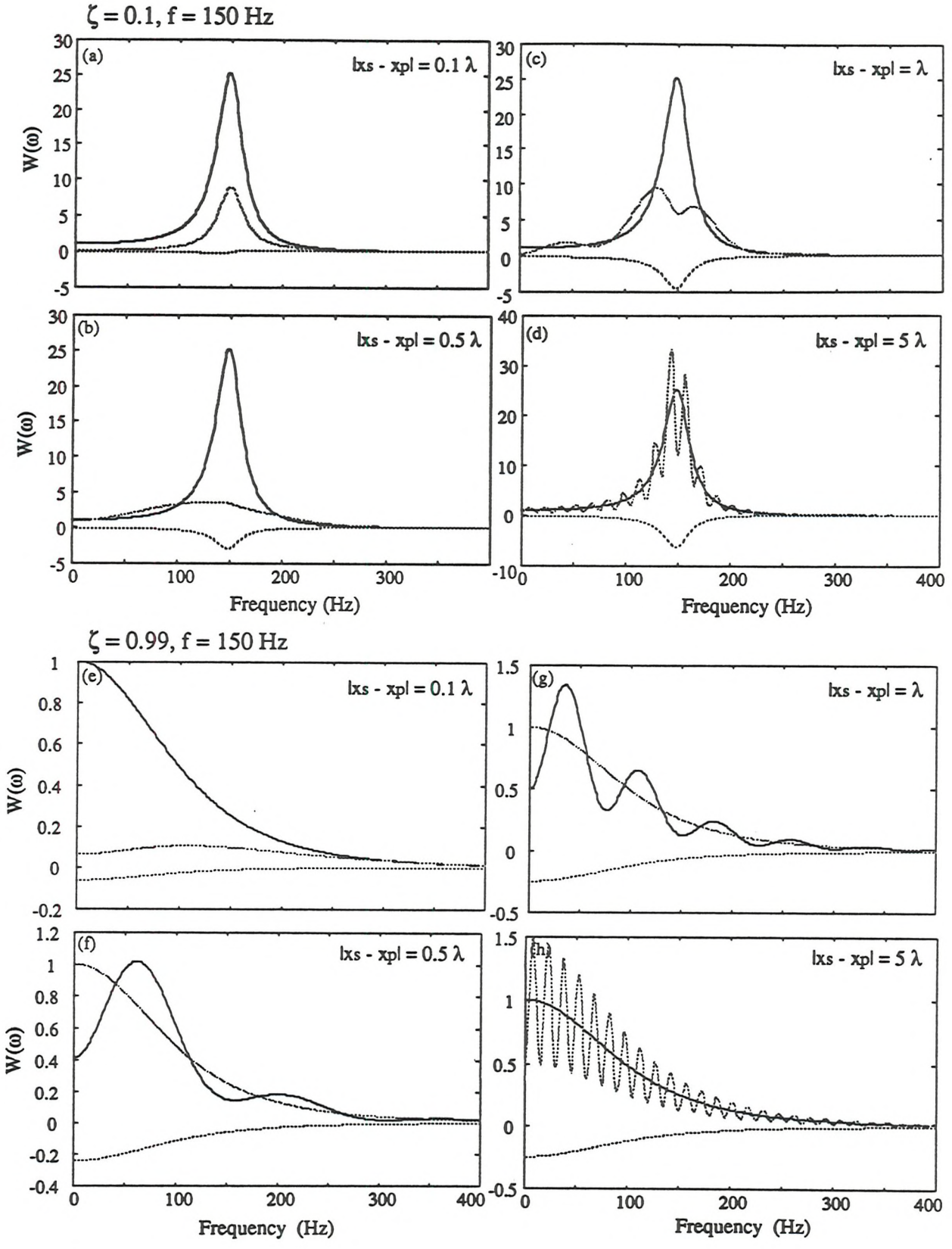

Figure 2.4. The primary source power spectral density before control (solid line) compared with that after control (grey line) and that of the secondary source (lower dashed line) for various values of the source separation distance where λ is the wavelength of the filter's centre frequency. Power spectral densities are the source responses to a primary shaping filter driven by unit amplitude white noise.

In the first example shown in figure 2.4a in which the sources are closely spaced at one tenth of a wavelength of the centre frequency of the shaping filter ω_n, the total sound power reduction is mostly due to primary source loading since the secondary source power spectral density is very close to zero over all frequencies. The total sound power reduction is therefore very close to that radiated if the primary signal were completely periodic owing to the high degree of determinism associated with this narrow band spectrum and the comparatively short distances over which a prediction of the signal is required. As the source separation distance is increased to one half of a wavelength shown in figure 2.4b, the primary signal cannot be predicted as effectively and consequently the secondary source sound power output equilibrium is destroyed resulting in a net sound power absorption. Note that at some frequencies, the primary source sound power output is now beginning to increase.

As the separation distance is increased still further to one wavelength, no further pronounced change in power spectral density can be observed from either source. However, as the source separation is increased to five wavelengths, the primary source sound power spectral density can be observed to have undergone a pronounced re-distribution of energy into into its constituent frequencies. This is of course due to the 3/2 - $\cos^2\omega\mu$ type modulation of the primary source spectral output as explained earlier. One can see that the increase in power output at some frequencies is roughly equal to the decrease in sound power at neighbouring frequencies, so that the total sound power output after control is approximately the same as before control. On the other hand, the secondary source power spectral density remains nearly constant at minus one quarter times that of the primary power spectral density.

Similar behaviour can be observed for the series of graphs shown in figures 2.4c - 2.4e for which the system frequency response is close to critically damped and therefore behaves as a form of low pass filter. Comparison of figures 2.4a - 2.4d and the corresponding graphs for the same source separation distance but for $\zeta = 0.99$ given in figures 2.4e - 2.4h, suggests that active sound power minimisation is most effective for narrow band signals. This observation is revealed more clearly in figure 2.2.

2.4. General aspects of predictability in the active control of random sound

The notion of predictability is extremely important in the active control of random sound fields. This is because it is not unusual for geometric constraints to demand that the propagation time between a secondary source and the desired cancellation point is greater than the propagation time between the primary source and the cancellation point. An

obvious but non-trivial example of where this occurs is the minimisation of the time averaged square pressure at a single free field point. This problem is discussed in detail in references [35] and [47]. When the point of cancellation is closer to the secondary source than the primary source, the optimal secondary source strength is essentially a delay in time equal to the difference in propagation times from the respective sources to the point of cancellation. In this configuration the pressure may be driven to zero for all time. This causal solution, which could have been written down by inspection, emerges quite simply and naturally from the causally constrained Wiener Hopf equation. When the converse is true however, such that the point of cancellation is closer to the primary source than the secondary source, the optimal time averaged reduction in the square pressure which is physically achievable is determined solely by the predictability of the primary source output.

From reference [45], one can show that the time averaged minimum square pressure at some free field point $\mathbf{r}_0$ which is *closer* to the primary source than the secondary source is given by

$$|p(\mathbf{r}_0,\omega)|^2 = Z_0 \int_0^\infty [1 - |U_o(\omega)|^2] G_{qpqp}(\omega)\, d\omega \qquad (2.73)$$

where $U_o(\omega)$ is the optimal predictor defined according to equation (2.31), Z_0 is the free space input impedance of the source and where $G_{qpqp}(\omega)$ is the spectral decomposition of the square pressure from the primary source with the secondary source turned off. Equation (2.73) is closely akin to the expression for the secondary source sound power output in equation (2.64). Just as the name suggests, the predictor filter $U_o(\omega)$ is the factor which completely specifies the fraction of the primary source power spectral density which may be perfectly predicted at any given frequency. For a primary source square pressure spectral density given by $G_{qpqp}(\omega)$, the corresponding square pressure spectral density which may be perfectly predicted $G_{UU}(\omega)$ (and therefore by implication cancelled), is simply

$$G_{UU}(\omega) = |U_o(\omega)|^2 G_{qpqp}(\omega) \qquad (2.74)$$

Using equation (2.74), the total predictable 'power' of the signal as fraction $\eta(\mu)$ of the original power can be written as

$$\eta(\mu) = \frac{\int_0^\infty G_{UU}(\omega)d\omega}{\int_0^\infty G_{qpqp}(\omega)d\omega} = \frac{\int_0^\infty |U_o(\omega)|^2 G_{qpqp}(\omega)d\omega}{\int_0^\infty G_{qpqp}(\omega)d\omega} \qquad (2.75)$$

where by definition $0 \leq \eta(\mu) \leq 1$. Although it is customary to refer to spectra of these kinds as 'powers', this does not of course refer to physical power in the conventional sense which has the units of Watts since this representation may be used to characterise a wide range of signals of various physical origins. Consider the original example where the form of the shaping filter is given by equation (2.33) driven by unit amplitude white noise. The power spectral density of the primary signal $G_{qpqp}(\omega)$ may be obtained from $|X_p(\omega)|^2$ to give

$$G_{qpqp}(\omega) = \frac{\omega_n^4}{(2\zeta\omega_n\omega)^2 + (\omega_n^2-\omega^2)^2} \qquad (2.76)$$

for which the optimal predictor $U_o(\omega)$ has been derived earlier. Using equations (2.35), (2.75) and (2.76), the fraction $\eta(\mu)$ of the primary signal energy which may be perfectly predicted at some time μ in the future is given by

$$\eta(\mu) = \frac{e^{-2\zeta\omega_n\mu}}{\omega_0^2} \left[(\omega_0\cos\omega_0\mu + \zeta\omega_n\sin\omega_0\mu)^2 + \omega_n^2\sin^2\omega_0\mu \right] \qquad (2.77)$$

The function above is less than, or equal to unity for all ζ and ω_n. For ζ which is equal to zero, $\eta(\mu)$ is exactly equal to unity for all values of μ and ω_n signifying that harmonic signals are perfectly predictable at any time in the future. For non zero values of ζ for which the primary signals are not wholly deterministic, it is extremely useful to be able to identify some characteristic temporal bandwidth $\mu_{0.5}$ of the signal for which the absolute predictability of the original primary source signal 'power' is less than, say, one half. One can therefore define a 3 dB predictability bandwidth $\mu_{0.5}$ according to

$$\eta(\mu_{0.5}) = 0.5 \qquad (2.78)$$

which will obviously be a function of the frequency bandwidth of the signal. For the form of spectrum given by equation (2.76), a convenient bandwidth of the signal is the 3 dB bandwidth $\omega_{0.5}$ defined as the frequency bandwidth within which the power spectral density is less than 3 dB below its peak value at resonance. The 3 dB bandwidth for the signal whose system frequency response function is given by equation (2.33) (or half power points) is given in many texts[45] and may be shown to be equal to

$$\omega_{0.5} = 2\zeta\omega_n \qquad (2.79)$$

The solution to equation (2.78), obtained numerically, is plotted below for various values of the filter damping ζ from which the filter 3 dB frequency bandwidth is obtained according to equation (2.79)

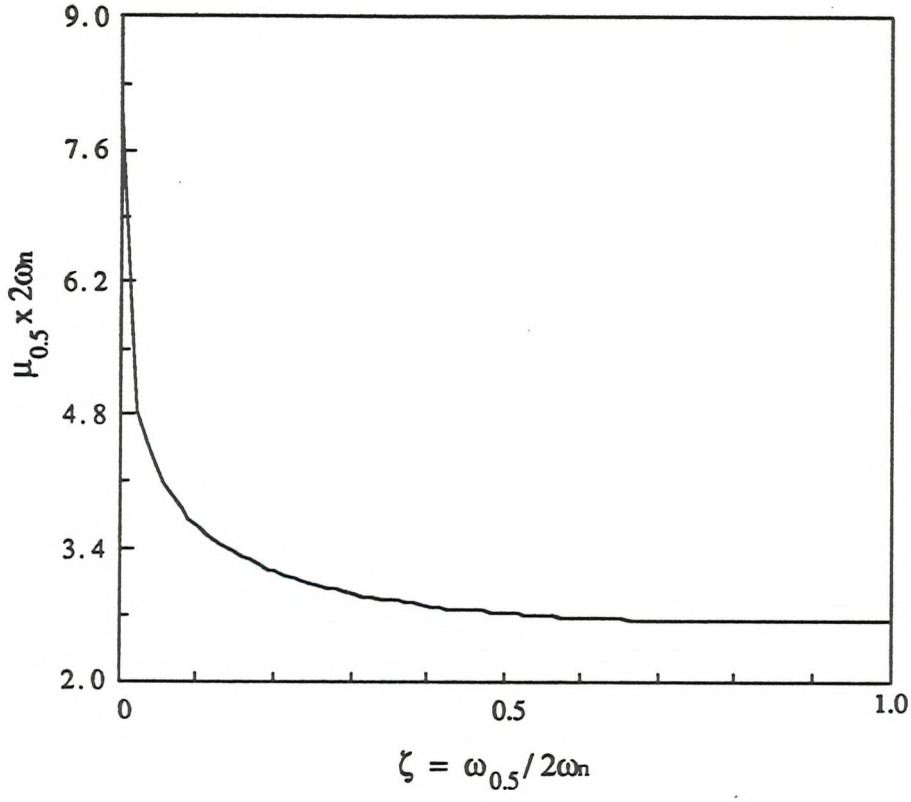

Figure 2.5. The time $\mu_{0.5}$ for which half the total primary signal energy is perfectly predictable versus damping ratio for second order primary source spectrum.

For small ζ, the relationship between the 3 dB frequency bandwidth $\omega_{0.5}$ and the corresponding 3 dB predictability bandwidth of the signal, as defined from $\eta(\mu_{0.5}) = 0.5$, is nearly reciprocal suggesting an approximate relationship of the form

$$\mu_{0.5}\omega_{0.5} \approx \text{constant} \qquad (2.80)$$

For large values of the filter damping ζ, the observed deviation from reciprocal behaviour in figure 2.5 can be explained due to the fact that the frequency bandwidth becomes increasingly ill-defined as the frequency response function of the shaping filter starts to become critically damped. For practical purposes, it is important to identify the order of magnitude of the constant on the right hand side of equation (2.80) so that one may obtain

useful guide-lines for the characteristic distances (in time) for which a given signal is predictable to within 3 dB of its actual value. Inspection of figure 2.5 for small ζ suggests that the constant in equation (2.80) may be estimated to be approximately equal to 0.5. The actual value of the constant of proportionality will depend on the precise characteristics of the primary source signal. As an example which reveals this reciprocal dependence explicitly, consider another form of primary source power spectral density $G_{qpqp}(\omega)$ given below

$$G_{qpqp}(\omega) = \frac{1}{1+\beta^{-2}\omega^2} \tag{2.81}$$

which is a form of low pass filter for which the time constant of the filter β characterises the rate of roll-off with increasing frequency. Unlike the previous example, the parameter β may take all values thereby encompassing both completely predictable signals for $\beta = 0$ and completely unpredictable signals for $\beta = \infty$. In the limit as β tends to infinity, the primary source power spectral density $G_{qpqp}(\omega)$ tends to unity at all frequencies for which the signal therefore has a white noise spectrum. On the other hand as β tends to zero, the shaping filter begins to roll off infinitely quickly thereby converging to a low pass filter which only allows d.c signals to pass. The 3 dB frequency bandwidth for this low pass shaping filter $\omega_{0.5}$, i.e., the frequency within which the response is less than one half of its peak response at $\omega = 0$, may be determined by inspection to give

$$G_{qpqp}(\omega_{0.5}) = 0.5\, G_{qpqp}(\omega)_{max} \quad \text{for} \quad \omega_{0.5} = \beta \tag{2.82}$$

One may follow an identical procedure as the previous example to show that the optimal predictor $U_o(\omega)$ for this spectral shape is simply

$$U_o(\omega) = e^{-\beta\mu} \tag{2.83}$$

which like the previous example in equation (2.77) is frequency independent. The total predictable signal energy as a fraction of the original energy $\eta(\mu)$ according to equation (2.75) may therefore be written as

$$\eta(\mu) = e^{-2\beta\mu} \tag{2.84}$$

The definition of the 3 dB predictability bandwidth $\mu_{0.5}$ defined by equation (2.78) therefore gives an exact reciprocal relationship between the two signal bandwidths of the form

$$\mu_{0.5}\omega_{0.5} = \frac{1}{2}\ln 2 \tag{2.85}$$

where $\frac{1}{2}\ln 2$ is approximately 0.35. Equations (2.80) and (2.85) arise as a consequence of the uncertainty principle. This is a statement of the physical law which says that the frequency bandwidth - time bandwidth product cannot be less than a certain minimum value[44]. This is essentially a mathematical phenomenon which expresses the inter-dependence of time and frequency which prevents arbitrary specification of signals in time and frequency simultaneously. Since the equivalent bandwidth of a function and its transform are reciprocal, it follows that

$$\text{Equivalent duration} \times \text{Equivalent bandwidth} \geq \text{constant} \qquad (2.86)$$

In the case of the bandwidths under discussion, it follows from the above argument that

$$\mu_{0.5}\omega_{0.5} \geq \text{constant} \qquad (2.87)$$

where the constant of proportionality, the bandwidth product, depends on how the bandwidths are defined. In the two cases considered, the bandwidth product appears to be typically equal to 0.5, but may be determined exactly for the form of signal which has the smallest bandwidth product. As Papoulis explains[44], the inequality is exactly satisfied for the *least* predictable signal at a *given* frequency bandwidth $\omega_{0.5}$ which occurs for signals which have a Gaussian power spectral density function for which the auto correlation function, the Fourier transform is therefore also Gaussian. To a good useful working approximation therefore, the characteristic time $\mu_{0.5}$ over which a stationary random signal is usefully predictable is governed by the approximate relationship

$$\mu_{0.5} \geq \frac{1}{\omega_{0.5}} \qquad (2.88)$$

although this formula will, in general, tend to provide a lower bound value according to the general form of the inequality indicated in equation (2.86).

2.5. The unconstrained minimum sound power output in a hard walled semi-infinite duct

As a simple model problem which embodies the essential features of sound power minimisation in reverberant enclosures, consider the same hard walled duct as before. Reflections are now introduced by means of a rigid termination added at one end shown in figure 2.6. Acoustic losses in the enclosure are introduced by way of dissipation at the duct termination which for simplicity is characterised by a real reflection coefficient r. Simple

analysis is only possible by assuming that the mechanism of energy dissipation at the duct termination is linear, causal and most importantly independent of frequency. The sound field in the duct is actively attenuated by the action of a secondary source $q_s(t)$ located *downstream* of the primary source $q_p(t)$ such that $x_s > x_p$. A secondary source located upstream of the primary source would clearly be badly positioned since it would be unable to absorb sound power radiated downstream of the figure.

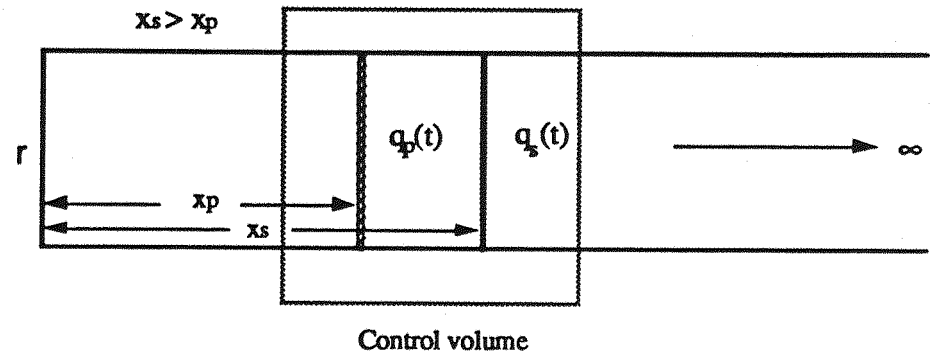

Figure 2.6 A semi-infinite duct with two idealised line sources of which one is a secondary source placed upstream of a primary source.

This geometry is intended to represent the characteristics of a simple reverberant space. The secondary source $q_s(t)$ is constrained to act causally with respect to the time history of the primary source in a way which minimises the total sound power radiated from the source pair. In doing so, the sound power radiated out of the control volume is also minimised, taking into account energy carried by propagating and reflected waves. Before investigating the causally constrained minimum sound power output, for comparative purposes, it is first necessary to establish the best that can be physically achieved when the secondary source is allowed to act non-causally and is therefore able to predict perfectly the output of the primary source. As has already been emphasised, this type of unconstrained optimisation is only relevant for harmonically varying sound fields.

Consider a frequency domain representation of the total sound power output from the source pair. Assuming that only plane waves are allowed to propagate, the total primary source pressure $p_p(\omega,x)$ in the duct from incident and reflected waves may be written thus

$$p_p(\omega,x) = Z_p q_p(\omega)\,(e^{-jk|x - xp|} + re^{-jk(x + xp)}) \qquad (2.89)$$

Similarly, the plane wave field from the secondary source $p_s(\omega,x)$ may also be written as the sum of incident and reflected waves in the form of

$$p_s(\omega,x) = Z_p q_s(\omega)\,(e^{-jk|x - x_s|} + re^{-jk(x + x_s)}) \qquad (2.90)$$

The total sound power W radiated into the duct from both sources acting simultaneously is simply the sum of primary source and secondary source contributions so that

$$W = W_p + W_s \qquad (2.91)$$

Recalling that only the component of the total acoustic pressure which is in-phase with the source strengths is able to radiate any sound power in the time average sense, one can write

$$W = \tfrac{1}{2}\Re\{\,(p_s(\omega,x_s) + p_p(\omega,x_s))q_s^*(\omega) \;+\; (p_s(\omega,x_p) + p_p(\omega,x_p))q_p^*(\omega)\,\} \qquad (2.92)$$

The acoustic pressures at x_p and x_s may be related to the source strengths $q_p(\omega)$ and $q_s(\omega)$ via their appropriate acoustic transfer impedances. We can thus introduce the following notation

$$\begin{aligned} Z(x_p|x_s) &= Z_p\,(e^{-jk(x_s - x_p)} + re^{-jk(x_s + x_p)}) \\ Z(x_s|x_p) &= Z_p\,(e^{-jk(x_s - x_p)} + re^{-jk(x_s + x_p)}) \\ Z(x_s|x_s) &= Z_p\,(1 + re^{-2jkx_s}) \\ Z(x_p|x_p) &= Z_p\,(1 + re^{-2jkx_p}) \end{aligned}$$

$$\text{for } x_s > x_p \qquad (2.93)$$

where reciprocity can be seen to apply. The total sound power W may now be written in terms of the appropriate acoustic transfer impedances to give

$$\begin{aligned} W = \tfrac{1}{2}\Re\{&(q_s(\omega)Z(x_s|x_s) + q_p(\omega)Z(x_p|x_s))q_s^*(\omega) \\ &+ (q_s(\omega)Z(x_s|x_p) + q_p(\omega)Z(x_p|x_p))q_p^*(\omega)\,\} \end{aligned} \qquad (2.94)$$

As previously demonstrated in section 2.1, the total sound power output from two sources acting together may be represented as a quadratic function of the complex secondary source strength $q_s(\omega)$ which lends itself to re-arrangement into the following standard form

$$W = q_s^*(\omega)Aq_s(\omega) \;+\; b^*q_s(\omega) \;+\; bq_s^*(\omega) \;+\; c \qquad (2.95)$$

The coefficients A, b and c may be identified as in the previous example to give

$$\begin{aligned} A = \tfrac{1}{2}\Re\{Z(x_s|x_s)\},\;\; b &= \tfrac{1}{2}q_p(\omega)\Re\{Z(x_p|x_s) + Z(x_s|x_p)\} \\ &\text{and } c = \tfrac{1}{2}|q_p(\omega)|^2\Re\{Z(x_p|x_p)\} \end{aligned} \qquad (2.96)$$

where c is the sound power from the primary source acting in isolation. The optimal solution which minimises this function has previously been derived and is re-written below

$$q_{so}(\omega) = -A^{-1}b \tag{2.11}$$

The existence of a unique minimum solution assumes the positive definiteness of A, namely $\Re\{Z(x_s|x_s)\} > 0$ which follows directly from the conservation of energy. A negative value would imply that more energy is flowing into the source from reflections at the termination than was originally radiated. Now writing $q_{so}(\omega) = H_o(\omega)q_p(\omega)$, from equation (2.11) the optimal transfer function may be shown to be equal to

$$H_o(\omega) = -\frac{\cos k(x_s - x_p) + r\cos k(x_s + x_p)}{1 + r\cos 2kx_s} \tag{2.97}$$

Note that $H_o(\omega)$, as in the free field case, is real indicating that the optimal secondary source either acts exactly in phase or out of phase with the primary source. The behaviour of the secondary source in this slightly more complex space can be visualised more easily in the time domain in terms of the optimal impulse response function $h_o(t)$ which is related to this frequency domain transfer function via the inverse Fourier transform

$$h_o(t) = \frac{1}{2\pi}\int_{-\infty}^{\infty} H_o(\omega)e^{j\omega t}\,d\omega \tag{2.13}$$

The optimal transfer function $H_o(\omega)$ may be expanded as a power series expansion providing $|r| < 1$ which gives

$$H_o(\omega) = -\frac{Z_p}{2}\left(e^{jk(x_s - x_p)} + e^{-jk(x_s - x_p)} + r(e^{jk(x_s + x_p)} + e^{-jk(x_s + x_p)})\right) x$$
$$(1 - r\cos 2kx_s + r^2\cos^2 2kx_s - r^3\cos^4 2kx_s \cdots\cdots (-r)^n\cos^n 2kx_s) \tag{2.98}$$

Employing De-Moivres theorem and noting Fourier transform pairs of the type

$$\cos\omega_0 t\, F(\omega) \overset{\mathcal{F}}{\leftrightarrow} \frac{1}{2}(f(t - t_0) + f(t + t_0)) \tag{2.99}$$

and after a little algebra one can show that $h_o(t)$ for minimising the total sound power output in the enclosure is an infinite row of weighted Dirac delta functions of the form

$$h_o(t) = \sum_{k=0}^{\infty} A_k \delta(t \pm \frac{(2k+1)x_s - x_p}{c}) + \sum_{k=0}^{\infty} B_k \delta(t \pm \frac{(2k+1)x_s + x_p}{c}) \tag{2.100}$$

where $A_k = a_k + ra_{k+1}$ and $B_k = ra_k + a_{k+1}$ and where the terms a_k are intimately related to binomial coefficients according to

$$\begin{aligned} a_0 &= a_0(r) = -(1/2 + 2r^2/2^3 + 6r^4/2^5 + 20r^6/2^7 \cdots \\ a_1 &= a_1(r) = (r/2 + 3r^3/2^4 + 10r^5/2^6 + 35r^7/2^8 \cdots \\ a_2 &= a_2(r) = -(r^2/2^3 + 4r^4/2^5 + 15r^6/2^7 + 56r^8/2^9 \cdots \\ a_3 &= a_3(r) = (r^3/2^4 + 5r^5/2^6 + 15r^7/2^8 + 84r^9/2^{10} \cdots \end{aligned} \tag{2.101}$$

$$\cdots \quad \cdots \quad \cdots \quad \cdots \quad \cdots \quad \cdots$$

$$a_k = a_k(r) = (-1)^{(k+1)} \sum_{k=0}^{\infty} \begin{bmatrix} k+2n \\ k+n \end{bmatrix} \left(\frac{r}{2}\right)^{(k+2n)}$$

$$\text{where } \begin{bmatrix} i \\ j \end{bmatrix} = \frac{i!}{j!\,(i-j)!}$$

This observation is significant since each set of coefficients in equation (2.101) forms a row of one half of Pascal's triangle for which the following recurrence relation holds

$$rA_{k-1} + 2A_k + rA_{k+1} = 0 \qquad \forall \text{ integer } k \tag{2.102}$$

The recursive structure of this equation follows directly from the presence of reflections in the enclosure and offers some insight into the structure of the optimal control process. Any amplitude term A_k appearing in the optimal impulse response function at some current time t exactly cancels with the sum of amplitude terms before and after, weighted by an amount equal to the reflection coefficient r. An identical recurrence relationship may also be written for the set of amplitude terms represented by B_k. Note that consistency with earlier work has been maintained since the free field result is recovered as the reflection coefficient r tends to zero. Putting $r \rightarrow 0$ in equation (2.98) yields

$$h_o(t) = -\frac{1}{2} [\, \delta(t - \mu) + \delta(t + \mu) \,] \tag{2.14}$$

where μ again symbolises the propagation time between the two sources $\mu = (x_s - x_p) / c_0$. There are several important features to observe from equations (2.100) and (2.101). First, the

impulse response function is perfectly symmetrical about the origin of time t = 0 so that the optimal secondary source strength is necessarily non-causal with respect to the primary source time history $q_p(t)$. This finding follows directly from the fact that $H_o(\omega)$ is real. Second, the optimal impulse response decays away with time at a rate determined solely by the reflection coefficient r at the duct termination. It is important to recognise that $h_o(t)$ given in equation (2.100) naturally lends itself to representation in terms of two independent infinite series. Those terms relating to the series of amplitudes A_k are responsible for controlling the radiation from the primary source radiated to the secondary source directly at a separation distance $(x_s - x_p)$. The terms associated with the series of amplitudes B_k are responsible for dealing with the reflected sound or equivalently, the sound field radiated from the 'image' source located at a distance $x_s + x_p$ from the secondary source. Recall that the non-causal optimal secondary source $q_{so}(t)$ is related to the time history of the primary source $q_p(t)$ via the convolution integral

$$q_s(t) = \int_{-\infty}^{\infty} h_o(\tau) q_p(t - \tau)\, d\tau \qquad (2.15)$$

The total time averaged minimum sound power output W_{min} from the source pair can be derived from

$$W_{min} = \lim_{T\to\infty} \frac{1}{2T} \int_{-T}^{T} [\, q_{so}(t)p(x_s,t) + q_p(t)p(x_p,t)\,]\, dt \qquad (2.103)$$

where p(x,t) refers to the total acoustic pressure at some position x and at some time t. Note that this operation is equivalent to substituting $q_{so}(\omega)$ into the equation (2.94) for the frequency dependent total sound power output W and averaging over all frequencies. However, a time domain interpretation of the control process makes it possible to identify the evolution of the total sound power from the source pair. This in turn enables one to establish the mechanism of control by which the total sound power output is minimised in this elementary reverberant space.

The cumulative total sound power output from the source pair $E_{min}(T)$ which determines the total acoustic energy radiated by the source pair from $t = -\infty$ *up to* some time T is given by

$$E_{min}(T) = \int_{-\infty}^{T} [\, q_{so}(t)p(x_s,t) + q_p(t)p(x_p,t)\,]\, dt \qquad (2.104)$$

The acoustic pressure p(x,t) as a function of time now involves four terms which may be written as

$$p(x,t) = Z_p \left[q_p\left(t - \frac{(x_p - x)}{c_0}\right) + r q_p\left(t - \frac{(x_p + x)}{c_0}\right) + q_s\left(t - \frac{(x_s - x)}{c_0}\right) + r q_s\left(t - \frac{(x_s + x)}{c_0}\right) \right]$$

$$\text{for } x_s > x_p \qquad (2.105)$$

By way of example, the cumulative total sound power from the source pair as a function of the time T is shown in figure 2.7 for r = 0.99. In this example the primary source radiation is in the form of a simple unit impulse at t = 0. The secondary source is placed at 2.12 m from the duct termination which is downstream of the primary source located at 1.67 m from the termination. While this analysis is really only appropriate for harmonic signals, the system response to a primary source emitting a unit pulse at t = 0 provides graphic illustration of the dynamic response of the control system. This will hopefully provide an understanding of the physical processes concerned.

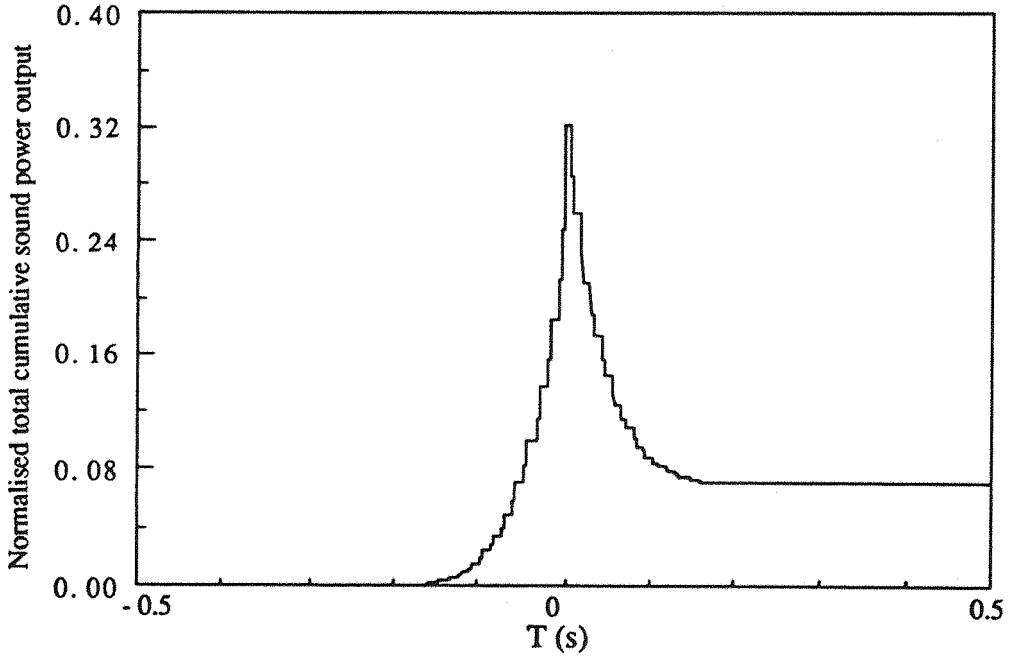

Figure 2.7. The total normalised cumulative sound power output from a source pair in a semi - infinite duct with a reflection coefficient r = 0.99 as a function of time T.

In this instance, negative time refers to the anticipatory action of the secondary source. Figure 2.7 clearly reveals the non-causal response of the optimal secondary source to the unit pressure pulse from the primary source at the origin of time. As a consequence of the high reflection coefficient in this example, the secondary source requires the time taken by many reflections to eventually attain the residual, steady state level of sound power output which in this case is a reduction by a factor of approximately 0.072. One can

establish more precisely the mechanism of control operating in the duct by resolving the total cumulative sound power output into the respective primary and secondary source contributions $E_p(T)$ and $E_s(T)$. These are plotted below

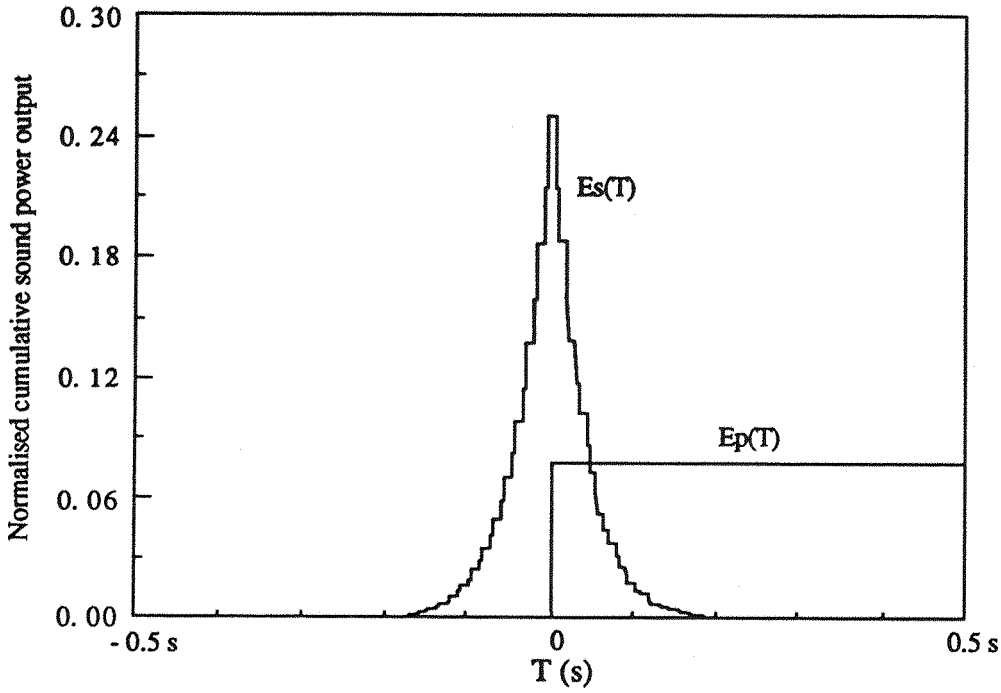

Figure 2.8. The cumulative normalised sound power output from the primary source and secondary source in a semi - infinite duct with a reflection coefficient r = 0.99 as a function of the time T.

There are two important features of this graph one should observe. First, the total energy radiated by the secondary source over a long time interval is exactly zero. Second, the primary sound power output is appreciably less than unity, its value in the absence of control. One is now able to draw some important conclusions relating to the optimal mechanism of control in this simple geometry. The reductions in the total sound power output from the source pair is due solely to the reduction in the sound power output from the primary source. This result is evident from figure 2.8 which shows that the time averaged secondary source contribution to the total energy in the duct is zero as previously observed in figure 2.3. In order to illustrate further the rôle of the secondary source in the minimisation process, the instantaneous secondary source sound power output $W_{so}(T)$ may be derived from the cumulative sound power output $E_{s_{min}}(T)$ via the relation

$$W_{so}(T) = \lim_{\Delta T \to 0} \frac{E_{s_{min}}(T+\Delta T/2) - E_{s_{min}}(T-\Delta T/2)}{\Delta T} \qquad (2.106)$$

$$= \frac{dE_{s_{min}}(T)}{dT} \qquad (2.107)$$

This function quantifies the time averaged acoustic energy radiated during the infinitesimally small time interval T - (1/2)dT and T + (1/2)dT (instantaneous sound power output) which for this example is plotted below

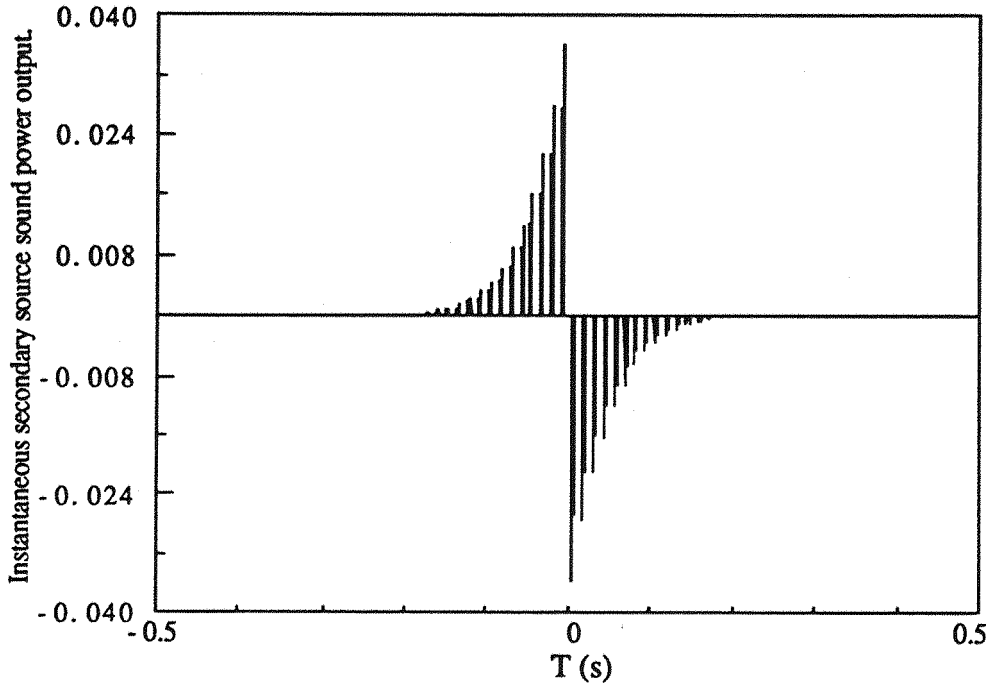

Figure 2.9. The instantaneous sound power output from the secondary source pair in a semi- infinite duct with a reflection coefficient r = 0.99.

The figure above provides graphic demonstration of the control mechanism from the point of view of the secondary source. The process of control commences an infinite time prior to t = 0 where the primary source starts radiating. In anticipation of this event, the secondary source sound power output increases steadily with time, peaking at a negative time equal to the propagation time μ between the two sources. Building up the secondary source sound power output gradually according to the behaviour indicated in figure 2.9 therefore involves less total sound power expenditure by the secondary source than achieving primary source loading with a single action as is necessary in free field, see equation (2.16). Summing the squares of the pressure amplitudes radiated from the secondary source along the infinite duct in figure 2.2c indicates that in free field, the total normalised sound power radiated by the secondary source in loading the primary source is exactly one half. This contrasts a value of only 0.27 in this simple reverberant space as indicated by the secondary source cumulative sound power output shown in figure 2.8 evaluated at T = 0.

This peak amplitude corresponds to the single pulse in the impulse response function sent to arrive at the primary source at t = 0 whose purpose is to load the primary source with the aim of reducing its sound power output. This process represents one of the elementary mechanisms of active sound control and explains why the time averaged primary source sound power output is less during control than before control. Taking this action has the effect of partially destroying the pressure at the primary source point. The acoustic pressure not cancelled at the primary source point is subsequently absorbed.

A short time after t = μ, only the secondary source acoustic pressure is remaining in the duct. The secondary source is then observed to engage in an infinitely long process of self absorption as revealed by the infinite series of infinitesimally short bursts of *negative* sound power output. Negative sound power output refers to energy flowing into the source which is the condition for sound power absorption. This infinite series of absorption terms can be seen to be a mirror image of the infinite series of terms culminating in the loading of the primary source at t = 0.

Once steady state conditions have been attained, the residual level of sound power output radiated from the source pair will ultimately depend upon the frequency and the level of reverberation in the enclosure. The precise level of sound power reduction W_{min} that can be produced at any given frequency is readily derived by substituting equation (2.97) for $q_{so}(\omega)$ into the expression for the total sound power output in equation (2.94) which gives

$$W_{min} = W_p \left[1 - \frac{(\cos k(x_s - x_p) + r \cos k(x_s + x_p))^2}{(1 + r \cos 2kx_s)^2}\right] \qquad (2.108)$$

Putting r = 0 recovers the free field minimum sound power output derived previously

$$W_{min}(\omega) = W_p [\, 1 - \cos^2 k(x_s - x_p) \,] \qquad (2.20)$$

The residual cumulative level of sound power reduction shown in figure 2.7 refers to the level of reduction averaged over all frequencies since the unit pulse of infinitesimal duration contains all frequencies to the same degree. One can show that the time averaged sound power reduction converges to some finite value for all values of the reflection coefficient r less than unity. For r which is exactly equal to unity, the cause of this apparent lack of convergence with time is due to the presence of an infinite series of discrete frequencies satisfying the relationship

$$1 + \cos 2kx_s = 0 \qquad (2.109)$$

where the corresponding value of $W_{min}(\omega)$ is equal to infinity. In physical terms, the condition above defines the set of frequencies for which there is a standing wave established between the secondary source and the completely hard walled termination (since r = 1). This standing wave pattern forms a pressure node at the secondary source point making it impossible to couple into the plane wavefield which therefore drives infinitely hard. On solving for $\cos 2kx_s = -1$, the critical distances for which $W_{min}(\omega)$ is singular corresponds to

$$x_s = \frac{(1 + 2n)\lambda}{4} \quad \text{where n is integer } 0, 1, 2, 3 \qquad (2.110)$$

2.6. The causally constrained minimum sound power output in a semi-infinite duct

In this section an analogous time domain analysis is undertake with the aim of constraining the secondary source strength to behave causally. As in the preceding section, the purpose of the secondary source is to minimise the total sound power radiated into the reverberant space. The time averaged sound power output from the source pair W is given by

$$W = \lim_{T\to\infty} \frac{1}{2T} \int_{-T}^{T} [\, q_s(t)p(x_s,t) + q_p(t)p(x_p,t) \,]\, dt \qquad (2.21)$$

Recalling that the total pressure in the duct p(x,t) is given by equation (2.107), the total sound power output W written in full is determined from

$$\begin{aligned} W = Z_p \lim_{T\to\infty} \frac{1}{2T} \int_{-T}^{T} [\, & q_s(t)(q_s(t) + rq_s(t - \tfrac{2x_s}{c_0})) \\ & + q_s(t)(q_p(t - \tfrac{(x_s - x_p)}{c_0}) + rq_p(t - \tfrac{(x_s + x_p)}{c_0})) \\ & + q_p(t)(q_s(t - \tfrac{(x_s - x_p)}{c_0}) + rq_s(t - \tfrac{(x_s + x_p)}{c_0})) \\ & + q_p(t)(q_p(t) + rq_p(t - \tfrac{2x_p}{c_0})) \,]\, dt \qquad \text{for } x_s > x_p \end{aligned} \qquad (2.111)$$

where $q_p(t)$ and $q_s(t)$, the primary source and secondary source time histories are linearly related by a *causal* impulse response function $h(\tau)$ defined by

$$q_s(t) = \int_0^\infty h(\tau) q_p(t - \tau)\, d\tau \qquad (2.24)$$

Noting that each source strength time history q(t) and its respective acoustic pressure p(t) are linearly related according equations (2.89) and (2.90) *providing* that the reflection coefficient is frequency independent. One can now derive the total sound power output from the source pair in exactly the same way as in the previous example. Substitution of the various terms produces

$$W = Z_p \lim_{T\to\infty} \frac{1}{2T} \int_{-T}^{T} \{ \int_0^\infty h(\tau_1) q_p(t - \tau_1) d\tau \, [\int_0^\infty h(\tau) q_p(t - \tau) d\tau + r \int_0^\infty h(\tau) q_p(t - 2x_s/c_0 - \tau) d\tau]$$

$$+ \int_0^\infty h(\tau) q_p(t - \tau) d\tau \; [\, q_p(t - \frac{(x_s - x_p)}{c_0}) + r\, q_p(t - \frac{(x_s + x_p)}{c_0}) \,]$$

$$+ q_p(t) [\int_0^\infty h(\tau) q_p(t - \frac{(x_s - x_p)}{c_0} - \tau) d\tau + r \int_0^\infty h(\tau) q_p(t - \frac{(x_s + x_p)}{c_0} - \tau) d\tau \,) \}$$

$$+ q_p(t) [\, q_p(t) + r\, q_p(t - \frac{(x_s + x_p)}{c_0}) \,] \qquad \text{for } x_s > x_p \qquad (2.112)$$

The minimum value of this function may be determined using exactly the same analytical procedure as outlined in Appendix 2.1 for the analogous one dimensional free field problem. It is a comparatively simple matter, if algebraically tedious, to show that the optimal impulse response function $h_o(\tau_1)$ which minimised the total sound power radiated into this simple reverberant space is determined from the solution of the following integral equation

$$[\int_0^\infty h_o(\tau_1) [\, r\rho_{pp}(\tau - \tau_1 - \frac{2x_s}{c_0}) + 2\rho_{pp}(\tau - \tau_1) + r\rho_{pp}(\tau - \tau_1 + \frac{2x_s}{c_0}) \,] \, d\tau_1$$

$$+ \rho_{pp}(\tau - \frac{(x_s - x_p)}{c_0}) + r\rho_{pp}(\tau - \frac{(x_s + x_p)}{c_0})$$

$$+ \rho_{pp}(\tau + \frac{(x_s - x_p)}{c_0}) + r\rho_{pp}(\tau + \frac{(x_s + x_p)}{c_0})] = 0$$

$$\text{for } x_s > x_p \text{ and } \tau > 0 \qquad (2.113)$$

Note that it is only the restriction on τ_1 and τ that imposes the constraint of causality.

The impulse response function given in equation (2.100) and (2.101) for the unconstrained problem is essentially the solution of this equation for pure tone signals owing to its perfect predictability. We have already seen that the concept of predictability has a well defined meaning in this context. For current purposes, it is sufficient to understand that harmonic signals represent one extreme of time history by virtue of being perfectly predictable. Sinusoidal functions also constitute an infinite set of ortho-normal functions for which all *periodic* signals may be de-composed. It therefore follows that all periodic signals (which also satisfy Dirichlet's conditions[48]) are completely predictable which is implicit in their periodicity. At the other extreme, white noise is totally unpredictable. By direct analogy with the impulse response function derived previously for the unconstrained example, it is convenient to resolve the optimal causal solution $h_o(t)$ into two components according to

$$h_o(\tau) = h_{o1}(\tau) + h_{o2}(\tau) \tag{2.114}$$

which upon substitution into equation (2.113) yields two independent equations of the form

$$\int_0^\infty h_{o1}(\tau_1) \left[r\rho_{pp}(\tau - \tau_1 - \frac{2x_s}{c_0}) + 2\rho_{pp}(\tau - \tau_1) + r\rho_{pp}(\tau - \tau_1 + \frac{2x_s}{c_0}) \right] d\tau_1$$

$$+ \rho_{pp}(\tau + \frac{(x_s - x_p)}{c_0}) + \rho_{pp}(\tau - \frac{(x_s - x_p)}{c_0}) = 0 \quad \text{for } x_s > x_p \text{ and } \tau > 0 \tag{2.115}$$

and

$$\int_0^\infty h_{o2}(\tau_1) \left[r\rho_{pp}(\tau - \tau_1 - \frac{2x_s}{c_0}) + 2\rho_{pp}(\tau - \tau_1) + r\rho_{pp}(\tau - \tau_1 + \frac{2x_s}{c_0}) \right] d\tau_1$$

$$+ r\rho_{pp}(\tau + \frac{(x_s + x_p)}{c_0}) + r\rho_{pp}(\tau - \frac{(x_s + x_p)}{c_0}) = 0 \quad \text{for } x_s > x_p \text{ and } \tau > 0 \tag{2.116}$$

The assignment of the right hand side of equation (2.113) to the two parts of the solution $h_{o1}(\tau_1)$ and $h_{o2}(\tau_1)$ indicated above is motivated by the form of the solution for the unconstrained optimum in equation (2.100). In this example, $h_o(\tau)$ has been shown to comprise two series of terms for dealing with the radiation from the real source and the

radiation from the so called 'image' source independently. The secondary source views the radiation from the primary source and its image as independent sources of sound even though one is just a delayed and diminished version of the other. This property is reflected in the mathematics as a de-coupling of the governing equation into two equations which may be solved independently.

For ease of analysis, consider the form of solution for which the primary signal $q_p(t)$ is Gaussian white noise such that the signal is totally uncorrelated with itself at any later time. In this case the control mechanism cannot rely on the predictability of the primary signal which which to anticipate the primary source signal. Correspondingly, the temporal correlation function for this limiting class of signal is a Dirac delta function so that the equations (2.115) and (2.116) above reduce to

$$\int_0^\infty h_{o1}(\tau_1)\left[r\delta(\tau - \tau_1 - \frac{2x_s}{c_0}) + 2\delta(\tau - \tau_1) + r\delta(\tau - \tau_1 + \frac{2x_s}{c_0}) \right] d\tau_1$$

$$+ \delta(\tau - \frac{(x_s - x_p)}{c_0}) = 0 \quad \text{for } x_s > x_p \text{ and } \tau > 0 \qquad (2.117)$$

and

$$\int_0^\infty h_{o2}(\tau_1)\left[r\delta(\tau - \tau_1 - \frac{2x_s}{c_0}) + 2\delta(\tau - \tau_1) + r\delta(\tau - \tau_1 + \frac{2x_s}{c_0}) \right] d\tau_1$$

$$+ r\,\delta(\tau - \frac{(x_s + x_p)}{c_0}) = 0 \quad \text{for } x_s > x_p \text{ and } \tau > 0 \qquad (2.118)$$

Note that the two terms $\delta(\tau + \frac{(x_s \pm x_p)}{c_0})$ which appear in equations (2.115) and (2.116) have been set equal to zero. This is because their arguments are positive (providing $x_s > x_p$) representing advances in time and are simply unit spikes which are only non - zero for negative τ and are therefore zero in accordance with the fundamental condition $\tau > 0$

$$\delta(\tau + \frac{(x_s \pm x_p)}{c_0}) = 0 \quad \text{for } x_s > x_p \text{ and } \tau > 0 \qquad (2.119)$$

Assume a solution consisting as before of an infinite row of Dirac delta functions for both $h_{o1}(\tau)$ and $h_{o2}(\tau)$. Because of the white noise statistics of the primary signal, there is no necessity to include an additional predictor term in the assumed form of the solution since there can be no prediction and therefore no loading of the primary source. For this special

case, the solution is assumed to comprise only *delays* in time with the appropriate amplitudes C_k and D_k which remain to be determined.

$$h_{o1}(\tau) = \sum_{k=0}^{\infty} C_k \delta(\tau - \frac{(2k+1)x_s - x_p}{c_0}) \tag{2.120}$$

$$h_{o2}(\tau) = \sum_{k=0}^{\infty} D_k \delta(\tau - \frac{(2k+1)x_s - x_p}{c_0}) \tag{2.121}$$

First, consider the form of the solution for $h_{o1}(\tau)$. Substituting in equation (2.117) the assumed form of the solution $h_{o1}(\tau_1)$ given by equation (2.120) yields the following recursion formula for the series of amplitude terms C_k

$$rC_{k-1} + 2C_k + rC_{k+1} = 0 \quad \text{for integer } k > 0 \tag{2.122}$$

which is subject to the boundary condition

$$rC_1 + 2C_0 + 1 = 0 \tag{2.123}$$

This is the same recurrence relation which governed successive amplitudes in the unconstrained problem discussed earlier in section 2.5. However, since this solution was unconstrained there was no boundary condition to be satisfied since the series was allowed to extend into negative time to minus infinity. Equation (2.122) constitutes a second order, homogeneous difference equation whose solution is straightforward using standard techniques[48]. Assume a solution of the form of a geometric series

$$C_k = r^k \alpha^{k+1} \tag{2.124}$$

Substitution of C_k into equation (2.122) yields the characteristic polynomial of the difference equation which is a quadratic in α, thus

$$r^2\alpha^2 + 2\alpha + 1 = 0 \tag{2.125}$$

Solving for the negative root of this equation since the positive root has a modulus greater than unity which therefore represents a divergent process which therefore cannot represent the minimum. We thus choose the solution

$$\alpha = \frac{-1 + \sqrt{1 - r^2}}{r^2} \tag{2.126}$$

Now since $-1 < \alpha < 0$, each amplitude term in the optimal impulse response function is of exactly opposite sign with the subsequent term and is therefore absorbed by it. The optimal causal solution for this part of the impulse response function may be written thus

$$h_{o1}(\tau) = \sum_{k=0}^{\infty} r^k \alpha^{k+1} \, \delta(\tau - \frac{(2k+1)x_s - x_p}{c_0}) \tag{2.127}$$

This function satisfies both the difference equation and the associated boundary condition and is therefore the complete solution (i.e., complementary function and particular integral). Performing an identical analysis for the part of the solution associated with $h_{o2}(\tau)$, one can show that

$$D_k = r^{k+1}\alpha^{k+1} \tag{2.128}$$

satisfies the required recurrence relation

$$rD_{k-1} + 2D_k + rD_{k+1} = 0 \quad \text{for integer } k > 0 \tag{2.129}$$

together with the additional boundary condition

$$rD_1 + 2D_0 + r = 0 \tag{2.130}$$

The solution for $h_{o2}(\tau)$ which is responsible for acting to reduce the radiation from the 'image' source may now be written as

$$h_{o2}(\tau) = \sum_{k=0}^{\infty} r^{k+1} \alpha^{k+1} \, \delta(\tau - \frac{(2k+1)x_s + x_p}{c_0}) \tag{2.131}$$

It is significant that $C_k = rD_k$ since the two processes associated with these terms operate in cascade separated by one reflection at the termination at $x = 0$. The set of optimal terms associated with $h_{o2}(\tau)$ are therefore identical to $h_{o1}(\tau)$ except for the additional muliplicative factor r. Assuming the uniqueness of the solution, the causally constrained optimal impulse response function for minimising the total sound power from the source pair in the presence of reflections is given by

$$h_o(\tau) = \sum_{k=0}^{\infty} r^k \alpha^{k+1} \delta(\tau - \frac{(2k+1)x_s - x_p}{c_0}) + \sum_{k=0}^{\infty} r^{k+1} \alpha^{k+1} \delta(\tau - \frac{(2k+1)x_s + x_p}{c_0})$$

$$\text{where } \alpha = (-1 + \sqrt{1 - r^2}) / r^2 \qquad (2.132)$$

It is instructive to compare the form of this causally constrained impulse response function with the analogous unconstrained function for the same geometry. These are compared below for r = 0.99

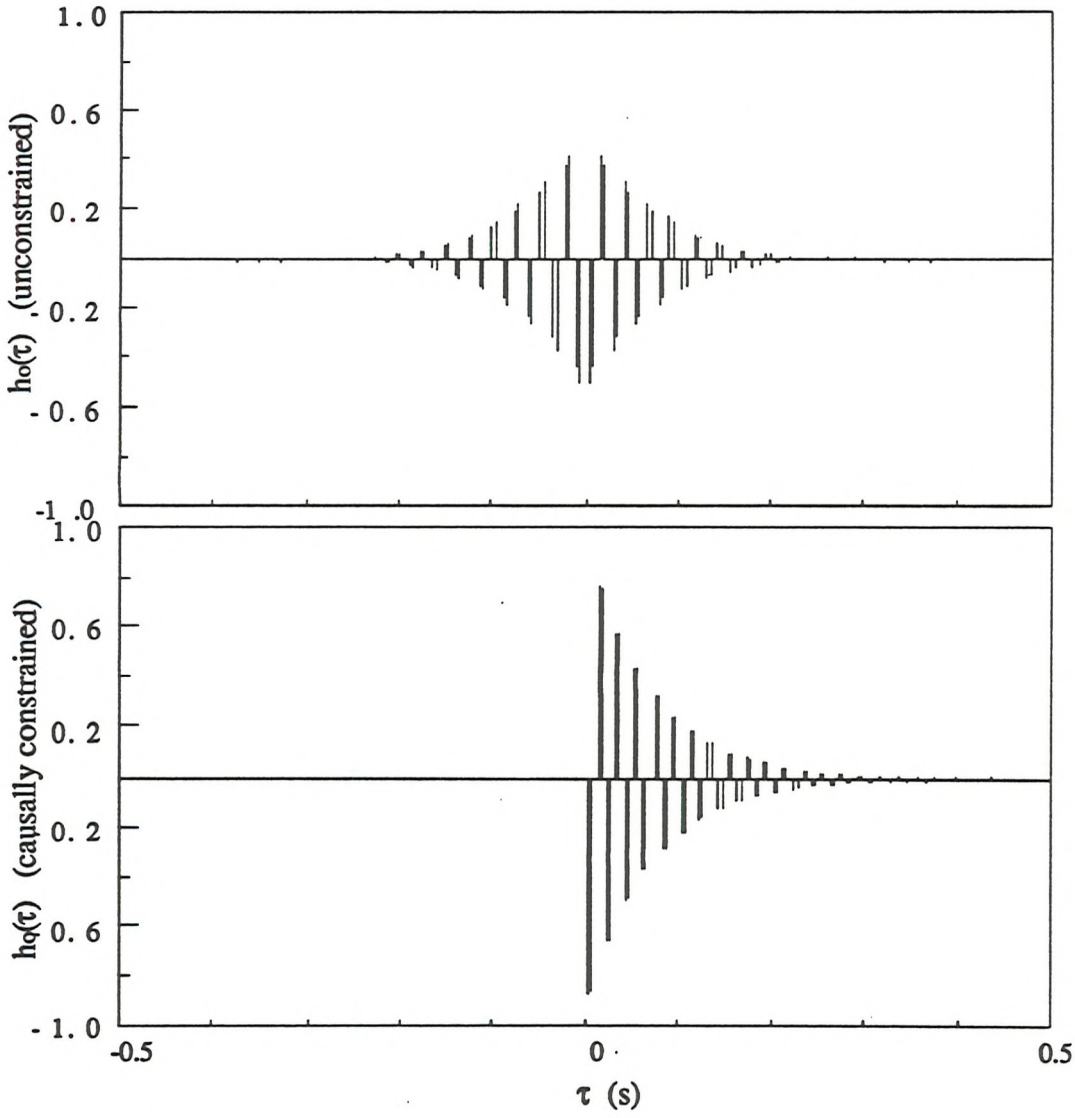

Figure 2.10. The unconstrained and causally constrained impulse response function for minimising the total sound power output in a semi-infinite duct with a reflection coefficient r = 0.99.

Notice that the terms in the impulse response functions above occur in pairs. These exist in order to suppress the radiation from the source and the radiation from the image source a short time later (for closely spaced sources where active control is most effective for finite bandwidth signals). One is now able to envisage the complexity of the impulse response functions for dealing with sound radiated into a fully enclosed sound field owing to the contributions from an infinite number of image sources. It is important to recognise that the causally constrained optimal impulse response function is *not*, in general the windowed non-causal impulse response function as might be interpreted from the work of some authors[49].

It is instructive to consider the limiting case of this series for the case where $r \rightarrow 0$ thereby removing the presence of reflections as in free space. Employing L'hopital's rule for the limit of the ratio of two functions simultaneously tending to zero such as

$$\frac{f(x)}{g(x)} \rightarrow \frac{f'(x)}{g'(x)} \quad \text{as } x \rightarrow 0 \tag{2.133}$$

then as $r \rightarrow 0$, α takes the limiting form

$$\alpha = \frac{-r\,(1 - r^2)^{-1/2}}{2r} \lim_{r \rightarrow 0} = -\frac{1}{2} \tag{2.134}$$

In a one dimensional free field space therefore, the optimal causal solution for white noise is simply

$$h_o(\tau) = -\frac{1}{2}\,\delta(\tau - \frac{(x_s - x_p)}{c_0}) \tag{2.135}$$

The optimal mechanism of control for white noise is therefore to absorb one half of the incident energy, a process which by summing the squares of the pressure amplitudes in the manner indicated in figure 2.2 shows a 25 % reduction in the original primary sound power output. This is shown again in a later graph. Again, it is instructive to calculate the cumulative sound power output as a function of time in order to establish the precise mechanism of control for this causally constrained controller. For this example however, the mechanism is particularly simple since controlling white noise can only be accomplished by a succession of delays which represent an infinite succession of absorption terms. One is now able to evaluate the causally constrained secondary source strength in response to a primary signal which is a unit spike of infinitesimal duration at $t = 0$. Evaluating the cumulative sound power output in the usual way for $r = 0.99$ as a function of time according to equation (2.106), yields the results shown in figure 2.11

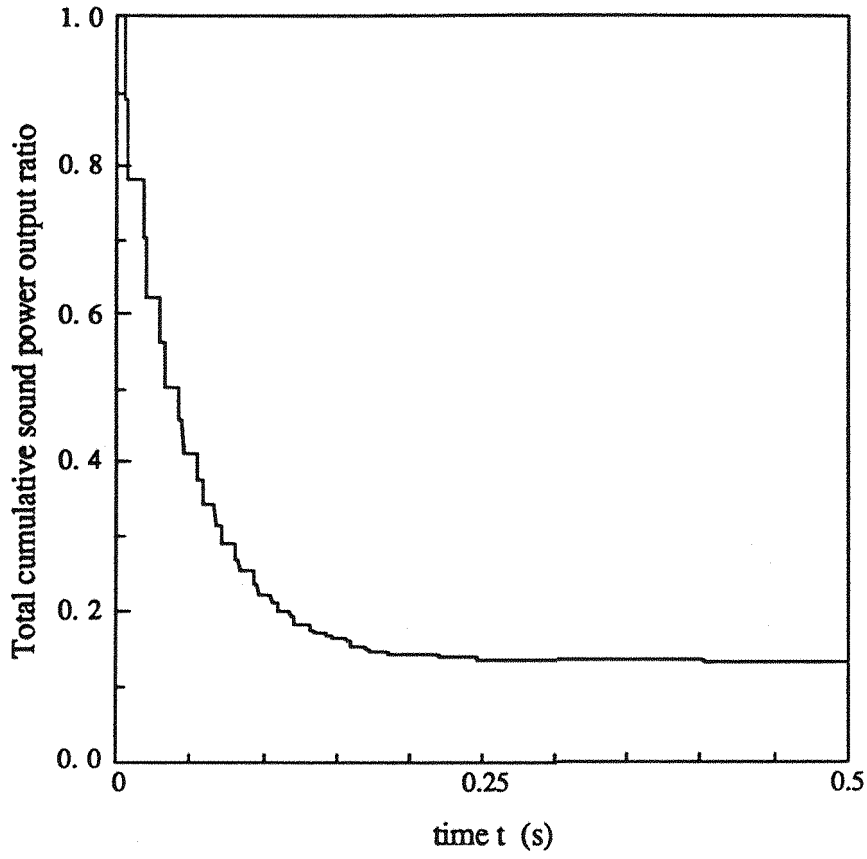

Figure 2.11. The total cumulative sound power output from a source pair in response to a unit pulse radiated by the primary source into a semi-infinite duct with a reflection coefficient r = 0.99.

The fact that the causally constrained optimal impulse response function is a simple infinite series of delays in time indicates that the *total* primary source sound power output in radiating white noise must remain unaltered by the causal action of the secondary source. The mechanism of control for this special problem must therefore be limited to the absorption of successive reflections since the secondary source is unable to anticipate the primary source radiation. However, it is important to recognise that even though the total primary source sound power is unchanged, the sound power radiated into its constituent frequencies has undergone a pronounced re-distribution according to the behaviour typified by equation (2.70).

The residual level of sound power reduction in the presence of reflections for primary signals in the form of a unit pulse (which also quantifies the sound power reduction for white noise signals) is evaluated from the type of numerical simulation outlined above which produced the results presented in figure 2.11. This simulation was repeated for a range of reflection coefficients r between 0 and 0.999, the results of which are plotted below. Also shown by way of comparison is the corresponding average result for harmonic primary sources.

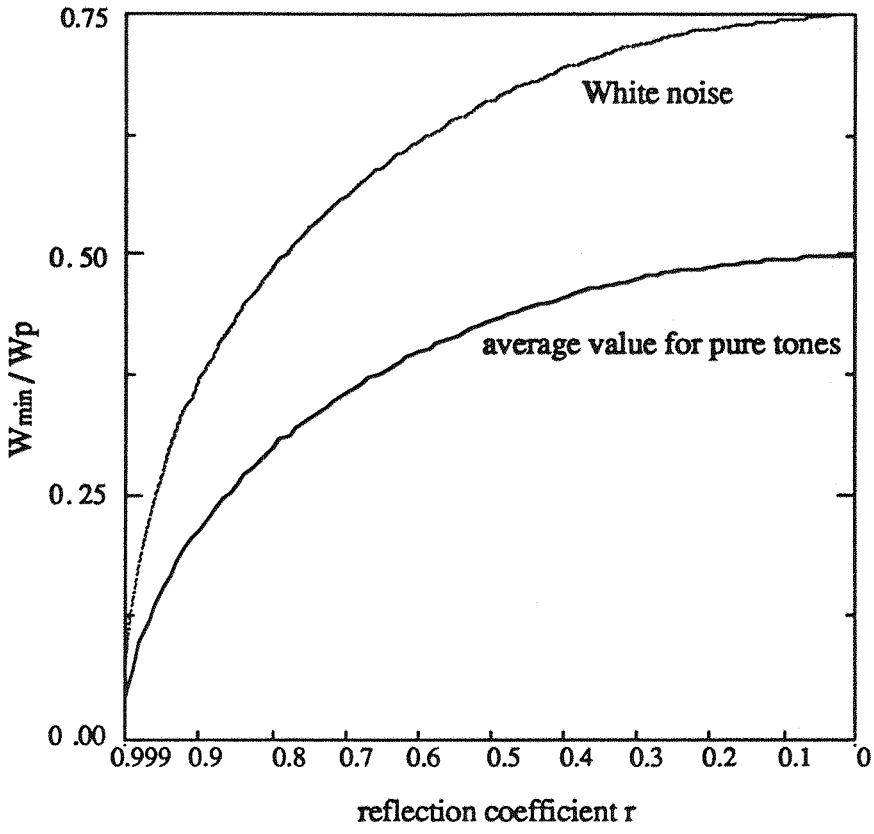

Figure 2.12. The time averaged total sound power output from a source pair in a semi-infinite duct versus the termination reflection coefficient r: Gaussian white noise (dashed line), completely predictable harmonic noise (continuous line).

Note that as the reflection coefficient tends to zero, in the case of white noise, the time averaged level of sound power reduction is exactly one quarter that of the primary source level, a result noted earlier. In the case of harmonic sources however, the averaged level of sound power reduction is reduced by exactly one half. Although the level of sound power reduction for arbitrary bandlimited signals has not been evaluated specifically, the results in figure 2.12 serves to place an upper and lower bound on the exact levels of sound power reduction which ultimately may be achieved for any stationary random signal.

2.7. Discussion and conclusion

This chapter has considered the active control of random, broadband noise giving special emphasis to the effects of reverberation. For simplicity of analysis, only sound propagating in one dimension has been investigated. Reverberation has been introduced in the simplest possible way by means of a single reflecting surface on which the form of acoustic dissipation is characterised by a real, frequency independent reflection coefficient.

It is believed that this elementary geometry retains all the important physical features of the more complicated three dimensional random sound field.

As a precursor to the more complex problem involving reflections, the total causally constrained free field minimum sound power output from a primary - secondary source pair has been derived. The primary source signal is mathematically modelled as the random output from some second order shaping filter driven by unit amplitude white noise. This choice of model enables the predominant frequencies in the signal to be varied according to the centre frequency of the filter, while the bandwidth of the signal (the more crucial factor) was adjusted according to the filter damping. Interpretation of the problem was approached from the point of view of the spectral output of each of the two sources in turn. The level of sound power reduction was found to diminish with increasing source separation distance and primary signal bandwidth.

One surprisingly subtle finding to arise from this investigation is that at an infinite series of harmonically related discrete frequencies, the total radiated sound power increases by up to a maximum of 3 dB but appears to more than compensated by reductions in sound power output at neighbouring frequencies which are also harmonically related. This re-distribution of energy amongst the constituent frequencies of the signal is pronounced and will certainly influence the subjective impression of the control procedure in accordance with the 'A' weighting curve. However, the general trend in sound power reduction over the entire frequency band is such that the total energy in the signal is less than in the absence of the secondary source. More specifically, in the limit as the primary signal bandwidth becomes increasingly greater eventually tending to an 'all pass' filter, the primary source sound power spectrum becomes modulated in a way which preserves the total original source sound power output. The secondary source power output on the other hand tends to minus one quarter of the primary source level before control signifying the absorption of one quarter of the incident energy. In the limit as the filter bandwidth becomes increasingly narrower, the primary signal appears increasingly like a sine wave. The total reduction in the sound power output was found to converge on the frequency domain result derived earlier in this chapter which delineates the absolute level of sound power reduction which may be physically achieved given perfect signal predictability.

The second half of this chapter has considered the effects of reverberation on broadband active noise control. Reflections are incorporated into the model problem by way of a single dissipative surface characterised by a real reflection coefficient whose value is independent of frequency. The model enclosure was chosen to take the form of a semi-infinite, hard walled duct constrained to support only plane waves. Again the total

minimum sound power radiated out of some control volume completely enclosing the primary - secondary source pair was sought. Despite the elementary nature of the chosen geometry, the derivation of the governing equation was found to be simple but its closed form solution for finite bandwidth primary signals was not. However, the optimal solution in terms of the transfer function between the sources was found to be derivable for the two limiting class of signals: Perfectly periodic signals, namely pure tones, and signals which are completely absent of periodic component and are therefore completely random i.e., Gaussian white noise signals.

In each case, the level of sound power reduction radiated into the simple enclosure was found to be highly dependent on the intensity of reverberation in the enclosure as determined by the reflection coefficient, becoming greater with increasing reverberation. At first glance it would appear paradoxical that the reduction in sound power increases with increasing spatial complexity as the presence of reflections implies. But this finding is readily explained when one realises that the dominant mechanism of energy reduction (both passive and active) is the absorption of sound power. Increasing the level of reverberant energy in the space therefore increases the amount of sound energy capable of being absorbed. As the optimal impulse response functions reveal, the absorption of sound in the presence of reflecting boundaries is not a single event, but is an infinite number of events possessing, in the case of a simple acoustic space, a high degree of recursive structure. Consequently, the steady state level of sound power reduction is a highly non-linear function of the reflection coefficient. The recursive action of the optimal secondary source strength time history may be exploited in a practical realisation, requiring only a small number of elementary delay elements.

In comparing the two impulse response functions, it becomes clear that the secondary source strength time history for the causally constrained minimum sound power output is *not* simply a windowed version of the unconstrained minimum sound power output. The inter-relationship between the two appears to considerably complex such that the steady state level of sound power reduction for the causally constrained case bears no immediately obvious relationship to the unconstrained minimisation in terms of the problem parameters. However, it is extremely encouraging to observe that the steady state level of sound power reduction for white noise at any value of the reflection coefficient is never less than 3 dB of the corresponding average value for pure tone signals.

APPENDIX 2

Appendix 2.1. The derivation of the Wiener - Hopf equation governing causally constrained free field minimum sound power output

Given the time domain expression for total sound power output W given in equation (2.27)

$$W = Z_p \Big[\int_0^\infty \int_0^\infty h(\tau)h(\tau_1)\, \rho_{pp}(\tau - \tau_1)\, d\tau\, d\tau_1 + \int_0^\infty h(\tau)\rho_{pp}\Big(\tau - \frac{|x_s - x_p|}{c_0}\Big)\, d\tau$$

$$+ \int_0^\infty h(\tau)\rho_{pp}\Big(\tau + \frac{|x_s - x_p|}{c_0}\Big)\, d\tau \Big] + W_p \qquad \text{(A2.1)}$$

for which the minimum is required with respect to the optimal impulse response function $h_o(\tau)$. This may be accomplished using the variational technique[42], a technique common in the calculus of variation. Assume that the impulse response function can be resolved into the optimal function $h_o(\tau)$ plus some unknown 'error' term $\varepsilon h_\varepsilon(\tau)$

$$h(\tau) = h_o(\tau) + \varepsilon h_\varepsilon(\tau) \qquad \text{(A2.2)}$$

Since any choice of the variational parameter ε will cause an increase in W, the total sound power output W must be stationary about $\varepsilon = 0$ i.e.,

$$\left(\frac{\partial W}{\partial \varepsilon}\right)_{\varepsilon=0} = 0 \qquad \text{(A2.3)}$$

On substitution of $h_o(\tau) + \varepsilon h_\varepsilon(\tau)$ for $h(\tau)$ into equation (A2.1) and performing the differentiation with respect to ε about $\varepsilon = 0$, only the term linear in ε will remain. Thus isolating the coefficient of ε yields

$$\int_0^\infty \int_0^\infty \big(h_\varepsilon(\tau_1)h_o(\tau_2) + h_o(\tau_1)h_\varepsilon(\tau_2) \big)\rho_{pp}(\tau_1 - \tau_2)\, d\tau_1 d\tau_2$$

$$+ \int_0^\infty h_\varepsilon(\tau_1)\rho_{pp}(\tau_1 - \mu)\, d\tau_1 + \int_0^\infty h_\varepsilon(\tau_1)\rho_{pp}(\tau_1 + \mu)\, d\tau_1 = 0 \qquad \text{(A2.4)}$$

Interchanging the dummy variables τ_1 and τ_2 on the product $h_o(\tau_1)h_\varepsilon(\tau_2)$ facilitates factorisation of the unknown error term $h_\varepsilon(\tau_1)$ which is completely arbitrary and, in general, not equal to zero leaving the following condition on $h_o(\tau_1)$

$$2\int_0^\infty h_o(\tau_1)\rho_{pp}(\tau - \tau_1)\, d\tau_1 + \rho_{pp}(\tau + \mu) + \rho_{pp}(\tau - \mu) = 0 \quad \text{for } \tau > 0 \qquad \text{(A2.5)}$$

Appendix 2.2. The derivation of the total primary source, and secondary source sound power output

Consider the secondary source sound power output thus

$$W_{so} = \lim_{T\to\infty} \frac{1}{2T} \int_{-T}^{T} q_{so}(t)p(x_s,t)\, dt \qquad \text{(A2.6)}$$

For the form of the second order primary signal given by equation (2.33), $q_s(t)$ has been shown to take the form

$$q_{so}(t) = -\frac{1}{2}[\, q_p(t - \mu) + Aq_p(t) + B\dot{q}_p(t)\,] \qquad \text{(A2.7)}$$

where

$$A = \frac{e^{-\zeta\omega_n\mu}}{\omega_0}(\,\omega_0\cos\omega_0\mu + \zeta\omega_n\sin\omega_0\mu\,) \quad \text{and} \quad B = \frac{e^{-\zeta\omega_n\mu}}{\omega_0}\frac{\omega_n}{8\zeta}\sin\omega_0\mu \qquad \text{(A2.8)}$$

Further note that

$$p(x_s,t) = Z_p[\, q_{so}(t) + q_p(t - \mu)\,] \qquad \text{(A2.9)}$$

Given the relationships above, one can show that W_{so} is derived from

$$W_{so} = \frac{1}{4}[\,(A^2 - 1)\rho_{pp}(0) + B^2\ddot{\rho}_{pp}(0)\,] \qquad \text{(A2.10)}$$

where $\ddot{\rho}_{pp}(0)$ denotes the correlation function of the time derivatives of the primary signal evaluated at zero time lag. The correlation function $\rho_{pp}(\mu)$ for this signal is given in standard texts[45]

$$\rho_{pp}(\mu) = \frac{e^{-\zeta\omega_n\mu}}{\omega_0}\frac{\omega_n}{8\zeta}(\omega_0\cos\omega_0\mu + \zeta\omega_n\sin\omega_0\mu) \qquad \text{(A2.11)}$$

from which one can determine $\ddot{\rho}_{pp}(0)$ via the following identity[44]

$$\rho_{\dot{p}\dot{p}}(\mu) = -\frac{\partial^2 \rho_{pp}(\mu)}{\partial \mu^2} \tag{A2.12}$$

which gives

$$\rho_{\dot{p}\dot{p}}(\mu) = \frac{e^{-\zeta\omega_n\mu}}{\omega_0}\frac{\omega_n^3}{8\zeta}(\omega_0 \cos\omega_0\mu + \zeta\omega_n \sin\omega_0\mu) \tag{A2.13}$$

Collectively, equations (A2.9) - (A2.13) are sufficient to determine W_{so}, which after a little algebra yields

$$W_{so} = \frac{W_p}{4}\left[\frac{e^{-2\zeta\omega_n\mu}}{\omega_0^2}\left(\omega_0^2\cos^2\omega_0\mu + \zeta\omega_n\omega_0 \sin 2\omega_0\mu + \omega_n^2(1+\zeta^2)\sin^2\omega_0\mu - 1\right)\right.$$

where (A2.14)

$$W_p = Z_p\rho_{pp}(0) = Z_p\omega_n / 8\zeta \tag{A2.15}$$

In a similar fashion the total sound power radiated by the primary source is given by

$$W_{po} = Z_p \lim_{T\to\infty}\frac{1}{2T}\int_{-T}^{T} q_p(t)\,[q_p(t) + q_{so}(t-\mu)]\,dt \tag{A2.16}$$

is also readily determined by noting the general form of the optimal secondary source strength $q_{so}(t) = -\frac{1}{2}[\,q_p(t-\mu) + Aq_p(t) + B\dot{q}_p(t)\,]$. Upon substitution of equation (A2.7) into W_{po} and expanding gives

$$W_{po} = \frac{1}{2}Z_p[\,\rho_{pp}(2\eta) + A\rho_{pp}(\eta) - B\rho_{p\dot{p}}(\eta) - 2\rho_{pp}(0)\,] \tag{A2.17}$$

The correlation function between the primary source time history and its derivative with respect to time, namely $\rho_{p\dot{p}}(\eta)$ is derived from $\rho_{pp}(\eta)$ via the identity[44]

$$\rho_{p\dot{p}}(\mu) = \frac{\partial}{\partial\mu}\rho_{pp}(\mu) \tag{A2.18}$$

to give

$$\rho_{p\dot{p}}(\mu) = -\frac{e^{-\zeta\omega_n\mu}}{\omega_0}\frac{\omega_n^3}{8\zeta}\sin\omega_0\mu \tag{A2.19}$$

Substitution of the various terms yields the total primary source sound power output W_{po}

$$W_{po} = W_p\left[1 - \frac{e^{-2\zeta\omega_n\mu}}{\omega_0^2}\left(\omega_0^2\cos^2\omega_0\mu + \zeta^2\sin^2\omega_0\mu + \zeta\omega_n\omega_0\sin 2\omega_0\mu\right)\right. \tag{A2.20}$$

CHAPTER 3

GLOBAL CONTROL OF HIGH FREQUENCY ENCLOSED SOUND FIELDS AND THE DIFFUSE FIELD

3.0. Introduction

The scope for active noise control has to a large degree been quantified for bounded spaces which support sound fields driven at low frequencies[12,22,23]. There has been considerable success in actively manipulating pure tone, low frequency enclosed sound fields for two reasons. First, the time taken between successive computing instructions places an upper bound on the frequency that can accurately be manipulated in real time. Second but more important is the spatial simplicity of the pressure distribution over the enclosure at low frequencies. The recent, rapid advances in digital technology has meant that the speed of computation is now no longer the severe constraint it once was. However, the difficulties associated with the spatial complexity of a reverberant sound field driven at high frequencies are inherent in the physical acoustics and consequently remain. It is therefore the physical characteristics of the acoustic field which dictates the fundamental limits on the levels of acoustic pressure attenuation that can be engineered via the use of active control technology.

At high frequencies the number of acoustic modes of the enclosure excited is large. On superposition, these modes interfere to form a pressure variation which is spatially complex. The ultimate task of active control is to reproduce this spatial pressure pattern exactly in anti-phase thereby nullifying the acoustic pressure throughout the entire space. Clearly this is not practicable (although possible in principle), when the primary source of noise is itself complex and distributed over distances which are large compared to the acoustic wavelength. The secondary source geometry is, by contrast, typically composed of compact, discrete transducer elements. The following few chapters are concerned with a limiting case of an enclosed sound field namely the diffuse field. In many respects, the idealised diffuse field represents a worst possible case from the point of view of applying active noise control. This study was primarily stimulated by the need to be able to identify an upper working frequency limit for which the application of active control within highly reverberant enclosed spaces driven at high frequencies is worthwhile.

The thrust of the work presented in this chapter is concerned with an analysis of the minimum sound power output of two closely spaced point monopole sources radiating into

a diffuse field environment. Providing that the sources are sufficiently close on the scale of the acoustic wavelength, destructive interference between the respective sound fields extends beyond their immediate near fields to encompass the entire space. Complete global suppression of the diffuse field is therefore a possibility for this rather unrealistic source geometry. Nevertheless, an analysis of this problem is able to yield results which offers considerable insight into the mechanisms by which the operation of one source can maximally reduce the sound power of another.

Conceivably, one could envisage minimising the total sound power radiated into an enclosure by appropriately adjusting the amplitude and phase of a secondary loudspeaker with the aim of minimising the sum of the square outputs from an array of microphones strategically located in representative points around the room. The sum of the squared outputs from such an array of control microphones is an approximation to the total acoustic potential energy in the enclosure at high frequencies. This follows directly from the linear relationship which exists between the sound power output W of the source, the total energy density e_p in the enclosure, and the space averaged square pressure $< |p(r)|^2 >$ in the room sustained by the source. From standard texts in acoustics[50] we have the well known relationships

$$e_p = \frac{4W}{Ac_0} = \frac{< |p(r)|^2 >}{2\rho c_0^2} \qquad (3.1)$$

where A is the total absorption in the enclosure in square metres, ρ and c_0 are the ambient density and the sound speed in the medium respectively. The results above are derived on the basis of an energy balance between the rate at which energy is supplied to the enclosure, determined by the source sound power output, and the rate of dissipation characterised by the total absorption A. Equation (3.1) is only valid when a state of energy equilibrium is achieved and is invalid for transient excitations. Real time algorithms and the associated hardware are now available, sufficiently economically, to render this methodology realistic enough to justify the lengthy, but enlightening analysis described in this chapter which deals primarily with the minimum sound power output of two closely spaced point monopole sources. This could be achieved in principle by driving one source (the secondary) to minimise the sum of the squared outputs from an array of microphones distributed around the room. Providing a large enough number of microphones were used, the sum of the squared outputs will provide a reasonable approximation to the total potential energy in the room which in turn is proportional to the total radiated sound power output as suggested by equation (3.1). It is first necessary to review some of the important diffuse field properties. Special emphasis is given to those properties which are known to dictate the absolute performance limits on the active control of this limiting class of sound field.

3.1 The diffuse sound field.

Consider a hard walled rectangular room with dimensions π x e x 1m as indicated in figure 3.1. These values provide for an irrational aspect ratio and therefore prevent modal degeneracy.

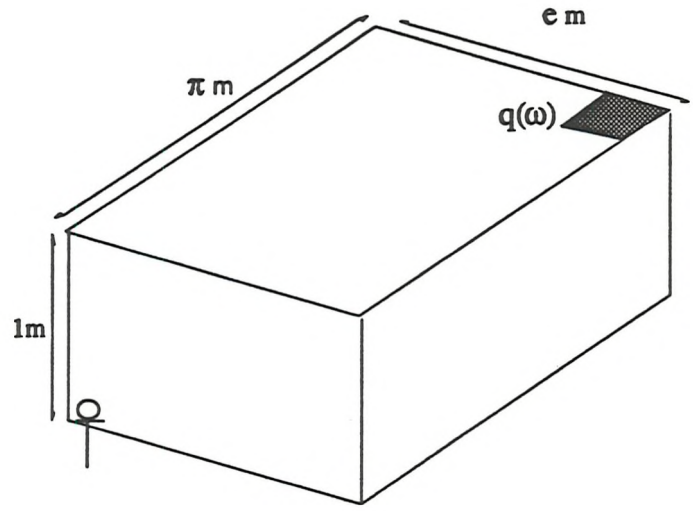

Figure 3.1 A three dimensional, hard walled enclosure which has been assigned an irrational aspect ratio. A rectangular piston type source is located at one corner.

The transfer impedance between a source of sound located in one corner of the room and the pressure response at the opposite diagonal is evaluated according to a superposition of acoustic modes as a function of frequency to give the spectrum shown in figure 3.2.

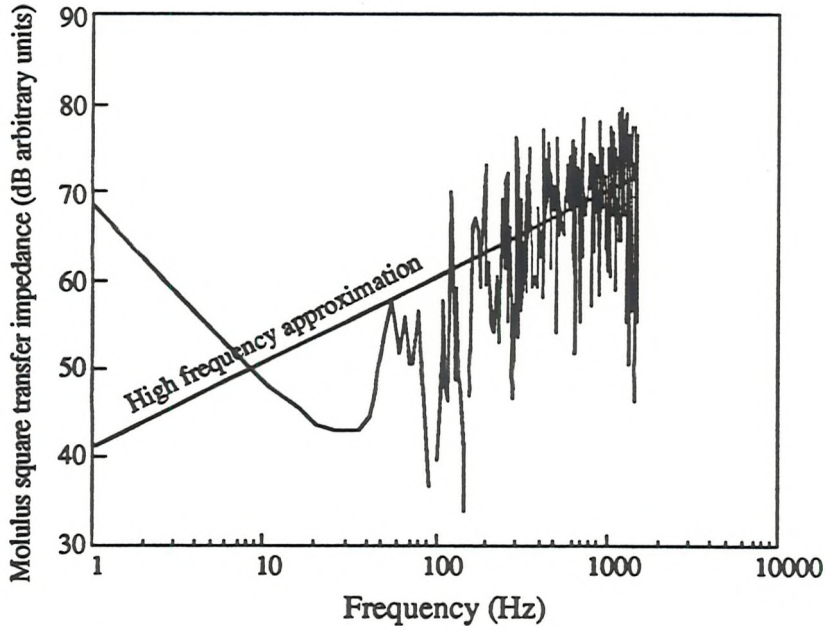

Figure 3.2 A typical Transmission response spectrum in a three dimensional sound field calculated below and above the Schröder frequency. Also shown is the high frequency limit derived in Appendix 3.1 which varies linearly with frequency.

Details of the computer simulation, which involves the superposition of many room modes, are left to chapter 4. Also plotted is the expression for the squared pressure high frequency limit which is derived in Appendix 3.1.

At low frequencies, one can identify individual distinct resonances of the sound field, each resonance being associated with a normal mode of the enclosure. At these frequencies, the sound field is dominated by a only small number of modes whose natural frequencies are close to, and centred around the excitation frequency. By virtue of the simple geometry and the wavelength which is comparatively long at low frequencies, the sound field may be fully characterised by a small number of orthogonal modes of the enclosure. Each mode contributes two degrees of freedom to the wave field by virtue of its complex amplitude. On superposition, the modes excited interfere to produce a simple spatial pattern[51]. The low frequency enclosed sound field may be regarded as being spatially deterministic in the sense that it can be described in terms of a few simple analytic functions (providing of course that the enclosure is of a simple geometry and that the walls are hard). In a reverberant space, a measurement of the acoustic pressure $p(\mathbf{r})$ at a point $\mathbf{r}$ is made up from two contributions. The first is the free space component $p_{FreeSpace}(\mathbf{r})$ which arrives at the measurement point directly from the source, assumed well away from the enclosure walls. The second is the scattered component $p_{Scattered}(\mathbf{r})$ which is radiated to the measurement point *via* wall reflections. One can therefore write

$$p(\mathbf{r}) = p_{FreeSpace}(\mathbf{r}) + p_{Scattered}(\mathbf{r}) \qquad (3.2)$$

As the frequency is raised, the number of modes having a natural frequency below a given frequency increases approximately as the cube of the excitation frequency[37]. The resonances of the sound field now cease to be distinct and adjacent modes begin overlap until individual resonances merge to form the characteristic high frequency spectrum shown in figure 3.2. The amount of overlap from neighbouring modes will depend on the modal bandwidth which is determined by the level of absorption in the room, compared with the density of modes which is governed solely by the enclosure volume. Increasing the acoustic damping therefore assists diffusion since the tails of each modal response curve overlaps with those from neighbouring modes. Excitation frequencies lying between modal resonant frequencies, therefore involve the tails of the responses from both upper and lower neighbouring modes.

While the component of the sound field radiated directly to the measurement point remains highly deterministic in the spatial sense, above some hitherto undefined critical frequency, the scattered sound field becomes highly unpredictable[52]. The reverberant,

scattered field now no longer lends itself to simple description in terms of the normal modes of the enclosure but is more appropriately represented as a random variable. Even though the reverberant, high frequency sound field is governed by well understood, causal deterministic laws, the spatially sampled sound field takes on all the characteristics of a random process which is more appropriately expressed by statistical models. Owing to random interference between simultaneously excited normal modes of the enclosure, point to point measurements of the sound field constitute a pseudo-random ensemble. One can now no longer speak in terms of the results obtained from single observations with certainty, but only in terms of the expected result obtained from a large number of similar experiments.

One can conceive of a sound field where scattering of the incident radiation by the walls of the enclosure is sufficiently uniform, that statistically, the sound field appears to be identical at all points within the bounded space. It is this basic property which forms the notion of the diffuse sound field. One accepted definition is given by Beranek[53]; *'In a diffuse sound field, there is an equal probability of energy flow in all directions'*. An alternative but equivalent definition has also been cited by Balachandran[54], *'A diffuse sound field comprises an infinite number of propagating plane waves with random phase relations arriving from uniformly distributed directions'*. These definitions attempt to define a sound field where there is no preferred location or direction such that all points in the space appear to be acoustically similar. Inherent in these definitions are the ideas of homogeneity and isotropy, the concepts of which form the basis of the last definition[55]; *'The statistical parameters characterising a diffuse sound field are spatially homogeneous and isotropic'*. This last definition represents a more rigourous statement of diffuseness and is the one that will be referred to in later work.

The concept of a diffuse sound field is clearly a convenient idealisation to which real sound fields only approximate. Different reverberant wave fields will inevitably exhibit different 'levels' of diffuseness. For example, a large, irregular room in which there are irregularly shaped scattering objects excited by white noise, will satisfy the criteria for diffuseness to a greater extent than a small, empty, regularly shaped enclosure excited by a low frequency pure tone. Similarly, at the boundary walls of an enclosure, the sound field must, by definition, comply with the boundary condition and so arrive at the walls with some pre-destined complex amplitude. Nevertheless, the diffuse wavefield remains a powerful concept in serving to model what would otherwise be an intangible problem from the point of view of theoretical analysis.

The principle of diffuseness applied to acoustic fields is frequently misunderstood. It is not uncommon for the concepts of diffuseness and the spatial uniformity of pressure to be confused. For example, a US standard test procedure maintains that perfect diffuseness is guaranteed by uniform pressure[56]. In fact, quite the opposite is true. While the acoustic pressure of a plane progressive plane propagating down a lossless, infinite waveguide is spatially uniform, it is far from diffuse since it is made to propagate in a prefered direction. Likewise, in a perfectly diffuse environment, the uniformity of pressure will be strongly dependent on the bandwidth of excitation. Broadband, random noise sources will excite a spatial pressure field that closely approaches spatial uniformity. But for pure tones, the expected deviation from its mean square value in a perfectly diffuse sound field has been shown to be ± 5.5 dB[57] which is roughly consistent with the behaviour of the computer simulation shown in figure 3.2. Far from being uniform therefore, the spatial diffuse wavefield represents a stochastic process which is both stationary and ergodic with respect to position. The stationarity of the diffuse field points to the invariance of the statistics with position while ergodic, refers to the equivalence of the statistics between an ensemble of similar diffuse wavefields and point to point measurements in any one.

Experiments undertaken by Schröder[58] analysing the behaviour of microwaves inside a rectangular microwave cavity, suggest that the onset of 'randomness' of the field variables appears above some critical frequency f_{sch}. This critical frequency, or Schröder frequency as it is now known, is defined as the frequency for which the average 3 dB bandwidth $\omega_{0.5}$ (half power points) of each mode $2\omega_n\zeta$ is equal to three times the average mode spacing. However, the average spacing between neighbouring modes is approximately equal to the reciprocal modal density. For the case when oblique modes are completely dominant, the reciprocal modal density is given by[37] $1/n(\omega) = 2\pi^2 c_0^3/V\omega^2$. Assuming that all modes are similarly damped such that $\zeta_n = \zeta$ we have the relationship

$$f_{sch} = (c_0/2\pi)\,(3\pi^2/\zeta V)^{1/3} \qquad (3.3)$$

where ω_n is the natural frequency of the n^{th} mode and ζ and V are the modal damping and enclosure volume respectively.

The approach adopted in formulating the diffuse field Schröder frequency f_{sch} is necessarily ad-hoc owing to the arbitrariness of the way the diffuse field has been defined. Indeed, Schröder's original diffuse field criterion was determined by the frequency in which the average modal spacing corresponds to one tenth of the 3 dB bandwidth. This was later ammended to one third in 1962[58] which is now the accepted criterion today. In the absence of a more rigourous and universally accepted guide-line, the condition under

equation (3.3) is derived must suffice as the standard by which reverberant sound fields are calibrated for diffuseness. A further reason for this choice of critical frequency is that the defining relation given by equation (3.3) may be conveniently re-written as a simple engineering formula in terms of the reverberation time T_{60}[58]

$$f_{sch} = 2000\sqrt{T_{60}/V} \tag{3.4}$$

where T_{60} and V are in S.I units.

The subject of 'random wave acoustics' was established during the 1950's and 60's mainly through the pioneering work of M. R. Schröder in what is now considered a classic paper published in 1954[59]. However, recognition of the statistical wave nature of high frequency reverberant sound fields may be found in the literature as far back as 1935 in a paper by Wente[60], who presents a discussion of diffuse field frequency irregularity and later in 1939 in a paper by Bolt and Roop[61], in which the distribution of natural frequencies in a three dimensional enclosure are discussed.

Paradoxically, the complexity of the diffuse wavefield serves to aid its analysis. A deterministic description of the diffuse sound field would render the form of the equations unusably complicated by virtue of the intricate structure of the high frequency reverberant field. A probabilistic approach turns out to be much simpler mathematically and has the considerable advantage of generality.

The results presented in the next few sections have been derived previously in terms of the acoustic pressure[59] but they will discussed here in terms of transfer impedance. Qualitative predictions concerning the levels of reduction afforded by active control strategies in the diffuse field require details about the acoustical impedance coupling two points in the sound field and not the absolute pressure at any one. Transfer impedance fields and pressure fields represent two different view points of the same process. They are only equivalent providing that the source has infinite internal impedance such that its volume velocity is independent of the pressure loading on its surface. In practice this assumption will be very nearly true. A description of the sound field in terms of the acoustical transfer impedance is more fundamental than that of pressure since it identifies the causal relationship between the source of excitation at one point, and the pressure response at another. A knowledge of the acoustic pressure simply identifies the response. We now consider some statistical properties fundamental to the diffuse wave field which will be found to be of importance in later work.

3.2. Statistical properties of the diffuse field transfer impedance

Consider a point source of sound with an elementary volume velocity density distribution $s(\omega,r_y) = q(\omega,r_y)\delta(r - r_y)$ located randomly within a reverberant enclosure at some point r_y. The source excites a pressure field $p(\omega,r_x)$. Any two points r_x and r_y in the enclosure are therefore acoustically coupled via a transfer impedance $Z(\omega,r_y|r_x)$ which is defined by

$$Z(\omega,r_x|r_y) = p(\omega,r_x) / q(\omega,r_y) \qquad (3.5)$$

where $q(\omega,r_y)$ is the volume velocity of the point source derived by integrating the volume velocity density $q(\omega,r_y) = \int_S s(\omega,r_y)dy$ over the extent of the infinitesimal source distribution S.

Here we assume that all acoustic parameters have been allowed to settle on their steady state values which usually occurs after time scales of the order of the reverberation time T_{60}. Furthermore, all acoustic variables are assumed to be harmonically modulated in time which may be introduced by the factor $e^{j\omega t}$. For the sake of brevity, the dependence on time will be omitted.

From the point of view of active noise control, a knowledge of the transfer impedance connecting two points in space is of fundamental importance. Large transfer impedances between control elements are desirable because secondary loudspeakers are required to exert a large influence at the points of control while least affecting the regions in the sound field where they are not required to act. Within the diffuse environment, the transfer impedance $Z(\omega,r_x|r_y)$ coupling two points r_y and r_x chosen at random is itself a random variable. We now seek to determine the statistical distribution of complex values $Z(\omega,r_x|r_y)$ for measurement points well away from the influence of directly transmitted sound, $|r_x - r_y| > R_c$ where R_c is the reverberation radius[37], the distance from the source for which the level of directly transmitted acoustic pressure and reverberant pressure are exactly equal. This is the case in many practical examples where the reverberant, scattered radiation completely dominates the direct field as is the case for large vibrating bodies for which the near fields are weak.

A sound wave transmitted between two points in space generally undergoes change in both its amplitude and phase. The transfer impedance coupling two points $Z(\omega,r_x|r_y)$ is therefore complex and may be considered to be the superposition of two *independent* impedance fields which are in quadrature. These are the in-phase reverberant component $\Re\{Z_r\} = \Re\{Z(\omega,r_x|r_y)\}$ (real) and the quadrature reverberant component $\Im\{Z_r\} = \Im\{Z(\omega,r_x|r_y)\}$ (imaginary), i.e., $Z(\omega,r_x|r_y) = \Re\{Z_r\} + j\,\Im\{Z_r\}$. Sound fields which are of

such complexity that they defy simple representation may be described as a superposition of many elementary, scattered waves z_k. Each elementary contribution z_k has an associated modulus $|z_k|$ and phase φ_k which are assumed statistically independent. Moreover, φ_k is assumed to be uniformly distributed between its principal arguments $I(-\pi, \pi)$, providing of course that the two points are well spaced and not too close to the walls (further away than a half a wavelength). Each oblique mode excited in the enclosure, for example, is a source of eight independent, elementary plane waves (four for tangential modes etc). The complex impedance field $Z(\omega,r_x|r_y)$ may therefore be represented by[62]

$$Z(\omega,r_x|r_y) = \frac{1}{\sqrt{N}} \sum_{k=1}^{N} |z_k|\, e^{j\varphi_k} \tag{3.6}$$

The representation of the diffuse field given above is as equally valid whether one interprets the elementary waves z_k as being derived from modal contributions or contributions from a large number of image sources. Equation (3.6) is intended to provide a qualitative description of the impedance field as an aid to obtaining statistical predictions about the diffuse field. It does not allow detailed quantitative statements to be made about any one wavefield, but embodies the statistical characteristics of a whole ensemble of similar wavefields.

If the number of elementary contributions N is large, then the transfer impedance $Z(\omega,r_x|r_y)$ appears as a random function of both r_x and r_y which consequently do not appear explicitly in equation (3.6). Furthermore, if one assumes that the excitation frequency is greater than the Schröder frequency then the diffuse field representation given above is also explicitly independent of frequency.

As the number of terms N approaches infinity, the statistical distribution of both the in-phase and quadrature parts of the impedance field converges on the Normal distribution (or Gaussian distribution) $N(\mu_z,\sigma_z^2)$. A completely general result is therefore obtained whose validity depends solely on the wavefield having the properties of 'diffuseness'. For $N\rightarrow\infty$, the probability density function of the real and imaginary parts of the diffuse field transfer impedance is therefore given by

$$f_Z(\Re\{z_r\}) \rightarrow \frac{1}{\sqrt{2\pi\sigma_{\Re Z}^2}} e^{-(\Re\{z_r\} - \mu_{\Re Z})^2 / 2\sigma_{\Re Z}^2} \tag{3.7}$$

and

$$f_Z(\Im\{z_r\}) \rightarrow \frac{1}{\sqrt{2\pi\sigma_{\Im Z}^2}} e^{-(\Im\{z_r\} - \mu_{\Im Z})^2 / 2\sigma_{\Im Z}^2} \tag{3.8}$$

where $f_Z(\Re\{z_r\})$ and $f_Z(\Im\{z_r\})$ represent probability density functions defined in elementary texts on statistics, see for example Mood and Graybill[63]. The same notation will be adopted here as adopted by Mood *et-al* whereby a subscripted upper case is used to denote the physical variable in question while lower case variables are used to represent the function variable. The terms $\mu_{\Im Z}$ and $\mu_{\Re Z}$ are the means and $\sigma^2_{\Im Z}$ and $\sigma^2_{\Re Z}$ are the variances of their respective probability density functions. This remarkable result follows from the central limit theorem in statistics[63] and applies whenever a single random event is itself the sum of a large number of independent random events, in this case elementary scattered waves.

Equations (3.7) and (3.8) describe how the probability of any one given value of the transfer impedance occuring in the diffuse field diminishes with increasing magnitude. This result is clearly intuitively correct since the likelihood of destructive interference between a large number of randomly phased terms must vastly exceed that of constructive interference. The form of the probability density function given by equations (3.7) and (3.8), is totally independent of the distribution of its constituent waves providing there are sufficient number of them. The Normal distribution is therefore a member of the appropriately named asymptotic distributions. The relevance of the central limit theorem to high frequency, reverberant pressure fields was first realised by Schröder[59].

The probability density function (p.d.f) may be characterised by its various moments. For a Normally distributed ensemble, all moments may be uniquely expressed in terms of its principal moments, the mean μ and variance σ^2. The statistical representation of the impedance field given by equation (3.6) suggests that within a diffuse field environment, the phase relationship between the acoustic pressure at a point to that of its source located further away than a wavelength, is completely random. The expectation of the complex transfer impedance which acoustically couples two well spaced points in the diffuse wavefield is therefore zero. Thus

$$< Z(\omega,r_x|r_y) > = < \Re\{Z_r\} > + j < \Im\{Z_r\} > = 0 \quad \text{for } |r_x - r_y| > R_c \qquad (3.9)$$

where $< >$ is used to denote expectation with respect to position. The mean values of the distribution in equations (3.7) and (3.8) are therefore likewise zero

$$\mu_{\Re Z} = < \Re\{Z_r\} > = 0 \qquad (3.10)$$

$$\mu_{\Im Z} = < \Im\{Z_r\} > = 0 \qquad (3.11)$$

Waves emanating from the source at a single frequency are subsequently scattered by the enclosure walls and therefore arrive at some distant point in the room with a change of phase which is completely uncorrelated with the phase of its source, see for example Ebeling[62]. This fact points to the statistical independence of the in-phase part of the transfer impedance from the quadrature part, providing the two points are well separated. The real and imaginary parts, $\Re\{Z_r\}$ and $\Im\{Z_r\}$ are therefore orthogonal which implies zero Covariance between the zero mean random variables. That is

$$<\Re\{Z_r\}\Im\{Z_r\}> = 0 \tag{3.12}$$

It is fundamentally important to recognise that $\Re\{Z_r\}$ and $\Im\{Z_r\}$ are only orthogonal as random variables. The physical processes by which they arise are not. This is because the physical system which enables the volume velocity at one point in space to give rise to acoustic pressure at another point constitutes a linear and causal process. The real and imaginary parts of the transfer impedance $Z(\omega,r_x|r_y)$ are therefore functionally related by the Hilbert Transform[64].

For points of observation well away from the source, it is implicit in the concept of the diffuse field that $\Re\{Z_r\}$and $\Im\{Z_r\}$ must be governed by identical statistical laws. It therefore follows that they must also exhibit identical levels of dispersion about their zero mean values so that

$$\sigma^2_{\Im Z} = \sigma^2_{\Re Z} = \sigma^2_Z \tag{3.13}$$

This property can be infered because the distribution of phase differences between two well separated points is uniform between the principal arguments. The joint probability density function $f_Z(\Re\{z_r\},\Im\{z_r\})$ for independent random variables is simply the product of their respective probability density functions $f_Z(\Re\{z_r\})$ and $f_Z(\Im\{z_r\})$ according to equations (3.7) and (3.8) thus

$$f_Z(\Re\{z_r\},\Im\{z_r\}) = f_Z(\Re\{z_r\})f_Z(\Im\{z_r\}) = \frac{1}{2\pi\sigma^2_Z}\, e^{-(\Re^2\{z_r\} + \Im^2\{z_r\})/2\sigma^2_Z} \tag{3.14}$$

A three dimensional representation of this equation is shown in figure 3.3 indicating that part of the diffuse field transfer impedance field which is in-phase of the source and that part of the diffuse field impedance field which is in quadrature with the source plotted on orthogonal axis

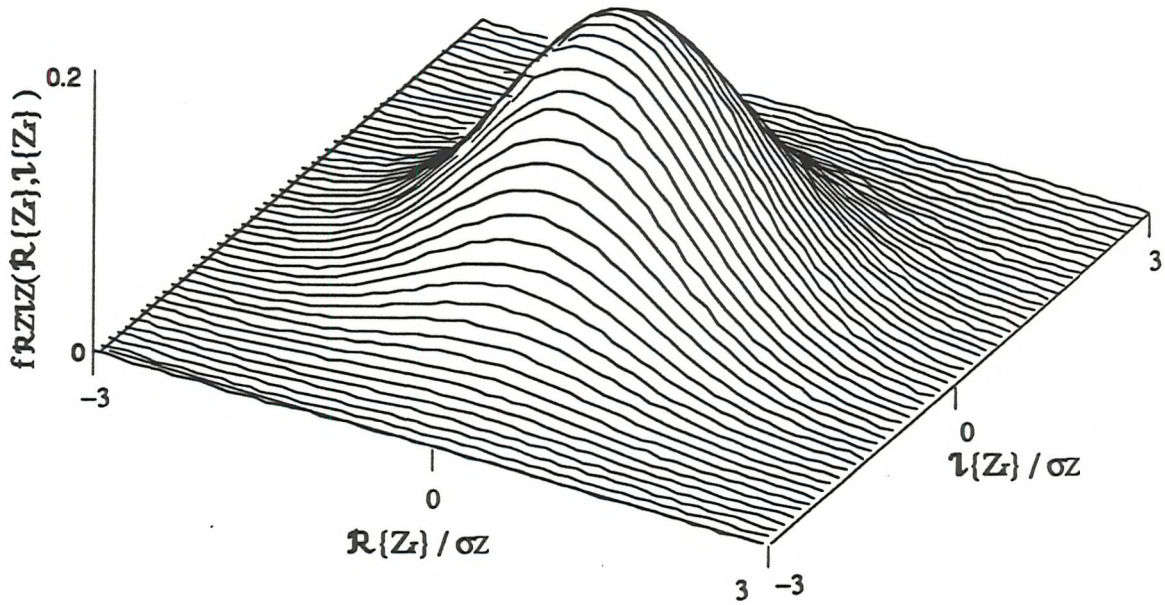

Figure 3.3 A three dimensional representation of the Joint Probability density function between the in-phase and quadrature parts of the transfer impedance between two well spaced points in the pure tone diffuse sound field.

While the form of the probability density function given by equation (3.14) is valid for all values of the transfer impedance and is therefore unbounded, more than 99.9 % of the complex transfer impedances that can possibly arise are contained within about three standard deviations from the mean value namely $\Re\{Z_r\}, \Im\{Z_r\} = \pm 3\sigma_z$. Not only is the mean of the probability density function zero according to equation (3.10) and (3.11), but also the most frequently occurring value (or modal value) which is identified from the peak of the joint probability density function. In accordance with equation (3.14) therefore, all measures of central tendency such as the mean, mode and median etc, are located on zero. This has important implications from the point of view of applying active noise control in diffuse fields. A control system attempting to engineer reductions in the sound pressure level could conceivably be unable to supply the necessary volume velocity in order to drive the point pressure to zero owing to poor coupling between the secondary source and the chosen point of cancellation. Moreover, in some instances, the secondary source strength required to perform the point pressure cancellation may be arbitrarily large which could have unfortunate consequences on the rest of the sound field.

The variance of both the in-phase and quadrature parts of the transfer impedance σ_Z^2 may be obtained from the defining equation

$$\sigma_Z^2 = <\Re^2\{Z_r\}> - <\Re\{Z_r\}>^2 = <\Im^2\{Z_r\}> - <\Im\{Z_r\}>^2 \qquad (3.15)$$

However, since $\Re\{Z_r\}$ and $\Im\{Z_r\}$ are zero mean processes, it follows that the variance must reduce to the expectation of the square of the value according to

$$\sigma_z^2 = <\Re^2\{Z_r\}> = <\Im^2\{Z_r\}> \tag{3.16}$$

The variance of both the real and the imaginary parts of the transfer impedance field are therefore identically equal to the expectation of their squared values. The space average modulus squared diffuse field impedance $<|Z_r(r)|^2>$ is given by $<|p(\omega,r)|^2>/|q(\omega)|^2$ where $|p(\omega,r)|^2$ refers to peak pressure amplitude squared. An expression for the space average high frequency square pressure $<|p(\omega,r)|^2>$ may be obtained if one replaces the infinite summation of acoustic modes by the appropriate integral taken over all possible modal natural frequencies. This is the basis of Schröder's principle[37]. The result of this modal integral is central to the analysis presented in this chapter and an outline derivation based on the analysis presented by Morse[65] is given in Appendix 3.1. The modal integral has been evaluated in order to obtain an expression for the space averaged squared pressure $<|p(\omega,r)|^2>$ which from Appendix 3.1 is given by

$$<|p(\omega,r)|^2> = |q(\omega)|^2 \frac{\rho^2\omega^2 c}{8\pi V k_0} \tag{3.17}$$

where V is the room volume and k_0 is the damping constant which is related to the total room absorption A ($= S\bar{\alpha}$) by the relationship[65]

$$k_0 = \frac{Ac}{8V} \tag{3.18}$$

In reality however, the total room absorption A (in m^2) is frequency dependent and one must refer to experimental data from representative absorbing materials in order to establish the empirical relationship describing the variation of A with frequency. Some experimental findings relating to the random incidence acoustic absorption coefficient $\bar{\alpha}$ versus logarithmic frequency for various acoustic materials are presented by Beranek[53]. Typical representative examples have been taken from this data and re-plotted on a linear frequency scale in figure 3.4 overleaf.

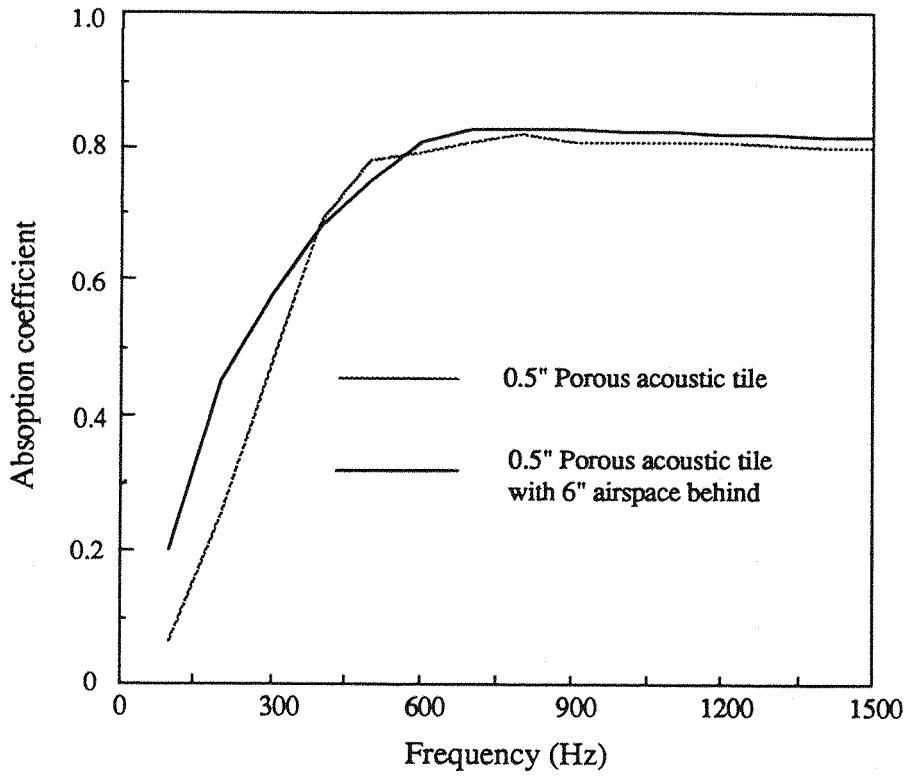

Figure 3.4. Experimental data taken from Beranek[53] indicating the variation of random incidence absorption coefficient with frequency for two samples of acoustic lining re-plotted on a linear frequency scale

The absorption coefficient plotted above appears to increase linearly with frequency up to about 600 Hz, above which the dissipative mechanism appears to change. Below this frequency however, which represents quite a large working bandwidth, one can reasonably propose an empirical dissipation law by which the total area of absorption increases linearly with frequency. This leads directly to the definition of a modal damping term ζ according to[45]

$$k_0 = \zeta\omega \tag{3.19}$$

. This is precisely the dissipation law arrived at by Sepmeyer[66]. The space averaged squared pressure may now be written as a linear function of frequency according to

$$< | p(\omega,\mathbf{r}) |^2 > = |q(\omega)|^2 \frac{\rho^2 \omega c_0}{8\pi\zeta V} \tag{3.20}$$

Assuming that the space average squared pressure is equi-partitioned between its in-phase and quadrature parts, one can therefore write

$$<\Re^2\{Z_r\}> = <\Im^2\{Z_r\}> = \frac{\rho^2\omega c_0}{16\pi\zeta V} \qquad (3.21)$$

As one may have anticipated, point to point measurements of the transfer impedance $Z(\omega,r_x|r_y)$ exhibit large variations in small enclosure volumes driven at low frequencies where the wavefield still exhibits modal behaviour. The comparatively large scatter of transfer impedance values arises from interference between single modes. Conversely, as the enclosure volume approaches infinity, the variance σ_Z^2 tends to zero whereby the wavefield becomes spatially uniform as the acoustics of the enclosure approach free field conditions. In this limiting case, each image source is located at infinity and mutually uncorrelated. Many authors regard this hypothetical limit to be the only perfect idealisation of diffuseness, see for example Bodlund[67].

Strictly speaking, the normal distribution is only an exact representation of the distribution of transfer impedance values as long as the number of random, independent constituent components tends to infinity. In practice, a good approximation to this asymptotic distribution is achieved from the summation of very few terms. In particular, a statistical distribution of transfer impedances very closely approaching that of equation (3.14) was obtained from a large random sample of transfer impedances calculated from a computer simulated, one dimensional sound field in a finite hard walled duct. The sound field was contrived to support only the first ten modes in ascending natural frequency, each excited to comparable amplitude. The Gaussian distribution of the in-phase and quadrature parts of the impedance field may therefore be regarded as a *weak* function of the wavefield and is therefore a poor indicator of diffuseness. Alternatively this property may be interpreted as a good descriptor of weakly diffuse fields.

3.3. The diffuse wavefield cross correlation function

While the spatially sampled diffuse wavefield exhibits all the characteristics of a random process, it is not without a significant degree of spatial structure. Specifically, the pressure at closely spaced neighbouring points in the diffuse wavefield may be shown to be highly correlated. The spatial cross correlation function $\rho(r_1, r_2,\omega)$ is the parameter which determines the degree of inter-dependence between adjacent points in the wavefield. Furthermore, this function offers insight into the coarse, large scale structure of the wave field upon which, the intricate, random spatial patterns occur arising from random interference between highly coherent waves (at a single frequency). The complex, spatial cross correlation function is defined by

$$\rho(r_1, r_2, \omega) = \frac{< Z(\omega, r_q|r_1) Z^*(\omega, r_q|r_2) >}{< |Z(\omega, r_q|r_1)|^2 >^{1/2} < |Z(\omega, r_q|r_2)|^2 >^{1/2}} \qquad (3.22)$$

Note that all transfer impedances are refered to a common source of sound at r_q.

The information contained in $\rho(r_1, r_2, \omega)$ emerges as one of the key parameters for determining the absolute performance limits on the active control of sound fields. A knowledge of the correlation function enables one to identify a correlation length, a characteristic distance which determines the extent over which the wave field is well correlated. The properties described by this function will be shown to be sufficiently fundamental to the mechanisms of diffuse field active control to warrant a brief discussion of some of its properties. The derivation summarised here is due to Cook *et-al*[68] although identical results have been derived from a modal viewpoint[52,69].

Consider a single frequency plane wave passing between two points r_1 and r_2 at an angle θ according to figure 3.5

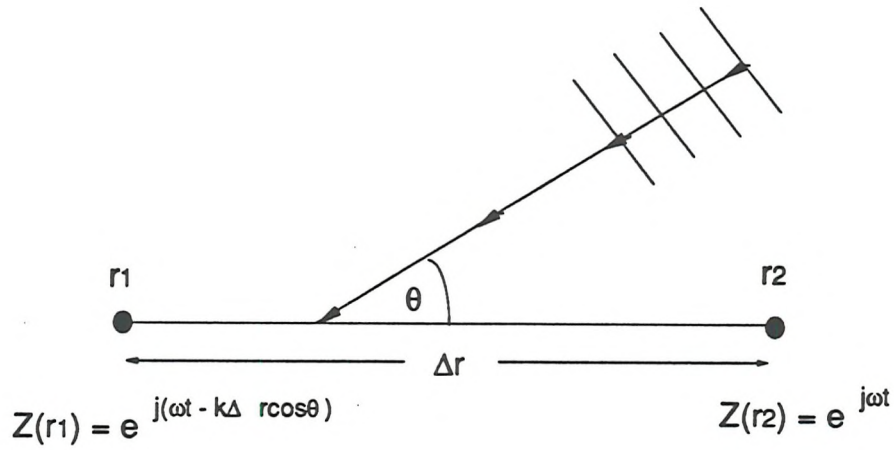

Figure 3.5 A single frequency plane wave passing between two points at an angle θ.

From equation (3.22), two points r_1 and r_2 are linearly correlated according to $\rho(r_1, r_2, \omega) = \exp\text{-}j(k\Delta r\cos\theta)$ where $\Delta r = | r_1 - r_2 |$. However, far from being a single plane wave arriving at any one single angle, the notional diffuse field comprises an infinite number of plane waves arriving from all elemental solid angles with equal probability. The diffuse field correlation function may be considered to represent the average value over waves arriving from all possible solid angles over 4π steradians. Taking a spherical co-ordinate system and averaging over all angles equally yields the result

$$\rho(r_1, r_2,\omega) = \frac{1}{4\pi} \int_0^{\pi} \int_0^{2\pi} [\cos(k\Delta r\cos\theta) - j\sin(k\Delta r\cos\theta)]\sin\theta d\theta d\phi = \frac{\sin k\Delta r}{k\Delta r} \quad (3.23)$$

The imaginary part is equal to zero since - cosθ (the anti-derivative of sinθ) is an even function. The real part is readily evaluated by using the simple change of variable x=cosθ.

This argument may be extended to deal with both two and one dimensional diffuse sound fields. In a two dimensional wavefield, the elementary waves have equal probability of arriving from any elemental angle located in a plane. Taking the average over all angles of incidence between 0 - 2π in the plane yields the result

$$\rho(r_1, r_2,\omega) = \frac{1}{2\pi} \int_0^{2\pi} [\cos(k\Delta r\cos\theta) - j\sin(k\Delta r\cos\theta)]\, d\theta = J_0(k\Delta r) \quad (3.24)$$

where $J_0(k\Delta r)$ is the zeroth order Bessel function which is a real function since the imaginary part integrates to zero. Similarly in one dimension the spatial cross correlation function may be written as

$$\rho(r_1, r_2,\omega) = \cos(k\Delta r) \quad (3.25)$$

The spatial correlation functions derived here are second order statistical properties of the diffuse field and depend only on the separation vector Δr between the points and not on their absolute locations i.e., $\rho(r_1, r_2,\omega) = \rho(\Delta r,\omega)$. This important result follows from the stationarity (homogeneity) of the diffuse field. More specifically, the correlation functions depend solely on the magnitude of the separation vector Δr which is a consequence of the isotropy of the diffuse field. Unlike the theoretical probability distribution function of complex impedance values in the diffuse field which is equally valid for narrow and broadband sources of excitation, the spatial correlation function is bandwidth sensitive. As Morrow explains[70], the correlation functions given by equations (3.23) - (3.25), may be inaccurate at a single frequency owing to the limited number of modes which can be excited. The problem is compounded if the modes are lightly damped. As the bandwidth is increased to admit more modes, the average correlation approaches the theoretical result where k now represents the mean of the upper and lower wavenumbers k_u and k_l respectively, $k = (k_l + k_u)/2$. A bandwidth sensitive discrepancy only appears for large bandwidths.

Figure 3.6 shows a comparison of the theoretical one, two and three dimensional diffuse field spatial correlation functions given by equations (3.23) - (3.25)

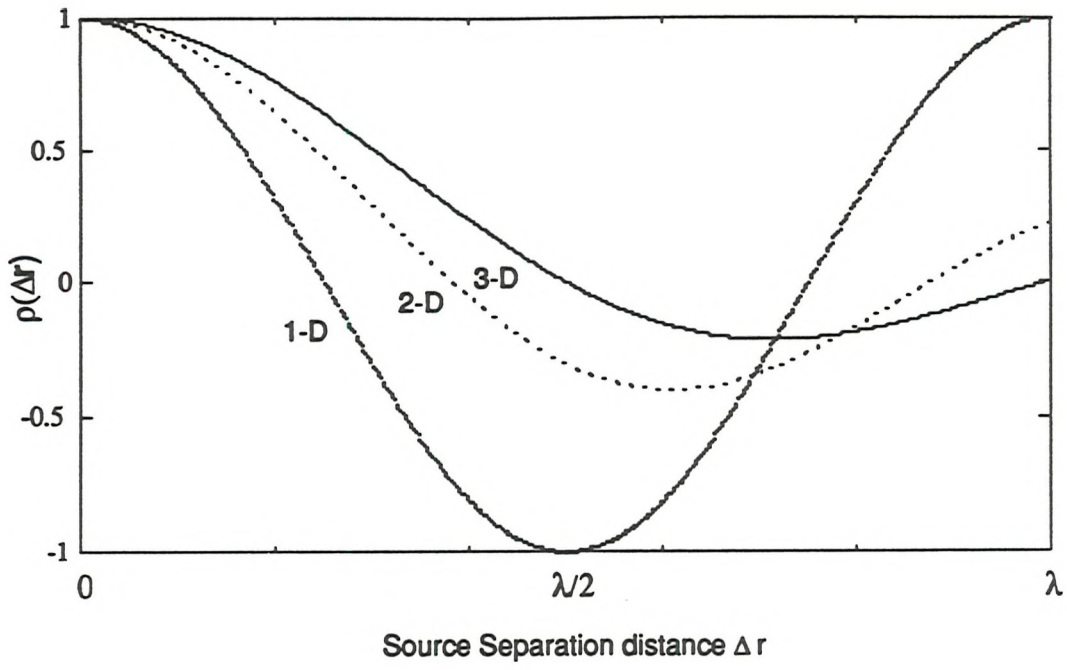

Figure 3.6 The theoretical one, two and three dimensional diffuse field spatial correlation functions versus separation distance.

The rate at which the correlation function decays with increasing separation distance provides some insight into the wave structure of the field. While a three dimensional diffuse field is 'held' together more tightly at close distances, points separated by more than say half a wavelength, possess less linear inter-dependence than either of the simpler fields. However, points which are located within one fifth of a wavelength of each other possess 80% mutual correlation. This property will be shown to be significant when we come to consider the zone of silence formed by the active cancellation of the pressure at a single point in the diffuse field. The spatial correlation function for various three dimensional anisotropic sound fields have been derived by Baxter[71] for which the form of the correlation functions indicate only small departure from the isotropic result given by equation (3.23). The differences are even less pronounced for small Δr, consequently the spatial correlation function may also be regarded as a poor indicator of diffuseness or again, a good descriptor of weakly diffuse fields.

In the next section, we consider the possibilities for obtaining global suppression of the sound field in a diffuse field environment for the rather special case where the primary source is compact and of monopole order. This problem was chosen because of the elementary nature of the primary source. A single discrete secondary loudspeaker is able to mimic the point monopole primary source by getting sufficiently 'close' such that the respective sound fields become highly correlated but in anti-phase and therefore tend to

interfere destructively. Ideally, the ultimate aim of any control strategy would be the complete global extinction of the primary sound field over the entire space. Even in free field where the evolution of the sound field in space is predictable in principle, this is extremely difficult to arrange for the reasons discussed in chapter 1. In the presence of reflecting boundaries, the problems are made substantially worse by complicated interference patterns arising from waves radiated by an infinite number of 'image' sources.

For this model problem outlined above, a realistic control strategy from the point of view of achieving good levels of global pressure reduction is to drive the secondary source in order to reduce the space averaged square pressure over the entire enclosure. Owing to the proportionality between the space averaged diffuse field square pressure and the sound power output of the source given by equation (3.1), a reduction in the average square pressure also implies a corresponding reduction in the potential energy density as sustained by sound power injected into the medium by the primary source, see again equation (3.1). In order to satisfy this requirement therefore, the secondary source must act at the primary source point thereby inhibiting its outflow of energy. Conceivably, a closely located secondary source could be driven with the same amplitude but in anti-phase of the primary source. This source geometry would form a single dipole arrangement whose radiation output is notoriously inefficient compared with a monopole source of the same source strength. However, as Nelson has demonstrated from a free field analysis[40], while this arrangement does afford some reductions in sound power output, it is not optimal and becomes progressively less optimal as the separation distance between the primary and secondary source increases. Indeed, for separation distances greater than about one wavelength, the primary and secondary source pressure fields are ill-matched thereby causing a doubling in the original squared pressure. We now consider the statistics of the optimal secondary source strength for minimising the sum of sound power outputs from itself and a closely spaced point monopole primary source which are both situated in a pure tone diffuse sound field.

3.4. The minimum sound power output from two closely spaced point monopole sources

Consider two closely spaced point monopole sources q_p and q_s located in a diffuse field environment at $\mathbf{r}_p$ and $\mathbf{r}_s$ whose volume velocity densities are respectively $q_p(\omega)\delta(\mathbf{r} - \mathbf{r}_p)$ and $q_s(\omega)\delta(\mathbf{r} - \mathbf{r}_s)$. This source configuration is shown schematically in figure 3.7 situated within an arbitrarily shaped control volume completely enclosing the source pair

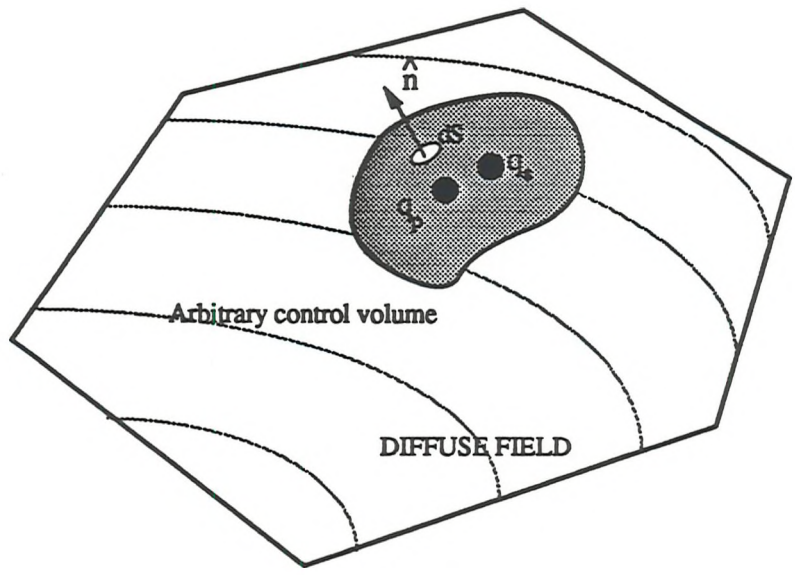

Figure 3.7. Two closely spaced monopole sources situated within a diffuse field environment completely surrounded by some arbitrary control volume.

We will now derive the minimum total sound power radiated from the closely spaced primary source and secondary source. As indicated in figure 3.7, this is equivalent to minimising the total sound power W radiated out of the control volume which may be calculated by integrating the acoustic intensity vector I(r) normal to the arbitrary surface of the control volume thus.

$$W = \int_S \mathbf{I}(\mathbf{r}).\hat{n}\, dS \tag{3.26}$$

where $\hat{n}$ is an outward unit vector normal to the surface of the control volume. This convention is adopted so that negative sound power refers to acoustic energy flowing into the source which is of course the condition for sound power absorption. The absorption of acoustic energy is clearly a possibility in a reverberant space as highlighted by the work in chapter 2. Equivalently, Levine[72] has shown that for elementary point sources, the sound power output may be constructed from the real part of the product of the source volume velocity and the pressure at the source point. This is because only the component of the acoustic pressure which is in-phase of the volume velocity makes any contribution to the time averaged sound power output. The orthogonal in-quadrature component, when multiplied by the source strength and averaged over a long time interval therefore converges to zero. Even though the acoustic pressure at the source point is infinite, only the resistive part of the pressure, which remains finite, transfers any energy to the medium since no energy is transported by the reactive part of the pressure.

The total acoustic pressure $p(\mathbf{r},\omega)$ at some point $\mathbf{r}$ in the field is given by the linear superposition of their respective sound fields according to

$$p(r,\omega) = q_p(\omega)Z_p(\omega,r_p|r) + q_s(\omega)Z_s(\omega,r_s|r) \tag{3.27}$$

From hereon, the dependence on ω will be omitted since above the Schröder frequency, acoustic variables have no explicit systematic frequency dependence. The monopole source of sound may be physically visualised as a sphere pulsating about some mean position with a small displacement amplitude whose time averaged volume input into the sound field is therefore zero. The point monopole source is a limiting case of the finite monopole source whose radius has collapsed to zero but whose source strength has nevertheless remained finite. The pressure at the 'surface' of this idealised point source is therefore infinite. In a reverberant space at frequencies above the Schröder frequency, the transfer impedances $Z_p(r_p|r)$ and $Z_s(r_s|r)$ may be resolved into their direct, free field components and random, reverberant components according to[73]

$$Z(r_p|r) = Z_d(r_p|r) + Z_r(r_p|r) \tag{3.28}$$

$$Z(r_s|r) = Z_d(r_s|r) + Z_r(r_s|r) \tag{3.29}$$

where the subscripts 'd' and 'r' are used to denote the direct, and reverberant components respectively.

The acoustic pressure in an unbounded medium $p_d(r_0,r)$, radiated directly by a point monopole source situated at a point r_0 of strength $q(\omega)$ to a point r is given by

$$p_d(r_0,r) = q(\omega)\, Z_d(r_0|r) \tag{3.30}$$

where

$$Z_d(r_0|r) = Z_0\, j\frac{e^{-jk\Delta r}}{k\Delta r} = Z_0\left[\frac{\sin k\Delta r}{k\Delta r} + j\frac{\cos k\Delta r}{k\Delta r}\right] \tag{3.31}$$

and where $\Delta r = |r_0 - r|$ and Z_0 is the monopole point resistance for harmonically varying sources given by[40]

$$Z_0 = \frac{\omega^2\rho}{4\pi c_0} \tag{3.32}$$

Following the work of Levine[72] for elementary point monopole sources, the sum of primary source and secondary source sound power outputs yields

$$W = \frac{1}{2}\,\Re\{p(r_s)\, q_s^* + p(r_p)\, q_p^*\} \tag{3.33}$$

The total acoustic pressure p(r) has contributions from both the primary source and the secondary source according to equation (3.27). In an identical manner to the procedure followed in chapter 2, substituting equation (3.27) for p(r) yields the total sound power output W as a quadratic function of the complex secondary source strength q_s which may be represented in the now standard form

$$W = q_s^* A q_s + b q_s^* + b^* q_s + c \tag{2.8}$$

where $A = \frac{1}{2}\Re\{Z(r_s|r_s)\}$, $b = \frac{1}{2} q_p \Re\{Z(r_p|r_s)\}$ and $c = \frac{1}{2}|q_p|^2 \Re\{Z(r_p|r_p)\}$ (3.34)

The terms $\Re\{Z(r_s|r_s)\}$ and $\Re\{Z(r_p|r_p)\}$ are the radiation resistances of the secondary source and primary source respectively. Recalling that the unique global minimum for this equation q_{so} is given by

$$q_s = q_{so} = -A^{-1}b \tag{2.11}$$

which enables the optimal secondary source strength to be written as

$$q_{so} = -\frac{\Re\{Z(r_p|r_s)\}}{\Re\{Z(r_s|r_s)\}} q_p \tag{3.35}$$

$$= -\frac{Z_0 \text{sinc}k\Delta r + \Re\{Z_r(r_p|r_s)\}}{Z_0 + \Re\{Z_r(r_s|r_s)\}} q_p \tag{3.36}$$

where $\text{sinc}k\Delta r = \text{sin}k\Delta r/k\Delta r$ and Δr is the source separation distance $|r_p - r_s|$.

The secondary source strength q_{so} which minimises the total sound power output radiated by the source pair will be susceptible to statistical fluctuations from point to point in the enclosure according to equation (3.36). The origin of this random variation arises from the presence of the terms $\Re\{Z_r(r_p|r_s)\}$ and $\Re\{Z_r(r_s|r_s)\}$ which as discussed earlier in this chapter, are mutually correlated normally distributed random variables. Scrutiny of equation (3.36) reveals that the optimal secondary source strength q_{so} has the potential to become singular. This would occur in the (unlikely but physically possibly) event that the secondary source sound power output radiated via wall reflections, which is proportional to $\Re\{Z_r(r_s|r_s)\}$, is exactly equal and opposite to the sound power directly radiated into the enclosure which is proportional to Z_0. This condition describes the simultaneous radiation and absorption of sound power by exactly the same amount from which the net sound power output of the secondary source is zero. Although this outcome is very rare, but possible in principle, it is highly likely that this event is sufficiently common in relative

terms to force the ill-conditioning of the statistics of the secondary source strength and related acoustic variables. In this event expectations such as $< q_{so} >$, for example, are equal to infinity. This has yet to be proved formally, but a full discussion indicating the conditions under which this is true is given in Appendix 3.2. However, in many respects this difficulty is of academic importance only and arises because of the very small probability of obtaining very large but negative values of the diffuse field source radiation resistance $\Re\{Z_T(r_S|r_S)\}$.

In the light of this difficulty we take a pragmatic approach and seek to obtain an estimate for the expectation of the optimal secondary source strength $< \hat{q}_{so} >$ for those source positions within the enclosure where $|\Re\{Z_T(r_S|r_S)\}| < Z_0$ for which the secondary source strength statistics are known to be 'well behaved'. The expectation is now taken over a modified, reduced ensemble of values in which 'rare' events arbitrarily defined by $|\Re\{Z_T(r_S|r_S)\}| \geq Z_0$ have been excluded. It is important to recognise that the probability density function of diffuse field radiation resistance $\Re\{Z_T(r_S|r_S)\}$ must posses positive skewness (third moment) owing to the fundamental condition[74]

$$- Z_0 \leq \Re\{Z_T(r_S|r_S)\} \leq \infty \tag{3.37}$$

which follows directly from the conservation of energy. However, for the range of diffuse field resistance values defined by $|\Re\{Z_T(r_S|r_S)\}| < Z_0$, it is believed that for all practical purposes $\Re\{Z_T(r_S|r_S)\}$ may still be closely represented as a zero mean Gaussian random variable.

Following standard techniques for dealing with the quotient of random variables[63], the optimal secondary source strength q_{so} may be rationalised by power series expansion which is *only* valid within the radius of convergence defined by $|\Re\{Z_T(r_S|r_S)\}| < Z_0$. All estimates of random quantities derived here therefore refer to the expectations of a finite sample size which from hereon will be symbolised by a 'hat', ^. To second order in $\Re\{Z_T(r_X|r_Y)\}/Z_0$, which will be denoted by γ, the optimal secondary source strength may be approximated by

$$q_{so} \approx q_p \left[-\text{sinc}k\Delta r + \frac{\text{sinc}k\Delta r\, \Re\{Z_T(r_S|r_S)\} - \Re\{Z_T(r_p|r_S)\}}{Z_0} \right.$$

$$\left. + \frac{\Re\{Z_T(r_p|r_S)\}\Re\{Z_T(r_S|r_S)\} - \text{sinc}k\Delta r\, \Re^2\{Z_T(r_S|r_S)\}}{Z_0^2} + \cdots \right]$$

$$\text{for } |\gamma| < 1 \tag{3.38}$$

The first term in the series expansion $-q_p \operatorname{sinc} k\Delta r$, is precisely the optimally adjusted secondary source strength for minimising the sound power output from the source pair in the free field[40]. One can therefore infer that this term only acts on the component of the primary field which is radiated to the secondary source directly. The remaining terms (which of obviously did not arise in the corresponding free field case) must therefore be responsible for suppressing the reverberant, scattered part of the primary sound power output. The infinite series expansion of the terms clearly indicates the recursive nature of the transfer function relating the optimal secondary source strength to the primary source. In evaluating the expectation $<\hat{q}_{so}>$, we note that for transfer impedance fields which are perfectly distributed zero mean Guassian random variables, one can write

$$<\Re\{Z_r(r_x|r_y)\}> = <\Re\{Z_r(r_x|r_x)\}> = 0 \qquad (3.39)$$

Now invoking the principle of reciprocity, the fundamental theorem which describes the invariance of the transfer impedance to interchange of measurement point and source point[37] one obtains the important result

$$\Re\{Z_r(r_x|r_y)\} = \Re\{Z_r(r_y|r_x)\} \qquad (3.40)$$

Also noting that for a fully diffuse three dimensional sound field, the in-phase components of the complex transfer impedance are spatially correlated according to[68] $\operatorname{sinc} k\Delta r$, namely

$$<\Re\{Z_r(r_s|r_s)\}\Re\{Z_r(r_s|r_p)\}> = <\Re^2\{Z_r(r)\}> \operatorname{sinc} k\Delta r \qquad (3.41)$$

where $<\Re^2\{Z_r(r)\}>$ denotes the space average squared, in-phase component of diffuse field radiation impedance. In order to extract the mean of the sum of terms given in equation (3.38), we note an important result in statistics. *The mean of a sum of random variables is simply the sum of their respective means.* This result is equally valid for correlated and uncorrelated random variables. Incorporating the results of equations (3.39) - (3.41) yields the following simple result

$$<\hat{q}_{so}> \approx -q_p \operatorname{sinc} k\Delta r \qquad \text{for } f \geq f_{sch} \text{ and } |\gamma| > 1 \quad (3.42)$$

Figure 3.8 shows a plot of the theoretical expectation given by equation (3.42) normalised with respect to q_p, as a function of the source separation Δr.

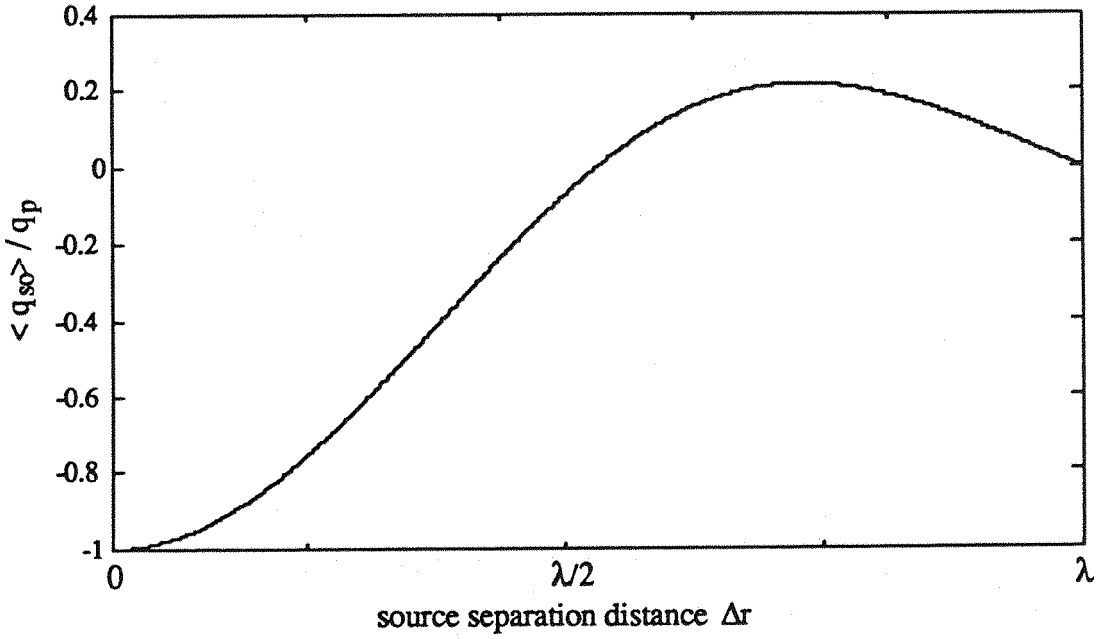

Figure 3.8 The expectation of the normalised secondary source strength for minimising the total sound power output of a closely spaced source pair in a diffuse sound field versus source separation distance.

As a consequence of taking the average value over all source positions, the components of the secondary source strength responsible for acting on the diffuse field part of the acoustic pressure converges to zero. This is because sound arriving at the secondary source via wall reflections undergoes a completely random phase change in relation to its original phase on leaving its source. The secondary source must respond by being exactly in-phase or out of phase with the primary source strength since only the resistive part of the transfer impedance has any bearing on the sound power transported into the medium. The averaging process will therefore cause this random component to vanish while the constant free field component of the solution remains.

An identical result has been derived by Nelson *et-al*[13] for minimising the total potential energy in the diffuse sound field. Indeed, this agreement should not be surprising owing to the proportionality which exists between sound power output and the corresponding potential energy in the diffuse field as given by equation (3.1). Nelson's result was formulated according to modal standpoint whereby the total potential energy was derived at by integrating over all modes to infinity. This formulation consequently produces the result appropriate to the limiting case of an infinite frequency. It is therefore hardly surprising to observe that the space average value converges on its equivalent free field result in the absence of reverberation.

This finding can be explained because in the limit as the frequency tends to infinity, the wavelength becomes vanishingly small compared to a typical dimension of the enclosure. In this limit, the wavefield therefore appears increasingly like a free field environment whereby the enclosure walls are effectively located at infinity.

3.5. The variance of the optimal secondary source strength

At finite frequencies the optimal secondary source strength given by equation (3.42) represents only an expected result which will be subject to a degree of statistical excursion centred about its mean. The principal descriptor of statistical departure is the variance $\hat{\sigma}^2_{q_{so}}$ defined by

$$\hat{\sigma}^2_{q_{so}} = < (q_{so} - < \hat{q}_{so} >)^2 > \qquad (3.43)$$

where again, the expectation only exists if one excludes the 'rare' events arbitrarily defined by $|\gamma| > 1$. Substituting equations (3.38) and (3.42) for q_{so} and $< \hat{q}_{so} >$ respectively, expanding and summing the expectations yields the result

$$\hat{\sigma}^2_{q_{so}} = \frac{< \Re^2\{Z_r\} >}{Z_0^2} [\, 1 - \mathrm{sinc}^2 k\Delta r \,] + \varepsilon_1$$

$$\text{for } |\gamma| < 1 \text{ and } f \geq f_{sch} \qquad (3.44)$$

All odd moments of the series expansion, i.e., the moments which characterise the asymmetry of the probability distribution about the mean (skewness) have been set equal to zero. Equation (3.44) represents only an approximate formula owing to the non-linearity of the exact expression for q_{so} given by equation (3.36). The second term ε_1 in equation (3.44) denotes the residual term, i.e., the term of next highest order which is non-vanishing neglected in the series expansion which can be shown to be of the order $O(\gamma^{-4})$.

Recalling that $< \Re^2\{Z_r\} >$ is proportional to ω and that Z_0 is proportional to ω^2, the residual term ε_1 appearing in equation (3.44) therefore has a frequency dependence which is of the order $O(\omega^{-6})$. At high frequencies this term makes only an insignificant contribution to the series summation compared with the leading term which is ω^{-3} dependent. Terms ε_1 and higher can therefore be omitted without incurring significant error at high frequencies. To a good level of accuracy, it would appear that the variance of the optimal secondary source strength for a given source separation distance is proportional to $< \Re^2\{Z_r\} > / Z_0^2$. This term represents one half the ratio of the space average diffuse field square pressure to the square of the in-phase, deterministic free field square pressure at the source point. At any given source separation distance Δr, the degree of variability exhibited by q_{so} from

point to point in the diffuse wavefield will therefore depend upon the level of acoustic 'signal to noise ratio' at the secondary source point.

In this context, 'signal' refers to the directly radiated contribution to the radiation resistance field Z_0 which is of course independent of the secondary source position. By contrast, the so called 'noise' term $\Re\{Z_r\}$ refers to the contribution to the radiation resistance which occurs via reverberant paths and is therefore a purely random function of the secondary source position. From equation (3.44), one can immediately verify that it is the relative magnitude of these respective contributions to the total pressure which dictates the absolute level of secondary source strength variance. This important ratio of terms $<\Re^2\{Z_r\}> / Z_0^2$ may be shown to have even more wide ranging significance which will now be discussed.

At any given point in an enclosure, the sound power W radiated by a point monopole source on its own into a reverberant environment is given by

$$W = \tfrac{1}{2} |q|^2 (Z_0 + \Re\{Z_r(r_s|r_s)\}) \tag{3.45}$$

From an earlier discussion it was argued that above the Schröder frequency the term $\Re\{Z_r(r_s|r_s)\}$ constitutes a zero mean Gaussian random process. By inspection, one can show that the mean μ_W of the source sound power output is simply $(1/2)\,|q|^2 Z_0$ which is equal to the free space value. Similarly, the variance σ_W^2 of the sound power output is given by $(1/4)\,|q|^4 <\Re^2\{Z_r\}>$. The ratio of the terms $<\Re^2\{Z_r\}> / Z_0^2$ appearing in equation (3.44) therefore symbolises the variance of the sound power output from a point monopole source normalised with respect to the square of its mean value according to

$$\frac{\sigma_W^2}{\mu_W^2} = \frac{<\Re^2\{Z_r\}>}{Z_0^2} \tag{3.46}$$

This quotient is commonly refered to as the 'relative variance' of the sound power output and has been discussed by a number a workers[75,76]. The discussion by Davy[77] is a particularly good review of the various theoretical approaches directed towards trying to evaluate this expression for real sound fields. Comparison with experimental data is also presented. Substituting equation (3.21) for the variance of the radiation resistance $<\Re^2\{Z_r\}>$ and equation (3.32) for the mean value Z_0, gives the result

$$\frac{<\Re^2\{Z_r\}>}{Z_0^2} = \frac{c_0^3 \pi}{\zeta V \omega^3} \tag{3.47}$$

Further simplification is possible by noting that the cube of the Schröder radian frequency ω_{sch}^3 is given by ($3\pi^2 c_0^3 / V\zeta$). By direct comparison with equation (3.3) the relative variance of the sound power output given by equation (3.47) may be re-written as a function of frequency normalised with respect to the Schröder frequency according to the surprisingly simple result

$$\frac{<\Re^2\{Z_r\}>}{Z_0^2} = \frac{1}{3\pi}\left[\frac{f_{sch}}{f}\right]^3 \quad \text{for} \quad f \geq f_{sch} \tag{3.48}$$

It must emphasised that this relationship is *only* valid at frequencies above the Schröder frequency for which the diffuse field assumptions are satisfied but below the frequency for which the room absorption ceases to increase linearly with frequency. This is about 600 Hz for some materials, see figure 3.4. Above this frequency, it may be shown from equation (3.17) that the relative variance varies as the square of the frequency. The factor of 1/3 which appears in equation (3.48) is an artefact of the arbitrary manner in which the Schröder frequency is defined. A more universal constant of the random wave field is the Modal overlap factor $M(\omega)$, an important parameter is statistical energy analysis, which is defined as the number of modes contained within the bandwidth $\Delta\omega$. The average number of modes in a unit frequency band is closely approximated by the reciprocal of the modal density $1/n(\omega)$. It therefore follows that

$$M(\omega) = \Delta\omega n(\omega) \tag{3.49}$$

Two modal overlap factors are commonly defined depending upon the frequency bandwidths one chooses to employ. One is the 3 dB bandwidth $\omega_{0.5}$ and the other is the noise bandwidth ω_N. Consider first the 3 dB bandwidth $\omega_{0.5}$ defined in chapter 2 which for the modal response function given by equation (A3.2), is equal to $2\omega_n\zeta$ where ω_n and ζ are the natural frequency and the damping ratio of the n^{th} mode respectively. It is well known that the asymptotic modal density in a three dimensional enclosure is given by ($V\omega^2 / 2\pi^2 c_0^3$) enabling the 3 dB modal overlap factor $M_{0.5}(\omega)$ to be determined from equation (3.49) to give

$$M_{0.5}(\omega) = \frac{c_0^3\pi^2}{\zeta V\omega^3} \tag{3.50}$$

where direct comparison with equation (3.47) reveals that

$$\frac{<\Re^2\{Z_r\}>}{Z_0^2} = \frac{1}{\pi M_{0.5}(\omega)} \tag{3.51}$$

The factor π appearing in the denominator of this equation may be absorbed into another modal overlap factor namely the 'noise' bandwidth modal overlap factor $M_N(\omega)$ which is again defined according to equation (3.49) but whose bandwidth ω_N is known as the noise bandwidth defined from

$$\omega_N = \int_0^\infty |A(\omega)|^2 \, d\omega \; / \; |A(\omega)|^2_{max} \tag{3.52}$$

where $A(\omega)$ is the modal response function given in equation (A3.2). According to their respective definitions, the different modal overlap factors, when they exist, may be shown to be directly related through $M_N(\omega) = \pi M_{0.5}(\omega)$[77]. The relative variance of the real part of the radiation impedance may now be written as

$$\frac{\sigma_W^2}{\mu_W^2} \approx \frac{<\Re^2\{Z_r\}>}{Z_0^2} = \frac{1}{M_N(\omega)} \tag{3.53}$$

The relative sound power variance has been rewritten in terms of the noise bandwidth to enable direct comparison with the result obtained by other workers. For example, Lyon[75] concludes that $\sigma_W^2 / \mu_W^2 = 27 / 16M_N(\omega)$. Jacobsen[76] on the other hand arrives at the similar, but nevertheless different result $\sigma_W^2 / \mu_W^2 = 1 / 2M_N(\omega)$. Although the various expressions differ, neither expression is more correct than the other. This is because the actual relative variance of the sound power output observed in practice has a frequency variation which is considerably more complex than either result suggests. See again the experimental results presented by Davy[77]. The arbitrariness of these various expressions arises from the differing assumptions relating to the modal spacing of the enclosed sound field which is exemplified by Maling[78], who, following the work of Lyon[75], gives the more general expression

$$\frac{\sigma_W^2}{\mu_W^2} = \frac{27g(M)}{16M_N(\omega)} \tag{3.54}$$

where g(M) is a function which varies from 1 to 0.5 as M, the modal overlap factor varies from zero to infinity. This function takes account of the difference between the two most popular models namely, the 'next neighbour' model and the Poisson model. In reality, the sound power variance will depend on the room geometry, inhomogeneities in the room absorption and other factors which will depend on the nature of the source. However, it is reassuring to observe that all of the various expressions predict a reciprocal dependence on the modal overlap factor and the result developed here in equation (3.53) will continued to be used.

Returning to the variance of the secondary source strength which may now be written in terms of the Schröder frequency according to

$$\hat{\sigma}^2_{q_{so}} \approx \frac{1}{3\pi} |q_p|^2 \left[\frac{f_{sch}}{f}\right]^3 [1 - \text{sinc}^2 k\Delta r]$$

$$\text{for } |\gamma| < 1 \text{ and } f \geq f_{sch}. \quad (3.55)$$

It would appear that for a given source separation distance Δr, the variance of the optimal secondary source strength is governed solely by the frequency of excitation relative to the Schröder frequency of the room. This function is plotted in figure 3.9 as a function of the source separation distance evaluated at one, two and three times the Schröder frequency

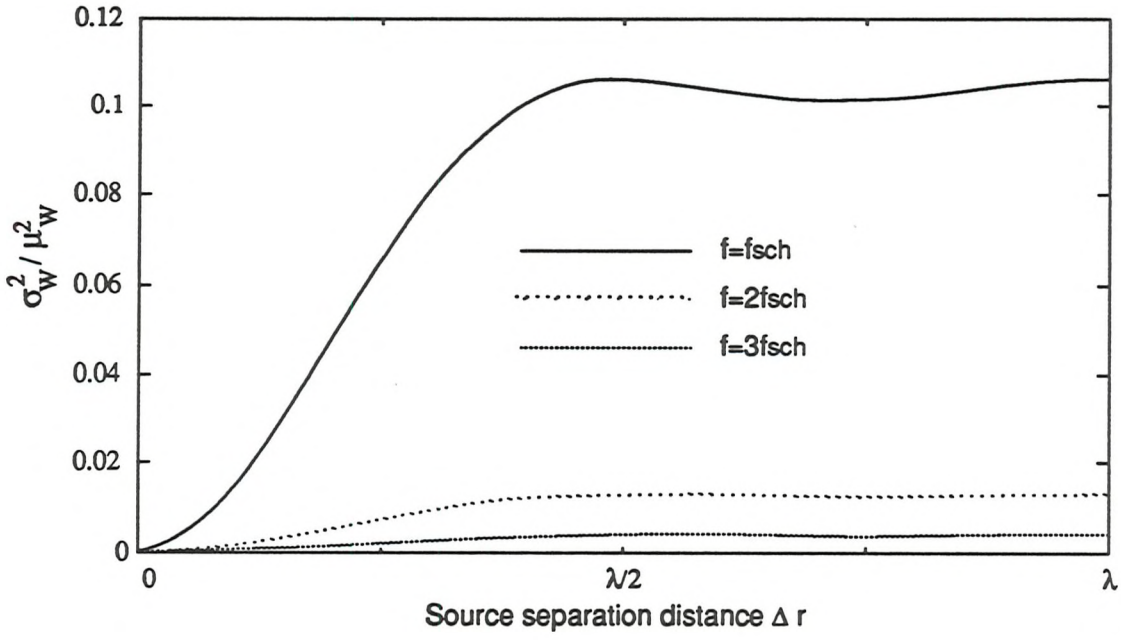

Figure 3.9 The theoretical variance of the secondary source strength required to minimise the total sound power output of a closely spaced source pair evaluated at one, two and three times the Schröder frequency.

The optimally adjusted secondary source strength q_{so} for minimising the total sound power output of a closely spaced source pair in a diffuse field environment has been shown to be susceptible to a level of variance which factorises into frequency dependent and source geometry dependent parts. The variance is observed to diminish inversely as the cube of the excitation frequency. This frequency dependence can be explained if one takes the view that the pressure loading at the secondary source, as it moves from point to point within the diffuse wavefield, has the characteristics of a signal superimposed on background noise to which one can attribute a signal to noise ratio.

The variance of the optimal secondary source strength $\sigma^2_{q_{so}}$ increases rapidly with increasing source separation Δr. As the sources move further apart, the level of random coupling between the source pair remains constant independent of the separation distance. The magnitude of the direct coupling however, progressively diminishes according to sinc$k\Delta r$. Consequently, the acoustic signal to noise at the secondary source, and correspondingly the source variance $\sigma^2_{q_{so}}$, steadily increases with increasing Δr. The source variance $\sigma^2_{q_{so}}$ rapidly converges to its asymptotic value $(1/3\pi)\,(f_{sch}/f)^3$ for separation distances greater than about half a wavelength. However, at large source separation distances the control strategy is largely ineffective as made clear in the next section.

3.6. Minimum sound power output

The minimum sound power output W_{min} as a consequence of the extremely complicated interaction between the secondary source q_{so} and the primary source q_p may be readily evaluated. Recall that the minimum value of the quadratic function given by equation (2.8) is equal to

$$W_{min} = c - b^* A^{-1} b \tag{2.17}$$

where all terms have previously been defined to give

$$W_{min} = \frac{1}{2}|q_p|^2 \left[Z_0 + \Re\{Z_r(r_p|r_p)\} - \frac{Z_0^2 \mathrm{sinc}^2 k\Delta r + 2Z_0 \mathrm{sinc}k\Delta r \Re\{Z_r(r_p|r_s)\} + \Re^2\{Z_r(r_p|r_s)\}}{Z_0 + \Re\{Z_r(r_s|r_s)\}} \right] \tag{3.56}$$

Note again the appearance of the term $(Z_0 + \Re\{Z_r(r_s|r_s)\})$ in the denominator of equation (3.56) which therefore also has a finite probability of being equal to zero causing W_{min} to become singular. At frequencies above the Schröder frequency however, the usual inequality can be applied for the vast majority of source positions within the enclosed sound field, $Z_0 > |\Re\{Z_r(r_s|r_s)\}|$ so that under this restriction, W_{min} lends itself to power series representation within the radius of convergence $|\gamma| < 1$. To second order in $\Re\{Z_r(r_s|r_s)\}/Z_0$, the minimum sound power output may be approximated by

$$W_{min} \approx \frac{1}{2}|q_p|^2 \Big[Z_0(1 - \mathrm{sinc}^2 k\Delta r) + \Re\{Z_r(r_p|r_p)\} + \mathrm{sinc}^2 k\Delta r\, \Re\{Z_r(r_s|r_s)\}$$

$$- 2\mathrm{sinc}k\Delta r\, \Re\{Z_r(r_p|r_s)\} + \frac{2\Re\{Z_r(r_p|r_s)\}\Re\{Z_r(r_s|r_s)\}\mathrm{sinc}k\Delta r - \Re^2\{Z_r(r_p|r_s)\}}{Z_0}$$

$$- \frac{\Re^2\{Z_r(r_s|r_s)\}\mathrm{sinc}^2 k\Delta r}{Z_0} + \cdots \Big] \qquad \text{for } |\gamma| < 1 \tag{3.57}$$

The first term, $1/2\ |q_p|^2\ Z_0(1 - \mathrm{sinc}^2 k\Delta r)$ is recognisable as the equivalent free space minimum sound power output in the absence of reverberation[40]. During the expectation process $< W_{min} >$, all odd moments have been set equal to zero, the diffuse field properties given by equations (3.39) - (3.41) have been employed, and the equalities

$$< \Re^2\{Z_r(r_p|r_s)\} > = < \Re^2\{Z_r(r_s|r_p)\} > = < \Re^2\{Z_r\} > \qquad (3.58)$$

have been noted to produce the considerably simpler expression

$$< \hat{W}_{min} > = \frac{1}{2} |q_p|^2 Z_0(1 - \mathrm{sinc}^2 k\Delta r) \left(1 - \frac{< \Re^2\{Z_r\} >}{Z_0^2} \right) + \varepsilon_2$$

$$\text{for } |\gamma| < 1 \text{ and } f \geq f_{sch} \qquad (3.59)$$

The residual term ε_2 again denotes the order of the next highest non-vanishing term which can be shown to be of the order $\varepsilon_2 \approx \mathbf{O}(\omega^{-4})$, which is clearly insignificant compared with the leading term which varies as ω^2. Recognising that

$$W_p = \frac{1}{2} Z_0 |q_p|^2 \qquad (3.60)$$

and recalling equation (3.48) for the relative source power variance, yields an expression for the expectation of the minimum sound power output $< \hat{W}_{min} >$ as a function of the normalised frequency of the form

$$< \hat{W}_{min} > \approx W_p (1 - \mathrm{sinc}^2 k\Delta r) \left(1 - \frac{1}{3\pi} \left[\frac{f_{sch}}{f} \right]^3 \right)$$

$$\text{for } |\gamma| < 1 \text{ and } f \geq f_{sch} \qquad (3.61)$$

Note that the free field limit is rapidly recovered as the excitation frequency tends to infinity i.e.

$$< \hat{W}_{min} > \rightarrow W_p (1 - \mathrm{sinc}^2 k\Delta r) \quad \text{as} \quad f / f_{sch} \rightarrow \infty \qquad (3.62)$$

where $W_p (1 - \mathrm{sinc}^2 k\Delta r)$ is the minimum sound power output in the absence of reverberation. This result may be regarded as the free field limit for the limiting case where the wavelength becomes vanishingly small corresponding to the frequency tending to infinity. However, at frequencies which are greater but comparable to the Schröder frequency, the expectation $< W_{min} >$ is appreciably less than can be achieved in free field. This finding helps to explain the presence of the terms additional to the free field solution in

equation (3.57). It is therefore reasonable to assume that the extra terms exist to suppress the component of the primary sound field scattered by the enclosure walls. The mechanism of control for this problem will be discussed in the next section. For excitation frequencies greater than the Schröder frequency, consider the ratio of terms given below

$$\frac{< \hat{W}_{min} > - (W_{min})_{ff}}{(W_{min})_{ff}} = \frac{1}{3\pi}\left[\frac{f_{sch}}{f}\right]^3 \quad \text{for } f \geq f_{sch} \qquad (3.63)$$

which has been evaluated from equations (3.69) and (3.70). This function determines the sound power reduction achieved by acting on the diffuse field part of the primary sound field as a fraction of the sound power reduction achieved through the attenuation of directly radiated sound. This equation shows that the addition of an optimally driven secondary source proximately located to a primary source radiating a pure tone at the Schröder frequency is only able to suppress an additional $1/(3\pi)^{th}$ (approximately 10 %) of the total sound power output than would be possible in the absence of enclosure walls under diffuse field conditions.

The space averaged sound power output $< \hat{W}_{min} >$ as a fraction of the primary source sound power output W_p is plotted below in figure 3.10 for integer multiples of the Schröder frequency. This function can be observed to rapidly converge to the free field limit at frequencies greater than about two times the Schröder frequency.

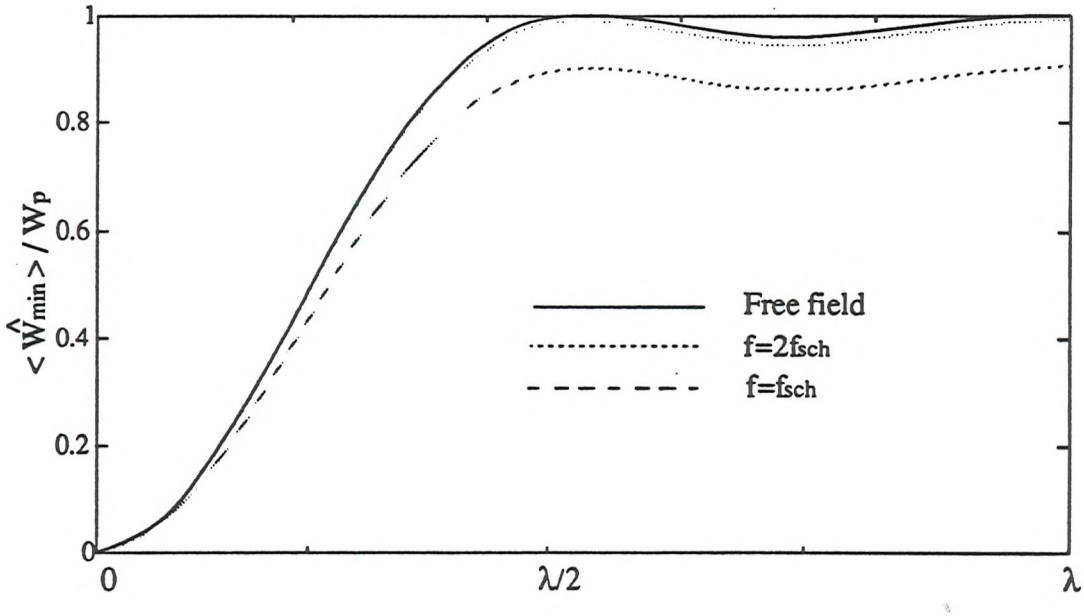

Figure 3.10 The expectation of the minimum sound power of a closely spaced source pair in a diffuse sound field versus source separation distance.

3.7. The variance of the minimum sound power output

The statistical fluctuations of the secondary source strength from point to point in the enclosure described by equation (3.55) will be ultimately exhibited as an uncertainty in the total sound power output. The variance associated with the optimally minimised sound power output may be derived directly from its defining relation given below

$$\hat{\sigma}^2_{W_{min}} = < (W_{min} - < \hat{W}_{min} >)^2 > \tag{3.64}$$

Substituting equations (3.57) and (3.59) for W_{min} and $< \hat{W}_{min} >$ respectively yields the surprisingly simple result

$$\hat{\sigma}^2_{W_{min}} = \frac{1}{4} |q_p|^4 < \Re^2\{Z_r\} > [1 - \text{sinc}^4 k\Delta r\,] + \varepsilon_3 \tag{3.65}$$

The derivation of this equation has necessitated the evaluation of the expectation $< \Re\{Z_r(r_p|r_p)\}\Re\{Z_r(r_s|r_s)\} >$ where both measurement points and source points are identically displaced. The quantities $\Re\{Z_r(r_p|r_p)\}$ and $\Re\{Z_r(r_s|r_s)\}$ may be shown to be spatially correlated according to $< \Re^2\{Z_r\} > \text{sinc}^2 k\Delta r$, the derivation of which is given in Appendix 3.3. The residual term ε_3 can be shown to be three orders of magnitude in frequency below the leading term i.e $\varepsilon_3 \approx O(\omega^{-2})$ which may therefore be neglected at high frequencies without incurring significant error. The sound power variance $\hat{\sigma}^2_{W_{min}}$ can be conveniently expressed non-dimensionally as a fraction of the primary sound power output squared W_p^2 according to

$$\frac{\hat{\sigma}^2_{W_{min}}}{W_p^2} \approx \left[\frac{< \Re^2\{Z_r\} >}{Z_0^2}\right] [1 - \text{sinc}^4 k\Delta r] \tag{3.66}$$

where from equation (3.48)

$$\hat{\sigma}^2_{W_{min}} \approx \frac{1}{3\pi} W_p^2 \left[\frac{f_{sch}}{f}\right]^3 [1 - \text{sinc}^4 k\Delta r]$$

$$\text{for } |\gamma| < 1 \text{ and } f \geq f_{sch} \tag{3.67}$$

This function is plotted below evaluated at one, two and three times the Schröder frequency for Δr ranging between zero and λ.

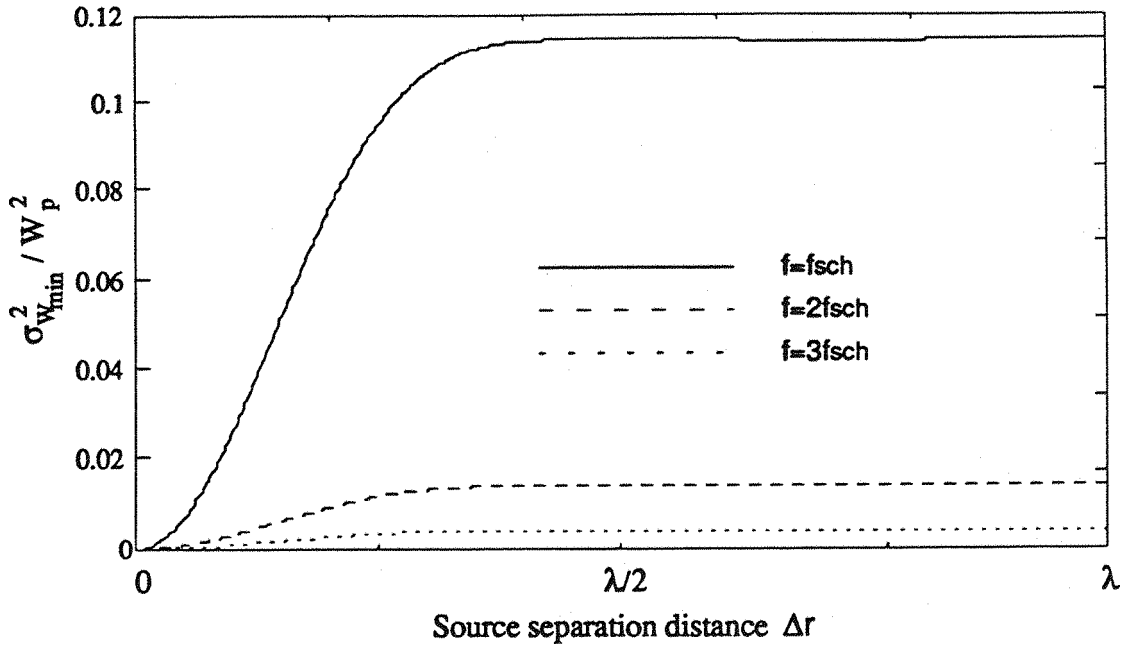

Figure 3.11 The theoretical variance of the minimum total sound power output of a closely spaced source in a diffuse sound field evaluated at one, two and three times the Schröder frequency.

Observe that the minimum sound power output from the source pair is highly susceptible to statistical fluctuations for source separation distances greater than about half a wavelength. These are the distances for which the level of sound power reduction is least such that the source pair is least constrained. The resulting sound power output therefore exhibits maximum variability as the source pair is moved around the enclosure reaching a maximum relative variance equal to $1/3\pi(f_{sch} / f)^3$. The dependence of the variance on the fourth power of sinckΔr is purely coincidental since both the real part of the transfer impedance and the three dimensional spatial correlation function vary as sinckΔr. This will clearly not be the case at frequencies below the Schröder cut off frequency f_{sch} where it is in general not possible to identify a spatially stationary correlation function. For source separation less than about one half of a wavelength however, the converse is true and the level of variance is diminished but highly sensitive to the source separation distance. The relative variance of both q_{so} and W_{min} can be observed to converge to the same value at any given frequency as the source separation distance steadily increases.

$$\frac{\hat{\sigma}^2_{W_{min}}}{W_p^2} = \frac{\hat{\sigma}^2_{q_{so}}}{|q_p|^2} \rightarrow \frac{1}{3\pi}\left[\frac{f_{sch}}{f}\right]^3 \qquad \text{for } \Delta r \rightarrow \infty \quad (3.68)$$

The relative variance derived here in equation (3.68) for the sound power output of the coupled, well separated source pair is identically equal to the relative variance exhibited by an isolated point monopole source allowed to radiate freely in the diffuse field, see equations (3.46) and (3.48). It would therefore appear, to the level of of accuracy afforded

by the truncated Taylor series expansion, that the introduction of a remotely positioned secondary source seeking to minimise the combined sound power outputs does not alter the original variance in primary source sound power output radiating in isolation. However, it is shown in the next section that the secondary source sound power output in any single experiment is exactly equal to zero from which the variance must also be equal to zero. Thus, the variance of the total sound power output is therefore equal to the sum of the variances of the primary and secondary source power contributions which indicates that the primary source sound power output is statistically independent of the presence of the secondary source providing they are well separated.

3.8. Mechanisms of sound power reduction in the diffuse field

The derivation of the optimal secondary source strength q_{so} and the corresponding diffuse field minimum sound power output W_{min} have yielded expressions which comprise the free field solution derived in reference [40], plus additional terms which depend on, and are simple functions of the reverberant field. It is therefore not unreasonable to suppose that the terms are responsible for acting on the direct field and reverberant field respectively. On the basis of this assumption it should be possible to identify the mechanism of diffuse field sound power minimisation.

Under free field conditions, an isolated point monopole source may have its total sound power output minimised by the introduction of a closely spaced secondary source of source strength $-q_p \text{sinc} k\Delta r$. This result is also the expected result in a diffuse field environment taken over all source positions. Surprisingly, the secondary source radiates no time averaged sound power itself since the *total* pressure at the secondary source point is arranged to be perfectly out of phase with its volume velocity[39]. The secondary source simply acts to present an additional pressure loading to the primary source thereby causing a reduction in its radiation efficiency. The same optimal control mechanism also operates in an enclosed space but the principal difference is that there are now both direct and indirect (via reflections from the walls) transmission paths connecting the two sources.

Some insight into the mechanisms of sound power minimisation are obtained if one considers the sound power output of the primary source and the secondary source in turn. The sound power output from the secondary source W_s in the presence of the primary source is given by

$$W_s = \tfrac{1}{2}\Re\{q_s^* \, p(r_s)\} \tag{3.69}$$

where $p(r_s)$ is the total acoustic pressure evaluated at the secondary source point r_s given by

$$p(r_s) = q_p Z(r_p|r_s) + q_s Z(r_s|r_s) \tag{3.70}$$

From equation (3.35), the optimal secondary source strength q_{so} has been shown to be equal to

$$q_s = q_{so} = -\frac{\Re\{Z(r_p|r_s)\}}{\Re\{Z(r_s|r_s)\}} q_p \tag{3.71}$$

The secondary source sound power output given in equation (3.69) can therefore be written as

$$W_s = \tfrac{1}{2}\Re\{-\frac{\Re\{Z(r_p|r_s)\}}{\Re\{Z(r_s|r_s)\}}[\, Z(r_p|r_s) - \frac{\Re\{Z(r_p|r_s)\}}{\Re\{Z(r_s|r_s)\}} Z(r_s|r_s)\ ]\, |q_p|^2\} \tag{3.72}$$

Taking the real part, one can shown that the term in square brackets is equal to zero

$$W_{so} = 0 \tag{3.73}$$

We now have formal verification of the behaviour observed in figure 2.8 of chapter 2 for the analogous one dimensional problem. From these findings, one can infer that even in a reverberant sound field, the total pressure at the secondary source point is arranged to be in quadrature to the complex secondary source strength. From the point of view of the governing equations, there is no distinction between free field transfer impedances and transfer impedances which involve reflections. The time averaged sound power output radiated by the secondary source when seeking to minimise the total sound power output is therefore zero in both free and enclosed sound fields. The same conclusion was arrived by Nelson *et-al* [39] for the analogous problem in free field. The reduction in the radiated sound power from the source pair is therefore due solely to pressure loading of the primary source by the secondary source. Clearly, this arrangement strives to achieve the optimal balance between the sound power outputs from the two sources which is obviously attained by setting the secondary source contribution to zero for pure tone fields.

Given that the time averaged secondary source sound power output is zero indicates that the secondary source sound power output associated with the loading of the primary source *exactly balances* with the sound power subsequently absorbed by secondary source.

Just as for the one dimensional sound power minimisation problem detailed in Chapter 2, the optimal transfer function relating the secondary source strength to the

primary source strength given in equation (3.36) is real. The Fourier transform of this real function of frequency is therefore perfectly symmetrical about t = 0 which is therefore non-causal with respect to the time history of the primary source signal. It would appear reasonable that the interpretation placed on the mechanism of sound power minimisation in the one dimensional example also directly applies to the control mechanism in this considerable more complex space. This is despite the fact that the time domain interpretation of the transmission response function in the three dimensional enclosed space is considerable more complicated[79].

Consider the system response to a unit primary pressure pulse at t = 0. For pure tone sound fields, the secondary source begins the process of reducing the total sound power output from the source pair an infinite time prior to the action of the primary source. The secondary source starts by continually building up its own power output such that successive terms in the optimal impulse response function are increasingly larger in magnitude. This infinite succession of events conspire to anticipate the action of the primary source which eventually culminate in the radiation of a pressure pulse just in time to meet the pulse leaving the primary source at t = 0. Note that the process of loading the primary source which takes place for t < 0 is achieved for minimum secondary source sound power expenditure. This has the effect of partially loading the primary source whose radiation impedance is consequently diminished. It is strongly suspected that figure 2.8 for the plane wave example in chapter 2 is therefore directly relevant to the three dimensional problem described here.

The acoustic energy which is radiated by the primary source is subsequently absorbed by the secondary source. However, since the secondary source is situated within a reverberant environment, it has the opportunity to continually absorb successive reflections. The precise details of how this is achieved in this more complicated three dimensional space is contained in the infinite series of recursive terms generated by the inverse Fourier transform of $(Z_0 + \Re\{Z_r(r_s|r_s)\})^{-1}$ which appear in equation (3.36). Successive terms in the series expansion have alternate signs so that each term is exactly in anti-phase with the previous term and is therefore absorbed under steady state conditions The general form of this behaviour in reverberant fields has been investigated numerically by Hough[80].

Consider the sound power from the primary source alone, namely

$$W_{po} = \tfrac{1}{2}\Re\{q_p^* \, p(r_p)\} \qquad (3.74)$$

One can readily show that this expression recovers the original result given in equation (3.58) whose statistics have already been investigated. Given that $W_{min} = W_{so} + W_{po}$ where it has been shown that $W_{so} = 0$, one can now state the following important result

$$W_{min} = W_{po} \tag{3.75}$$

which is an exact relationship for point sources and is valid for *individual* experiments and is therefore not in any sense an average result. So far we have shown that the problem discussed in this chapter is simply a three dimensional extension of the considerably simpler one dimensional example discussed at length in chapter 2. In chapter 2, one observed that for random broadband sources of noise, the causally constrained secondary source was limited to the absorption of sound. This restriction must also be true for this three dimensional example when the two sources are well separated. This is the subject of the next section.

3.9. The maximum sound power absorption of a point monopole source in the pure tone diffuse field

The previous section was concerned with the *total* minimum sound power output from a closely spaced source pair situated within a diffuse field. Whilst the secondary source acted to reduce its own sound power output in accordance with the criterion of minimisation, the secondary source also took equal account of the sound power output from the primary source. In this section we consider the closely related problem of minimising the secondary source sound power output taking *no* account of the effects on the primary source. This example constitutes a particularly important problem since it is highly relevant to the large number of cases where the primary source signal is random broadband noise and its predictability is consequently poor. This example is also pertinent to the large number of real cases for which the primary source is a large distributed body such that pressure loading on it will be largely ineffective for these more representative source types. In both cases, the optimal control mechanism will be restricted to the active absorption of the incident primary sound field.

Assume that the secondary source is irradiated by some monochromatic primary source field $p_p(\mathbf{r})$ of hitherto unspecified spatial characteristics. The sound power output W_s from the point secondary source may be constructed from the expression

$$W_s = \tfrac{1}{2}\Re\{q_s^* \, p(\mathbf{r}_s)\} \tag{3.76}$$

It is important to recognise that in the cost function W_s of equation (3.76) (the secondary source sound power output), there is no account taken of the sound power radiated by the primary source and therefore does not respond to the action of the primary source in any systematic anticipatory fashion. There is therefore a possibility that in some cases the secondary source may inadvertently 'suck' energy from the primary source while in other cases, inhibit the pressure radiated from the primary source. This was the finding of Bullmore according to the results obtained from a series of systematic computer simulations of the sound field in a shallow box of low modal density[51].

Putting $p(r_s) = p_p(r_s) + q_s Z(r_s|r_s)$ in equation (3.76) and following exactly the same procedure as before, the secondary source sound power output as expressed by equation (3.76) may be constructed as a quadratic function of the secondary source strength according to

$$W_s = \frac{1}{2} q_s \Re\{Z_{rad}\} q_s^* + \frac{1}{4} q_s p_p^*(r_s) + \frac{1}{4} q_s^* p_p(r_s) \qquad (3.77)$$

where comparison with equation (2.8) and its solution $q_s = q_{so}$ given in equation (2.11) yields the completely general result

$$q'_{so} = - \frac{p_p(r_s)}{2\Re\{Z_{rad}\}} \qquad (3.78)$$

where for the sake of brevity $Z_{rad} = Z(r_s|r_s)$ denoting the secondary source radiation impedance. All quantities for which only the secondary source sound power has been minimised will now be referenced with the symbol (') so as to make the distinction between the former problem for which the minimum of the total sound power was sought. In this example, the secondary source strength is exactly in anti-phase with the primary source pressure arriving at the secondary source point. The minimum secondary source sound power output W'_{so} may be derived from equation (2.17) to give the expression

$$W'_{so} = - \frac{|p_p(r_s)|^2}{8\Re\{Z_{rad}\}} \qquad (3.79)$$

The maximum sound power capable of being absorbed by a given source type is therefore inversely proportional to its radiation resistance. Although this result is only valid for point monopole sources, equation (3.79) helps to explain why a quadrupole source of sound is a more efficient absorber of sound than a dipole source, which in turn is a more efficient absorber than a monopole source[40]. The primary square pressure $|p_p(r_s)|^2$ may be re-written in terms of the sum of the squares of the resistive and reactive part of the transfer impedance between the two sources according to

$$W_{sp} = -\frac{\Re^2\{Z(r_p|r_s)\} + \Im^2\{Z(r_p|r_s)\}}{8\Re\{Z_{rad}\}} |q_p|^2 \qquad (3.80)$$

Most importantly note that W_{sp} is negative providing that the radiation resistance of the point secondary source $\Re\{Z_{rad}\}$ is positive which is of course guaranteed by the conservation of energy principle. Now consider the influence on the primary source sound power output W'_p where

$$W'_p = \tfrac{1}{2}\Re\{q_p^* p(r_p)\} \qquad (3.81)$$

On substitution of equation (3.78) for q'_{sp}, one can show that the primary source sound power output W'_p is modified by the behaviour of the secondary source which is now equal to

$$W'_p = \tfrac{1}{2}|q_p|^2 [\,\Re\{Z(r_p|r_p)\} + \frac{\Im^2\{Z(r_p|r_s)\} - \Re^2\{Z(r_p|r_s)\}}{2\Re\{Z_{rad}\}}\,] \qquad (3.82)$$

The first term is the primary source sound power output radiated into the reverberant space in the absence of the secondary source. The second term therefore quantifies the *change* in the primary source sound power output due to the sound field from the secondary source. It is emphasised that any modification to the primary source sound power output is wholly inadvertent. By inspection, this additional term may be positive or negative depending on whether the primary source pressure at the secondary source is mostly reactive or resistive. It is enlightening to consider the behaviour of this function for the two well defined cases corresponding to when the secondary source is located very close to the primary source, and very far from the primary source.

When the sources are very close compared to the acoustic wavelength, to a good approximation the source pair behave as if they were in free field so that one can omit diffuse field terms to a good level of accuracy. One can therefore show that the sound power output of the primary source is considerably *increased* at these distances. This increase is overwhelming due to the very large reactive component of pressure at the secondary source point compared with the resistive contribution $\Im^2\{Z(r_p|r_s)\} >> \Re^2\{Z(r_p|r_s)\}$ which will have the effect of 'sucking' energy from the primary source. This phenomenon has also been observed by Nelson *et-al*[81].

Now, consider the more important and practically orientated problem where the points sources are well separated and outside the influence of directly transmitted sound. Clearly, the squared reactive component of primary pressure $|q_p|^2\Im^2\{Z(r_p|r_s)\}$ will on

average equal the square resistive pressure $|q_p|^2 \Re^2\{Z(r_p|r_s)\}$ so that when the space average is taken, the second set of terms in equation (3.82) averages to zero. For this limiting geometry, the primary source sound power output is, on average, unchanged and therefore equal to its average diffuse field value W_p, the free field sound power output

$$< W'_p > = W_p \qquad \text{for } |r_s - r_p| >> \lambda \qquad (3.83)$$

The control mechanism is now limited to the absorption of the sound field which is scattered close to the secondary source. Recalling that $Z_{rad} = Z_0 + Z_r(r_s|r_s)$, taking equation (3.80) as a series expansion to second order, neglecting small terms and then performing the expectation in the usual way shows the maximum secondary source sound power absorption may be closely approximated by

$$< \hat{W}'_{so} > \approx - \frac{< |p_{pr}(r)|^2 >}{8Z_0} \left(1 + \frac{1}{M_N(\omega)} \right) \qquad (3.84)$$

where the hat '^' is used to denote that the usual restriction, namely $|\Re\{Z_r(r_s|r_s)\}| < Z_0$ has been applied. The subscript 'r' has been again used to indicate diffuse field pressures outside the influence of directly radiated sound. One can immediately verify that $< W'_{so} > \leq 0$ which indicates that the primary sound field which is incident on the secondary source is absorbed, or at worst left unchanged corresponding to $W'_{so} = 0$. The secondary source cross sectional area of absorption can be readily evaluated by recognising that the average diffuse field sound intensity modulus $< |I_{pr}(r)| >$ is properly defined even though the average *net* sound intensity vector $< I_{pr}(r) >$ is zero. One can envisage a hypothetical surface of unit area randomly orientated in the field. The sound field on one side of this notional surface may be regarded as semi-diffuse which is perfectly counteracted by an identical sound field on the other side. The net sound intensity passing through one side of this hypothetical surface has been related to the space average square pressure in the field. From standard acoustical texts[65]

$$< |I_{pr}(r)| > = \frac{< |p_{pr}(r)|^2 >}{8\rho c_0} \qquad (3.85)$$

where $< |p_{pr}(r)|^2 >$ refers to the space averaged diffuse field square pressure amplitude sustained by the primary source. Substituting equation (3.85) for $< |I_{pr}(r)| >$ into equation (3.84) and recalling that $Z_0 = \omega^2\rho / 4\pi c_0$, yields the important result

$$< \hat{W}'_{SD} > \approx - < |I_{pr}(r)| > \frac{\lambda^2}{\pi} \left(1 + \frac{1}{M_N(\omega)} \right) \tag{3.86}$$

where λ is the acoustic wavelength. The expectation of the secondary source sound power output $< W'_{SD} >$ is now in the form of an acoustic intensity times a cross sectional area of absorption. At frequencies well above the Schröder frequency therefore, the maximum secondary source sound power absorption may therefore be accurately represented by

$$< \hat{W}'_{SD} > \approx - < |I_{pr}(r)| > \frac{\lambda^2}{\pi} \tag{3.87}$$

One can employ exactly the same approach to derive an approximate expression for the relative variance of the maximum sound power absorption which is given by

$$\frac{\sigma^2_{\hat{W}'_{SD}}}{\mu^2_{\hat{W}'_{SD}}} \approx \frac{1}{M_N(\omega)} \tag{3.88}$$

where the mean value $\mu_{W'_{SD}}$ given by equation (3.87) has been used.

The isotropy of the diffuse wavefield suggests that the diffuse field bombards the secondary source from all angles equally. The area of absorption S_{absorb} must therefore take the form of a sphere of surface area $4\pi a^2$ which has the point secondary source at its centre. Equating $4\pi a^2$ to λ^2 / π enables one to solve for the radius of absorption of the hypothetical sphere 'a' on the surface of which all sound is absorbed on average. Solving for 'a' gives

$$S_{absorb} \approx \frac{\lambda^2}{\pi} \quad \text{and} \quad a \approx \frac{\lambda}{2\pi} = k^{-1} \tag{3.89}$$

This diffuse field cross sectional area of absorption S_{absorb} given by equation (3.89) is exactly four times the area of absorption for a free field plane wave incident on the optimally absorbing point monopole source, namely $\lambda^2 / 4\pi$. This result was deduced by Nelson *et-al*[82]. In this case, the cross sectional area of absorption takes the form of a circle, normal to the plane wave front, whose radius is *also* equal to $\lambda/2\pi$. Despite the fact that the point monopole secondary source can only match itself to the acoustic pressure at a single point in the wavefield, the effective cross sectional area of absorption has a linear dimension which is comparable to the acoustic wavelength. This finding suggests that the influence of the perfectly absorbing source extends much further than its physical dimension which indicates that acoustic energy is somehow diffracted towards the point

source. An optimal absorber of sound is therefore an optimal diffractor. See, for example, the diffraction intensity patterns given in reference [39] for the free field plane wave example.

The free and diffuse field cross sectional areas of absorption are fully consistent with the idea that the optimally absorbing point source creates around itself, a sphere of influence of radius $\lambda / 2\pi$ on whose surface, all sound is absorbed. In the case of an incident plane wave, the normal projection of the sphere onto the plane wave front is precisely the circle of absorption of radius k^{-1} identified by Nelson *et-al* in reference [82]. A fully diffuse field however, will see the full benefit of the hypothetical sphere of influence and its cross sectional area of absorption is increased accordingly. One can therefore infer that the total cross sectional area of absorption of a point monopole source is an intrinsic property of the source type, completely characterised by its radiation resistance, and is independent of the form of the primary pressure field.

Inspection of equation (3.78) shows that the optimal secondary source cross sectional area of absorption S_{absorb} is also insensitive to the proximity of the enclosure walls. Consider, for example, the case of a point secondary source situated at a distance d from a perfectly rigid wall of an enclosure supporting a diffuse field. Assuming that the source is well away from other sources and boundaries, the average square pressure $< |p(r)|^2_{wall} >$ is given by[37]

$$< |p(r)|^2_{wall} > = < |p(r)|^2 > [\ 1 + \text{sinc}2kd\ ] \tag{3.90}$$

Similarly, superposition of the directly radiated field and the field radiated from the 'image' source, which is effectively separated by a distance 2d, gives equation (3.91) for the increased radiation resistance of a point source near to a perfectly reflecting boundary

$$(Z_{rad})_{wall} = Z_{rad} [\ 1 + \text{sinc}2kd\ ] \tag{3.91}$$

where diffuse field terms are negligible providing 2d is small compared to the wavelength. The ratio of the terms near to the wall, which determines the maximum sound power capable of being absorbed, is therefore *independent* of the source position relative to the enclosure boundaries. Similar scaling rules also exist for sources in the corners and other wall intersections of the room. From equation (3.79), one can therefore write

$$< W'_{so} > = \frac{< |p(r)|^2 >}{\Re\{Z_{rad}\}} = \frac{< |p(r)|^2_{wall} >}{\Re\{(Z_{rad})_{wall}\}} \tag{3.92}$$

The optimal absorption of sound is only possible by presenting to the oncoming primary wavefield an apparent optimal impedance. From the point of view of the incident sound field, it is entirely irrelevant whether this impedance is active or passive in origin. The optimised passive absorption of acoustic energy is the function of the Helmholtz resonator[48]. This device consists simply of a rigid enclosure of air communicating with the external medium through a small opening which is usually in the form of a narrow neck. The Helmholtz resonator has the properties of mass by virtue of the oscillating slug of air in the neck of the device, stiffness by virtue of the compliance of the enclosed gas and an associated resistance as a consequence of viscous forces at the opening. This arrangement may be optimally tuned to a *single* given frequency and the absorption of sound maximised at that frequency. It is generally well established that the absorption cross sectional area of this device in the diffuse field at resonance is also λ^2 / π where λ is the acoustic wavelength[83].

A further discussion on the absorption of sound by a passive 'receiver' is presented by Shaw[84] who shows that the maximum sound power absorbed at a given frequency is given by $(\lambda^2 / \pi) (|p(r)|^2 / 8\rho c_0)$ which is identical to the expression derived in equation (3.87). Shaw proceeds to demonstrate that the maximum area of absorption occurs when the radiation resistance of the secondary source equals the internal resistance of the source. This condition defines the resonance of the device which is precisely the definition for the Helmholtz resonator to be maximally effective. However, Shaw appears to use the plane wave intensity to obtain a value for the diffuse field cross sectional area of absorption which differs from the value derived here in equation (3.89) by a factor of four. The obvious advantage of using an active source is that in principle, one is able obtain maximum sound power absorption over a band of frequencies simultaneously whereas the Helmholtz resonator is a high Q system carefully tuned to a single frequency[50]. The Helmholtz resonator may therefore be regarded as the passive analogue of the optimally absorbing point monopole source.

The reduction in the total radiated sound power from the source pair W'_{min} even though only the secondary source contribution has been included in the cost function of equation (3.76), is simply the sum of individual source outputs $W'_p + W'_{so}$. From equations (3.80) and (3.81)

$$W'_{min} = \frac{1}{2} |q_p|^2 \left[\Re\{Z(r_p|r_p)\} - \frac{3\Re^2\{Z(r_s|r_p)\} - \Im^2\{Z(r_s|r_p)\}}{4\Re\{Z(r_s|r_s)\}} \right] \qquad (3.93)$$

Intriguingly, this expression gives a disproportionate weighting to the resistive part of the transfer impedance in favour of the reactive part by a factor of three. The total sound power output from the source pair may therefore be dramatically increased for closely spaced

sources where the reactive transfer impedance vastly exceeds the resistive part. This remark is particularly relevant to point sources. However for well separated sources, taking a series expansion and then the expectation in the usual way yields the anticipated result

$$<\hat{W}'_{min}> \approx W_p \left[1 - \frac{<\Re^2\{Z_r(r)\}>}{2Z_0^2}\right] \tag{3.94}$$

where from equations (3.84) - (3.86), one can write

$$<\hat{W}'_{min}> = W_p - <|I_{pr}(r)|> \frac{\lambda^2}{\pi} \tag{3.95}$$

as expected. This expression contrasts with the previous result for the minimum *total* sound power reduction given by equation (3.59). Using equation (3.87), for large separation distances one can now write

$$<\hat{W}_{min}> = <\hat{W}'_{min}> - <|I_{pr}(r)|> \frac{\lambda^2}{\pi} \tag{3.96}$$

The additional reduction of sound power output when the *total* sound power output is minimised is of course due to the ability of the secondary source to load the primary source since the transmission path of sound from the secondary source to the primary source is known in this case as part of the information fed into the cost function of equation (3.33). In the present example, however, where only the secondary source sound power output is minimised, this transfer function is *not* known to the cost function of equation (3.74) and the action of the secondary source is limited to the absorption of the incident primary source energy. It is no coincidence that the extra sound power reduction acquired through optimal loading of the primary source is *exactly equal* to the sound power reduction attained through optimal absorption by the secondary source. Thus the mechanisms of sound power absorption and reductions in sound power caused by pressure loading possess strong similarities. One principal difference is that pressure loading takes place at the primary source while sound power absorption invariably takes place at the secondary source.

In order to illustrate further the interchangability of the secondary source as a source of sound and as an equivalent area of absorption, consider the energy balance equation below. This fundamental relation expresses the equivalence between the rate at which energy is injected into the enclosure to the rate of increase in potential energy plus the rate of dissipation of energy determined by the total area of absorption A. We now apply this equation to the expected values of the sound power and potential energy (this is usually

implied in most texts books on acoustics[37] but usually not stated). In this example there are two sources of sound power input into the enclosure $< W'_{so} >$ and $< W'_p >$ so that

$$V\frac{d<e_{po}>}{dt} + \frac{c_0 A}{4} < e_{po} > = < W'_p + W'_{so} > \tag{3.97}$$

According to equation (3.87), for well separated sources W'_{so} merely acts to absorb the incident scattered energy whose minimum value is given by the equation

$$< W'_{so} > \approx - \frac{< |p_{pr}(r)|^2 >}{8\rho c_0} \frac{\lambda^2}{\pi} \tag{3.98}$$

The total diffuse field potential energy density in the enclosure is linearly related to the space averaged squared pressure via, $< e_{po} > = < |p_{pr}(r)|^2 > / 2\rho c_0^2$ and so equation (3.97) may be re-arranged to give

$$V\frac{d<e_{po}>}{dt} + \frac{c_0}{4}(A + \frac{\lambda^2}{\pi}) < e_{po} > = < W'_p > \tag{3.99}$$

Thus, when the secondary is optimally driven with the aim of minimising the secondary source sound power output, it becomes indistinguishable from an additional element of passive absorption. Equation (3.99) describes the dynamic growth of sound from a source which is switched on at some time t = 0. The effect of the secondary source is to effectively slow down this exponential increase in sound pressure level in the enclosure. More importantly however, the steady state equilibrium potential energy level is now less than in the absence of control since acoustic energy is now dissipated at a faster rate. From standard texts[37], the steady state solution of this equation is simply

$$\lim_{t\to\infty} < e_{po} > = \frac{4 < W'_p >}{(A + \frac{\lambda^2}{\pi})c_0} \tag{3.100}$$

Now dividing by the level of potential energy E_p sustained in the absence of the secondary source, namely $4<W_p> / Ac_0$, and noting that $< W'_p > = W_p$ from equation (3.83), gives the average steady state reduction in potential energy resulting from sound power absorption

$$\frac{< e_{po} >}{e_p} = \left(1 + \frac{\lambda^2}{A\pi}\right)^{-1} \tag{3.101}$$

For large enclosures at high frequencies in which there is a high level of absorption by the enclosure walls or other objects in the room, the additional active term λ^2/π will be negligible. However, for small rooms where the Schröder frequency is low, this additional active contribution may be significant compared to the existing passive absorption before active control. By way of example, consider a medium size cubical room with an internal volume of 100 m^3 whose walls are evenly lined with a 0.5 " thick acoustic tiles. Using values of absorption coefficient $\bar{\alpha}$ taken from Beranek[53] plotted in figure 3.4, and noting equations (3.18) and (3.19) suggests that for this size room the Schröder frequency f_{sch} is approximately equal to 160 Hz. The total room absorption as determined from $S\bar{\alpha}$ is shown below together with the area of active absorption λ^2/π plotted down to 0 Hz even though the theory is clearly invalid below the Schröder frequency. However, significant departure from this value at low frequencies *is* anticipated according to the form of the relative variance given in equation (3.88). Equation (3.89) is therefore plotted to 0 Hz merely to suggest that the active absorpton of sound is considerably more effective as a mechanism of control at low frequencies due to the resonant nature of the sound field. The active absorber simply acts to damp out the resonance for which the effective area of absorption appears extremely large

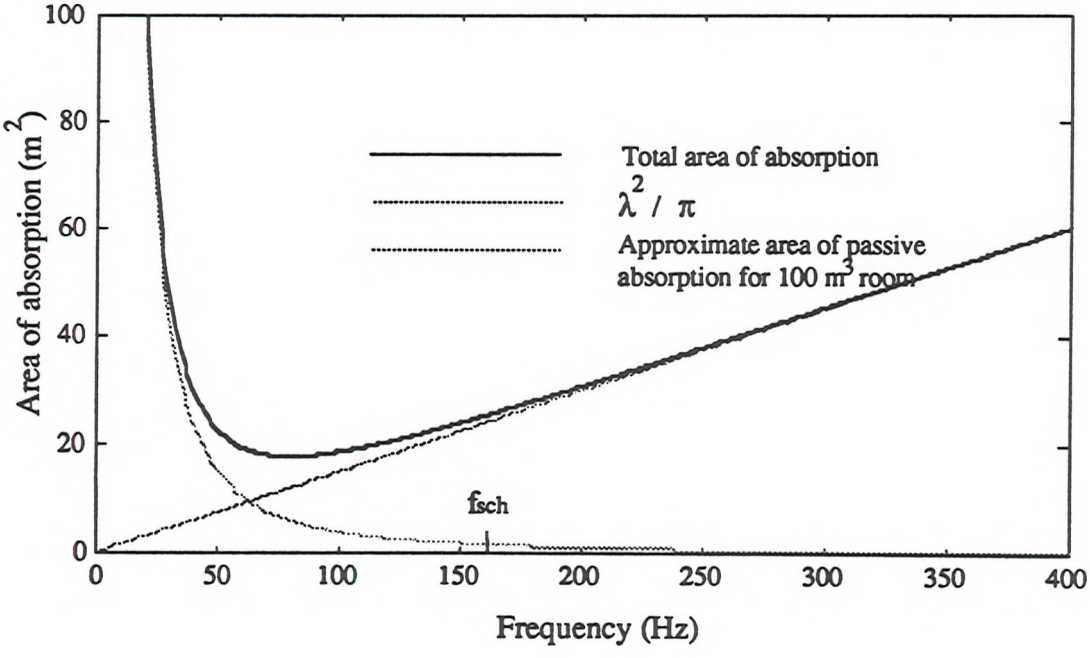

Figure 3.12. A comparison of the total passive absorption in a medium sized room (100 m^3) with the area of active absorption afforded by an optimally absorbing point monopole source.

The level of potential energy reduction achievable for this illustrative example has been calculated in accordance with equation (3.101) and is plotted in figure 3.13 overleaf, where again experimental data presented by Beranek has been used.

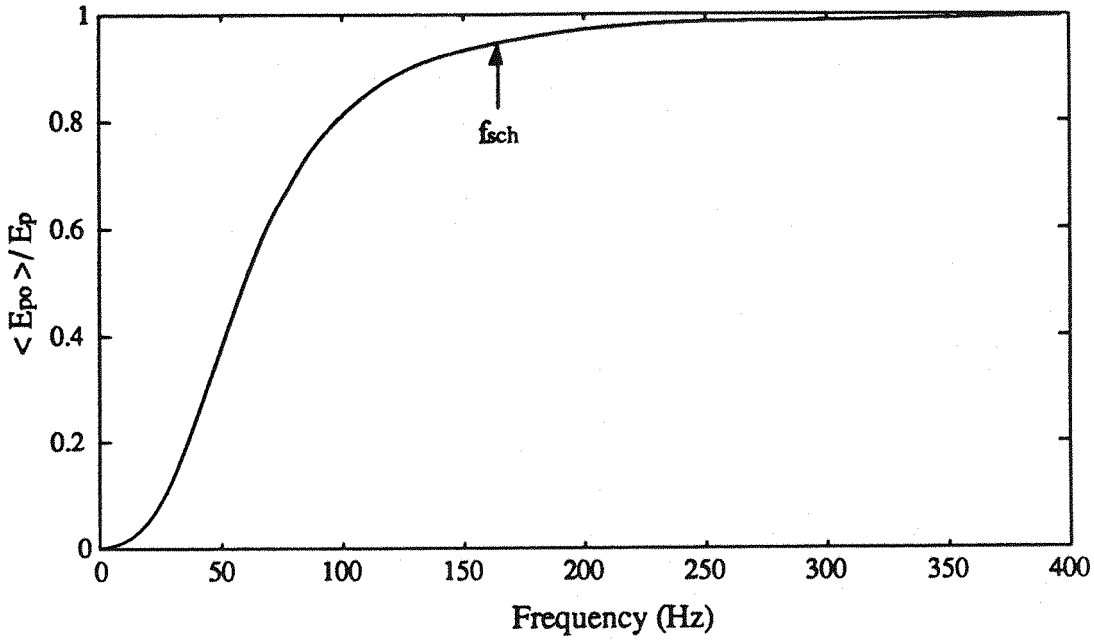

Figure 3.13. The residual potential energy in a medium sized room (100 m^3) as afforded by an optimally absorbing point monopole source in a diffuse field.

At high frequencies, the additional area of active absorption provides only a negligible supplement to the existing passive absorption provided by the acoustic tiles. At frequencies close to 100 Hz however, both the active and passive elements of absorption are, on average, observed to be roughly comparable in effective size (although physically of very different sizes). For this size of enclosure and damping characteristics, the benefits derived from the active absorber are only significant at frequencies below 75 Hz whereby the total absorption in the room is predominantly active in origin. However, it must be remembered that it is not strictly correct to extrapolate these results for frequencies very far below the Schröder frequency. Nevertheless, these results at least serve to identify the average maximum level of sound power absorption at low frequencies to within an order of magnitude even though they are susceptible to extremely large levels of variance as identified by equation (3.88). At frequencies well above the Schröder frequency, only small departures from the expected level of sound power absorption given by equation (3.87) is anticipated. Figure 3.12 nicely illustrates the philosophy behind active noise control, clearly demonstrating how active and passive control may be employed simultaneously to provide noise reduction over opposite ends of the frequency spectrum.

At the Schröder frequency, according to figure 3.13, the optimal absorption of sound affords a level of reduction in the potential energy which is of the order of only 10 %. This value appears to be characteristic of the typical levels of reduction obtainable at this frequency, falling to about 1 % at twice the Schröder frequency, when seeking to minimise energetic quantities in a diffuse field environment, see again figure 3.10.

3.10. The pressure changes in the vicinity of a perfectly absorbing point monopole

The preceding section was given to the investigation of the optimally absorbing point monopole source in a pure tone diffuse sound field. For well spaced sources, it was shown that the mechanism of sound power reduction was restricted to the absorption of sound which impinges upon the source. Just as in the case of a free field plane wave incident on a perfectly absorbing point monopole source[39], the absorption of sound in a reverberant field will, on average, influence the otherwise uniform spatial distribution of pressure throughout the enclosure. An intensity plot showing the flow of energy in and around a point monopole source seeking to optimally absorb an incident harmonic plane wave is presented by Bullmore[51]. In this section we seek to establish the size and extent of similar spatial effects on the near field pressure from a perfectly absorbing point monopole in a pure tone diffuse sound field.

For well separated sources, the source strength of the optimally absorbing point monopole has been derived in equation (3.78)

$$q'_{so} = - \frac{Z(r_p|r_s)}{2\Re\{Z(r_s|r_s)\}} q_p \qquad (3.78)$$

For ease of analysis, it is necessary to restrict the range of secondary source positions within the room for which the direct field from the secondary source is much greater than the reverberant field such that $Z_0 >> \Re\{Z_r(r_s|r_s)\}$. For these cases the secondary source strength q'_{so} is closely approximated by

$$q'_{so} \approx -q_p \, Z(r_p|r_s) / 2Z_0 \qquad (3.102)$$

which is therefore small compared to q_p.
This not unreasonable simplification ensures that the algebra remains manageable which otherwise would tend to obscure the underlying physics. Neglecting the reverberant contribution from the secondary source and using equation (3.102) enables the total pressure $p(r_s + \Delta r)$ at a distance Δr from the secondary source to be written as

$$p(r_s + \Delta r) \approx p_p(r_s + \Delta r) - p_p(r_s) \, j \frac{e^{-jk\Delta r}}{2k\Delta r} \qquad (3.103)$$

Taking the square of the modulus $|p(r_s + \Delta r)|^2$ yields

$$|p(r_s + \Delta r)|^2 \approx |p_p(r_s + \Delta r)|^2 - p_p^*(r_s + \Delta r)\, p_p(r_s)\, j\frac{e^{-jk\Delta r}}{2k\Delta r} + p_p(r_s + \Delta r)\, p_p^*(r_s)\, j\frac{e^{jk\Delta r}}{2k\Delta r} + |q_p|^2 \frac{|p_p(r_s)|^2}{(2k\Delta r)^2} \quad (3.104)$$

Now taking the expectation $< |p(r_s + \Delta r)|^2 >$ and using the relationships

$$< p_p(r_s + \Delta r)\, p_p^*(r_s) > + < p_p^*(r_s + \Delta r)\, p_p(r_s) > = < |p_{pr}(r)|^2 > \rho(\Delta r) \quad (3.105)$$

yields the simplified result

$$< |p(r_s + \Delta r)|^2 > \approx < |p_{pr}(r)|^2 > \left(1 + \frac{1}{(2k\Delta r)^2} - \rho(\Delta r)\, \frac{\sin k\Delta r}{k\Delta r} \right) \quad (3.106)$$

Now putting $\rho(\Delta r) = \sin k\Delta r / k\Delta r$ for pure tone three dimensional diffuse sound fields, the expectation for the square pressure in the vicinity of a perfectly absorbing point monopole source can now be written as

$$< |p(r_s + \Delta r)|^2 > \approx < |p_{pr}(r)|^2 > \left(\frac{1 + 4\,[(k\Delta r)^2 - \sin^2 k\Delta r]}{(2k\Delta r)^2} \right) \quad (3.107)$$

A plot of this function is given below for $r_s = 0$. Also indicated is a circle of radius $\lambda/2\pi$ symbolising the sphere whose surface is the average cross sectional area of absorption.

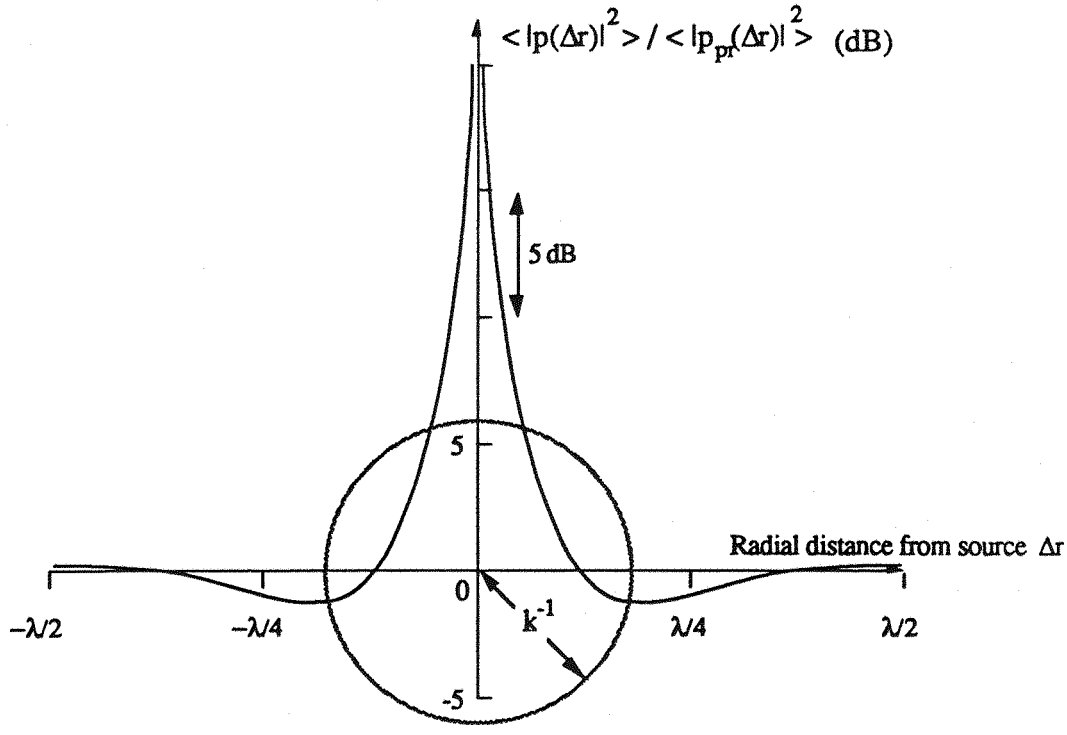

Figure 3.14. The expected square pressure ratio on axis of a perfectly absorbing point monopole source in a pure tone diffuse sound field shown as a solid line. The circle denotes a cross section through the maximum sphere of absorption.

The average effect of sound power absorption in the immediate vicinity of the point source is quite clearly a sinusoidal modulation the square pressure well into the far field of the source but whose amplitude diminishes inversely as the square of the radial distance from the source. Beyond a few wavelengths from the source however, the square pressure has recovered the original primary source value in the absence of control. Observe that the maximum level of attenuation is only about 3 dB. This contrasts the equivalent free field plane wave example[39] where a maximum reduction of approximately 5 dB is apparent at a distance of 0.05 λ from the source. This level of difference arises because in the diffuse field, the reduction in the square pressure is now distributed equally in all radial directions owing the isotropy of the field whereas for the plane wave example, the reduction in pressure is concentrated on the side of the source which firsts impacts with the plane wave.

3.11. Discussion and conclusion

This chapter has studied the possibilities for active noise control in diffuse fields for producing reductions in the acoustic pressure which extend considerably further than the immediate near fields of the sources to encompass the entire space bounded by the enclosure walls. This is what is meant by global control. Recognising that this is an unrealistic objective for the vast majority of real primary sources which are commonly, large and irregularly shaped vibrating bodies, the total minimum sound power output of two closely spaced elementary point sources has been derived. Although this source configuration is in many respects an over simplification of the type of control problem encountered in reality, the problem embodies all of the important features of the more general high frequency enclosed sound field problem.

The early part of this chapter has been given to clarification of what is meant by 'diffuseness' together with a brief survey of some of its important characteristic properties. According to the relevant literature, it would appear that there are two popular conceptions of diffuseness. One envisages a definite state of perfect diffuseness as might be true of the pressure at a single point surrounded by an infinite number of uncorrelated point sources. The other is more useful and less rigourous which conceives only of a probabilistic state of diffuseness which says that energy has an equal probability of arriving from any angle equally. This is fundamentally different from the first idealisation where energy *is* arriving from all angles equally. It is the latter definition which will be used in this thesis.

In many respects, the derivation of the minimum sound power output of two closely spaced diffuse field point sources is simply an extension of the free field analysis

presented by Nelson *et-al*[40]. There are, however, many fundamental differences which will be summarised here by way of conclusion. In the free field, the minimum sound power output is a deterministic function of the source separation distance and the frequency of excitation. Carrying out an identical experiment in the diffuse field introduces random uncertainties which arise due to extremely complicated interference patterns formed by the superposition of a large number of simultaneously excited acoustic modes of the enclosure. One can therefore only identify the levels of sound power reduction by way of a mathematical expectation with respect to varying source position. As in the one dimensional example discussed in chapter 2, the presence of reflected sound enhances the performance of the control process inasmuch that more sound power can be reduced than in the free field. This is of course due to the absorption of reflected sound.

Diffuse field quantities are also subject to levels of dispersion from point to point in the enclosure whereas free field quantities are not. It has been generally found that the secondary source strength and the minimum sound power output are susceptible to levels of variation which are highly dependent on the source separation distance. The results obtained in the two environments are reconciled at high frequencies where the means of the diffuse field quantities approach their free field counterparts as the frequency is raised. Similarly, the expected level of excursion from the mean, characterised by the variance, becomes systematically lessened as the frequency is increased, indicating that the diffuse field is, in essence, approaching free field conditions.

One other fundamental property of diffuse field sound power minimisation is the absorption of reverberant acoustic energy. The absorption of diffuse field energy is considered to be sufficiently important and fundamental to the active control of enclosed sound fields that it has been investigated separately in this chapter. There has always been an element of uncertainty surrounding the ability of elementary sources to extract energy from rooms, although it is generally accepted that it is an inefficient strategy at high frequencies. In an attempt to address this problem directly, the maximum high frequency sound power absorption has been derived. Fortunately, the diffuse field is one of the small number of sound fields where there exists a simple relationship between the average sound intensity in the field and the space average diffuse field square pressure. This relationship has enabled the cross sectional area of absorption to be derived which is shown to take the form of a sphere whose radius is approximately equal to k^{-1} where k is the acoustic wavenumber.

This important relationship is by no means original and has been previously deduced by a number of workers seeking to derive the maximum cross sectional of

absorption for a Helmholtz resonator at resonance in a diffuse field. It is therefore gratifying to observe the consistency between the two cases, since it is entirely irrelevant whether the impedance condition necessary for optimal absorption of sound power is obtained actively or passively. The significant difference is of course that the passive device is only effective at resonance which therefore only occurs at a single frequency. By contrast, the active device offers the possibility for broadband suppression of acoustic energy as highlighted by Olson[3].

In practical terms, the optimal absorption of sound power has only a negligible influence on the global sound field which is simple to evaluate. The sound power absorbed by the secondary source is ultimately manifest as a re-distribution of the square pressure which become sinusoidally modulated along radial lines from the source. The modulation amplitude diminishes as the square of the radial distance from the source such that the influence of the point source is negligible further than about a wavelength. Extrapolating the cross sectional area of absorption down to low frequencies (where it is not strictly valid) reveals that for medium sizes rooms, of the order of 100 m^3, the reduction in potential energy is only significant, say less than 3 dB, for frequencies below about 50 Hz. However, the variance between successive measurements of the source sound power absorption at these frequencies is extremely large making the mean value an inappropriate indicator of central tendency

APPENDIX 3

Appendix 3.1. The derivation of the space averaged squared pressure in the high frequency limit

This Appendix presents in more detail the derivation outlined by Morse[65] for the squared pressure high frequency limit. For a point monopole sources located at some point $\mathbf{r}_q$, the acoustic pressure at $\mathbf{r}$ is given by

$$p(\mathbf{r},\omega) = q \sum_{n=0}^{\infty} a_n(\omega)\psi_n(\mathbf{r}_q)\psi_n(\mathbf{r}) \qquad \text{(A3.1)}$$

where $\psi_n(\mathbf{r}_q)$ is the n^{th} normal mode of the enclosure evaluated at the source position. For a three dimensional enclosure, n represents a triple index set denoting a trio of modal integers (n_1,n_2,n_3). The modal response function $a_n(\omega)$ is is given by

$$a_n(\omega) = \frac{\rho c_0^2}{V} A_n(\omega) \text{ where } A_n(\omega) = \frac{(1/\Lambda_n)\,\omega}{2k_0\omega - j(\omega_n^2 - \omega^2)} \qquad \text{(A3.2)}$$

where k_0 is the room damping which is related to the total room absorption A by $k_0 = (Ac_0 / 8V)$ and where Λ_n is a source factor which is equal to unity for sources well away from boundaries. The average square pressure $< |p(\mathbf{r},\omega)|^2 >$ taken over all points in the room (keeping $\mathbf{r}_q$ fixed) is determined from equation (A3.1) and (A3.2) to give

$$< |p(\mathbf{r},\omega)|^2 > = |q|^2 \frac{\rho^2 c_0^4}{V^3} \sum_{n=0}^{\infty} \frac{(1/\Lambda_n)^2\,\omega^2}{(2k_0\omega)^2 + (\omega_n^2 - \omega^2)^2} \psi_n^2(\mathbf{r}_q) \int_V \psi_n^2(\mathbf{r})\, dV \qquad \text{(A3.3)}$$

where it has been assumed that only modes of the same modal index n do not integrate to zero due to the orthogonality of the modes normalised thus

$$\int_V \psi_n^2(\mathbf{r})\, dV = \Lambda_n V \qquad \text{(A3.4)}$$

$$\int_V \psi_n(\mathbf{r})\psi_m(\mathbf{r}) dV = 0 \qquad \text{(A3.5)}$$

The average square pressure over all space is therefore determined from

$$< |p(r,\omega)|^2 > = |q|^2 \frac{\rho^2 c_0^4}{V} \sum_{n=0}^{\infty} \frac{\omega^2}{(2k_0\omega_n)^2 + (\omega_n^2 - \omega^2)^2} \psi_n^2(r_q)\, \Lambda_n^{-1} \qquad \text{(A3.6)}$$

The product of terms $\psi_n^2(r_q)\, \Lambda_n^{-1}$ is defined as the 'source factor' E(S)[65] whereby

E(S) = 1	for sources well away from room boundaries.	
E(S) = 2	"	" on walls.
E(S) = 4	"	" on edges.
E(S) = 8	"	" in corners.

The space averaged square pressure is now given by

$$< |p(r,\omega)|^2 > = |q|^2 \frac{\rho^2 c_0^4}{V^2} E(S) \sum_{n=0}^{\infty} \frac{\omega^2}{(2k_0\omega_n)^2 + (\omega_n^2 - \omega^2)^2} \qquad \text{(A3.7)}$$

The modal summation written above may be shown to take a well defined form in the high frequency limit. Equation (A3.7) is as summation over all modal natural frequencies ω_n. At 'high' frequencies, the modal density is sufficiently high that the discrete variable ω_n may be replaced by the continuous variable u and the summation replaced by an integral. This is the essence of Schröder's principle[37]. Assuming that only terms ω_n close to ω make significant contributions to the summation, one can therefore write

$$< |p(r,\omega)|^2 > \approx |q|^2 \frac{\rho^2 c_0^4}{V^2} E(S) \int_0^{\infty} < |A_n(\omega)|_u^2 > \left(\frac{dN}{d\omega}\right)_{\omega=u} du \qquad \text{(A3.8)}$$

The term (dN / dω) is the asymptotic modal density ($\omega^2 V / 2\pi^2 c_0^3$) evaluated at the centre frequency $\omega = u$ and the term $< |A_n(\omega)|_u^2 >$ is the average modal coupling factor given by equation (A3.2) also evaluated at $\omega = u$. This approximation gives

$$< |p|^2 > \approx |q|^2 \frac{\rho^2 c_0 \omega^2}{2V\pi^2} E(S) \int_0^{\infty} \frac{u^2\, du}{(2k_0 u)^2 + (u^2 - \omega^2)^2} \qquad \text{(A3.9)}$$

Assuming that $k_0 << \omega$, then small error is incured if one sets the lower limit of the integral to $-\infty$ and if one puts $(u^2 - \omega^2) = (u - \omega)2u$ (since the only $u \approx \omega$ contributes greatly to the integral). Also putting $x = u - \omega$, the integral now reduces to

$$\int_{-\infty}^{\infty} \frac{u^2\,du}{(2k_0u)^2 + (u^2 - \omega^2)^2} \approx \frac{1}{4}\int_{-\infty}^{\infty} \frac{dx}{k_0^2 + x^2} \qquad \text{(A3.10)}$$

which is a standard integral whose solution is given by

$$\frac{1}{4}\int_{-\infty}^{\infty} \frac{dx}{k_0^2 + x^2} = \frac{\pi}{4k_0} \qquad \text{(A3.11)}$$

The space averaged squared pressure $< |p(r,\omega)|^2 >$ in the high frequency limit is therefore closely approximated by[65]

$$< |p(r,\omega)|^2 > \approx |q|^2 \frac{\rho^2 c_0 \omega^2}{8V\pi k_0} E(S) \qquad \text{(A3.12)}$$

Appendix 3.2. A discussion on the existence of the space averaged secondary source strength for minimising the conbined sound power outputs from itself and a closely spaced point primary source

One can demonstrate the ill-conditioning of q_{so} as determined from equation (3.36) by showing that its expectation value over all space is equal to infinity. Re-writing equation (3.36) as the sum of two terms yields

$$q_{so} = -\frac{Z_0 \text{sinc} k\Delta r}{Z_0 + \Re\{Z_r(r_s|r_s)\}} q_p - \frac{\Re\{Z_r(r_p|r_s)\}}{Z_0 + \Re\{Z_r(r_s|r_s)\}} q_p \qquad \text{(A3.13)}$$

Consider the mathematical expectation of the first term in equation (A3.13). It is sufficient to show that if the expectation of either term is infinite, then $< q_{so} >$ is also infinite. Earlier work has argued that $\Re\{Z_r(r_s|r_s)\}$, which for brevity will be represented by $\Re\{Z_r(r)\}$, is a zero mean normally distributed random variable whose probability density function is given by

$$f_Z(\Re\{z_r\}) = \frac{1}{\sqrt{2\pi\sigma_z^2}} e^{-\Re^2\{z_r\}/\sigma_z^2} \qquad \text{(A3.14)}$$

Unlike the behaviour of a perfect Gaussian random variable, the probability density function of the diffuse field radiation resistance $\Re\{Z_r(r_s|r_s)\}$ must have positive skewness (third moment) by virtue of the fundamental restriction[74]

$$-Z_0 \leq \Re\{Z_r(r_s|r_s)\} \leq \infty \tag{A3.15}$$

which follows directly from energy conservation. It is obvious that in the absence of any external primary sound field, the sound power flowing into the secondary source through absorption of the reflected sound cannot exceed the original power radiated into the space directly.

The mean (or first moment) of the first term in equation (A3.13) may be formally evaluated from the integral of the function taken over all possible radiation resistance values $\Re\{Z_r(r)\}$ given in equation (A3.13) weighted by the probability density function as indicated below

$$< \frac{-Z_0 \text{sinc} k\Delta r}{Z_0 + \Re\{Z_r(r)\}} > = - \int_{-Z_0}^{\infty} \frac{f_Z(\Re\{z_r\}) Z_0 \text{sinc} k\Delta r}{Z_0 + \Re\{Z_r(r)\}} d\Re\{z_r\} \tag{A3.16}$$

which upon substitution of $f_Z(\Re\{z_r\}$ in equation (A3.16) yields

$$= - \frac{Z_0 \text{sinc} k\Delta r}{\sqrt{2\pi\sigma_z}} \int_{-Z_0}^{\infty} \frac{e^{-\Re^2\{z_r\}/\sigma_Z^2}}{Z_0 + \Re\{Z_r(r)\}} d\Re\{z_r\} \sim \int_{-1}^{\infty} \frac{e^{-x^2}}{1+x} dx = \infty \tag{A3.17}$$

Reference to tables of integrals[85] indicates that this expectation does not exist inasmuch that the integral fails to converge. One can therefore infer that the proper mathematical expectation of the optimal secondary source $< q_{so} >$ is also equal to infinity. This is of course unhelpful and very misleading since the closely spaced source pair is tightly coupled at close separation distances and consequently only a small departure in the secondary source strength from one source position to the next is anticipated. This surprising and unfortunate result is an artefact of the mathematical model and not some ill-conditioning in the governing physics as will soon become apparent. In terms of the mathematics, a plot of the general form of the integrand $I = e^{-x^2}(1+x)^{-1}$ appearing in the divergent integral of equation (A3.17) indicates the cause of this unfortunate ill-conditioning.

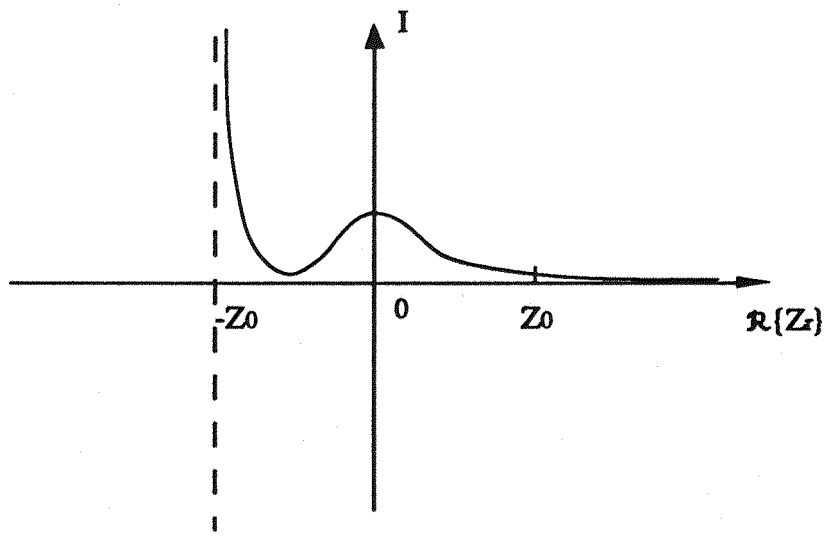

Figure A3.1 The general form of the integrand in equation (A3.17)

Observe from equation (A3.17) that as $\Re\{Z_r\}$ tends to plus infinity, the integrand decays to zero faster than $e^{-\Re^2\{z_r\}}$ and is therefore well behaved in this limit. The ill-conditioning of the integral is therefore almost certainly due to the singularity in the integrand I and the corresponding behaviour of the probability density function in the vicinity of $\Re\{Z_r\} \approx -Z_0$. In physical terms, this condition describes the situation where the sound power radiated into the medium directly is exactly counterbalanced by sound power flowing into the source by absorption. Unfortunately, the behaviour of the *assumed* form of the probability density function in this region does not assist the convergence of the integral. It is of course arguable that the distribution of radiation resistances is *not* Gaussian in the immediate vicinity of $-Z_0$ but some other more rapidly varying function for which the integral in equation (A3.17) is convergent. To the authors knowledge, there are no references made to this phenomenon in the published literature, in the absence of which, the distribution of radiation resistances of a point source radiating into a diffuse field environment will continue to be assumed Gaussian. However, convergence of this integral is only guaranteed providing the probability density function $f_Z(\Re\{z_r\})$ behaves like x^n in the vicinity of $-Z_0$, where a necessary and condition on 'n' is that $n > 1$.

Assuming a Gaussian probability density function for the distribution of diffuse field radiation resistances, one may obtain a very *approximate* estimate (within an order of magnitude) of how likely q_{so} is of being singular. This may be obtained by re-writing the term in the expression for the secondary source strength q_{so} in the form of

$$\frac{Z_0 \text{sinc}k\Delta r}{Z_0 + \Re\{Z_r(r)\}} = \frac{\text{sinc}k\Delta r}{1+\gamma} \qquad \text{(A3.18)}$$

where γ represents the real part of the ratio of reflected to directly transmitted sound $\Re\{Z_T(r)\}/Z_0$. Assume that γ is a zero mean, normally distributed random variable whose variance is given by the mean of the square $<\gamma^2>$. The standard deviation σ_γ is therefore given by $<\gamma^2>^{1/2}$. For convenience of computation, further assume that γ extends from minus infinity to plus infinity. Given that the cause of the non-convergence of the integral in equation (A3.17) is due to a singularity in the integral appearing at $\gamma = 1$, one can readily show that this is a remote occurrence. The probability that γ will equal, or exceed unity is equivalent to evaluating the probability that γ will equal, or exceed a number $<\gamma^2>^{-1/2}$ standard deviations from the mean. For normally distributed random variables, this exceedance likelihood is determined from the complementary error function given by

$$P(\gamma \geq 1) = 1 - \mathrm{Erf}(<\gamma^2>^{-1/2}) \qquad \text{(A3.19)}$$

where the Error function Erf(x) is the cumulative normal distribution defined by

$$\mathrm{Erf}(x) = \sqrt{\frac{2}{\pi}} \int_0^x e^{-u^2}\, du \qquad \text{(A3.20)}$$

This function is not expressible in terms of elementary functions and is therefore tabulated[85]. The tendency of γ to take small values less than unity is best illustrated by way of example. Consider the case of two closely spaced point sources in which the average resistive part of the scattered sound is one half the directly radiated part namely $<\gamma^2>^{1/2} = 1/2$. Tables indicate that the probability that γ is equal or greater than unity namely $P(\gamma \geq 1)$, is given by

$$P(\gamma \geq 1) = 1 - \mathrm{Erf}(2) \approx 0.04 \qquad \text{(A3.21)}$$

In this example, less than 4 % of diffuse field source positions have *more* sound power radiated into the medium via wall reflections than sound power radiated directly. However, it is only when the sound power contributions from the two transmission paths are exactly equal (and opposite) which causes the integral to diverge. The probability that this condition is exactly satisfied and consequently the secondary source strength is equal to infinity is considerable less than 4 %.

Appendix 3.3. The derivation of the expectation $<\Re\{Z_T(r_p|r_p)\}\Re\{Z_T\{r_s|r_s)\}>$

Consider the expectation $<\Re\{Z_T(r_p|r_p)\}\Re\{Z_T\{r_s|r_s)\}>$, where the subscripts "p" and "s" denote the transfer impedance from the primary source at r_p evaluated at r_p and the transfer impedance from the secondary source at r_s evaluated at r_s respectively.

The point transfer impedance $\Re\{Z_T(r_S|r_S)\}$ may be expressed relative to $\Re\{Z_T(r_S|r_p)\}$, the transfer impedance from the secondary source at r_S to the point r_p in terms of its correlated and uncorrelated parts $\Re\{Z_T(r_S|r_p)\}_{cs}$ and $\Re\{Z_T(r_S|r_p)\}_{us}$ respectively

$$\Re\{Z_T(r_S|r_S)\} = \Re\{Z_T(r_S|r_p)\}_{cs} + \Re\{Z_T(r_S|r_p)\}_{us} \tag{A3.22}$$

where the subscripts "cs" and "us" denote perfectly correlated and perfectly uncorrelated with respect to the pressure from the secondary source at r_S.

$$<\Re\{Z_T(r_p|r_p)\}\Re\{Z_T(r_S|r_S)\}> = <\Re\{Z_T(r_p|r_p)\}\Re\{Z_T(r_S|r_p)\}_{cs}>$$

$$+ <\Re\{Z_T(r_p|r_p)\}\Re\{Z_T\{r_S|r_p)\}_{us}> \tag{A3.23}$$

Invoking the principle of reciprocity, the source and point of observation may be interchanged thus

$$<\Re\{Z_T(r_p|r_p)\}\Re\{Z_T(r_S|r_S)\}> = <\Re\{Z_T(r_p|r_p)\}\Re\{Z_T(r_p|r_S)\}_{cp}>$$

$$+ <\Re\{Z_T(r_p|r_p)\}\Re\{Z_T(r_p|r_S)\}_{up}> \tag{A3.24}$$

By definition, one can write

$$<\Re\{Z_T(r_p|r_p)\}\Re\{Z_T(r_p|r_S)\}_{up}> = 0 \tag{A3.25}$$

where now $\Re\{Z_T(r_p|r_S)\}_{cp}$ represents that part of the pressure at r_S perfectly correlated with the pressure at r_p from the source at r_p. Following the work of Cook *et-al* [68]

$$<\Re\{Z_T(r_p|r_p)\}\Re\{Z_T(r_p|r_S)\}_{cp}> = <\Re\{Z_T(r_p|r_p)\}\Re\{Z_T(r_p|r_S)\}> \text{sinc}k\Delta r \tag{A3.26}$$

Equation (3.23) may now be re-written

$$<\Re\{Z_T(r_p|r_p)\}\Re\{Z_T(r_S|r_S)\}> = <\Re\{Z_T(r_p|r_p)\}\Re\{Z_T(r_p|r_S)\}> \text{sinc}k\Delta r \tag{A3.27}$$

where by definition of the spatial correlation function given by equation (A3.23)

$$<\Re\{Z_T(r_p|r_p)\}\Re\{Z_T(r_S|r_S)\}> = <\Re^2\{Z_T\}> \text{sinc}^2k\Delta r \tag{A3.28}$$

CHAPTER 4

LOCAL CONTROL IN THE PURE TONE DIFFUSE SOUND FIELD

4.0. Introduction

Global reductions in the acoustic pressure of a diffuse field has been shown to be physically possible for the geometry discussed in chapter 3 in which the primary source of noise is an elementary point monopole and the secondary source is also a point monopole but close to the primary source. This contrived source geometry is blatantly not representative of typical noise sources which are often large, irregularly shaped complex vibrating bodies. For these more realistic kind of sources, global silence is only guaranteed providing the primary source and secondary source are geometrically similar and exactly superposed, or if there are an infinite number of secondary sources[13]. One other approach for global reductions in the sound pressure level is the absorption of diffuse field sound power but this strategy is found to be ineffective at high frequencies. It soon becomes clear that global extinction of the pressure field over the entire space is unrealistic for this kind of wave field and one must seek to apply active noise control in a more pragmatic fashion.

One of the simplest and most obvious ways to engineer reductions in the sound pressure level in *any* harmonically excited sound field is to employ a single secondary loudspeaker in order to drive the acoustic pressure at a single point to zero. In this chapter we consider this active control strategy for those cases where the secondary source is remote (many wavelengths) from the primary source. In the case of an infinite duct supporting only plane waves, this control strategy is sufficient, in principle, to secure complete silence downstream of the secondary source[86]. Surprisingly, the spatial extent of the reduction in the sound pressure level for the important limiting case of the diffuse field has only recently been quantified[87]. The phrase ' zone of quiet ' is coined here to describe the spatial region of pressure reduction centred on the point of control in the diffuse field. The term 'zone' is carefully used to suggest that the region of attenuation does not extend appreciably far from the control point, but is confined to localised regions within the diffuse field compared to the acoustic wavelength. Not only is a quantitative assessment of the diffuse field zone of quiet important in that it identifies a worst possible case, but also because it has considerable practical implications. It is worth noting that in the two enclosures where active noise control has been contemplated (the interior of cars and the interior of medium size propeller aircraft), the Schröder frequency has been experimentally

estimated at being between 100 Hz and 150 Hz. This frequency band is well within the frequency range of many important noise sources such as an aeroplane propeller which radiates a series of pure tones harmonically related to the blade passage frequency, or the firing frequency of four cylinder internal combustion engines in cars[88]. When applying localised active control to this type of sound field, one must address three important considerations, namely:

(i) The local effects: The shape and size of the space averaged square pressure profile around the point of cancellation where the respective sound fields are highly correlated, and ultimately a full quantification of the diffuse field quiet zone.

(ii) Global changes: The effect on the average square pressure well away from the point of control where the respective sound fields are uncorrelated (the change in the potential energy of the sound field).

(iii) Secondary source strength requirements: The statistical distribution of secondary source strengths required to bring about the point cancellation at any arbitrary point generated by a source located at some arbitrary position.

Clearly, the facets of the problem listed above are inextricably inter-related. For example, harmonic secondary source strengths which are necessarily large compared with the primary source strength are able to cause significant increases in the average square pressure in the enclosure. This in turn has a detrimental effect on the size of the quiet zone about the control point. In this chapter, all three considerations are systematically investigated from a theoretical standpoint and subsequently validated using computer simulated models.

4.1. The cancellation of the pressure at a single point

Consider the enclosed sound field shown in figure 4.1 in which there are two harmonic sources $q_p(\omega)$ and $q_s(\omega)$ located at $\mathbf{r}_s$ and $\mathbf{r}_p$ respectively radiating at a single frequency which is presumed to be greater than the Schröder frequency. The secondary source is driven from the primary source with the aim of cancelling the acoustic pressure at some arbitrarily chosen point $\mathbf{r}_0$ in the enclosure to zero.

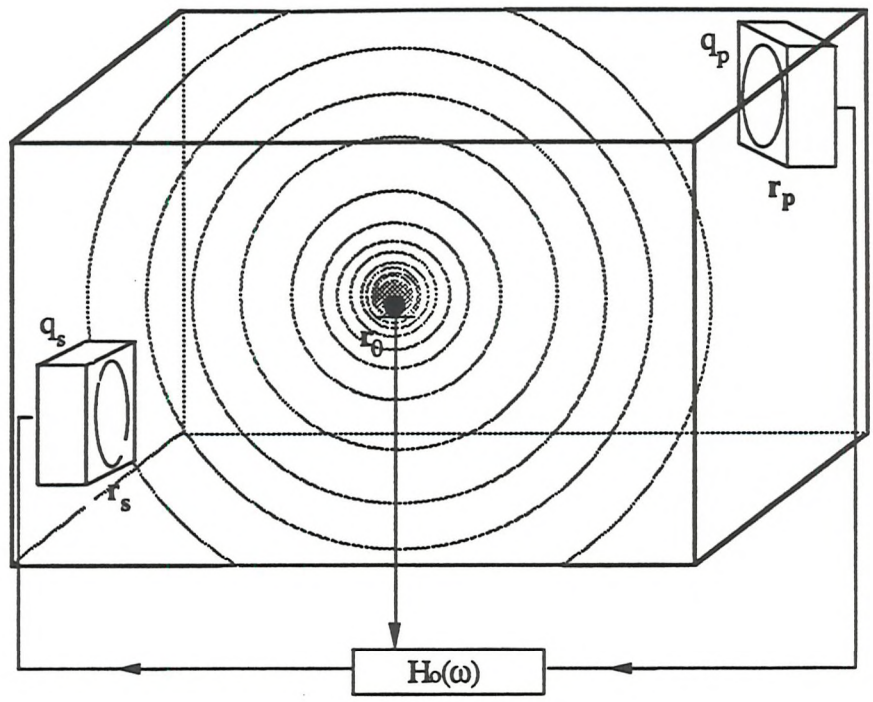

Figure 4.1 A schematic representation of the primary and secondary sources radiating within an enclosure where the secondary source is driven by the primary source via a transfer function $H_o(\omega)$ *so as to drive the pressure at ro to zero.*

No assumption is made here concerning the nature of the source distributions. For small amplitude oscillations, linear superposition applies so that

$$p(\mathbf{r}) = q_p Z(\mathbf{r}_p|\mathbf{r}) + q_s Z(\mathbf{r}_s|\mathbf{r}) \tag{4.1}$$

where the current notation has been introduced in Chapter 3. Again the dependence on frequency has been omitted since all acoustic variables of interest are statistically similar above the Schröder frequency. In principle, the linearity of the superposed acoustic fields allows for any one point $\mathbf{r}_0$ in the sound field to be driven to zero i.e., $p(\mathbf{r}_0) = 0$ for a unique secondary source strength q_{so} which is given by

$$q_{so} = H_o q_p \tag{4.2}$$

The optimal secondary source strength has been written in this way to indicate that it is derived from the primary source strength via a linear transformation which is the transfer function of the notional electronic controller. By inspection of equation (4.2), the transfer function H_o which secures the complete cancellation of the acoustic pressure at $\mathbf{r}_0$ is simply given by

$$H_o = - \frac{Z(r_p|r_0)}{Z(r_s|r_0)} \tag{4.3}$$

Writing $r = r_0 + \Delta r$, the acoustic pressure $p(r_0 + \Delta r)$ at a distance Δr from the point of cancellation on r_0 is now given by

$$p(r_0 + \Delta r) = q_p \left[Z(r_p|r_0+\Delta r) - \frac{Z(r_p|r_0)}{Z(r_s|r_0)} Z(r_s|r_0+\Delta r) \right] \tag{4.4}$$

With reference to equation (4.4), one can identify two distinct spatial regimes. The first is broadly defined by $\Delta r < \lambda/2$, the region in which the primary field $p_p(r)$ and the secondary field $p_s(r)$ are highly correlated. The second is where the point of observation is far from the point of cancellation roughly defined by $\Delta r > \lambda$, the region in which the sound fields are generally unconstrained and therefore uncorrelated such that $< p_p(r)p_s(r) > = 0$. Both regions have been investigated with the aid of a computer model whose details are the subject of the next section.

4.2. Computer model of the pure tone diffuse sound field

A good diffuse field model must be able to emulate the properties discussed in the first half of Chapter 3. There are perhaps three such mathematical models which comply with these requirements, namely the stochastic model, the free wave model and the geometrical acoustical model or ray model. All three are surveyed in an excellent review paper by Jacobsen[76]. For current purposes, our requirements are best served by the normal mode model. The acoustic pressure at any arbitrary point in the sound field is evaluated from a summation of acoustic modes which although computer intensive, is able to afford a statistical representation of the sound field that is not possible from either geometric or ray models. This model has proved successful for performing low frequency computer simulations for aiding the prediction of sound pressure level reductions in low modal density sound fields[51]. The same model will continue to be used here and is outlined below.

The model starts with the homogeneous wave equation of equation (2.2) whose solution leads to a generalised expression for the sound field in terms of an infinite sum of the normal modes of the room ψ_n weighted with the appropriate complex amplitude $a_n(\omega)$. For computational convenience, the series is truncated to N modes which is taken to be sufficiently large that the residual pressure contained by the higher order neglected in the finite summation is negligible. Each mode is an eigenfunction of the wave equation which in addition satisfies the boundary conditions of the room. Each eigenfunction has an

associated eigenvalue which is closely related to the natural frequency of the n^{th} mode ω_n. The acoustic pressure $p(r,\omega)$ in the enclosure may therefore be approximated by the finite summation of the modes thus

$$p(r,\omega) = \sum_{n=0}^{N} a_n(\omega)\psi_n(r) \tag{4.5}$$

For a three dimensional enclosure, n represents a triple index set denoting a trio of modal integers (n_1,n_2,n_3). The amplitude of modal excitation $a_n(\omega)$ is calculated from the sum of primary source and secondary source contributions which for generalised source strength density distributions $Q_s(\omega,r_s)$ and $Q_p(\omega,r_p)$ is given by[65]

$$a_n(\omega) = A_n(\omega)\left[\int_{S_p} Q_p(\omega,r_p)\psi(r_p)dr_p + \int_{S_s} Q_s(\omega,r_s)\psi_n(r_s)dr_s \right] \tag{4.6}$$

where the integration is taken over the respective source surfaces S. For the simplest possible source geometry in which the source distributions are simple point monopoles $Q_p(\omega,r_p) = q_p(\omega)\delta(r - r_p)$ and $Q_s(\omega,r_s) = q_s(\omega)\delta(r - r_s)$, the integrations reduce to straightforward multiplications

$$a_n(\omega) = A_n(\omega)\left[q_p(\omega,r_p)\psi(r_p) + q_s(\omega,r_s)\psi_n(r_s) \right] \tag{4.7}$$

The term $A_n(\omega)$ is the frequency dependent modal coupling factor

$$A_n(\omega) = \frac{\rho c_0^2}{V} \frac{\omega}{2\xi\omega_n\omega - j(\omega_n^2 - \omega^2)} \tag{4.8}$$

By comparison with equation (4.1), the transfer impedances may be represented as a series summation in terms of the orthogonal modes of the enclosure

$$Z(r_p|r) = \sum_{n=0}^{N} A_n(\omega)\psi_n(r_p)\psi_n(r) \tag{4.9}$$

and

$$Z(r_s|r) = \sum_{n=0}^{N} A_n(\omega)\psi_n(r_s)\psi_n(r) \tag{4.10}$$

The diffuse field transfer impedance may now be considered to comprise a large series of second order resonators each associated with an orthogonal modes of the

enclosure. It is the assumption of a large number of significantly contributing terms which forms the basis of statistical diffuse field theory.

In principle, the properties of the diffuse wavefield are insensitive to the exact form of the constituent room modes ψ_n which are a function of the room geometry and boundary conditions only. For computational simplicity, the room supporting the diffuse field was chosen to be a hard walled rectangular enclosure whose mode shapes are known to be simple three - fold sinusoids[65]. The room dimensions were chosen to be the independent, fundamental constants π x e x 1m so as to provide for an irrational aspect ratio and therefore prevent modal degeneracy. This precaution ensures that the room modes encompass the frequency range more uniformly so that the sound field appears less resonant since the acoustic response comprises significant contributions from a large number of modes. The reverberation time T_{60} was set to 0.5s corresponding to a modal damping ζ equal to about 0.0014. Using the simple engineering formula given in equation (3.4), the Schröder frequency f_{sch} for this sound field can be calculated to be 738 Hz. The frequency of excitation was set to 1500 Hz, more than twice the Schröder frequency which hopefully will compensate for the high degree of symmetry associated with the rectangular geometry which will tend to focus the sound field. The international standard which advises on the construction of reverberation rooms for diffuse field measurements, ISO 2638, strongly recommends against the use of parallel walls.

The acoustic pressure was computed according to equation (4.5). Incorporating all modes with a natural frequency below 2 kHz was found to be sufficient to ensure a series representation of the acoustic pressure to within 0.2 dB of its value using many tens of thousand modes. Modal convergence is further assured by ensuring that the measurement point is well away from the enclosure boundaries and not close to the point source of sound. In practice, satisfactory modal convergence was achieved from the summation N, of nearly 8000 room modes. Before proceeding to simulate the effects of active control of diffuse fields, the simulated sound field was tested for diffuseness inasmuch as it complies with the properties discussed in the first half of chapter 3.

First, an estimate of the average square pressure $< |\hat{p}|^2 >$ was obtained from over 200 simulations of the sound field. The hat '$\wedge$' is used to denote random quantities which are not true expectations but estimates owing to the finite sample size. In each case, both the source position and the measurement position were randomly altered within the enclosure with the constraint that for each simulation they remain further than a wavelength apart and further than half a wavelength from the walls. The mean value of the relatively

small sample was calculated to be within 0.1 dB of the theoretically predicted result given by equation (3.20) $< |p|^2 > = |q|^2\rho^2\omega c_0 / 8\pi\zeta V$.

Second, the spatial cross correlation function $\rho(\Delta r)$ was computed according to equation (3.22) for 440 simulations of the sound field. In each case, both the source position and the measurement position were randomly positioned within the enclosure although the orientation of Δr remained fixed with respect to the enclosure. The result, calculated for Δr between zero and two wavelengths at 100 equal intervals, is shown in figure 4.2 together with the theoretically predicted result $\rho(\Delta r) = \text{sinc}k\Delta r$.

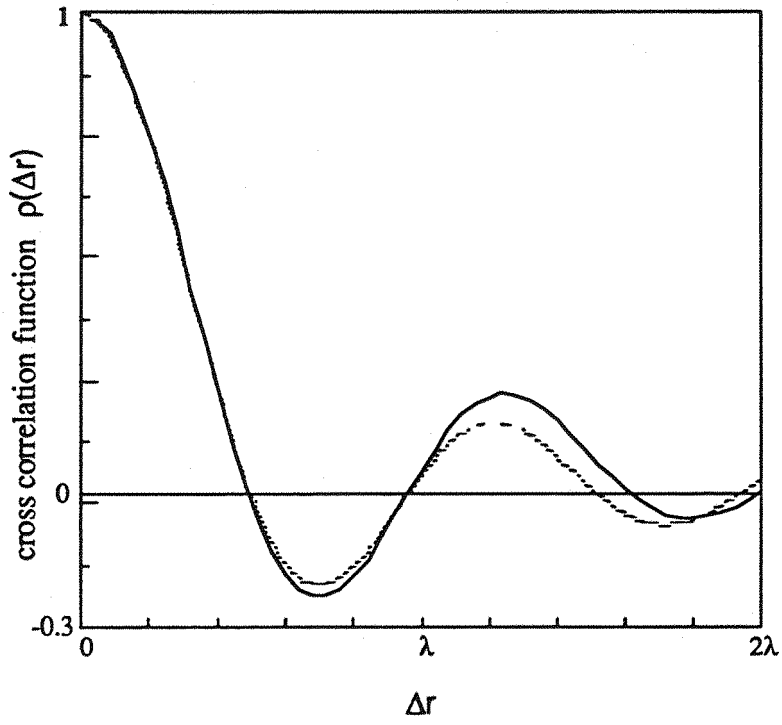

Figure 4.2 The simulated cross correlation function of the simulated diffuse sound field obtained from 440 measurements (dashed line), together with the theoretical result $\rho(\Delta r) = \text{sinc}k\Delta r$ *(solid line).*

A good fit to the expected form is obtained for Δr up to about one wavelength, above which, the curves begin to exhibit appreciable departure. This is a common experience in diffuse field correlation measurement which can usually be resolved by the incorporation of more measurements into the space average[89] or taking the correlation between pressures which comprise a narrow band of frequencies[70]. For Δr less than half a wavelength however, a good fit to the theoretical expectation is achieved from an average comprising less than twenty simulations. This is precisely the region which governs the variation in square pressure about the point of cancellation as will become clear in the next section. However, these standard tests serve to validate the diffuseness of the hypothetical sound field in so far as they allow an objective assessment for which other fields may be

compared. Neither test permits an unequivocal appraisal of the sound field diffuseness and it is therefore generally accepted that these properties are fairly insensitive diffuse field indicators.

4.3. Zones of quiet ($\Delta r < \lambda/2$)

This section presents a derivation of the expected value of the square pressure $< | p(r_0 + \Delta r) |^2 >$ in the vicinity of the cancellation point. This is the region where Δr is small compared to the acoustic wavelength such that the primary and secondary sound fields are highly correlated and therefore destructively interfere to a substantial degree. Assuming linearity of the primary and secondary source pressures, one can write

$$p(r_0 + \Delta r) = p_p(r_0 + \Delta r) + p_s(r_0 + \Delta r) \tag{4.11}$$

Consider the expectation $< | p(r_0 + \Delta r) |^2 >$. Multiplying out the terms and then taking the expectation yields four terms

$$< | p(r_0 + \Delta r) |^2 > = < | p_p(r_0 + \Delta r) |^2 > + < | p_s(r_0 + \Delta r) |^2 >$$

$$+ < p_p^*(r_0+\Delta r)\, p_s(r_0+\Delta r) > + < p_p(r_0+\Delta r)\, p_s^*(r_0+\Delta r) > \tag{4.12}$$

The first two terms may be summed together to produce the sum of the squared 'self pressures' in mutual isolation, assumed uncorrelated which takes the form of

$$< | p(r_0 + \Delta r) |^2_{self\ pressure} > = < | p_p(r_0 + \Delta r) |^2 > + < | p_s(r_0 + \Delta r) |^2 > \tag{4.13}$$

The second set of two terms, denoted by $< p(r_0 + \Delta r)^2_{Interference} >$, describes the manner in which the partially correlated sound fields interact about the point of cancellation thus

$$< p(r_0+\Delta r)^2_{Interference} > = < p_p^*(r_0+\Delta r)\, p_s(r_0+\Delta r) > + < p_p(r_0+\Delta r)\, p_s^*(r_0+\Delta r) > \tag{4.14}$$

This is the crucial term which must be negative for destructive interference to occur and ultimately determines the shape of the quiet zone. However, the size of the diffuse field zone of quiet and the increase in the pressure well away from the point of cancellation are predominantly governed by the statistical inter-dependence between the pressure fields $p_s(r)$ and $p_p(r)$ of which nothing has hitherto been presumed.

At the point of cancellation on r_0, the pressure fields are arranged to exactly cancel. The expectation $< p(r_0+\Delta r)^2_{Interference} >$ must therefore be negative in the region of the

quiet zone roughly identified by $\Delta r < \lambda/2$. Within this region, the primary and secondary sound fields are negatively correlated thereby causing partial destructive interference.

In terms of a quantitive description of the diffuse field quiet zone, the interference term $< p(r_0+\Delta r)^2_{Interference} >$ is of principal interest since it governs exactly how the combined sound fields recover from being exactly in antiphase on r_0, to being totally uncorrelated at points well away from the point of cancellation. Consider the expectation of the first term in equation (4.14), namely

$$< p_p^*(r_0+\Delta r)\, p_s(r_0+\Delta r) > \tag{4.15}$$

Each pressure term appearing in equation (4.15) may be resolved into two orthogonal pressure components. The first, given by $p(r_0+\Delta r)_c$ is perfectly correlated with the pressure at r_0. The second is the component of the pressure $p(r_0+\Delta r)_u$ which is perfectly uncorrelated with the pressure at r_0. These pressure components are formally defined by

$$p^*(r_0)p(r_0+\Delta r)_c = |p(r_0)|^2\, \rho(\Delta r) \tag{4.16}$$

and

$$< p^*(r_0)p(r_0+\Delta r)_u > = 0 \tag{4.17}$$

Note that the right hand side of equation (4.16) has been directly related to the spatial correlation function of the sound field $\rho(\Delta r)$. This is because it is precisely this function which, by definition, characterises the causal mechanism describing the linear inter-relation between the correlated pressure at $r_0+\Delta r$ with the pressure at some other point r_0. The decomposition of the signal into correlated and uncorrelated parts is usually a technique reserved for time histories[90]. However, the analogies between random time sequences and the spatially sampled transfer impedances between two randomly position points in the diffuse wavefield have already been recognised in chapter 3 where it was found to be convenient to describe the spatially sampled diffuse wavefield as a stochastic process that was both stationary and ergodic with respect to position. Thus, for the purpose of the analysis, some of the ideas usually associated with random time histories are carried over to the randomly sampled, spatial sound field. Time t is now replaced by **r** denoting measurement position. Substituting the decomposed pressures into expression (4.15) gives

$$< p_p^*(r_0+\Delta r)\, p_s(r_0+\Delta r) > = < [p_p^*(r_0+\Delta r)_c + p_p^*(r_0+\Delta r)_u]\, [p_s(r_0+\Delta r)_c + p_s(r_0+\Delta r)_u] > \tag{4.18}$$

Writing $p_p^*(r_0+\Delta r)_c = p_p^*(r_0)\rho(\Delta r)$ and $p_s(r_0+\Delta r)_c = p_s(r_0)\rho(\Delta r)$ one obtains

$$< p_p^*(r_0+\Delta r)\, p_s(r_0+\Delta r) > =$$
$$< \{p_p^*(r_0)\rho(\Delta r) + p_p^*(r_0+\Delta r)_u\}\{p_s(r_0)\rho(\Delta r) + p_s(r_0+\Delta r)_u\} > \quad (4.19)$$

On multiplication and expansion of the terms, to a good level of approximation, three of the four terms which subsequently appear may be set equal to zero. The first is the term $< p_p(r_0+\Delta r)_u\, p_s(r_0+\Delta r)_u >$ which for well separated sources signifies the product of small terms and is therefore very close to zero in the region of the quiet zone where the primary and secondary are highly correlated. The two remaining terms, $< p_p(r_0+\Delta r)_u\, p_s(r_0) >$ and $< p_s(r_0+\Delta r)_u\, p_p(r_0) >$ are identically zero following directly from equation (4.17) providing that $p_s(r_0)$ and $p_p(r_0)$ are equal and opposite at r_0 according to

$$p_s(r_0) = -p_p(r_0) \quad (4.20)$$

This leaves just one non-zero term, namely

$$< p_p^*(r_0+\Delta r)\, p_s(r_0+\Delta r) > = < p_p^*(r_0) p_s(r_0) > \rho^2(\Delta r) \quad (4.21)$$

In exactly the same way, an identical result can also be obtained for the second term in equation (4.14) thus

$$< p_p(r_0+\Delta r)\, p_s^*(r_0+\Delta r) > = < p_p(r_0) p_s^*(r_0) > \rho^2(\Delta r) \quad (4.22)$$

Only the parts of the primary and secondary sound fields which are perfectly correlated cause destructive interference. The residual pressure that one ultimately perceives $< | p(r) |^2 >$ is therefore formed from the parts of the primary and secondary pressure fields which are mutually uncorrelated. The uncorrelated fraction of the total square pressure becomes progressively greater with increasing Δr while the correlated part correspondingly diminishes.

The expectations $< p_p(r_0) p_s^*(r_0) >$ and $< p_p^*(r_0) p_s(r_0) >$ are readily evaluated by recognising that the total pressure at the point of cancellation is identically zero. This is both true in any one single experiment and also true in the average sense from a large number of similar experiments. The two pressure contributions $p_s(r_0)$ and $p_p(r_0)$ are therefore exactly in anti-phase in accordance with equation (4.20) and so form a *new* boundary condition of the sound field given by

$$< | p_s(r_0) + p_p(r_0) |^2 > = 0 \quad (4.23)$$

Simple re-arrangement of equation (4.23) leads to

$$< p_p(r_0)p_s^*(r_0) > = < p_p^*(r_0)p_s(r_0) > = -\frac{1}{2}[\, < |\, p_p(r)\,|^2 > + < |\, p_s(r)\,|^2 >] \qquad (4.24)$$

Noting that $< |\, p_p(r_0)\,|^2 > = < |\, p_p(r)\,|^2 >$ and $< |\, p_s(r_0)\,|^2 > = < |\, p_s(r)\,|^2 >$ and substituting equation (4.24) into equation (4.12) gives the important final result[87]

$$< |\, p(r_0+\Delta r)\,|^2 > = [\, < |\, p_p(r)\,|^2 > + < |\, p_s(r)\,|^2 >]\, [\, 1 - \rho^2(\Delta r)\,] \qquad (4.25)$$

Further simplification follows from the proportionality between q_{so} and q_p so that the space averaged square secondary pressure $< |\, p_s(r)\,|^2 >$ is a simple scalar multiple of the space averaged primary square pressure $< |\, p_p(r)\,|^2 >$. From equation (3.20)

$$< |\, p_p(r)\,|^2 > = |\, q_p\,|^2 \frac{\rho^2 \omega c_0}{8\zeta\pi V} \quad \text{and} \quad < |\, p_s(r)\,|^2 > = |\, q_p\,|^2 < |H_o|^2 > \frac{\rho^2 \omega c_0}{8\zeta\pi V} \qquad (4.26)$$

where from equation (4.25), one can write

$$< \frac{|p(r_0+\Delta r)|^2}{|p_p(r)|^2} > \; = \; [\, 1 + < |H_o|^2 >]\, [\, 1 - \rho^2(\Delta r)\,] \qquad (4.27)$$

This expression for the space averaged zone of quiet in a generalised sound field which is characterised by the spatial correlation function $\rho(\Delta r)$, is an important result in the theory of active noise control. The usefulness of the result stems from its generality since no assumption has yet been made concerning the diffuseness of the wave field. The validity of the analysis therefore extends to all sound fields which are stationary with respect to position such that $\rho(r_1,r_2) = \rho(\,|r_1 - r_2|\,)$. This result is particularly relevant to diffuse sound fields whose spatial correlation functions are well defined, see Chapter 3. Equation (4.27) is therefore important in determining the size and extent of the quiet obtained in the high frequency limit, enabling one to make judgements relating to the effectiveness of active control in this type of acoustic environment.

Following from the stationarity of the diffuse field (see chapter 3), the level of square pressure attenuation steadily decreases with the absolute distance from the control point. The space averaged quiet zone about the point of null pressure is therefore a sphere. At the origin of the hypothetical sphere defined by $\Delta r = 0$, the secondary sound field is arranged to be perfectly correlated, but in anti-phase with the primary field consequently $< |\, p(r_0)\,|^2 > = 0$. Moving a short distance away from r_0 however, and the residual square

pressure increases, not instantaneously, but smoothly owing to the correlated inter-dependence of neighbouring diffuse field points. The respective pressures $p_p(r)$ and $p_s(r)$ therefore become increasingly uncorrelated with increasing Δr until the residual square pressure $< | p(r_0 + \Delta r) |^2 >$ is eventually raised above that of the original square pressure in the absence of control.

This simple result provides an intuitively correct description of the way in which two sound fields, which are constrained to be exactly in anti-phase at a single point, interact around the immediate vicinity of the point of null pressure. The result describes how the square pressure recovers smoothly from zero at r_0, to eventually attaining its asymptotic value $< | p_p(r) |^2 > + < | p_s(r) |^2 >$ as $\Delta r \rightarrow \infty$. This implicitly assumes that the correlation function between two points tends to zero as the distance between them tends to infinity. This assumption is generally valid for most sound fields although there are exceptions, notably the one dimensional sound field which is discussed in Appendix 4.1. With reference to figure 3.6 showing plots of the correlation functions for simple diffuse sound fields, the three dimensional diffuse field quiet zone will, on average, exhibit a more gradual change in the sound pressure level about the point of null pressure than either of the simpler sound fields. Nevertheless, the differences in the behaviour of the correlation functions are not pronounced for small Δr. While both $|H_0|^2$ and the spatial correlation function $\rho(\Delta r)$ influence the size of the diffuse field quiet zone, it is the square of the transfer function $|H_0|^2$ (and ultimately, the square of the secondary source strength) which emerges as by far the most important factor away from the point of control. As refered to earlier, it is the value of $|H_0|^2$ which quantifies the statistical inter-dependence between the primary and secondary pressure fields. The statistical properties of this function will be studied in detail shortly.

By way of verification, computer simulations were undertaken. The amplitude and phase of the secondary source strength q_{so} was calculated so as to drive the pressure at a point 3/8 along the longest diagonal to zero. The computer simulated experiment was repeated 200 times where in each case, both primary and secondary point sources were randomly positioned in the enclosure under the condition that they were not allowed within one wavelength of any of the enclosure boundaries, or one of the longest diagonal of the enclosure. The modulus square pressure was calculated at 100 equally spaced points, one and half wavelengths either side of the point of control along the longest diagonal. The average value from 200 simulations of the square pressure, as a fraction of the primary square pressure in the absence of control, is shown in figure 4.3. Also shown is the function $< | p(r_0+\Delta r) |^2 > = 4 < | p_p(r) |^2 > [1 - \mathrm{sinc}^2 k\Delta r]$ which appears to provide good agreement to the simulated curve.

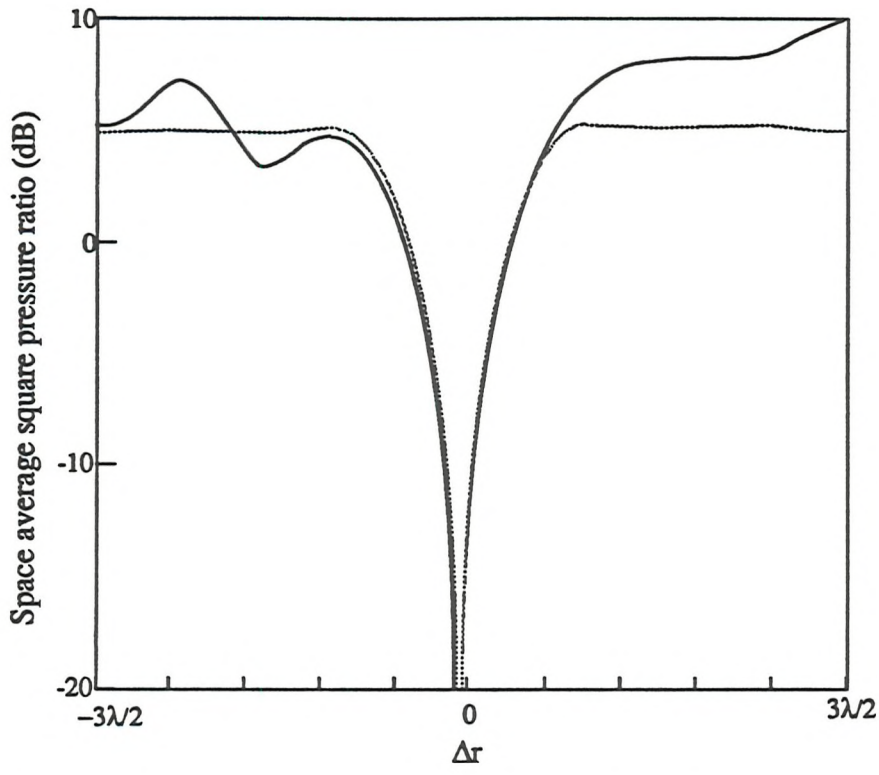

Figure 4.3 The average square pressure about a point of cancellation as a ratio of the square pressure in the absence of control obtained from 200 computer simulations in a pure tone diffuse sound field. Also shown is the function 4 [1 - $\text{sinc}^2 k\Delta r$].

One can therefore infer that for *this* simulation the average square pressure contribution from the secondary source is approximately three times the average primary source contribution namely $< | p_s(\mathbf{r}) |^2 > \approx 3 < | p_p(\mathbf{r}) |^2 >$.

The computer simulated experiment was repeated for another set of 200 simulations corresponding to a completely different set of 200 random primary and secondary source positions. While the general shape of the new diffuse field quiet zone was found to be preserved compared to the first simulation, the increase in square pressure well away from the control point was observed to change. In fact, the first computer simulation was found to be unrepeatable from one set of ensemble averages to the next. While the result presented in figure 4.3 is specific to this computer simulation, it was generally found that good agreement to the general theoretical result given by equation (4.27) was obtained provided that the values of $< | \hat{p}_s(\mathbf{r}) |^2 >$ were suitably adjusted to fit the simulated data. Values of the square secondary pressure $|p_s(\mathbf{r})|^2$ in any one computer simulation, were frequently found to deviate significantly from the averaged square primary pressure $< | p_p(\mathbf{r}) |^2 >$. In order to explain this lack of repeatability one is compelled to investigate the statistics of the square of the modulus of the optimal secondary source strength $| q_{so} |^2$. This is the quantity which

linearly couples into the secondary square pressure contribution to the sound field and ultimately the total potential energy in the enclosure. One can nevertheless make some important remarks on the basis of a small number of computer simulations regarding the behaviour of the diffuse field pressure in the vicinity of the point of null pressure

For 'sensibly' behaved values of the secondary source strength (of the order of the primary source strength), the zone of quiet $2\Delta r_{0.1}$, the distance over which the residual sound pressure level is 10 dB below the primary sound pressure level, is typically one tenth of the acoustic wavelength. Furthermore, according to figure 4.3 the residual space averaged square pressure is less than the original space average primary square pressure within a sphere of diameter equal to about one third of the acoustic wavelength. Outside of this sphere however, active control is observed to have a detrimental effect on the rest of the sound field. It must be emphasised that these values are only intended to provide general guideline relating to the characteristic distances involved in canceling the pressure at a point to zero in a pure tone diffuse sound field. Experience has shown that individual simulations can exhibit very large variations in the predicted square pressure well away from the point of cancellation, an explanation for which is given in section 4.4.

In forcing the pressure at a single point to zero, one is imposing a degree of certainty into the random pressure field which otherwise would be absent. It therefore seems intuitively plausible that this additional constraint must be at the expense of increased levels of pressure well away from the point of cancellation. While this finding is true in this case, this generalisation need not necessarily be true. Consider, for example, the case of a small solid ball bearing located within a room. Even though the particle velocity of the enclosed sound field is constrained to be zero at the surface of the solid sphere, experience has shown that this localised constraint has no measurable influence on the rest of the sound field.

It is instructive to consider the form of $1 - \rho^2(\Delta r)$ for the one, two and three dimensional diffuse wave fields in the region of small Δr where the spatial correlation functions are respectively $\cos k\Delta r$, $J_0(k\Delta r)$ and $\mathrm{sinc} k\Delta r$. Employing standard power series expansions to leading term, for $\Delta r < \lambda/10$

$$\rho(\Delta r) = \cos k\Delta r, \quad 1 - \rho^2(\Delta r) \approx (k\Delta r)^2 \tag{4.28}$$

$$\rho(\Delta r) = J_0(k\Delta r), \quad 1 - \rho^2(\Delta r) \approx \tfrac{1}{2}(k\Delta r)^2 \tag{4.29}$$

$$\rho(\Delta r) = \mathrm{sinc} k\Delta r, \quad 1 - \rho^2(\Delta r) \approx \tfrac{1}{3}(k\Delta r)^2 \tag{4.30}$$

where a systematic relationship appears to exist relating the coefficients of $(k\Delta r)^2$, the leading term in the series expansion, to the number of dimensions characterising the sound field. The space averaged zone of quiet in the three dimensional diffuse field therefore recovers from zero at a rate approximately three times slower than the one dimensional diffuse sound field for the same square pressure increase.

The expression for the quiet zone about a point of cancellation in a generalised sound field has been further substantiated by considering the form of the quiet zone obtained in a simple one dimensional sound field. The details of the derivation are left to Appendix 4.1. The expression is derived first from first principles, and then again using the generalised formula of equation (4.27). Both approaches are shown to lead to equation (4.31) given below

$$<< |p(\Delta x)|^2 >> = 2 << |p_p|^2 >> \sin^2 k\Delta x \qquad (4.31)$$

where Δx is the distance from the point of cancellation. This exercise is useful in highlighting the need to average over *both* the position of the point of cancellation and the positions of the sources (which in this case is determined by the duct length). Double parentheses have therefore been used to indicate two-fold averaging. Using the 10 dB level of sound pressure level reduction as the criterion of quiet, the quiet zone $2\Delta x_{0.1}$ may therefore be calculated according to

$$\frac{<< |p(\Delta x)|^2 >>}{<< |p_p|^2 >>} = 0.1 \quad \text{for} \quad 2\Delta x_{0.1} = 0.072\lambda. \qquad (4.32)$$

Equation (4.32) suggests that the one dimensional zone of quiet is periodic along the length of the duct repeating every wavelength by virtue of the periodicity implicit in the one dimensional diffuse field spatial correlation function $\cos k\Delta x$. Further verification of the general result in equation (4.27) for the three dimensional diffuse field has been established experimentally, the results and details of which are left to chapter 6.

4.4. Secondary source strength statistics

The findings of the earlier sections were useful in serving to establish the size and extent of the sound pressure level reductions one could expect as a consequence of driving a diffuse field pressure at a point to zero. The level of attenuation was found to be sufficiently localised around the point of cancellation to justify the description, 'quiet zone'. Having roughly quantified this region, the next step must then be an appraisal of the

necessary hardware requirements in terms of the power amplification and the secondary source volume velocity requirements. This exercise provides some idea as to the acoustic input needed into the existing sound field in order to bring about the point cancellation of the acoustic pressure. This is the purpose of the current section.

Ideally of course, one would like to achieve the cancellation of the pressure while expending least effort. However, experience has shown that in some cases the optimal secondary source strength $|q_{so}|$ is very much less than that of the primary source strength $|q_p|$, while in other cases, very much more. The optimal source strength $|q_{so}|$ is therefore a random quantity which is some unpredictable random function of both primary and secondary source positions and point of cancellation positions. Ultimately, one would like to know the exact theoretical probability density function of $|q_{so}|$, enabling all measures of central tendency such as the mean, mode and median to be calculated. Furthermore, this information would enable a precise quantification of the likelihood of failure to cancel perfectly the pressure, assuming that any reasonable control strategy would include some upper bound value, above which the control system could not operate.

The linear relationship between the complex secondary source strength q_{so} and that of the primary source q_p was established in section 4.1 and shown to be equal to

$$H_o(\omega) = \frac{q_{so}}{q_p} = -\frac{Z(\mathbf{r}_p|\mathbf{r}_0)}{Z(\mathbf{r}_s|\mathbf{r}_0)} \tag{4.3}$$

For the purpose of this analysis, it is assumed that $\mathbf{r}_p$, $\mathbf{r}_s$ and $\mathbf{r}_0$ are located further that a wavelength from each other so that $Z(\mathbf{r}_s|\mathbf{r}_0)$ and $Z(\mathbf{r}_p|\mathbf{r}_0)$ are statistically independent. Furthermore, it is assumed that the point of cancellation $\mathbf{r}_0$ is well away from the influence of directly transmitted radiation. From previous work, we know that $Z(\mathbf{r}_p|\mathbf{r}_0)$ and $Z(\mathbf{r}_s|\mathbf{r}_0)$ are complex quantities which may change independently in each of its degrees of freedom, the real and imaginary parts. Using established notation one can write

$$q_{so} = -\frac{\Re\{Z(\mathbf{r}_p|\mathbf{r}_0)\}+j\,\Im\{Z(\mathbf{r}_p|\mathbf{r}_0)\}}{\Re\{Z(\mathbf{r}_s|\mathbf{r}_0)\}+j\,\Im\{Z(\mathbf{r}_s|\mathbf{r}_0)\}}\, q_p \tag{4.33}$$

Rationalising equation (4.33) in terms of its real and imaginary parts, $\Re\{q_{so}\}$ and $\Im\{q_{so}\}$ respectively, yields a quotient whose numerator has an equal probability of being less than, or greater than zero while the denominator remains positive definite. We can therefore reasonably conclude that the expectation of the complex source strength q_{so}, taken over all possible secondary source positions and points of cancellation, is zero

$$< q_{so} > = 0 \tag{4.34}$$

This result is consistent with experience since the secondary source is only able to drive *any* arbitrary point pressure to zero providing it can change freely and independently in both its amplitude and phase. This is in many respects a trivial, commonsense result. More important is the expectation value of the secondary source strength modulus $< |q_{so}| >$ which is by definition phase insensitive and a measure of the effort provided by the control system as well as having obvious practical implications. We start by considering the statistical properties of $|q_{so}|^2$ which from equation (4.33) is given by

$$|q_{so}|^2 = \Re^2\{q_{so}\} + \Im^2\{q_{so}\} = \frac{|Z(r_p|r_0)|^2}{|Z(r_s|r_0)|^2} |q_p|^2 \tag{4.35}$$

Now each of the square impedance terms $|Z(r_x|r_y)|^2$, in the numerator and denominator of equation (4.35) comprise the sum of the squares of its real and imaginary parts according to

$$|Z(r_x|r_y)|^2 = \Re^2\{Z(r_x|r_y)\} + \Im^2\{Z(r_x|r_y)\} \tag{4.36}$$

both of which are assumed to be zero mean Gaussian random variables. To test this hypothesis for consistency with the computer simulated model, both the real and imaginary parts of the transfer impedance between two well spaced points in the enclosure was calculated according to equation (4.9) and (4.10) for a total of 15,000 times. In each case, all source positions were prevented from being closer than a wavelength, both from each other, and all of the enclosure boundaries. The resulting probability density function for the real part and imaginary parts of the transfer impedance was calculated from the 15,000 point ensembles. The probability density function appropriate to the real part, normalised with respect to the standard deviation σ_z, is shown in figure 4.4 together with the theoretical Gaussian probability density function according to the central limit theorem given by equation (3.7).

A good fit to the expected form is observed between the distribution obtained from the computer simulated ensemble and the theoretically expected result. Similar agreement was also obtained for the quadrature part of the transfer impedance, $\Im\{Z(r_x|r_y)\}$. The general form of the probability density function can be explained because the likelihood of destructive interference between a large number of randomly phased contributions exceeds that of constructive interference. Zero is therefore the mean value and also the most commonly occurring value.

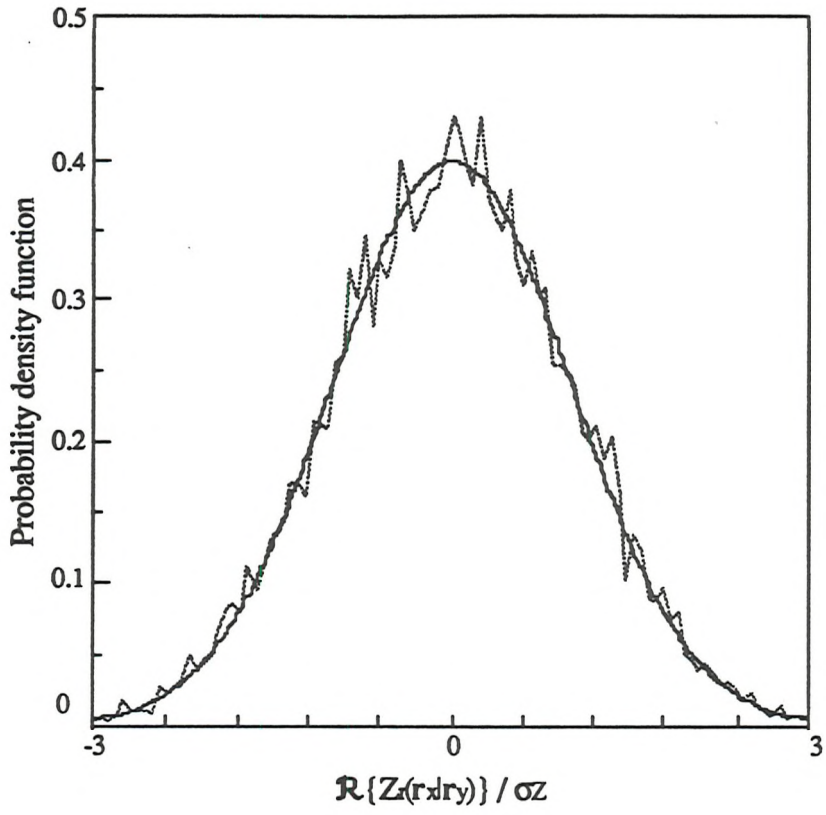

Figure 4.4 The simulated probability density function of the in-phase part part of the diffuse field transfer impedance (dashed line). Also shown is the theoretical result obtained as a consequence of the central limit theorem given by equation (3.7), (solid line).

As a practical aside note that the computer simulated data presented in this chapter was obtained from a single computer run lasting nearly 72 c.p.u hours on a VAX 11-750 computer. The rectangular enclosure chosen for the computer simulations has dimensions equal to π x e x 1m whose volume is therefore equal to slightly more than 700 cubic wavelengths at 1.5 kHz. Assuming that this also corresponds to the number of independent source and measurement positions, 15,000 values of all the appropriate acoustic variables were calculated in order to provide for a good statistical sample and therefore ensure good statistical representations of all possible outcomes.

Now $|q_{so}|^2$ is derived from the ratio of the squares of the absolute values of transfer impedance terms according to equation (4.35). Writing $|Z(r_x|r_y)|^2$ as the sum of the squares of its real and imaginary parts according to equation (4.36), suggests that $|Z(r_x|r_y)|^2$ is subject to statistical fluctuation from point to point in the enclosure which varies as the sum of the squares of two independent normally distributed random variables. Clearly, the independence of the terms relies on r_x and r_y being separated by more than a wavelength. This is precisely the definition of the Chi squared distribution χ^2_2, which are assigned two degrees of freedom by virtue of the number of its independent parts, in this case the real

and imaginary parts (or equivalently, amplitude and phase). From standard texts[63], the Chi squared random variable with two degrees of freedom has a probability density function given by

$$f_X(x) = \frac{1}{2}\exp(-x/2) \quad \text{where} \quad X = |Z(r_x|r_y)|^2 / \sigma_Z^2 \tag{4.37}$$

where σ_Z^2 is the variance of $|Z(r_x|r_y)|^2$ which has already been defined in equation (3.16) and (3.21). This distribution function is also known as the Poisson or exponential probability density function. Note that equation (4.37) could have equally been derived by substituting $|Z(r_x|r_y)|^2 = \Re^2\{Z(r_x|r_y)\} + \Im^2\{Z(r_x|r_y)\}$ into the joint density function between $\Re\{Z(r_x|r_y)\}$ and $\Im\{Z(r_x|r_y)\}$ given by equation (3.14). The theoretical result was again tested against the distribution of values obtained from a large computer simulated ensemble. The number of samples in the ensemble was again 15,000 where all source positions and cancellations positions were subject to the usual constraints. The resulting probability density function normalised with respect to the variance σ_Z^2, is shown in figure 4.5 together with the expected distribution given by equation (4.37). Good agreement is observed.

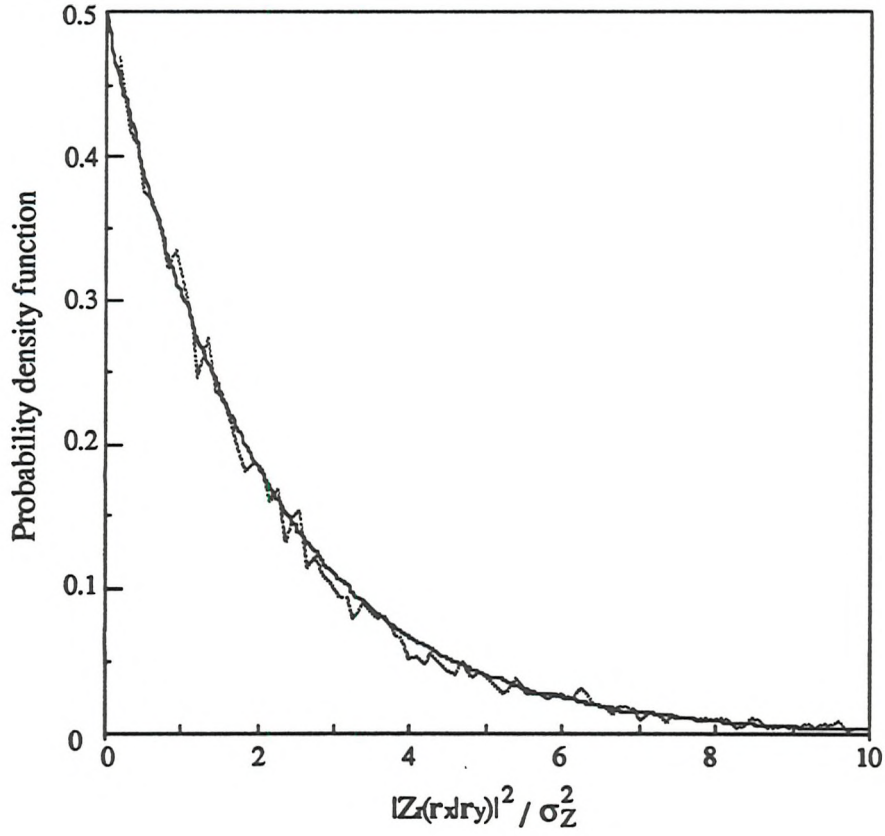

Figure 4.5 The probability density function of the modulus square value of the transfer impedance coupling two well spaced points in the diffuse field obtained from a computer simulated sample (dashed curve), together with the theoretical curve VS theory (solid line)

The variance calculated from the 15,000 point sample has also indicated a good fit to the theoretical result given by equation (4.37). Note that this probability density function is a monotonically, exponentially decreasing function whereby small values of the squared transfer impedance are systematically more likely to occur than large values.

With reference to equation (4.35) for the square of the modulus of the optimal secondary source strength $|q_{so}|^2$, the ease with which two well separated points in the diffuse sound field can become weakly coupled may give rise to practical difficulties if the secondary impedance term $|Z(r_s|r_0)|^2$ happens to be small compared with that of the primary transfer impedance term $|Z(r_p|r_0)|^2$. In this event, $|q_{so}|^2$ will be required to be proportionately greater than that of the primary $|q_p|^2$, in order to overcome the weaker impedance that couples the secondary source to the chosen point of cancellation at r_0 according to equation (4.35). One could therefore anticipate the ill-conditioning of the statistics associated with the square pressure and square pressure related energetic quantities as observed in computer simulations. One can therefore write $|H_o|^2$ as the ratio of two Chi squared random variables, each possessing two degrees of freedom which are presumed independent providing the primary source and secondary source are further than a wavelength apart. From equation (4.35), one can write

$$|H_o|^2 = \frac{|q_{so}|^2}{|q_p|^2} = \frac{(\chi^2_2)_{qp}}{(\chi^2_2)_{qs}} \tag{4.38}$$

It is a fairly straightforward matter to derive the resulting probability density function from the ratio of random variables although usually, the integrals which result cannot usually be solved in closed form. However, much tedious algebra can be avoided by recognising that all random quantities which comprise the ratio of independent Chi square random variables have been extensively investigated in connection with problems of statistical inference where the variance is unknown[63]. Random quantities of this type have a known probability density function denoted by $F(\nu_1,\nu_2)$, where ν_1 refers to the number of degrees of freedom in the numerator. In the present case, the defining parameters of the probability density function, $\nu_1 = \nu_2 = 2$ are an intrinsic property of the complex wavefield (possessing independent amplitude and phase). From standard texts in statistics, the F(2,2) probability density function is given by

$$f_V(v) = \frac{1}{(1+v)^2} \quad \text{where} \quad V = |H_o|^2 \tag{4.39}$$

The F(2,2) probability density function can be observed to provide good agreement with distribution of 15,000 computer simulated values shown in figure 4.6. The details of the simulation remain as before.

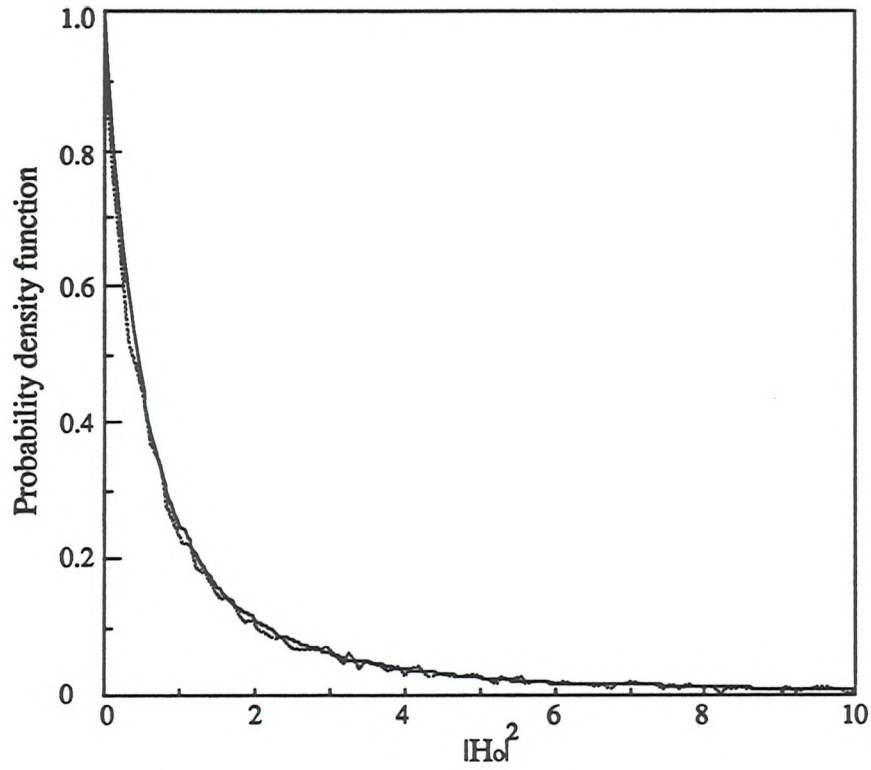

Figure 4.6 The calculated density function of the square modulus of the transfer function $|Ho(\omega)|$ obtained from a 15,000 computer simulated sample (dashed line), together with the F(2,2) density function (solid line).

The distribution obtained from the computer simulated ensemble and the theoretical result are observed to closely agree.

Firstly note that the F(2,2) density function is also a monotonically decreasing, unbounded function which can, in principle, take arbitrarily large values and whose modal (most likely) value is zero. Now since the square pressure contribution from the secondary field $< |p_s|^2 >$ is linearly related to $< |q_{so}|^2 >$ via $|H_o|^2$ according to equation (4.26), one can conclude that the most likely increase in the square pressure as a result of driving a point pressure to zero in a diffuse sound field is zero. While this surprising result is clearly unexpected, it disguises the fact that extremely large values of $|H_o|^2$ are sufficiently likely to arise, as a consequence of unfortunate coupling between the secondary source and the chosen point of cancellation, to force the ill-conditioning of the associated statistics. This conclusion is borne out by the mean value of the F(2,2) probability density function.

Given a random quantity X whose probability density function is $f_X(x)$, the mean value μ_x is formally defined by

$$\mu_x = \lim_{u \to \infty} \int_{-\infty}^{u} x f_X(x) dx \tag{4.40}$$

For the present example

$$< |q_{so}|^2 > = |q_p|^2 \lim_{u \to \infty} \int_0^u \frac{x}{(1+x)^2} \, dx \tag{4.41}$$

$$= |q_p|^2 \lim_{u \to \infty} \left[\ln(1+u) - \frac{u}{1+u} \right] = \infty \tag{4.42}$$

The expectation $< |q_{so}|^2 >$ therefore fails to converge but diverges very slowly to infinity like ln(x) and is therefore undefined. Strictly speaking, the spatial averaging operation should be indicated by the use of double parentheses << (.) >> to denote that the average value is taken over all primary source *and* secondary source positions. However, as demonstrated overleaf it is the average taken over all secondary source positions which causes the expectation value not to converge and is entirely independent of the statistical behaviour of the primary source transfer impedance. The implications for active noise control in the diffuse sound field are significant. Any quadratic function of the pressure after the cancellation of the pressure at a point, such as the square pressure, potential energy, acoustic intensity and sound power *etc* all have a linear dependence on $|q_{so}|^2$ and are therefore similarly undefined. All higher moments of the F(2,2) probability density function such as the variance, are likewise undefined and diverge even more rapidly than $< |q_{so}|^2 >$.

The result also has important engineering implications from the point of view of contriving diffuse field control strategies. Any additional constraint made on the secondary source, however weak, will assist the convergence of the ensemble mean value. While this is generally true, there are some control configurations (see chapter 6) which despite being very well behaved from point to point within the diffuse field, posses a mathematical expectation which is also equal to infinity. For these cases the mean value is a misleading indicator of first order behaviour as discussed at length in chapter 6. Nevertheless, trying to establish a control technique which is less prone to large secondary source strength requirements is the motivation for the work presented in chapters 5 and 6.

In appraising the current problem, it is important to recognise that it is the inability of the secondary source to couple well into the point of cancellation that is the sole cause of the ill-conditioning of the statistics of all square pressure related variables. The observed ill-

conditioning is dependent on the acoustic coupling between the primary source and the point of cancellation. This conclusion can be asserted because of the following basic result in statistics. The expectation of the product of independent random variables X and Y, $< XY >$ is simply the product of their expectations, $< X >< Y >$. From equation (4.35)

$$< |H_o|^2 > = < |Z(r_p|r_0)|^2 > \; < \; |Z(r_s|r_0)|^{-2} > \tag{4.43}$$

The first factor $< |Z(r_p|r_0)|^2 >$ is certainly well behaved whose mean is convergent and determined from equation (3.21). The observed lack of convergence must therefore be attributed to the second factor which only involves the expectation of the secondary source transfer impedance term $< |Z(r_s|r_0)|^{-2} >$. This is the term which is solely responsible for the ill-conditioning of the statistics associated with $|q_{so}|^2$ whereby $< |Z(r_s|r_0)|^{-2} > = \infty$. Any control strategy aimed at circumventing this difficulty must focus on the inability of the secondary source to couple into the chosen point of cancellation by imposing on the secondary source additional constraints, see Chapter 5.

The second important feature worthy of note, is that the form of the F(2,2) probability density function according to equation (4.39) is completely insensitive to the properties of the sound field such as the enclosure volume, room damping and the frequency of excitation etc (providing it is higher than the Schröder frequency). This is manifest by the complete absence of the impedance variance σ_Z^2 in equation (4.39) which is of course sound field specific according to equation (3.21), where $\sigma_Z^2 = \sigma_Z^2 (V, \zeta, \omega)$. This property is fundamental to the F distribution which also explains why this probability density function is so useful in problems of hypothesis testing. The simple function governing the theoretical distribution of $|q_{so}|^2$, therefore has surprising generality and applies equally to *all* diffuse fields. The explanation is simple and lies in the way the variance σ^2 of a normally distributed ensemble $N(\mu,\sigma^2)$, merely acts to linearly scale the distribution according to

$$N(\mu,\sigma^2) \; = \; \sigma N(\mu,1) \tag{4.44}$$

As a consequence of this basic identity, the variance σ_Z^2 of the diffuse field transfer impedance emerges as a common factor in both the numerator $< |Z(r_p|r_0)|^2 >$ and the denominator $< |Z(r_s|r_0)|^2 >$ which therefore cancels in the quotient. It follows that all quotients containing functions of normally distributed random variables are therefore independent of its variance provided they are the same for the numerator and denominator. The results which follow for the secondary source strength statistics are completely general, independent of either enclosure volume, source geometry or frequency of excitation, but a sole property of the diffuseness of the wavefield inasmuch as the in-phase

and quadrature part of the acoustic impedance are normally distributed and independent. This result has even greater generality since it not only applies to the elementary system under discussion here, but is equally valid to more sophisticated control control schemes which utilise an array of secondary loudspeakers and microphones, see chapter 5. One is now in a position to state an important result in the theory of active control. All secondary source strength statistics in the high frequency, enclosed sound field are *invariant* to the details of the sound field as long as the spatially sampled complex sound field is distributed as a bivariate Gaussian distribution between its in-phase and quadrature parts. This condition is certainly satisfied at frequencies above the Schröder frequency and most likely valid for a significant range of frequencies below.

The probability density function of the transfer function modulus $|H_o|$ may be obtained directly from that of $|H_o|^2$ by a simple change of variable $U = \sqrt{V}$ in equation (4.39) following an analysis exactly analogous to the change of variable in an indefinite integral. The probability density function $f_V(v)$ is formally defined by

$$f_V(v) = \lim_{\Delta v \to 0} \frac{F(v-\Delta v/2 \, , \, v+\Delta v/2)}{\Delta v} \tag{4.45}$$

where F(v) is the cumulative distribution function such that $F(v-\Delta v/2 \, , \, v+\Delta v/2)$ denotes the probability of V lying somewhere between $v-\Delta v/2$ and $v+\Delta v/2$. One can therefore write

$$F(v-\Delta v/2 \, , \, v+\Delta v/2) \approx f_V(v)\Delta v \tag{4.46}$$

where Δv is small. From equation (4.39), it follows that

$$F(v-\Delta v/2 \, , \, v+\Delta v/2) \approx \frac{1}{(1+v)^2}\Delta v \tag{4.47}$$

Putting $u = \sqrt{v}$ where $U = |H_o|$, then $v = u^2$ and $\Delta v \approx 2u\Delta u$ for small u one can now write

$$F(u-\Delta u/2 \, , \, u+\Delta u/2) \approx \frac{2u}{(1+u^2)^2}\Delta u \tag{4.48}$$

From the definition of the probability density function

$$f_U(u) = \lim_{\Delta u \to 0} \frac{F(u-\Delta u/2 \, , \, u+\Delta u/2)}{\Delta u} = \frac{2u}{(1+u^2)^2} \tag{4.49}$$

The probability density function of the optimal secondary source strength $|q_{so}|$ has been derived. For the sake of completeness, the square root of each of the 15,000 points in the ensemble employed to verify the distribution of $|H_o|^2$ was taken. The resulting probability density function obtained from the computer simulated ensemble is shown in figure 4.7 together with the theoretical result of equation (4.49).

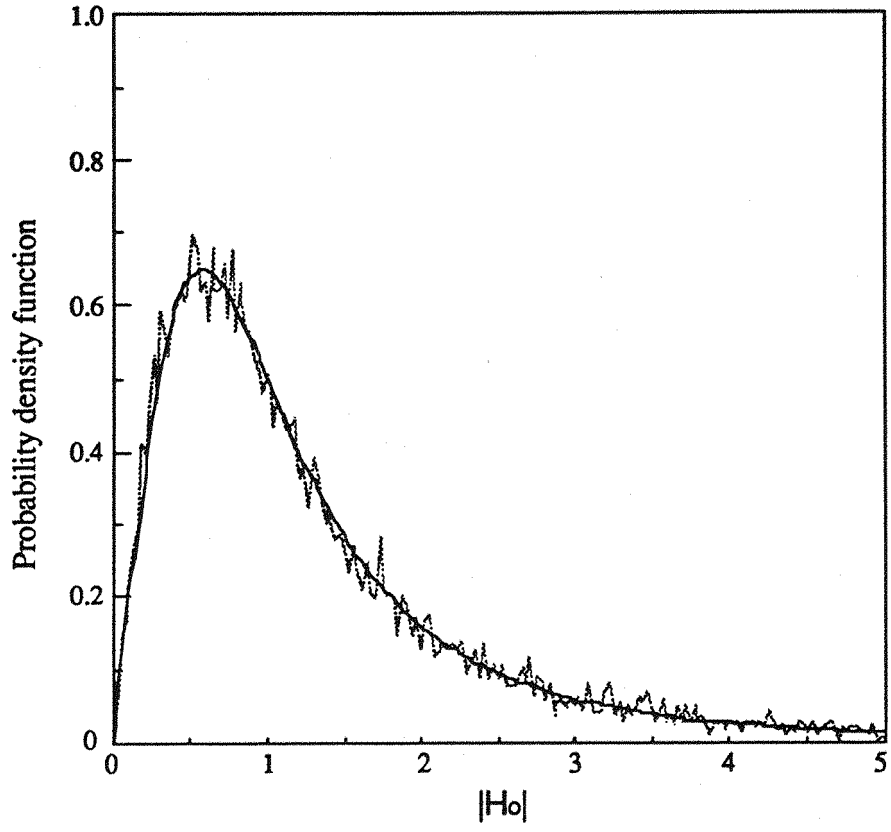

Figure 4.7 The probability density function of the secondary source strength |qso| necessary to drive a point pressure to zero in a pure tone diffuse sound field. Results from computer simulations(dashed line) and the theoretical result (solid line).

As expected, the distribution obtained from the simulated data and the distribution function denoting the theoretical curve of convergence as the ensemble size tends to infinity, are in good agreement.

The behaviour of the function shown in figure 4.7 is observed to be a radical departure from the behaviour of the F(2,2) density function owing to the non-linearity of the transformation $X \rightarrow \sqrt{X}$. It is interesting to observe that while the most probable value of $|H_o|^2$ is zero according to equation (4.39), $|H_o|$ takes zero as its *least* probable value. In fact $|H_o|$, (and therefore by implication $|q_{so}|$) can never be zero where from equation (4.49)

$$f_U(0) = 0 \tag{4.50}$$

This quite surprising result can be explained if one considers the form of the probability density function of the root mean square (r.m.s) diffuse field pressure $|p_r(r)|$. Making the same change of variable, namely $X \rightarrow \sqrt{X}$ in the probability density function for the modulus of the square of the pressure $|p_r(r)|^2$ given in equation (4.37), one can show that independent samples of the root mean square diffuse field pressure are distributed as a Rayleigh random variable whose probability density function is written below

$$f_X(x) = 2xe^{-x^2} \quad \text{where } X = |p_r(r)| / < |p_r(r)| > \tag{4.51}$$

This function is plotted in most texts on statistics[63]. The same conclusion was arrived by Waterhouse for example[73]. This function suggests that even though both the in-phase and the quadrature part of the diffuse field pressure have a most likely (or modal) value equal to zero, the modulus of the complex pressure can never be zero since $f_X(0) = 0$. A traverse of a measurement microphone along some arbitrary trajectory in the diffuse field will never encounter a pressure null. One can therefore infer that there is therefore never any one point of cancellation position where the secondary source is required to switch off and consequently there will always be some residual pressure which requires cancellation. This point of view is wholly consistent with form of the probability density function for the modulus of the optimal secondary source strength given in equation (4.49).

Inspection of the probability density function $f_U(u)$ in equation (4.49), reveals that the distribution of q_{so} is uni-modal thereby possesses a single maximum value which therefore suggests that there is only one single most likely occurring value $|q_{so}|_{mode}$. At the modal value, $f_U(u)$ is stationary with respect to u

$$\frac{df_u(u)}{du} = 0 \quad \text{at} \quad |q_{so}| = |q_{so}|_{mode} \tag{4.52}$$

Performing the differentiation and solving yields

$$|H_o|_{mode} = \frac{1}{\sqrt{3}} \tag{4.53}$$

Further noting that $|q_{so}| = |q_p|\,|H_o|$ leads to

$$|q_{so}|_{mode} = \frac{1}{\sqrt{3}}\ |q_p| \tag{4.54}$$

The most probable value of the secondary source strength for driving a randomly chosen diffuse field point to zero is appreciably smaller (by a factor of 0.577) than the primary source strength whose wavefield it is attempting to cancel. This result is in complete agreement with the most commonly occurring simulated value shown in figure 4.7. The mean value of the probability density function given by equation (4.49) also exists and may be formally calculated from equation (4.40) to give

$$< |q_{so}| > = |q_p| \int_0^{\infty} \frac{2u^2}{(1 + u^2)^2} \, du = |q_p| \frac{\pi}{2} \tag{4.55}$$

The ensemble mean actually obtained from the 15,000 computer simulated values was calculated to be 1.563 times that of the primary source strength , i.e., within 1/2 % of the theoretical expectation given by equation (4.55). This result, at first glance appears to be surprising since one could have reasonably anticipated some kind of reciprocal process to exist between the primary source and the secondary source. Specifically, the pressure at a point is driven to zero regardless of whether one regards the primary source to be acting on the secondary source to impose the point of cancellation, or *vica-versa*. In this event the mean of the transfer function $|H_o|$ would be therefore unity. This is obviously not the case and the active (secondary) source is subject to a level of statistical constraint which, on average, requires a source strength which is slightly more than one and a half times that of the primary source strength. Unfortunately however, a formal assessment of the source strength variance as conventionally defined does not exist.

Consider the cumulative distribution function $F_U(u)$. This function defines the probability that U lies between 0 and u, i.e., $P(0 \leq U < u)$ which is derived from the probability density function $f_U(u)$ as indicated below

$$F_U(u) = \int_{-\infty}^{u} f_Y(y) \, dy \tag{4.56}$$

For the form of the probability density given by equation (4.49), the cumulative distribution function is determined from

$$F_U(u) = \int_0^{u} \frac{2y}{(1 + y^2)^2} \, dy \tag{4.57}$$

$$F_U(u) = 1/2 - 1/2 \cos(2\tan^{-1}u) \quad \text{where } U = |H_o| \tag{4.58}$$

The theoretically derived result given above and the cumulative distribution of computer simulated data are of course in close agreement as shown by figure 4.8

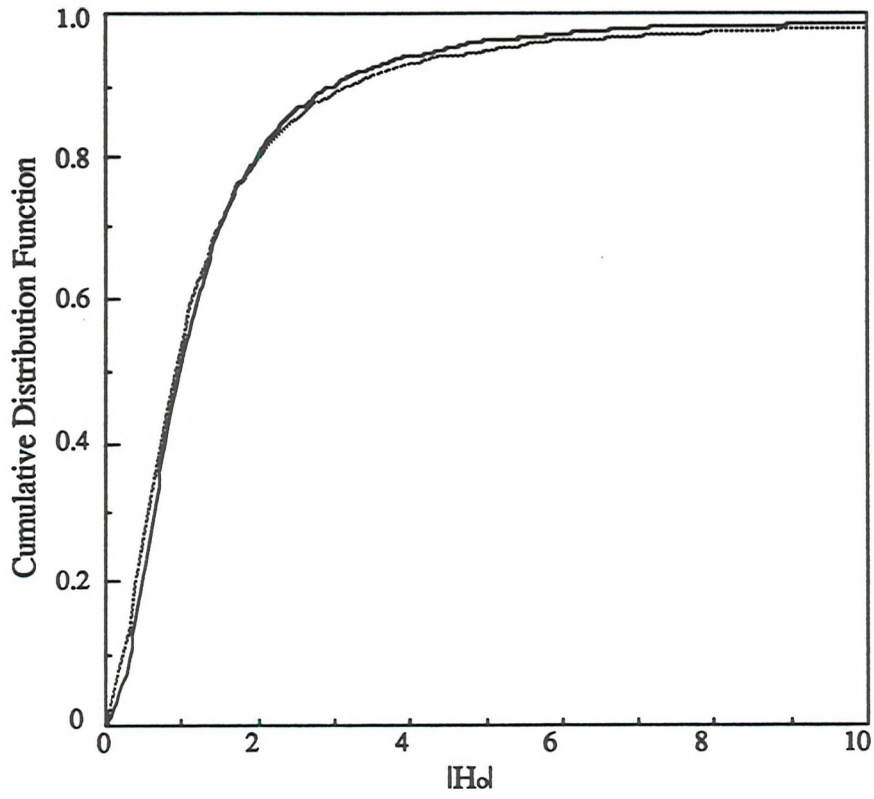

Figure 4.8 The cumulative distribution of computer simulated values of |Ho| *(dashed line) together with the theoretically derived cumulative distribution function* $1/2 - 1/2\cos(2\tan^{-1}x)$ *(solid line)*

Despite the unlikely form of the function $F_U(u)$ given in equation (4.58), rational values are obtained for $u = 1/\sqrt{3}$, 1 ,2 ,3 and 7 which are tabulated below

$\|H_o\|$	$1/\sqrt{3}$	1	2	3	7
$F_U(u)$	0.25	0.5	0.8	0.9	0.98

By virtue of the identity $F_X(x) = 1 - F_X(1/x)$ which exists for cumulative distribution functions[63], further rational values are also obtained for $u = \sqrt{3}$, 1/2, 1/3 and 1/7. By inspection, the median value of the absolute value of the transfer function $|H_o|_{med}$ is unity which implies that $|q_{so}|$ has equal probability of being less than, or greater than that of the primary source strength $|q_p|$ such that

$$|q_{so}|_{med} = |q_p| \tag{4.59}$$

This is clearly a general finding which is equally valid for all sound fields for which no restriction is imposed on the positioning of either the primary source or secondary source. This is because $Z(r_p|r)$ and $Z(r_s|r)$ are taken from the same ensemble of values in any given sound field such that there is an equal probability of either the primary source or secondary source impedance being less than, or greater than the other. Increasing $|q_{so}|$ to twice that of the primary source strength raises the number of points at which the complete cancellation of the pressure is possible to 80 %. Further increasing the secondary source-primary source strength ratio to exactly seven now means that exactly 98 % of all point cancellations that may be demanded of the secondary source are possible, although most likely at the expense of significantly raised potential energy levels. However, there still remains exactly 2 % of cases which defy complete cancellation owing to the inability of the secondary source to provide sufficient influence at the chosen point of cancellation owing to the weak acoustic coupling between them.

All three descriptors of the central tendency of the modulus of the optimal secondary source strength have been shown to be simply related to elementary mathematical constants. More significantly is that all of these first order statistics are typically of the order of the primary source strength itself. These results indicate that on average, active control of diffuse fields is within the physical capabilities of commonly available acoustic transducers which helps to provide some important guide-lines for the necessary secondary source strength requirements. In general terms, one should ensure that the maximum volume velocity of the secondary loudspeaker is at least equal to the volume velocity of the primary source strength in order to guarantee a reasonable chance of ensuring the perfect cancellation of the pressure at the chosen point of cancellation.

4.5. The potential energy statistics before and after the active cancellation at a point

In addition to having important practical relevance, it is useful to be able to provide a statistical description of the response of the enclosure to the active cancellation of the pressure at a single point, in terms of its potential energy. A knowledge of the enclosure potential energy before and after control serves to provide a single index relating to the cost of driving the pressure in the enclosure to zero. Furthermore, it enables one to asses the benefits of localised acoustic attenuation around the point of control set against the probabilistic rise in the potential energy level. Unlike for low modal density case where the

change in potential energy is in many respects predictable[51], in the case of the diffuse field one can only make general statistical statements about the probability of increased levels of potential energy. This is the aim of the current section.

The potential energy E_p in a harmonically excited enclosure, can be closely approximated by the finite sum of square modal amplitudes[65] according to

$$E_p = \frac{V}{4\rho c_0^2} \sum_{n=0}^{N} |a_n|^2 \tag{4.60}$$

Equation (4.60) simply expresses the total potential energy in the enclosure to the sum of the potential energies of its constituent modes. Each complex modal amplitude a_n, comprises the sum of primary and secondary modal amplitudes according to equation (4.7)

$$a_n = A_n(\omega) \left[q_p(\omega)\psi_n(r_p) + q_s(\omega)\psi_n(r_s) \right] \tag{4.7}$$

When the primary source and secondary source are related such that cancellation of the pressure is assured at some chosen point in the field, the residual potential energy E_{pres} under these conditions is given by

$$E_{pres} = \frac{V}{4\rho c_0^2} \sum_{n=0}^{N} |A_n(\omega)|^2 \, | \, q_p\psi_n(r_p) + q_{so}\psi_n(r_s) \, |^2 \tag{4.61}$$

Providing the primary and secondary sources are well separated, then apart from the small sphere of pressure reduction centred on the point of cancellation where the respective sound fields are highly correlated (typically a small fraction of a wavelength), the primary and secondary sound fields are everywhere else uncorrelated. The primary and secondary sources may be regarded as two mutually uncorrelated sources radiating into the enclosure such that the enclosure potential energy is simply the sum of their individual contributions. This approximation is equivalent to assuming that the space average of the cross modes $< \psi_n(r_s)\psi_n(r_p) >$ is equal to zero which is of course only valid when all the linear dimensions of the enclosure are much greater than the acoustic wavelength. Recalling that q_{so} and q_p are linearly related by the transfer function H_o, the residual potential energy E_{pres} can be approximated as

$$E_{pres} \approx \frac{V}{4\rho c_0^2} |q_p|^2 \left[\, | \sum_{n=0}^{N} A_n(\omega)\psi_n(r_p) \, |^2 + |H_o|^2 \, | \sum_{n=0}^{N} A_n(\omega)\psi_n(r_s)|^2 \, \right] \tag{4.62}$$

If E_{pp} denotes the primary source contribution to the enclosure potential energy in the enclosure according to

$$E_{pp} = \frac{V}{4\rho c_0^2} |q_p|^2 \left| \sum_{n=0}^{N} A_n(\omega)\psi_n(r_p) \right|^2 \tag{4.63}$$

then to a good approximation one can write

$$E_{pres} \approx E_{pp} [\, 1 + |H_o|^2 \,] \tag{4.64}$$

where it is been assumed that in any single simulation

$$\left| \sum_{n=0}^{N} A_n(\omega)\psi_n(r_p) \right|^2 \approx \left| \sum_{n=0}^{N} A_n(\omega)\psi_n(r_s) \right|^2 \tag{4.65}$$

Assuming that the potential energy in the room is proportional to the sound power output, following from equation (3.1) in chapter 3, the potential energy generated by a single point monopole source will also exhibit a level of variance which is inversely proportional to the modal overlap factor $1 / M_N(\omega)$. Above the Schröder frequency therefore, the likelihood of significant departure between successive measurements of the potential energy for different source positions is very small. More will be said about this shortly. This simplification is therefore a good approximation in diffuse sound fields supported by large enclosure volumes which are driven at high frequencies.

Equation (4.64) represents a considerable simplification over the exact expression given by equation (4.61). Further justification for this approximation follows because the variance of the square transfer function $|H_o|^2$ compared with unity, is much larger than the variance of the primary source potential energy E_{pp} compared with its mean value. The extremely large statistical variation in the residual potential energy is therefore predominantly due to the large variance of the square of the secondary source strength as compared to the variance incured from varying the source positions. As will soon become clear, all moments of the probability density function associated with the primary source potential energy E_{pp} are formally defined where by contrast, none of the moments are defined for the F(2,2) probability density function which governs the statistical behaviour of $|H_o|^2$. The residual potential energy statistics are therefore predominantly dictated by $|H_o|^2$ which are subject to extremely large variations from point to point within the diffuse wavefield while those of E_{pp} remain negligible by comparison.

For the case of a single source radiating freely within an enclosed space, the primary potential energy E_{pp}, is simply the sum of a large number of squared terms $|a_n|^2$. Invoking the central limit theorem suggests that in the limit as the number of significantly contributing terms tends $|a_n|^2$ to infinity, the distribution of values of E_{pp} approaches the normal distribution $N(\mu_E,\sigma_E^2)$ centred about its mean value μ_E with a variance σ_E^2 according to

$$f_X(x) = \frac{1}{\sqrt{2\pi}\sigma_E} e^{-(x-\mu_E)^2/2\sigma_E^2} \qquad (4.66)$$

where $X = E_{pp} / \langle E_{pp} \rangle$ defined by equation (4.63), and $\mu_E = \langle \hat{E}_{pp} \rangle$, the ensemble mean arising from the finite sample size.

By way of verification, the primary (monopole) source potential energy was computed according to equation (4.63) for 15,000 random source positions although not within half a wavelength of the walls in any one simulation. The probability density function of the resultant ensemble is shown in figure 4.9 together with the theoretical curve with the same relative variance namely $\sigma_E^2 / \mu_E^2 = 0.0246$.

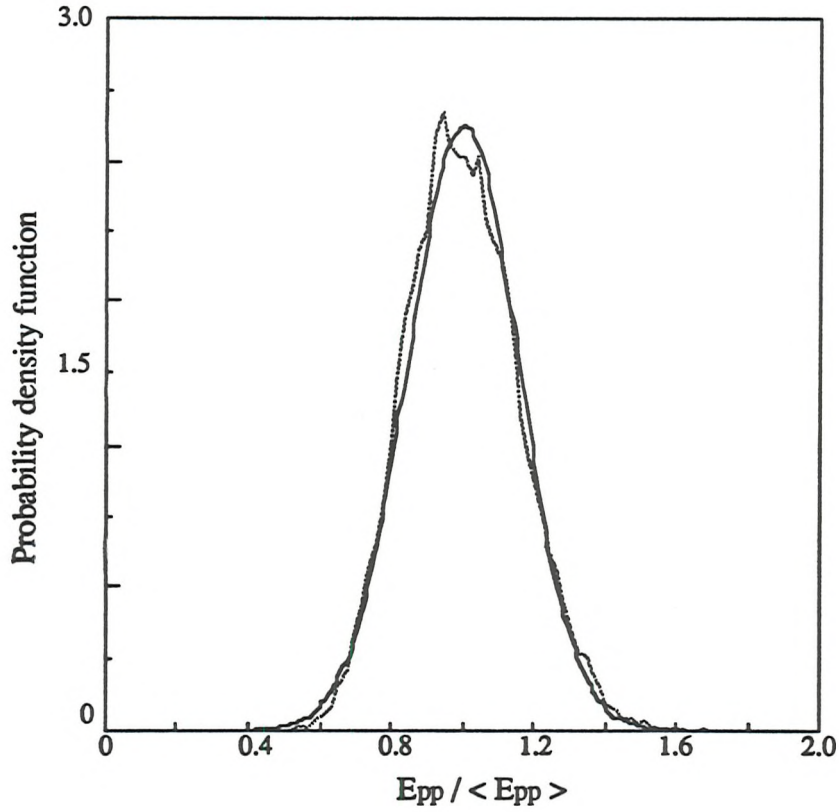

Figure 4.9 The distribution of 15,000 computer simulated values of the primary source potential energy before control (dashed line) together with the theoretical normal curve with the same variance - square mean ratio of 0.0246 (solid line).

Reasonable agreement is observed serving to demonstrate the small degree of dispersion associated with measurements of source potential energy in the diffuse sound field. Before proceeding to evaluate the influence of the secondary source, it is instructive to consider the origin of the potential energy variance σ_E^2. On the basis of an energy balance relating the sources and sinks of acoustic energy in a room, one can write down a direct relationship between the sound power of a source W and the steady state level of potential energy E_p subsequently sustained by the source. This result is given in many acoustical texts and is given below

$$< E_p > = \frac{2V}{Ac_0} < W > \tag{4.67}$$

All of the results derived in chapter 3 for the relative variance of the sound power output are now directly relevant to the potential energy. From equations (3.56) and (3.61), the relative variance of the potential energy is given by

$$\frac{\sigma_E^2}{\mu_E^2} = \frac{\sigma_W^2}{\mu_W^2} = \frac{1}{3\pi}\left[\frac{f_{sch}}{f}\right]^3 \quad \text{for} \quad f \geq f_{sch} \tag{4.68}$$

$$\frac{\sigma_E^2}{\mu_E^2} = \frac{1}{M_N(\omega)} \tag{4.69}$$

The distribution of primary source potential energies shown in figure 4.9 was obtained at a frequency of 1500 Hz within an enclosure whose Schröder frequency was estimated to be 738 Hz. From equation (4.68), the theoretically predicted value of the relative variance may be calculated to be 0.013 which is clearly an underestimate of the observed value of 0.0246. The possible ambiguities in relating the relative variance of the sound power output, which in turn is equal to the relative variance of the potential energy is discussed in chapter 3. In this example, the simulated value is considerably closer to Lyon's formula which gives a value for the relative variance equal to 0.022.

The figure above shows that the source potential energy E_{pp} rarely deviates by more than about two standard deviations from the mean value which for this room geometry, modal damping etc, is about $0.3 < \hat{E}_{pp} >$. However computer simulations have shown that the observed level of excursion about the mean value is profoundly altered once the secondary source has been introduced into the wavefield seeking to drive some diffuse field point pressure to zero. A theoretical justification for this finding now follows.

Assuming that equation (4.64) is a good approximation to the residual potential energy after the active control at a point within the diffuse sound field, we now seek to determine the resulting probability density function $f_Y(y)$. Given that the probability density function of both E_{pres} and $|H_o|^2$ are now known and have each been shown to be a good fit to computer simulated data, we require the probability density function of their product namely $E_{pp}\,[\,|H_o|^2 + 1\,]$. From an analysis exactly analogous to the transformation of variables in a double integral whose details are left to Appendix 4.2, it can be shown that

$$f_Y(y) = \frac{1}{\sqrt{2\pi\sigma_E^2}} \int_0^1 u e^{-(yu - \mu_E)^2/\sigma_E^2}\, du \quad \text{where} \quad Y = E_{pres} / \langle E_{pp} \rangle \qquad (4.70)$$

This integral may be further expanded in terms of the tabulated error function Erf(x) defined in chapter 3 to give

$$f_Y(y) = \frac{\sqrt{\pi}\,\mu_E}{2y^2} \left[\mathrm{Erf}\left(\frac{y - \mu_E}{\sqrt{2}\,\sigma_E}\right) - \mathrm{Erf}\left(\frac{\mu_E}{\sqrt{2}\sigma_E}\right) \right] + \frac{\sigma_E}{2\sqrt{2}} \left[\frac{e^{-(y - \mu_E)^2/2\sigma_E^2} - e^{-\mu_E^2/2\sigma_E^2}}{y^2} \right] \qquad (4.71)$$

By way of comparison with computer simulated data, E_{pres} was computed for 15,000 primary source, secondary source and cancellation positions all of which were constrained to lie further than a wavelength from each other or the walls. Figure 4.10 shows the probability density function of the residual potential energy as computed from equation (4.61) 15,000 times, together with the theoretical curve of equation (4.70) shown overleaf. Note that as before in the absence of control, the ensemble has been normalised with respect to the space averaged primary potential energy $\langle \hat{E}_{pp} \rangle$.

The curves are observed to be in close agreement. Comparing figure 4.10 with the previous graph, figure 4.9 for the distribution of primary source potential energies demonstrates how even this simple elementary control scheme can have potentially disastrous consequences in terms of the global sound pressure level. Previously, the primary source radiating in isolation was shown to excite a level of potential energy that was only capable of small excursions from the mean. On the introduction of the secondary source however, the enclosure potential energy is observed to frequently reach levels many times that of $\langle \hat{E}_{pp} \rangle$. This behaviour is exemplified by the mean and standard deviation of the potential energy both before and after control as calculated from the 15,000 point ensemble.

Before active control:

$$< \hat{E}_{pp} > = < \hat{E}_{pp} > \quad \text{and} \quad \hat{\sigma}_{Ep} \approx 0.16 < \hat{E}_{pp} > \tag{4.72}$$

and after active control:

$$< \hat{E}_{pres} > \approx 10 < \hat{E}_{pp} > \quad \text{and} \quad \hat{\sigma}_{Epres} \approx 175 < \hat{E}_{pp} > \tag{4.73}$$

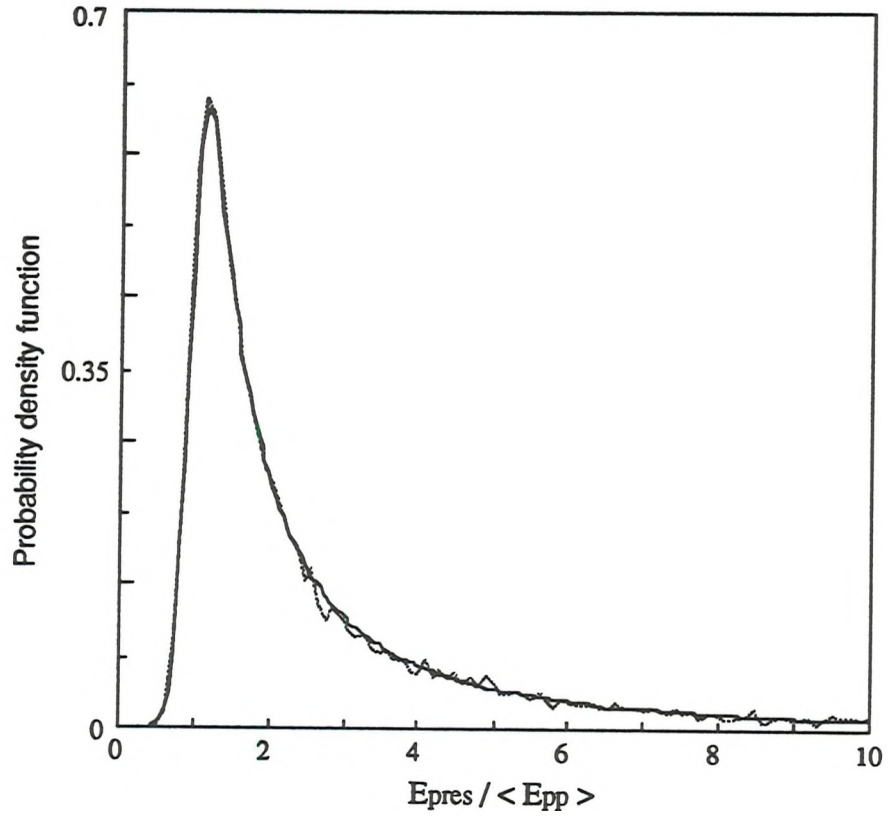

Figure 4.10 The distribution of computer simulated values of the residual potential energy according to equation (4.67) (dashed line and theoretical curve of equation (4.70)

The close match between the distribution of simulated values and the theoretical probability density function given by equation (4.70) is perhaps not surprising given that the statistics of the residual potential energy are predominantly governed by the statistics of $|H_o|^2$ whose probability density function has already been shown to provide a good fit to the simulated data.

For $E_{p_{res}}$ greater than $< \hat{E}_{pp} >$, the probability density function falls off as y^{-2} for large y where the probability density function of $|H_o|^2$ is dominant. Near $E_{p_{res}} \approx < E_{pp} >$ however, where the secondary source contribution to the total potential energy is negligible, the resulting density function is predominantly governed by that of E_{pp}. This

accounts for the small tail on the probability density function for E_{pres} less than $< E_{pp} >$. Now since linear expectation is commutative for independent random variables such as

$$< E_{Pres} > = < E_{pp} > [< |H_o|^2 + 1 >] \tag{4.74}$$

where

$$< |H_o|^2 + 1 > = < |H_o|^2 > + 1 = \infty \tag{4.75}$$

One can therefore conclude that the expectation of the potential energy produced as a consequence of driving a point pressure to zero in a pure tone diffuse sound field is also infinite

$$< E_{Pres} > = \infty \tag{4.76}$$

One can apply similar reasoning to the space averaged square pressure and all square pressure related variables so that with reference to equation (4.27), *the true expectation of the diffuse field zone of quiet is zero.*

The most likely increase in enclosure potential energy however, is only fractionally above that of the primary contribution. Inspection of figure 4.10 indicates that

$$(E_{Pres})_{mode} \approx 1.15 < E_{pp} > \tag{4.77}$$

Note that putting $\partial f_Y(y) / \partial y = 0$ and rearranging the orders of differentiation and integration indicates that the peak of the probability density function $(E_{Pres})_{mode}$ must always be greater than $< E_{pp} >$ for all $\sigma_E^2 > 0$. Equation (4.77) is clear verification that despite the overall poor conditioning of the control scheme, it is possible to find a source and cancellation position whereby a point of null pressure can be actively imposed on the existing sound field without significantly influencing the rest of the sound field. Indeed, it is the most probable outcome.

From equation (4.56), the information implicit in equation (4.70) for the probability density function of E_{pres} can be more meaningfully expressed as the cumulative distribution function given below

$$F_Y(y) = \frac{1}{\sqrt{2\pi\sigma_E}} \int_0^y \int_0^1 u e^{-(xu - \mu_E)^2 / \sigma_E^2} \, du \, dx \tag{4.78}$$

The function above together with the cumulative distribution obtained from computer simulated values is shown in figure 4.11, where it is not surprising to observe that the two graphs are in excellent agreement. Small statistical fluctuations due to the finite sample size are now smoothed due to the integration process.

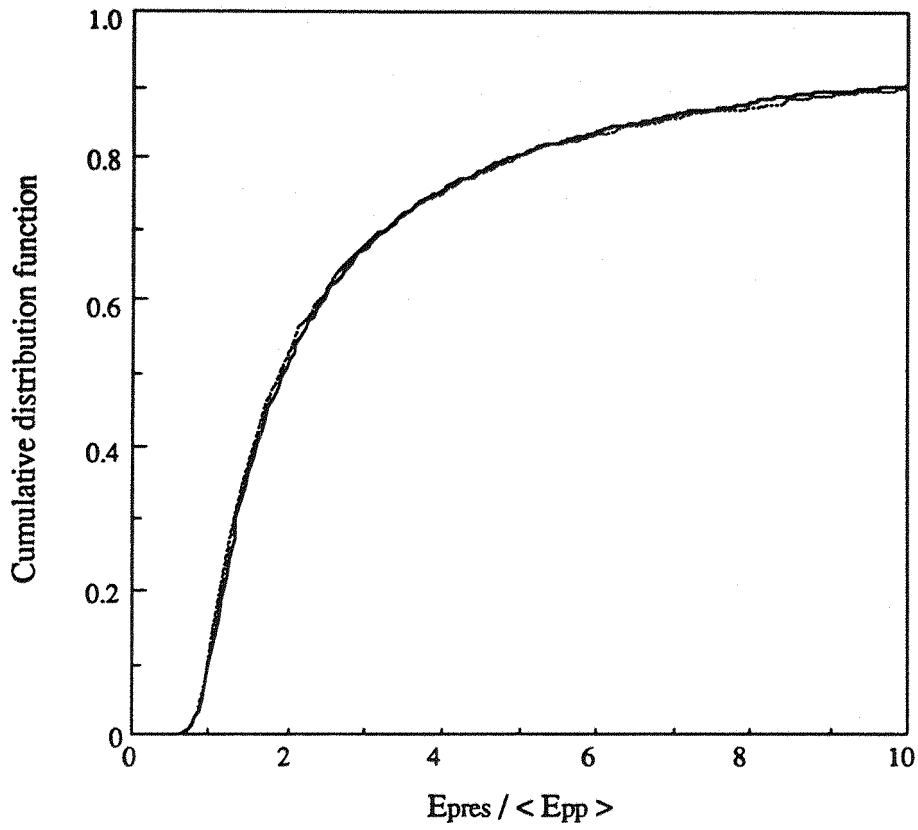

Figure 4.11 The cumulative distribution function of the residual potential energy after driving a random point pressure to zero in a pure tone diffuse sound field. Results from a computer simulated ensemble (dashed line) and the theoretical result of equation (4.78) (solid line).

The principal feature to note from the above figure is how slowly the curves approach unity. Specifically, observe that there is a 10 % chance that driving some randomly selected point in the diffuse sound field to zero will incur a penalty of at least a ten fold increase in the residual potential energy. A further illustration of the unfortunate consequences of imposing point control in the diffuse field is that there is now a less than 10 % chance that the residual potential energy will be less than the averaged primary source potential energy E_{pp}. Previously, with the primary source in isolation it was exactly 50 % . Lastly, note that the median of the probability density function is very nearly twice $< E_{pp} >$ that is

$$(E_{pres})_{med} \approx 2 < E_{pp} > \qquad (4.79)$$

This can be explained if one considers the important asymptotic case whereby the enclosure volume V tends to infinity. Correspondingly, the transfer impedance variance tends to zero, $\sigma_E^2 \rightarrow 0$ as indicated by equations (3.16) and (3.21). In this hypothetical limit, the variance of the potential energy generated by a single source in the enclosure tends to a Dirac delta function centred on the mean μ_E value according to

$$f_X(x) \rightarrow \delta(x - \mu_E) \quad \text{for} \quad V \rightarrow \infty \tag{4.80}$$

where $X = E_{pp}$. It is a straightforward matter to show that in the limit of infinite enclosure volume, the probability density function of the residual potential energy takes on the particularly simple form

$$f_Y(y) \rightarrow \frac{1}{y^2} \quad \text{as} \quad V \rightarrow \infty \quad \text{for} \quad y \geq 1 \tag{4.81}$$

where $Y = E_{pres} / E_{pp}$. Furthermore, the cumulative distribution function $F_Y(y)$ is correspondingly simple

$$F_Y(y) \rightarrow \frac{y - 1}{y} \quad \text{as} \quad V \rightarrow \infty \quad \text{for} \quad y \geq 1 \tag{4.82}$$

For this limiting case, the modal value is unity and the median value is exactly two. Figure 4.9 therefore represents graphic illustration of the difficulties connected with applying active noise control to sound radiated into diffuse field environment.

4.6. Discussion and conclusion

The physics relating to the deceptively simple problem of actively cancelling a point pressure to zero in a pure tone diffuse sound field has been extensively investigated. The simplicity of the single channel control scheme employing just a single loudspeaker and a single microphone has been acknowledged. Nevertheless, the simple analyses presented in this chapter has served to provide considerable insight into the mechanisms by which two highly complex, incongruous sound fields superpose, where one is pre-arranged to be equal and opposite with the other at some pre-determined point in space.

Elementary statistical methods have been employed in order to establish the theoretical variability of all the key physical parameters connected with the diffuse sound field. Primarily, a theoretical assessment of the so called diffuse field 'zone of quiet' about the point of control and equally importantly, a probabilistic description of the diffuse field potential energy as a result of the secondary sound field. Subsequent verification of all the postulated results were obtained from the statistical behaviour of a large number of

computer simulations, which is thought to provide a reasonable alternative to real experimental data. In all cases, the theoretical results were shown to provide good agreement with computer simulated experiments.

The space averaged square pressure profile about the point of cancellation was evaluated and shown to be solely determined by the spatial correlation of the sound field. However, it was found to be impossible to make any general, universal predictions concerning the actual size of the diffuse field quiet zone (of say the -10 dB level). The average behaviour of one set of ensemble averages consisting of fifty simulations was found to be quite different from another set, although the shape of the square pressure profile remained preserved in each case. As a general guideline, a 10 dB reduction was found to typical within a region confined to about one tenth of the acoustic wavelength, with the important *proviso* that the secondary source strength is typically of the order of the primary source strength for which there was found to be no guarantee.

The cause of this apparent lack of consistency was traced to the ill-conditioning of the statistics associated with the square of the secondary source strength $|q_{so}|^2$, the quantity which couples linearly into the square pressure of the sound field. Significantly, the mean of $|q_{so}|^2$ was shown to be undefined in the mathematical sense and was therefore proved to be infinite. Moreover, the expectation value of the unconstrained optimum $< |q_{so}|^2 >$ was shown to be on the borderline of convergence as governed by the integral of the probability density function, multiplied by x, integrated to infinity. It therefore seems reasonable that convergence of $< |q_{so}|^2 >$ can therefore be assured by imposing additional constraints on the secondary source strength which, in principle could be arbitrarily small. This would would force the convergence of the expectation value and therefore the expectation value of all square pressure related variables. This hypothesis forms the basis of the work presented in Chapter 5 and 6.

A consideration of the statistics relating to the secondary source strength required to impose the point of null pressure in the diffuse sound field has also yielded some valuable results. Perhaps the most important, is that the probability density function of the secondary source strength is completely independent of the details of the sound field such as acoustic damping, room volume and excitation frequency, assumed greater than the Schröder frequency. The validity of the result rests solely on the sound field being in a state of 'diffuseness'.

Last, an analysis of the theoretical probability density function of the diffuse field potential energy before and after control was undertaken. These results were particularly

informative inasmuch as they provide a single global index relating to the penalty incurred as a consequence of the driving a point pressure to zero. One can consider the enclosure potential energy to represent a measure of the average diffuse field square pressure. Inspection of the probability density function reveals how easily the imposition of control can force the residual potential energy to reach many times its value in the absence of the secondary source. In fact, the mean value of the potential energy calculated from 15,000 computer simulations, exhibits a ten fold increase as a consequence of the control, although this value is not particularly meaningful given that its standard deviation was even larger by another order of magnitude. The true expectation of both the mean and the variance of the optimal secondary source strength were both calculated to be equal to infinity which therefore serve as a caution regarding the consequences of applying active noise control to the diffuse sound field.

Although specific tests have not been carried out, it is strongly suspected that many of the results established in this chapter may be applied to other types of sound field which do not comply with the rigourous requirements of diffuseness. Indeed, the formula describing the space averaged zone of quiet about a point of cancellation is valid for any sound field whose spatial correlation function is properly defined and which is stationary with respect to measurement position. Furthermore, it is generally acknowledged that the Gaussianity of both the real and imaginary parts of the complex transfer impedance is not restricted to only the diffuse impedance field but is a reasonable description of less reverberant wave fields. The precise area of validity remains to be identified.

As a closing remark, it is probably worth noting the implications for driving a point pressure to zero which comprises a broadband range of frequencies. The analysis the outlined in this chapter appears to show that the unconstrained optimum q_{so} is a poorly conditioned random variable which has a significant likelihood of 'blowing' up. Attempting to control a broadband range of frequencies at a point suggests that the difficulties are compounded since ill-conditioning may occur any one frequency. The problems are not as severe as at first they appear because all the physical variables associated with the diffuse field are highly correlated in frequency as well as in space[59]. Thus, establishing satisfactory behaviour at one frequency ω_0 will ensure sensible results at another frequency $\omega_0 + \Delta\omega$, as governed by the form of the frequency dependent correlation function $< q_{so}(\omega_0) q_{so}(\omega_0 + \Delta\omega) >$ which remains to be determined.

APPENDIX 4

Appendix 4.1

The cancellation of the pressure at a single point in a one dimensional diffuse sound field

Consider a hard walled, lossless duct of length L which is constrained to support only plane waves, figure A4.1. At either end of the duct defined by x=0 and x=L, are situated idealised piston sources pulsating about their mean positions.

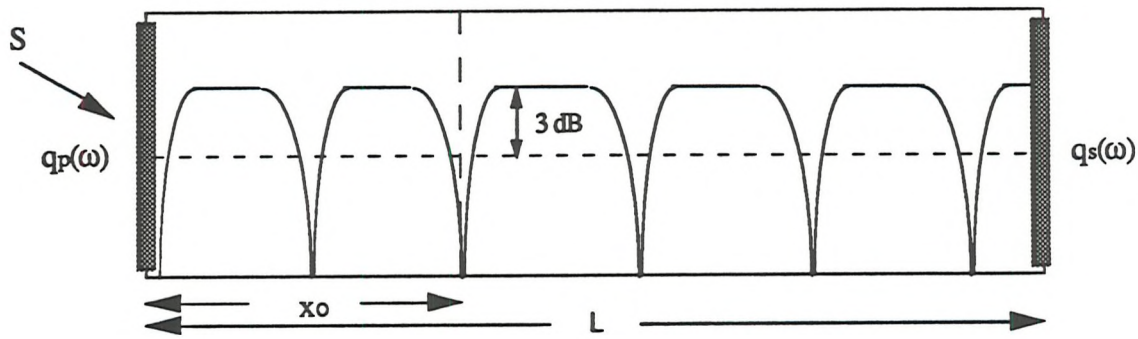

Figure A4.1 A conceptual model of a hard walled duct which is contrived to support only plane waves. At either end are primary and secondary line sources, of which the secondary is driven to cancel the pressure at x_0 to zero. Average residual square pressure (solid line), Average primary square pressure level (dashed line).

Assuming that the duct is hard walled with a uniform cross sectional area S and the acoustic particle velocity is equal to the respective source velocities at the ends. The pressure p(x) inside the duct is given by[37]

$$p(x) = \frac{Z}{\sin kL}\left[q_p \cos k(L - x) + q_s \cos kx \right] \qquad (A4.1)$$

where Z is the duct, plane wave impedance $Z = -j\rho c_0 / 2S$.

Equation (A4.1) is consistent with the 'travelling wave' model of the sound field which is built up following an infinite succession of reflections at the terminations. Consider the radiation impedance of the primary source $(Z_{rad})_p$ in the absence of the secondary source. Putting $q_s = 0$, the primary pressure $p_p(x = 0)$ may be represented as

$$p_p(x=0) = \frac{-jq_p\rho c_0}{2S \sin kL} \cos kL \qquad (A4.2)$$

The radiation impedance of the primary source in the absence of the secondary source is therefore determined from

$$(Z_{rad})_p = \frac{p_p(x=0)}{q_p} = -j\frac{\rho c_0}{2S}\cot kL \qquad (A4.3)$$

which is purely reactive. Equation (A4.3) is the radiation impedance of a closed pipe with rigid terminations as discussed in detail by Kinsler *et-al*[50]. The resonances of the duct f_n, can be identified with the singularities of cotkL to give

$$(f_n)_{qs=0} = \frac{nc_0}{2L} \qquad (A4.4)$$

Now consider the one dimensional sound field in the duct where both the primary and secondary sources are radiating simultaneously, but whose source strengths are linearly related such that the pressure at x_0 is driven to zero. Following from equations (4.2) and (4.3), the total acoustic pressure at x_0 may be driven to zero for a secondary source strength given by $q_{so} = q_p H_o$ where the transfer function H_o is given by

$$H_o = -\frac{\cos k(L - x_0)}{\cos kx_0} \qquad (A4.5)$$

The total pressure in the duct is now equal to

$$p(x) = \frac{-jq_p\rho c_0}{2S\sin kL}\left[\cos k(L - x) - \frac{\cos k(L - x_0)}{\cos kx_0}\cos kx\right] \qquad (A4.6)$$

The primary source radiation impedance is profoundly altered by the presence of the secondary sound field which has now changed to

$$(Z_{rad})_p = \frac{p_p(x=0)}{q_p} = -j\frac{\rho c_0}{2S}\left[\frac{\cos kL\cos kx_0 - \cos k(L - x_0)}{\sin kL\cos kx_0}\right] \qquad (A4.7)$$

Employing standard trigonometric identities, one can show that all terms which are dependent on the length of the duct L, cancel in the quotient of equation (A4.7), leaving the primary source radiation impedance $(Z_{rad})_p$ as a sole function of the point of cancellation x_0 to give

$$(Z_{rad})_p = j\frac{\rho c_0}{2S}\tan kx_0 \qquad (A4.8)$$

Equation (A4.8) is precisely the radiation impedance of an open ended pipe of length x_0. The result of the point cancellation therefore, is to effectively isolate the remainder of the

pipe x > L from the influence of the primary source. A similar result has been derived by Trinder *et-al*[91]. The addition of the secondary source, from the point of view of the primary source, has been to create a new boundary condition since the new sound field is effectively 'clamped' at x_0. This was also the conclusion arrived at by Curtis *et-al.*[10]. The new resonances are now more sparsely located in frequency which may be identified from the values of kx_0 which cause $\tan kx_0$ to be infinite. Physically, this arises from the infinite build up of reflected sound which constructively interfere on each reflection and eventually form an anti-node of infinite magnitude at the primary source position. In practice acoustic damping will tend to regulate the response at the anti-node in which event this idealised model will no longer be accurate. The new resonant frequencies of the primary source $(f_n)_{qs=qso}$ now correspond to

$$(f_n)_{qs=qso} = \frac{(n+1)c_0}{4x_0} \qquad \text{(A4.9)}$$

From the point of view of the primary source, the closed, finite duct is indistinguishable from a shortened duct of length x_0 with an open end. An alternative, but equivalent acoustic space is that of a duct with some hypothetical infinitesimally thin pressure release mechanism located around the perimeter walls at a distance x_0 from the primary source. This arrangement of passive elements would also form a pressure null across a cross section of the duct at x_0. Thus, the effect of applying active control is to alter the boundary conditions of the space which previously were determined solely by the properties of the walls of the enclosure. Being able to identify an equivalent acoustic space with the same effective boundary conditions begs the question as to whether one can describe the new sound field in terms of *new* acoustic modes i.e., new eigenfunctions appropriate to the geometry and the new equivalent boundary conditions. Depending of course on the extent of the active control applied throughout the space, the new modes shapes would be correspondingly modified and therefore by implication, the new resonant frequencies of the enclosure would also differ from their values in the absence of control. A shift in the new resonant frequencies of the enclosure could have unfortunate consequences in terms of the overall sound pressure level in the enclosure.

Attempts to reconcile the mode shapes derived from finite element analysis in an enclosure with the same effective boundary conditions in terms of an array of pressure nulls, and the square pressure response at resonance due to the action of the secondary sources has so far been inconclusive. The spectrum of the radiation impedance of a plane piston type source in a shallow rectangular box at low frequencies was shown to change in the presence of an array secondary sources driven to cancel the pressure at an equal number of points. Unfortunately, the new resonances of the primary source radiation impedance were poorly correlated with the finite element predictions. However, for the purposes of

the problem under discussion here, the cancellation of the pressure at a point in a three dimensional enclosure is believed to cause only a minor perturbation of the mode shapes. At high modal densities such that $M(\omega) >> 1$, where modal behaviour is obscured owing to the large number of overlapping modes, the frequency response of the enclosure is identical in the statistical sense both before and after control.

Proceeding to calculate the space averaged zone of quiet for this one dimensional sound field, the total acoustic pressure in the duct p(x) may be calculated from equation (A4.6). Putting $x = x_0 + \Delta x$, expanding and collecting terms yields

$$|p(x)|^2 = |q_p|^2 Z^2 \left[\sin^2 k(L - x_0) + 2\cos k(L - x_0)\sin k(L - x_0)\tan kx_0 + \cos^2 k(L - x_0)\tan^2 kx_0 \right] \sin^2 k\Delta x \qquad \text{(A4.10)}$$

Keeping the point of cancellation on x_0 fixed, and averaging over all duct lengths L, yields the simplified expression

$$< |p(x_0 + \Delta x)|^2 > = < |p_p|^2 > [\ 1 + \tan^2 kx_0\ ] \sin^2 k\Delta x \qquad \text{(A4.11)}$$

where $< >$ denotes the expectation over L and where the following relations have been used, $< \sin k(L - x_0) \cos k(L - x_0) > = 0$ due to the orthogonality of the elementary functions and

$$|q_p|^2 Z^2 < \cos^2 k(L - x_0) > = |q_p|^2 Z^2 < \sin^2 k(L - x_0) > = < |p_p|^2 > \qquad \text{(A4.12)}$$

Now averaging over all points of cancellation on x_0, one can show that the average value of $\tan^2 kx_0$ is finite. This is despite the finite number of singularities in one period of the function arising from those points where the secondary source is completely unable to couple into the sound field.

$$< \tan^2 u > = \frac{1}{2\pi} \int_0^{2\pi} \tan^2 u\, du = 1 \qquad \text{(A4.13)}$$

where $< >$ now denotes the expectation over x_0. Further noting that $< \tan x_0 > = 0$, the one dimensional quiet zone when averaged over all duct lengths and cancellation positions $<< |p(\Delta x)|^2 >>$, may be shown to be equal to

$$<< |p(\Delta x)|^2 >> = 2 < |p_p|^2 > \sin^2 k\Delta x \qquad \text{(A4.14)}$$

Equation (A4.14) indicates that as a consequence of nullifying the pressure at a single point in the duct the square pressure is, on average, increased by a maximum of 3 dB. This relationship is indicated in figure A4.1. This result could equally have been derived from the more general relationship obtained in the early part of this chapter in equation (4.27).

The one dimensional quiet zone has the same dependence on the separation distance Δx as that predicted by the general formula given by equation (4.27) in terms of the one dimensional diffuse field correlation function $\cos k\Delta x$ since $1 - \rho^2(\Delta x) = \sin^2 k\Delta x$. Also note that from equation (A4.5)

$$H_o^2 = \cos^2 kL + \sin 2kL \tan kx_o + \sin^2 kx_o \qquad \text{(A4.15)}$$

Further noting that

$$< \cos^2 kL > = < \sin^2 kx_o > = \frac{1}{2} \qquad \text{(A4.16)}$$

and

$$< \sin 2kL \tan kx_o > = 0 \qquad \text{(A4.17)}$$

One can therefore show that $< |H_o|^2 > = 1$ so that according to equation (A4.15)

$$< |p_p|^2 > = < |p_s|^2 > \qquad \text{(A4.18)}$$

Putting $1 - \rho^2(\Delta r) = \sin^2 k\Delta x$ and $< |p_p|^2 > = < |p_s|^2 >$ into equation (4.27) recovers the result originally in equation (A4.14) derived from first principles.

Appendix 4.2

The probability density function of the residual potential energy after the cancellation of the pressure at a point

Given $X_1 = |H_o|^2$ whose probability density function is $f_{x1}(x_1) = (1+x_1)^{-2}$ (A4.19)

and $X_2 = E_{pp}$, whose density function is $f_{x2}(x_2) = \dfrac{1}{\sqrt{2\pi\sigma_E^2}} e^{-(x_2-\mu_E)^2/2\sigma_E^2}$ (A4.20)

The probability density function $f_Y(y)$ is required where $Y = E_{pres}$ defined by

$$Y = X_2(1+X_1) \qquad \text{(A4.21)}$$

From an analysis exactly analogous to the transformation of variables in the evaluation of a double integral, it may be shown[63] that if X_1 and X_2 are jointly continuous random variables with a probability density function $f_{X_1,X_2}(x_1,x_2)$ and $Y_1 = g_1(x_1,x_2)$ and $Y_2 = g_2(x_1,x_2)$ define one to one transformations, then the joint probability density function $f_{Y_1,Y_2}(y_1,y_2)$ may be obtained from equation (A4.22)

$$f_{Y_1,Y_2}(y_1,y_2) = |J|\ f_{X_1,X_2}(g_1^{-1}(y_1,y_2),\ g_2^{-1}(y_1,y_2)) \tag{A4.22}$$

where $|J|$ is the Jacobian determinant of the transformation defined by

$$|J| = \begin{vmatrix} \frac{\partial x_1}{\partial y_1} & \frac{\partial x_1}{\partial y_2} \\ \frac{\partial x_2}{\partial y_1} & \frac{\partial x_2}{\partial y_2} \end{vmatrix} \tag{A4.23}$$

However, in the present case, only one transformation is required, the one relating to the residual potential energy defined from equation (A4.21). It is therefore necessary to introduce some elementary dummy transformation whose density function function will remain undetermined

$$Y_2 = X_2 \tag{A4.24}$$

enabling the Jacobian $|J|$ of the transformations to be constructed according to equation (A4.23)

$$|J| = \frac{1}{1+y_2} \qquad \text{for } y_2 > 0 \tag{A4.25}$$

The joint probability function $f_{Y_1,Y_2}(y_1,y_2)$ is readily constructed since $f_{Y_1}(y_1)$ and $f_{Y_2}(y_2)$ are independent which is therefore simply their product

$$f_{Y_1,Y_2}(y_1,y_2) = f_{Y_1}(y_1)\, f_{Y_2}(y_2) = \frac{\frac{1}{\sqrt{2\pi\sigma_E^2}} e^{-(x_2-\mu_E)^2/2\sigma_E^2}}{\sqrt{2\pi}\,\sigma_E\,(1+y_2)^2} \tag{A4.26}$$

Incorporating the results of equations (A4.19), (A4.20) and (A4.25)

$$f_{Y_1,Y_2}(y_1,y_2) = \frac{e^{-\left[\frac{y_1}{1+y_2}-\mu_E\right]^2/2\sigma_E^2}}{\sqrt{2\pi}\,\sigma_E\,(1+y_2)^3} \tag{A4.27}$$

The marginal density function $f_{Y1}(y_1)$ of the residual potential energy may be determined by integrating out y_2 over the joint density function

$$f_{Y1}(y_1) = \int_0^\infty f_{Y1,Y2}(y_1,y_2)\, dy_2 \qquad \text{(A4.28)}$$

$$f_{Y1}(y_1) = \frac{1}{\sqrt{2\pi}\sigma_E} \int_0^\infty \frac{e^{-\left[\frac{y_1}{1+y_2} - \mu_E\right]^2/2\sigma_E^2}}{(1+y_2)^3}\, dy_2 \qquad \text{(A4.29)}$$

which may be considerably simplified by the change of variable $u = (1+y_2)^{-1}$

$$f_{Y2}(y) = \frac{1}{\sqrt{2\pi}\sigma_E} \int_0^1 u e^{-(y_2 u - \mu_E)^2/\sigma_E^2}\, du \qquad \text{(A4.30)}$$

CHAPTER 5

ENGINEERING ZONES OF QUIET IN THE PURE TONE DIFFUSE SOUND FIELD

5.0. Introduction

The potential difficulties inherent in using active control to cancel the pressure at a point in diffuse fields were exposed in Chapter 4. In that chapter the results of a study of the behaviour of the unconstrained optima were presented in terms of the secondary source strength, zone of quiet and the residual potential energy. The variables are necessarily unconstrained because the cancellation of the point pressure is achieved with no regard for the magnitude of effort required, or the subsequent effect on the sound field globally. In this respect, the problem is artificially formulated and is therefore wholly unrealistic of the type of approach one would ultimately employ in practice.

One of the principal results to emerge so far in this thesis is an expression for the region of confinement in which the acoustic pressure is attenuated below that of the primary level. The so called diffuse field quiet zone has been shown to be restricted to length scales which are typically a small fraction of the acoustic wavelength. Unfortunately, this was only achieved at the expense of significantly raised levels of the potential energy over the entire enclosure. The best one can do therefore, is to try to extend this region of attenuation over a wider region as possible while at the same time leaving the rest of the sound field as least affected as possible. It soon becomes clear that these requirements are to a certain degree inconsistent when using a secondary source which is remote from the cancellation point.

The work presented in this chapter comprises an investigation into some various control schemes which attempt to capitalise on the diffuse field properties with the aim of improving on the typical levels of attenuation documented in the last chapter. It was demonstrated that extremely large values of the diffuse field square pressure were sufficiently likely to occur that the average value over all space is equal to infinity. The cause of this ill-conditioning was attributed to the inability of the secondary source to provide, on average, sufficient influence at the chosen point of cancellation. It is this unexpected result which forms the starting point behind the control strategies presented in this chapter. The strategies investigated include constraining the secondary source strength to be below some limiting value (hard limiting), minimising a cost function which includes control effort as well as measured error signals (soft limiting) and minimising the sum of

the squares of the pressures at two closely spaced microphones. An initial discussion of these strategies was presented in reference [92]. Some empirical findings pertinent to multi-channel control are also presented.

5.1. Hard Limiting

Up until now, the necessary secondary source strengths have been allowed to take arbitrarily large values so that all of the probability density functions associated with the physical variables under discussion were of course unbounded. That is to say, for example, that the probability of the secondary source strength required to be say, many thousands times greater than the primary source strength is finite. This would result in correspondingly large increases in the potential energy by roughly the same order of magnitude. The outcome described here is clearly absurd, however, the example serves to highlight the fallacious assumptions giving rise to these unfortunate statistics.

Any real control system powered by a real amplifier and subject to the finite dynamic range of its transducers will possess an upper-bound value in terms of its maximum acoustic power output. Above this maximum value, the control system would fail to operate satisfactorily. Furthermore, driving a secondary loudspeaker above some critical level will inevitably introduce non-linearities into the response of the loudspeaker as well as having an adverse affect on the sound field globally. Clearly, with each control system one can associate a maximum source strength $|q_{so}|_{max}$, either built into the control system by the engineer according to some pre-determined criterion, or as an unfortunate artefact of the limited hardware. The purpose of this section is to examine the consequences of this limitation, known as 'hard limiting', both in terms of the quiet zone and the corresponding increase in the space averaged square pressure level.

In the case where the secondary source strength is completely unconstrained, the probability density function of the square of the absolute value of the transfer function $V = |H_o|^2$ is given by

$$f_V(v) = \frac{1}{(1+v)^2} \qquad \text{for } 0 \leq V \leq \infty \qquad (5.1)$$

where the interval within which the probability density function is non-zero is now stated explicitly. Now suppose that the distribution of secondary source strengths is prevented from being greater than some pre-determined maximum value, say $|q_{so}|_{max}$ such that

$$|q_{so}|_{max} = q_p|H_o|_{max} \qquad (5.2)$$

In statistical terms, the F(2,2) probability density function is now truncated to some maximum value V_{max} where $V_{max} = |H_0|^2_{max}$. All values of V less than V_{max} still have the same *relative* likelihood of occurrence although the *absolute* likelihood is increased by a factor α at the expense of a zero probability of V being greater than V_{max}. Truncation of the ensemble of values has the effect of 'stretching' the probability density function in the interval of validity as described by equation (5.3) below

$$f_V(v) = \alpha \frac{1}{(1+v)^2} \qquad \text{for } 0 \leq V \leq V_{max} \tag{5.3}$$

where α remains to be determined and represents some linear, dimensionless scaling constant greater than unity. One can conceive of a real situation where the position of the secondary loudspeaker is re-adjusted until perfect cancellation of the acoustic pressure is achieved while ensuring that the secondary source strength required lies within the allowed interval. In nearly all cases, the primary source position will be fixed and the point of cancellation will also be fixed, being largely dictated by, for example, the car driver's ear position.

The value of α is obviously determined by the value of V_{max} which may be readily evaluated by exploiting the fact that the area under under a probability density function is equal to unity. From equation (5.3)

$$\alpha \int_0^{v_{max}} \frac{1}{(1+v)^2} dv = 1 \tag{5.4}$$

Solving for α yields

$$\alpha = [\, F_V(v_{max}) \,]^{-1} = \frac{1 + v_{max}}{v_{max}} \tag{5.5}$$

where obviously

$$\alpha \geq 1 \tag{5.6}$$

The resulting probability density function of the hard limited ensemble may now be written as

$$f_V(v) = \frac{1 + v_{max}}{v_{max}} \frac{1}{(1+v)^2} \qquad \text{for } V \leq V_{max}. \tag{5.7}$$

and

$$f_V(v) = 0 \qquad \text{for } V > V_{max}. \tag{5.8}$$

By way of illustration, the ensemble of unconstrained values employed in the distribution of values shown in figure 4.6 was edited to exclude all those values greater

than 3 so that $V_{max} = 3$ in which case $\alpha = 4/3$. In this example therefore, $|q_{so}|_{max} = \sqrt{3}\,|q_p|$. The theory and the simulated distribution of values are compared in figure 5.1.

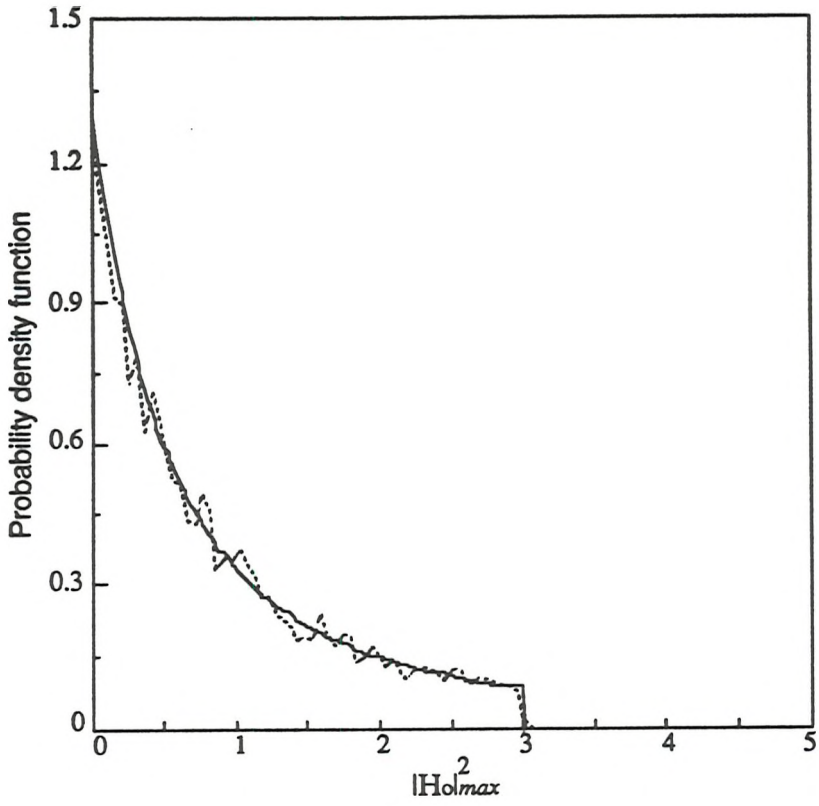

Figure 5.1 The probability density function of an ensemble of values of $|H_o|^2$ *constrained not to exceed 3. Simulated data (dashed line), theoretical curve (solid line).*

It is instructive to consider the mean of this hard limited probability density function which now must converge on some finite value since all of the moments associated with the truncated distribution are now derived from integrals evaluated within finite limits. From equation (4.40), the mean value of the distribution is readily obtained from

$$< |H_o|^2_{hard} > = \frac{1 + v_{max}}{v_{max}} \int_0^{v_{max}} \frac{v}{(1+v)^2}\, dv \qquad (5.9)$$

$$= \frac{1 + v_{max}}{v_{max}} \ln (1 + v_{max}) - 1 \qquad (5.10)$$

As previously remarked, $< |H_o|^2_{hard} >$ will tend to infinity as the level of constraint is gradually lifted such that v_{max} tends to infinity. A graph showing the expectation of the normalised potential energy as calculated from $< |H_o|^2_{hard} > + 1$ is shown below versus $|q_{so}|_{max}$. Also indicated for integer fractions of $|q_p| / |q_{so}|_{max}$ is the cumulative distribution function determined from equation (4.58) for the unconstrained problem. These values are exact except when a decimal point is indicated! The graph is most meaningful for values of

$|q_p| / |q_{so}|_{max}$ greater than unity for which the corresponding variance in the normalised potential energy is small in relative terms.

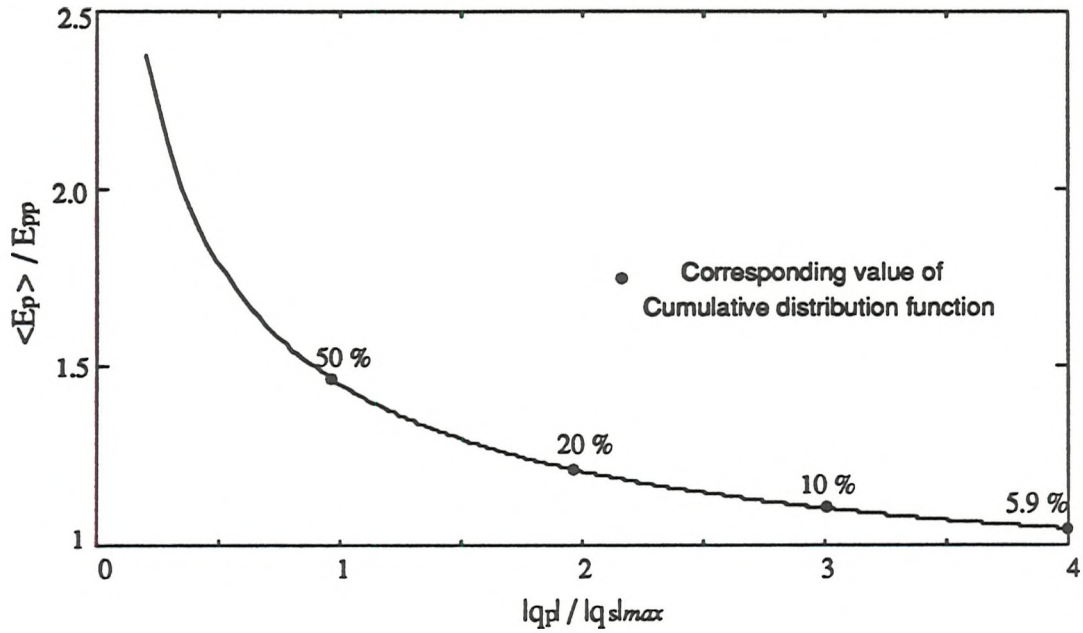

Figure 5.2. The expectation of the normalised potential energy resulting from driving a point pressure to zero when hard limiting is imposed.

The graph is valuable in providing guide-lines relating to the first order behaviour of the residual diffuse field square pressure together with the likelihood of achieving its perfect cancellation at a single point. It is extremely encouraging to note that for even quite useful values of V_{max}, the corresponding expectation value of the normalised potential energy remains within tolerable limits. This behaviour is an immediate consequence of how slowly the mean value diverges to infinity as governed by equation (5.10). In fact logarithmic increase is the slowest of all elementary functions just as exponential growth (the inverse function) is the fastest. For example, setting an upper bound for the maximum secondary source strength to say twice the primary source strength i.e., $|q_{so}|_{max} = 2\,|q_p|$, provides for an 80 % chance of being able to cancel perfectly some pressure at an arbitrarily chosen point to zero. Providing the secondary source strength is not allowed to exceed this value, the expectation in the diffuse field potential energy will increase by only 1.8 dB.

Precisely how this simple theory translates to the actual space averaged diffuse field quiet zone is readily evaluated. Recalling equation (4.25), which for the case when hard limiting is being applied, is given by

$$< |\hat{p}(r_0 + \Delta r)|^2 > = < |\hat{p}_p(r)|^2 > [1 + < |H_o|^2_{hard} >] (1 - \hat{\rho}^2(\Delta r)) \qquad (5.11)$$

The hat '^' is used to suggest that the random variables are now only estimates owing to the finite sample size so as to make the distinction from proper expectations due to the fact that some of the possible outcomes have been excluded. For a fully diffuse, three dimensional sound field, for $k\Delta r << 1$ the term $1 - \hat{\rho}^2(\Delta r)$ has a particularly simple power series

$$1 - \hat{\rho}^2(\Delta r) \approx \tfrac{1}{3}(k\Delta r)^2 \tag{5.12}$$

Recalling that $1 + < |H_o|^2_{hard} > = \dfrac{1 + v_{max}}{v_{max}} \ln(1 + v_{max})$ from equation (5.10), setting the right hand side of equation (5.11) to 0.1 and solving for $2\Delta r_{0.1}$ shows that to a good approximation, the -10 dB zone of quiet may be written as

$$\frac{2< \Delta r_{0.1} >}{\lambda} \approx \frac{u_{max}}{\pi} \sqrt{\frac{0.3}{(1+u^2_{max}) \ln(1+u^2_{max})}} \tag{5.13}$$

where $U_{max} = |H_o|_{max}$. This expression is plotted in figure 5.3 versus the reciprocal transfer function $|q_p| / |q_{so}|_{max}$. Below this figure is shown the cumulative distribution function also plotted against the reciprocal transfer function $(U_{max})^{-1}$

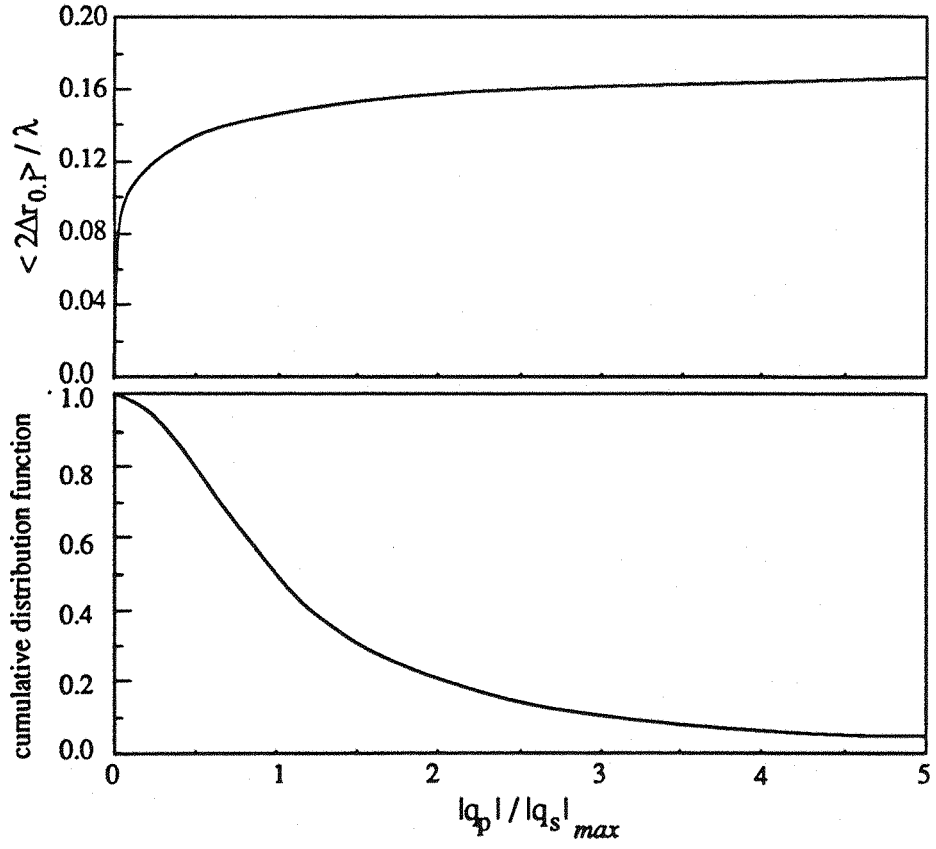

Figure 5.3 The expected value of the diffuse field quiet zone versus $|qp| / |q_{so}|_{max}$. *Also shown is the cumulative distribution function of equation (4.58), also as a function of* $|qp| / |q_{so}|_{max}$.

Values of the secondary source strength which are prevented from exceeding, say ten times that of the primary source strength where $|q_p| / |q_{so}|_{max} = 0.1$ (which accounts for more than 99% of cases) gives rise to an expected value for the size of quiet zone typically equal to one tenth of a wavelength. For this example the expected increase in potential energy is by a factor of 2.4 (approximately equal to 4 dB). In the absence of any upper-bound value imposed on the distribution of secondary source strengths corresponding to $|q_p| / |q_{so}|_{max} = 0$, the true, unconstrained expectation is zero. However, upper bound values of the secondary source strength which are of the order of the primary source strength, are sufficient to secure an expectation value for the diffuse field quiet zone of about 0.15 wavelengths. Unfortunately, the probability of achieving perfect cancellation of the pressure diminishes rapidly.

The statistical distribution of hard limited secondary source strengths can also be derived. Following an analysis identical to that presented in the last chapter, one can show that

$$f_U(u) = \frac{1+u_{max}^2}{u_{max}^2} \frac{2u}{(1+u^2)^2} \qquad \text{for } u \leq U_{max} \tag{5.14}$$

and

$$f_U(u) = 0 \qquad \text{for } u > U_{max} \tag{5.15}$$

where $U_{max} = |H_o|_{max}$.

Of principal interest from this theoretical probability density function is the mean which may be calculated from

$$< |q_{so}|_{hard} > = |q_p| \frac{1+u_{max}^2}{u_{max}^2} \int_0^{u_{max}} \frac{2u^2}{(1+u^2)^2} du \tag{5.16}$$

where the simple change of variable $u = \tan u'$ yields

$$< |q_{so}|_{hard} > = |q_p| [\frac{(1+u_{max}^2)\tan^{-1} u_{max} - u_{max}}{u_{max}^2}] \tag{5.17}$$

The variance is now also defined according to equation (5.18), providing some useful information relating to the typical variation one can expect from successive experiments

$$\sigma^2_{|q_{so}|} = < |q_{so}|^2_{hard} > - < |q_{so}|_{hard} >^2 \tag{5.18}$$

where $< |q_{so}|^2_{hard} >$ can be evaluated from

$$< |q_{so}|^2_{hard} > = |q_p|^2 \frac{1+u^2_{max}}{u^2_{max}} \int_0^{u_{max}} \frac{2u^3}{(1+u^2)^2}\, du \qquad (5.19)$$

From equation (5.17) and (5.19) the variance of the unconstrained secondary source strength can be shown to have the complicated form

$$\sigma^2_{|q_{so}|} = \Big[\frac{1+u^2_{max}}{u^2_{max}} \ln(1 + u^2_{max}) + 2\frac{1+u^2_{max}}{u^3_{max}} \tan^{-1} u_{max} - \frac{(1+u^2_{max})^2}{u^4_{max}} (\tan^{-1} u_{max})^2 - \frac{1}{u^2_{max}} - 1 \Big] |q_p|^2 \qquad (5.20)$$

The mean value according to equation is plotted below for U^1_{max} between zero and four and the region, shaded gray, represents the interval between plus and minus one standard deviation $\sigma_{|q_{so}|}$ from the mean value according to equation (5.21).

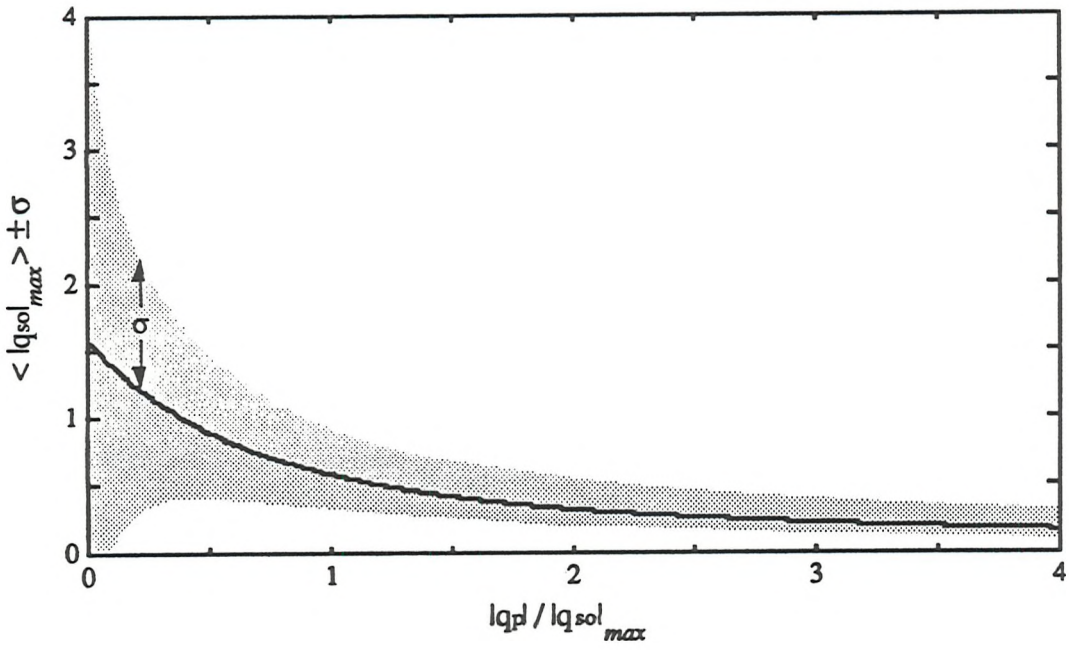

Figure 5.4. The mean of the hard limited secondary source strength plotted against the reciprocal transfer function $|q_p| / |q_{so}|_{max}$. The shaded region denotes the values contained within plus and minus one standard deviation from the mean.

The function plotted in the figure above falls surprisingly slowly from its unconstrained, asymptotic value of $\pi / 2$ at $|q_p| / |q_{so}|_{max} = 0$. Such is the gradual rate of descent of this function that varying $|q_{so}|_{max}$ from infinity down to a value equal to the primary source strength $|q_p|$ results in little more than a halving of its associated mean value. Now that all possible outcomes are constrained to lie in a finite interval, all of the moments associated

with the distribution are now properly defined. As anticipated, the function asymptotes to infinity as the level of constraint is gradually removed such that $|q_p| / |q_{so}|_{max}$ approaches zero. However, for a upper-bound value of $|q_{so}|_{max} = 2|q_p|$ there is an 80 % chance of perfectly canceling the pressure for which the expected increase in the mean square pressure is only raised by a factor of 1.38.

The analysis in this section is, in essence, an investigation into the divergence and convergence properties of the relevant variables. It nevertheless serves to demonstrate that the active control of the diffuse sound field is not as poorly conditioned as the former analysis has initially indicated. Indeed, upper bound values for the secondary source strength which are only slightly greater than the primary source strength, provide sufficient input into the sound field to be able to cancel the pressure at the majority of cancellation point positions while incurring only small increases in the space averaged square pressure over the sound field globally. Figure 5.3 indicates that for $|q_{so}|_{max} = 2|q_p|$ the size of the quiet zone is approximately 0.13λ. However, upper bound values of the secondary source strengths which are reasonably large exhibit only small variations from point to point within the diffuse sound field enabling the optimal secondary source strength requirements to be anticipated to within an acceptable level of accuracy. For the current example, the secondary source variance is approximately $0.25\ |q_p|^2$ corresponding to a standard deviation of about $0.5\ |q_p|$. Not surprisingly, the level of variance depends strongly on the level of freedom assigned to the control system which is of course determined by the size of the upper bound value $|q_{so}|_{max}$. The difficulty in applying these figures to any real example however, is being able to quantify the primary source strength. This is a notoriously difficult measurement for large, complex vibrating bodies.

In practice, one should allow for a maximum secondary source volume velocity when seeking to cancel the pressure in a high frequency, enclosed sound field to be typically twice that of the primary source. This ratio strives to achieve a level of compromise between standing a reasonable chance of accomplishing perfect cancellation of the pressure at the desired point, forming a reasonable size quiet zone while ensuring against too large an increase in the average diffuse field square pressure.

5.2. The under determined problem: Employing many secondary sources to minimise the pressure at a single point

In the next two sections, elementary multi-channel control schemes are considered from the point of view of their statistical behaviour in a diffuse field environment. In all of the following, it is assumed that the in-phase part, and quadrature part of the complex

transfer impedance between two well separated diffuse field points are bivariate Gaussian random variables. Consider a pure tone diffuse sound field in which there are many *independently* positioned secondary sources employed to reduce the square pressure at the same point r_0 according to some hitherto unspecified criterion. This arrangement is shown schematically in figure 5.5.

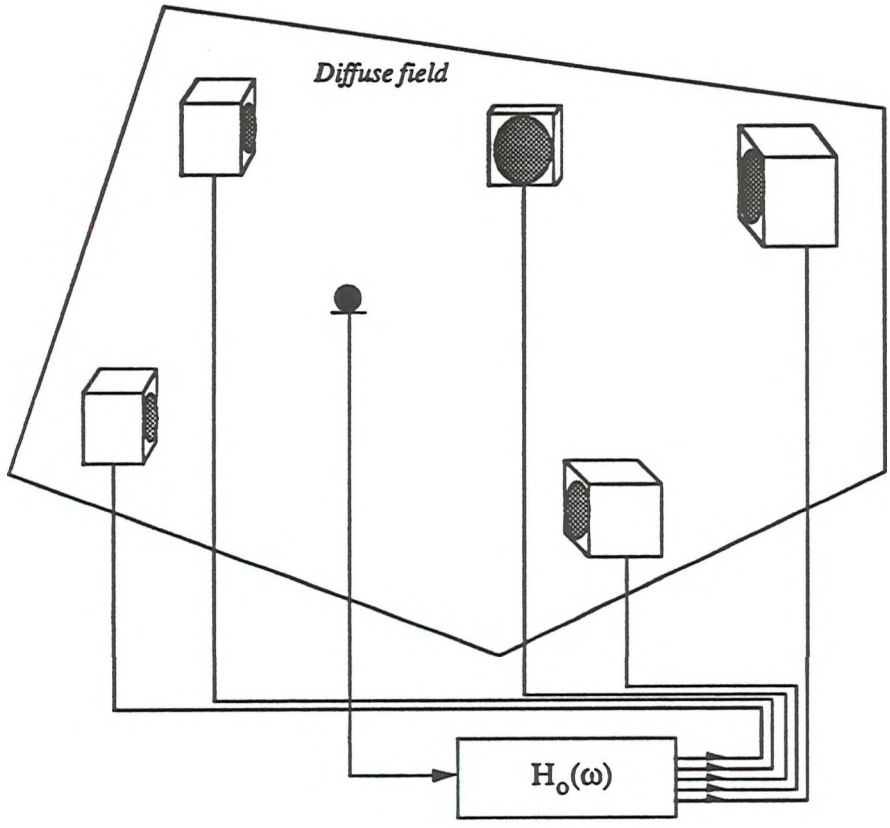

Figure 5.5 An illustration of a number of secondary sources acting to minimise the square pressure at one single point in a pure tone diffuse sound field.

In terms of a proper control formalism, consider the cost function J_p constructed according from the sum of 'cost' and 'effort' terms

$$J_p = |p(r_0)|^2 + \beta \underline{q}_s^H \underline{q}_s \qquad (5.21)$$

The term β is a user determined 'effort' weighting constant. The term $\underline{q}_s$ denotes a vector of secondary source strengths $\underline{q}_s^T = [q_{s1}\ q_{s2}\ q_{s3}\ \ldots\ q_{sj}]$ and 'H' denotes the Hermitian conjugate transpose. This new cost function J_p now includes an additional term $\beta \underline{q}_s^H \underline{q}_s$ which is the sum of the modulus squared secondary source strengths, the control effort, which ensures that the effort provided by the control system by way of the secondary source strengths required to perform the reduction in the acoustic pressure are fully accountable. The secondary source strengths can no longer take arbitrary large values since this would now

tend to dominate the cost function. In this event the effort would be directed towards regulating its own volume velocity output and the reduction in the pressure would emerge as a minor priority by comparison. The level of attenuation produced at the control point will therefore be somewhat diminished. For most source positions however, the additional term $\beta \underline{q}_s^H \underline{q}_s$ will represent only a minor perturbation on the actual square pressure $|p(r_0)|^2$ and only small losses in the actual achievable pressure reduction will be incurred. The process just described is sometimes refered to as soft limiting

Specifying the problem more precisely, the vector of optimally adjusted secondary source strengths $\underline{q}_s$ is now required which satisfies the optimisation criterion

$$\frac{\partial J_p}{\partial q_{s1}} = \frac{\partial J_p}{\partial q_{s2}} = \cdots = \frac{\partial J_p}{\partial q_{sj}} = 0 \qquad (5.22)$$

where it is now tacitly assumed that setting the differential of the cost function with respect to a complex secondary source strength zero represents the following operations

$$\frac{\partial J_p}{\partial q_{sj}} = \frac{\partial J_p}{\partial \Re\{q_{sj}\}} = \frac{\partial J_p}{\Im\{q_{sj}\}} = 0 \qquad (5.23)$$

The solution to this multi-variable optimisation problem is accomplished using the following procedure: The cost function J_p in equation (5.21) is expanded into the standard Hermitian quadratic form using $p(r_0) = p_p(r_0) + \underline{Z}(r_s|r_0)\, \underline{q}_s$

$$J_p = p_p(r_0)^* p_p(r_0) + p_p(r_0)^* \underline{Z}(r_s|r_0)\underline{q}_s + \underline{q}_s^H Z^H(r_s|r_0)\, p_p(r_0) +$$

$$\underline{q}_s^H [\, \underline{Z}(r_s|r_0)^H \underline{Z}(r_s|r_0) + \beta \underline{I}\,]\, \underline{q}_s \qquad (5.24)$$

where in this case $\underline{Z}(r_s|r_0)$ is a (1 x M) vector and where the superscript H is used to denote the Hermitian transpose which is an operation composed of taking the transpose and the complex conjugate successively and where $\underline{I}$ is the identity matrix whose order is determined by the number of points of cancellation. Inspection of equation (5.24) shows that it has precisely the quadratic form considered in Chapter 3. However, in this multi-variable problem, scalar quantities are now replaced by their corresponding vector and matrix equivalent variables. The coefficient $\underline{A}$, is now a matrix of transfer impedances coupling each of the secondary sources to the point of cancellations and the vectors $\underline{b}$ and $\underline{c}$ may be identified in a similar way. Recognising this property[13] enables the unique, global

minimum of this complex function to be determined in an exactly analogous way to the single channel case from the formula

$$\underline{q}_s = \underline{q}_{so} = - \underline{A}^{-1} \underline{b} \tag{5.25}$$

which leads to the general solution

$$\underline{q}_s = -[\, \underline{Z}(r_s|r_0)^H \underline{Z}(r_s|r_0) + \beta I \,]^{-1} \; \underline{Z}(r_s|r_0)^H p_p(r_0) \tag{5.26}$$

This generalised formula reduces to the following simple expression for the single source case (L = M = 1)

$$q_{so} = - \frac{Z(r_p|r_0)}{Z(r_s|r_0)+\beta} \, q_p \tag{5.27}$$

One can verify immediately that the result of constructing the cost function in this manner is to simulate an *effective* transfer impedance from the secondary source to the point of cancellation which is identical to the physical transfer impedance with some constant impedance impedance term β superimposed. All the first order diffuse field transfer impedance statistics discussed in chapter 3, are effectively translated from zero to some pre-determined non-zero value β.

For the two source case, the optimal secondary source strength vector according to equation (5.26) gives

$$q_{s_1} = - \frac{Z^*(r_{s1}|r_0) Z(r_p|r_0)}{|Z(r_{s1}|r_0)|^2 + |Z(r_{s2}|r_0)|^2 + \beta} \, q_p \tag{5.28}$$

$$q_{s_2} = - \frac{Z^*(r_{s2}|r_0) Z(r_p|r_0)}{|Z(r_{s1}|r_0)|^2 + |Z(r_{s2}|r_0)|^2 + \beta} \, q_p \tag{5.29}$$

Equations (5.28) and (5.29) reveals the inter-dependence between the two secondary sources. The respective magnitudes of the two sources correspond, in some sense, to the ease with which each source is able to couple into the point of cancellation at r_0. In the extreme case where $|Z(r_{s1}|r_0)|$ is much greater then $|Z(r_{s2}|r_0)|$, then correspondingly, $|q_{s_1}|$ will be much greater than $|q_{s_2}|$ such that q_{s_2} will tend to turn off. In the event that $|Z(r_{s1}|r_0)| = |Z(r_{s2}|r_0)|$, the total effort will be equi-partitioned between the two sources so that $|q_{s_1}| = |q_{s_2}|$.

Unfortunately, the statistical behaviour of the secondary source strengths defined by equations (5.28) and (5.29) is not amenable to simple analysis. Particularly, the expectation $[< |q_{s_1}|^2 > + < |q_{s_2}|^2 >] / |q_p|^2$, is required which is of principal interest since

it determines the expected increase in the diffuse field square pressure. Nevertheless, this expectation may be closely approximated using very simple numerical techniques. The real and imaginary parts of the complex transfer impedance $Z(r_{s1}|r_0)$, $Z(r_{s2}|r_0)$ and $Z(r_p|r_0)$ were each assigned a value taken from an independent, normally distributed ensemble produced with the aid of a random number generator. The secondary source strengths q_{s_1} and q_{s_2} were then evaluated according to equations (5.28) and (5.29) and the exercise repeated a total of 15,000 times for each value of β. The average value $[< |q_{s_1}|^2 > + < |q_{s_2}|^2 >] / |q_p|^2$ was subsequently calculated from the resulting ensemble as a function of β between 0 and 0.1 which is shown plotted in figure 5.6.

Consistent with the underlying control philosophy, the expectation of the sum of the square source strengths remains within acceptable limits over the range of β. Introducing an additional source has the effect of adding to the controller an additional degree of freedom which enables the total effort required to be distributed between the two sources according to a least squares criterion specified in equation (5.21). The total volume velocity directed towards driving the point pressure to zero will shift towards the secondary source which is best coupled to the control point.

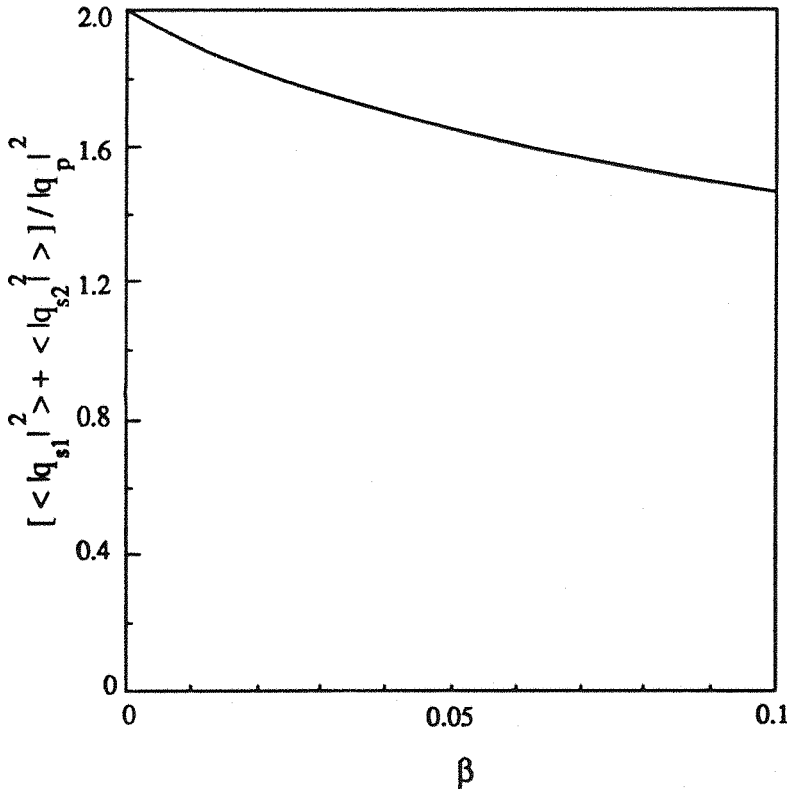

Figure 5.6 The expectation of the sum of the squares of the two secondary sources both of which are constrained to act at the same point in a pure tone diffuse sound field versus the soft limiting parameter β.

According to figure 5.6, the ensemble mean remains unexpectedly well behaved even as β tends to zero. The normalised sample mean eventually converges on two for a value of β which is exactly equal to zero. The result is particularly surprising because for $\beta = 0$, the optimal solution to $J_p = 0$ is now longer unique, but equally satisfied for an infinite set of values corresponding to

$$q_{s_1} Z(r_{s1}|r_0) + q_{s_2} Z(r_{s2}|r_0) = -p(r_0) \tag{5.30}$$

The solution to this apparent paradox lies in the fortunate choice of cost function J_p. Employing a technique common in the calculus of variations for finding the extrema of constrained functions[48], we now seek to show that posing the problem in this way and letting β tend to zero has unwittingly lead us to an important limiting case. In the next section it is shown that for the particular case where $\beta = 0$ corresponds to the unique set of source strengths for achieving perfect cancellation of the point pressure for minimum least squares effort. In the diffuse sound field, the minimum total square source strength also corresponds to the minimum secondary source sound power output.

5.3. Cancellation of the pressure at a point using multiple secondary sources for least squares effort

Consider again the configuration in which two secondary sources q_{s_1} and q_{s_2} are made to act at the same point r_0, the total pressure is therefore given by

$$p(r_0) = q_p Z(r_p|r_0) + q_{s_1} Z(r_{s1}|r_0) + q_{s_2} Z(r_{s2}|r_0) \tag{5.31}$$

Now consider the usual cost function J_p which is constructed from the square of the pressure at the point of cancellation

$$J_p = p(r_0)^* p(r_0) \tag{5.32}$$

The aim of this section is to derive the vector of optimal secondary source strengths $\underline{q}_{so}^T = [\, q_{so1}, q_{so2} \,]$ which makes $J_p = 0$ subject to the *additional* constraint that $\underline{q}_s^H \underline{q}_s$ is a minimum. Note that it is only this additional constraint which ensures the consistency of putting $p(r_0) = 0$. Employing the method of Lagrange's undetermined multipliers, consider some new real cost function φ which is constructed from

$$\varphi = \underline{q}_s^H \underline{q}_s + \lambda^* p(r_0) + \lambda p^*(r_0) \tag{5.33}$$

On substituting for $p(r_0)$, one can therefore write

$$\varphi = \underline{q}_s^H \underline{q}_s + \lambda[\, q_p^* \underline{Z}^*(r_p|r_0) + \underline{q}_s^H \underline{Z}^*(r_s|r_0)\,] + \lambda^*[\, q_p \underline{Z}(r_p|r_0) + \underline{q}_s^T \underline{Z}(r_s|r_0)\,] \tag{5.34}$$

The term λ is some arbitrary complex scalar constant known as the Lagrange multiplier. The vector of optimal secondary source strengths $\underline{q}_{so}$ must further satisfy

$$\frac{\partial \varphi}{\partial \lambda} = \frac{\partial \varphi}{\partial \Re\{\lambda\}} + j\frac{\partial \varphi}{\partial \Im\{\lambda\}} = 0 \tag{5.35}$$

which is equivalent to setting $J_p = 0$ which puts the pressure at the control point equal to zero. On performing the differentiation one obtains

$$q_p \underline{Z}(r_p|r_0) + \underline{q}_{so}^T \underline{Z}(r_s|r_0) = 0 \tag{5.36}$$

which is of course precisely the original condition on the secondary source strengths for achieving perfect cancellation at r_0 whose solution was found to correspond to an infinite set of non-unique secondary source strengths. Equation (5.35) can be made consistent by ensuring that the pressure is only driven to zero for an optimal secondary source strength vector $\underline{q}_{so}$ which maintains least squares effort. However since at $\underline{q}_s = \underline{q}_{so}$ the pressure $p(r_0) = 0$, equation (5.36) is equivalent to setting derivative of the cost function φ to zero with respect to the vector of secondary source strengths according to

$$\frac{\partial \varphi}{\partial \underline{q}_s} = 0 \tag{5.37}$$

Equation (5.33) is a standard Hermitian quadratic form in $\underline{q}_s$ which may be readily solved to give

$$\underline{q}_{so} + \lambda \underline{Z}^*(r_s|r_0) = 0 \tag{5.38}$$

Together, equations (5.35) and (5.38) form a pair of consistent set of simultaneous equations in $\underline{q}_{so}$ which are readily solved to produce the unique, solution for the vector of optimal secondary source strengths which sets the vector of pressures $p(r_0)$ to zero while maintaining a minimum value for the sum of squared source strengths of the form given by equation (5.39)

$$\underline{q}_{so} = -\, \underline{Z}^*(r_s|r_0)\, [\, \underline{Z}(r_s|r_0)^T \underline{Z}^*(r_s|r_0)]^{-1}\, \underline{Z}(r_p|r_0) q_p \tag{5.39}$$

where there is no requirement to determine λ and is therefore undetermined. Equation (5.39) is precisely the form of equation (5.25) for vanishingly small β. For the case where two sources are acting at one point, performing the matrix inverse is trivial so one can therefore write

$$q_{so_1} = - \frac{Z^*(r_{s1}|r_0)Z(r_p|r_0)}{|Z(r_{s1}|r_0)|^2 + |Z(r_{s2}|r_0)|^2} q_p \tag{5.40}$$

$$q_{so_2} = - \frac{Z^*(r_{s2}|r_0)Z(r_p|r_0)}{|Z(r_{s1}|r_0)|^2 + |Z(r_{s2}|r_0)|^2} q_p \tag{5.41}$$

Consider the sum of squares of the moduli of the secondary source strengths as a ratio of the square of the primary source strength as indicated below

$$\frac{|q_{so1}|^2 + |q_{so2}|^2}{|q_p|^2} = \frac{|Z(r_p|r_0)|^2}{|Z(r_{s1}|r_0)|^2 + |Z(r_{s2}|r_0)|^2} \tag{5.42}$$

From previous work, it has been established that in a diffuse field, the numerator is a random variable which is distributed as a Chi squared distribution with two degrees of freedom. By similar reasoning the denominator is, by definition, a Chi squared random variable with four degrees of freedom. Assume that all sources are located further than a wavelength apart so that the numerator will be independent from the denominator. One can therefore infer that the quotient of Chi squared random variables given in equation (5.42) has the probability density function of an F(2,4) random variable. From standard statistical texts[63], the F(2,4) probability density function takes the form of

$$f_V(v) = \frac{1}{(1+v/2)^3} \quad \text{where} \quad V = [\, |q_{so1}|^2 + |q_{so2}|^2 \,] / |q_p|^2 \tag{5.43}$$

Notice the similarity in the form of this function with the F(2,2) probability density function for the single channel unconstrained problem. The mean value of this distribution now exists and may be determined in the usual way to give

$$< |q_{so1}|^2 + |q_{so2}|^2 > = |q_p|^2 \int_0^\infty \frac{v}{(1+v/2)^3} dv = 2\,|q_p|^2 \tag{5.44}$$

For well spaced secondary sources, the average effort will be equally distributed between the two sources from which one can infer that $< |q_{so1}|^2 > = < |q_{so2}|^2 > = |q_p|^2$. The variance is not defined however.

A single secondary source acting alone to cancel the pressure at a point in the diffuse field has a space averaged square source strength which is infinite. Now dividing the total effort between two independently positioned sources according to the least squares criterion specified in equation (5.33) has been proved to be considerably more beneficial in terms of the total sound power injected into the sound field. The expectation of the sum of the square values in this two source case is less than when only one source is used even though the outcomes are identical inasmuch as the diffuse field point pressure is driven to zero in both cases. The total square effort is now mathematically convergent and of a magnitude which makes the scheme viable for many practical applications although clearly costly in terms of hardware and computational resources.

For two well separated secondary sources, each source makes the same contribution to the space averaged square pressure as the primary source in isolation thereby causing a three fold increase in the space averaged diffuse field square pressure which is approximately equal to 5 dB. The 10 dB quiet zone $2\Delta r_{0.1}$ for this two source problem can be calculated to be about approximately one tenth of an acoustic wavelength. In contrast, the expected value for the quiet zone in the single source case is zero.

An identical argument can be reasoned for the three source case. The probability density function of the sum of the squares of a trio of well separated sources $V = [\, |q_{so1}|^2 + |q_{so2}|^2 + |q_{so3}|^2 \,] \,/\, |q_p|^2$ which are driven to cancel the pressure at a point to zero, while maintaining least squares effort, can be shown to randomly distributed with the F(2,6) probability density function given below

$$f_V(v) = \frac{1}{(1+v/3)^4} \quad V = [\, |q_{so1}|^2 + |q_{so2}|^2 + |q_{so3}|^2 \,] \,/\, |q_p|^2 \qquad (5.45)$$

Both the mean and the variance are now defined for three independently positioned secondary sources owing to the rapidity with which the probability density function decays away. The argument can be generalised for M well separated secondary sources acting at the same point for the least squares effort. The probability density function of the sum of the squares of the optimal source strengths is given by the F(2,2M) function whose probability density function is of the general form

$$f_V(v) = \frac{1}{(1+v/M)^{M+1}} \quad \text{where } V = \sum_M |q_{soM}|^2 \,/\, |q_p|^2 \qquad (5.46)$$

A plot of this function is shown below for M = 1, 2, 3 and 4.

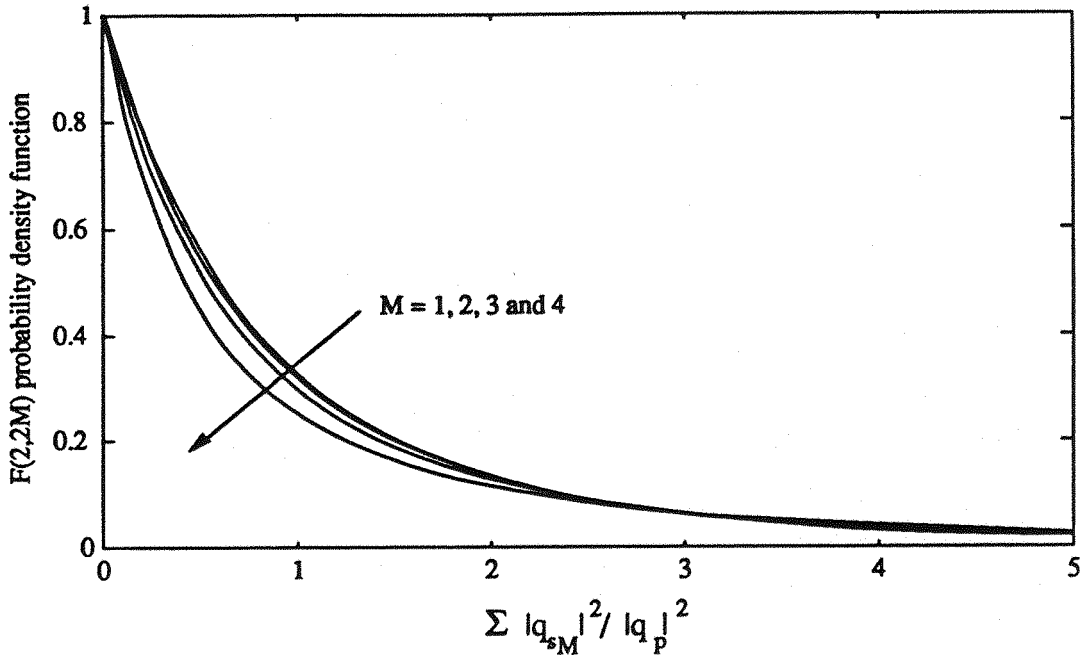

Figure 5.7. Plots of the F(2,2M) probability density function for M = 1, 2, 3 and 4

Using equation (4.40), it is a simple matter to show that the mean of the F(2,2M) distribution is M/(M - 1) which for independently positioned secondary source corresponds to an expectation value for the square of each of the secondary source strengths individually $< |q_{soM}|^2 >$ which are equal to

$$< |q_{soM}|^2 > = |q_p|^2 / (M - 1) \qquad (5.47)$$

which is finite providing M > 1. Despite the fact that dividing the total effort between a number of independently positioned points appears to have only a (surprisingly) small effect on the probability density function of the sum of the squares of the secondary source strengths as indicated in figure 5.7, the effect on the average value is significant. Not surprisingly, this mean value steadily diminishes as the number of secondary source M introduced to cancel the point pressure increases. However, the benefits obtained in terms of the global sound field derived from increasing the number of sources quickly depreciates and the principle of 'diminishing returns' soon starts to apply. It is interesting to observe that as the number of secondary sources introduced to assist in cancelling the same diffuse field pressure is increased, the *total* square pressure contribution from the cluster of secondary sources M / (M - 1) tends to unity which therefore equals the primary source square pressure contribution acting in isolation $< |p_p(r)|^2 >$. This important limiting case represents a doubling, or 3 dB increase in the average global square pressure. A two fold increase in the diffuse field square pressure therefore represents the smallest increase physically achievable when one seeks to cancel the pressure at a point in a diffuse field by a

loudspeaker or loudspeaker array which is remote from the point of cancellation. The expected value for the quiet zone for this best possible case can be calculated to be about one eighth of the acoustic wavelength. A doubling in the global square pressure will be shown to be also the least possible increase possible when we come to consider the problem of minimising the sum of the squares of the pressures at a number of well spaced points using a multiplicity of secondary sources.

By way of illustration, the square pressure was calculated one and a half wavelengths either side of a point of cancellation produced by two well separated secondary source optimally driven so as to maintain a total least squares secondary source strength. The computer simulated experiment was repeated twenty times in the computer simulated sound field where for each simulation, both the primary source and the secondary source pair was randomly positioned although prevented from being closer than one wavelength from each other and all of the enclosure boundaries in each case. The average square pressure reduction obtained from twenty such simulations is shown below in figure 5.8. In this example, good agreement is established by the theoretical curve $2.7(1 - \text{sinc}^2 k\Delta r)$ indicating that the mean square pressure contribution from the secondary source is approximately $< |\hat{q}_s|^2 > \approx 1.7 < |q_p|^2 >$. Note that this is close to the expected value of two as predicted by equation (5.47).

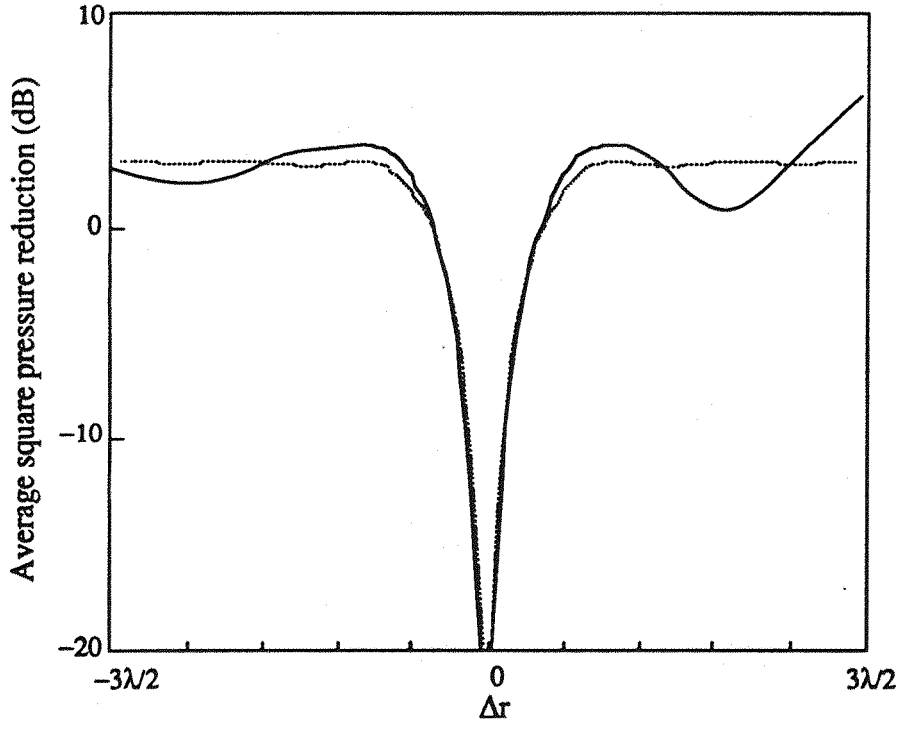

Figure 5.8 The zone of quiet about a point of cancellation formed by two independently positioned secondary sources seeking to maintain a least squares secondary source strength. The computer simulation is shown as solid line and the theory is represented by a dashed line.

Comparison of figure 5.8 with the zone of quiet produced by a single unconstrained source shown in figure 4.3 demonstrate the benefits derived from using two well spaced sources. On average, the square pressure level produced well away from the point of cancellation is approximately 2 dB below the single source unconstrained level. The benefits obtained here in terms of the pressure increase well away from the point of cancellation are of course transfered to the size of the quiet zone which is now nearly 0.15 of the acoustic wavelength. This value compares with one tenth of a wavelength for the single source case. Introducing the number of secondary sources still further to three is not expected to produce a dramatic improvement on this result.

5.4. The over-determined problem

In the preceding section, a number of secondary sources were employed over and above the single source absolutely necessary to cancel the pressure at a point. The redundancy of sources were shown to be useful in order to ensure that the expected increase in the diffuse field square pressure remains low.

This section is concerned with the converse problem where a number of secondary sources are used to minimise the sum of the squared pressures at an even greater number of microphones. Where there are more points of minimisation than secondary sources, the control configuration is known as over-determined. Obviously, the perfect cancellation of the acoustic pressure at each point is no longer achievable. Undoubtedly, the most successful approach for achieving a reduction in the sound pressure level which extends over a wide area is to minimise the sum of the square pressures at a distributed number of points. This type of least squares approach forms the basis of a large part of modern control theory which may be cast in the guise of a quadratic minimisation problem for which there exists a well defined, unique solution. We will first consider the statistics of the secondary source strength and the subsequent degree of acoustic reduction in the field will then be discussed.

Consider the case where M secondary sources are required to minimise the sum of the square pressures at L points in the sound field. It is assumed that the problem is over determined so that $M \leq L$, otherwise the control geometry is under determined. The vector of L complex pressures $p(\mathbf{r})$ is related to the vector of M complex secondary source strengths $\underline{q}_s$ via

$$\underline{p}(\mathbf{r}) = \underline{q}_s \underline{Z}(\mathbf{r}_s|\mathbf{r}_0) + q_p \underline{Z}(\mathbf{r}_p|\mathbf{r}_0) \qquad (5.48)$$

where $\underline{Z}(r_s|r_0)$ now represents an (L X M) matrix of complex transfer impedance terms coupling each of the measurement points to each of the secondary sources and where $\underline{Z}(r_p|r_0)$ denotes a (1 X L) vector of transfer impedance terms which couple each of the measurement points to the primary source (only one primary source is assumed). Writing equation (5.48) in full gives

$$\begin{bmatrix} p(r_1) \\ p(r_2) \\ . \\ . \\ . \\ p(r_L) \end{bmatrix} = \begin{bmatrix} Z_s(r_1|r_{s1}) & Z_s(r_2|r_{s1}) & . & . & Z_s(r_M|r_{s1}) \\ . & . & . & . & . \\ . & . & . & . & . \\ . & . & . & . & . \\ Z_s(r_1|r_{sL}) & Z(r_2|r_{sL}) & . & . & Z_s(r_M|r_{sL}) \end{bmatrix} \begin{bmatrix} q_s(r_{s1}) \\ q_s(r_{s2}) \\ . \\ . \\ q_s(r_{sM}) \end{bmatrix} + \begin{bmatrix} Z_p(r_1|r_p) \\ Z_p(r_2|r_p) \\ . \\ . \\ Z_p(r_L|r_p) \end{bmatrix} q_p(\omega) \tag{5.49}$$

The problem of finding the vector of optimal secondary source strengths $\underline{q}_{so}$ is reduced to a standard problem in linear algebra. Now given that there are more equations (points of minimisation) than unknowns (secondary sources), one is compelled to seek a least squares solution. An exact solution to the equation $\underline{p}(r) = 0$ is only possible for $M \geq L$. The vector of optimal secondary source strengths $\underline{q}_{so}$ for minimising the sum of the squares of the acoustic pressures $\underline{p}(r)^H\underline{p}(r)$ is well known and given by[14]

$$\underline{q}_{so} = -[\, \underline{Z}(r_s|r_0)^H \underline{Z}(r_s|r_0) \,]^{-1} \underline{Z}(r_s|r_0)^H \underline{p}_p(r) \tag{5.50}$$

which is the familiar least squares regression formula. This result has successfully been applied to a wide range of active control problems[14,39,51]. Typically, the best possible reduction of some energetic quantity is usually desired which readily lends itself to this kind of analysis since energy related variable naturally arise as quadratic functions of the source strengths. The total acoustic potential energy in an enclosure is just such an example.

In a diffuse field environment, each of the complex transfer impedance terms appearing in equation (5.49) exhibits well defined statistical behaviour. The in-phase and quadrature parts of the respective terms $Z(r_{si}|r_j)$ are known to form a joint Gaussian process according to the argument proposed in Chapter 3 providing that the secondary sources and the control points are well separated namely $|\, r_{si} - r_j \,| > \lambda$. Further assuming that all of the secondary sources are separated by more than a wavelength (which in practice means that all error microphones are well separated) enables one to make the further simplifying assumption that all of the complex impedance terms are themselves mutually uncorrelated. Considerable effort was directed towards attempting to determine theoretically, the probability density function of the square of the optimal secondary source

strengths defined via equation (5.50). Unfortunately without success. Nevertheless, considerable insight into the multi-channel diffuse field problem was gained by the use of Monte-Carlo methods.

The fact that all of the impedance terms appearing in equation (5.49) may be described in terms of independent, normally distributed random variables forms the basis of Monte-Carlo simulations. The level of statistical fluctuation experienced by any one single diffuse field secondary source seeking to minimise the sum of the squares of the pressures at a number of well separated points was simulated on the computer. Each of the real and imaginary parts of the transfer impedance terms appearing in equation (5.50) were assigned a normally distributed, zero mean random value taken from a random number generator. The variance of the random number series was pre-determined and arranged to be approximately equal to that obtained from the computer simulated model. This in turn was in approximate agreement with the variance predicted by equation (3.21), although, this precaution is of course not strictly necessary. For the case of L sensors and M secondary sources, this procedure is represented symbolically below

$$
\begin{aligned}
&\text{For } i = 1,L \\
&\qquad \text{For } j = 1,M \\
&\qquad\qquad \Re\{ Z(r_{si}|r_j) \} \equiv N_1(0,\sigma_Z^2): \quad \Im\{ Z(r_{si}|r_j) \} = N_2(0,\sigma_Z^2) \\
&\qquad \text{Next } j \\
&\text{Next } i \\
&\text{For } j = 1,L \\
&\qquad\qquad \Re\{ Z(r_p|r_j) \} = N_3(0,\sigma_Z^2): \quad \Im\{ Z(r_p|r_j) \} = N_4(0,\sigma_Z^2) \\
&\qquad \text{Next } j \\
&\qquad\qquad \text{where } \sigma_Z^2 = \rho^2 \omega c_0 / 16\pi\zeta V
\end{aligned}
\qquad (5.51)
$$

The source strength of a single secondary source necessary to minimise the sum of the square pressures at one, two, three and four independent points was evaluated according to equation (5.50). In each case, the simulation was repeated 5,000 times for different transfer impedance values and the modulus of the secondary source strength $|q_{si}|^2$ was calculated for each. The probability density functions for each ensemble of values was calculated. Each computer simulated distributions of values appears to be in close agreement with the Pareto probability density function $f_V(v,N)$ given by[63]

$$f_V(v,N) = \frac{N}{(1+v)^{1+N}} \tag{5.52}$$

where N is the Pareto parameter. In this set of four examples, the Pareto variable N, the sole descriptor of the distribution, appears to correspond to the number of points of minimisation such that N = L. The calculated probability density function of the squares of the secondary source strength together with their respective Pareto distributions are shown in figure 5.9 for N equal to two, three and four. Also shown for comparison is the F(2,2) probability density function for the single channel case. By inspection of equation (5.52), the F(2,2) probability density function is a special case of the Pareto distribution for N = 1.

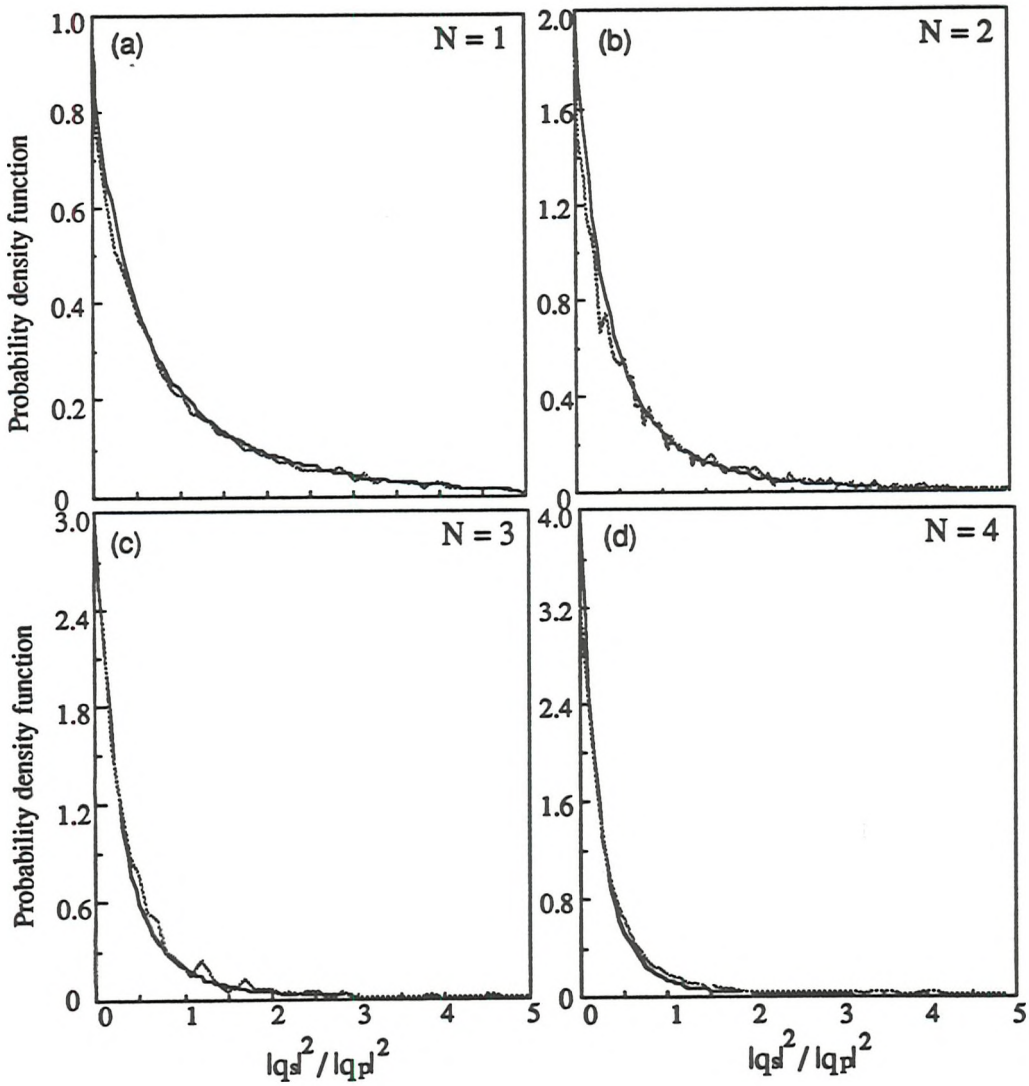

Figure 5.9 The calculated probability density function of the square of the secondary source strength required to minimise the sum of the square pressure at (a) One point, the F(2,2) density function, (b), Two well separated points, (c), Three points and (d), Four points all shown as a dashed line. Also shown is their respective Pareto functions for N = 1, 2, 3 and 4 respectively, shown as a solid line.

It is instructive to consider the mean value of the Pareto probability density function as a function of the governing variable N which has been found to have meaningful physical significance in this case. It is a simple matter to show that the mean value of the random variable x_N namely $< x_N >$ which is governed by the Pareto probability density function with a Pareto variable N according to equation (5.52) is simply

$$< x_N > = \frac{1}{N-1} \tag{5.53}$$

which remains finite for $N > 1$.

On the basis of this set of Monte-carlo simulations, the expectation of the square of the secondary source strength $< |q_{soL}|^2 >$ necessary to minimise the sum of the square pressures at L independent diffuse field points may therefore be written as

$$< |q_{soL}|^2 > = |q_p|^2 / (L - 1) \tag{5.54}$$

Notice the resemblance to the form of the expectation in equation (5.47) for each secondary source strength in the overdetermined problem $|q_p|^2 / (M-1)$. In the under-determined case, the pressure is set to zero and the sum of square efforts is minimised. In the over-determined case, the sum of square pressures is minimised although the no constraint is imposed on the secondary source strength. The apparent interchangability between the number of sources M and the number of points of minimisation L between the over-determined and under-determined source configurations suggests the existence of some kind of reciprocal process between the two control schemes.

In the absence of any formal analysis, one cannot be absolutely certain that the Pareto function is the correct generalised probability density function for describing the variation of square secondary sources constrained in this fashion. However, a high degree of confidence in this choice of function is justified for several reasons. First, The Pareto distribution provides a good fit to the simulated data; second, the function reduces to the F(2,2) probability density function which is known to be correct for the special case where $N = 1$, and last, statistical trends are correctly predicted as the number of secondary sources are increased.

The effect of using a multiplicity of secondary sources to minimise at a number of well separated points was also investigated using the same Monte-Carlo technique. Equation (5.50) was evaluated 5,000 times with the appropriate complex transfer impedances so as to mimic the behaviour of two secondary sources minimising the square pressure at three points ($M = 2, L = 3$) and three secondary sources minimising the sum of square pressure at five points ($M = 3, L = 5$). Intriguingly, the Pareto density function

seems to have surprising generality and even appears to adequately describe the variation of square secondary source strengths for this higher order system. In this case however, the Pareto variable N now appears to correspond to the ratio of the number of points of cancellation to the number of secondary sources

$$N = \frac{L}{M} \tag{5.55}$$

where the generalised formula of equation (5.52) is valid as a probability density function even for fractional values of N. The distribution of simulated values for the two examples together with their respective Pareto density functions is shown below. Figure 5.10a and figure 5.10b show the probability density functions for the M = 2, L = 3 and M = 3, L = 5 examples respectively where good agreement is apparent in each case.

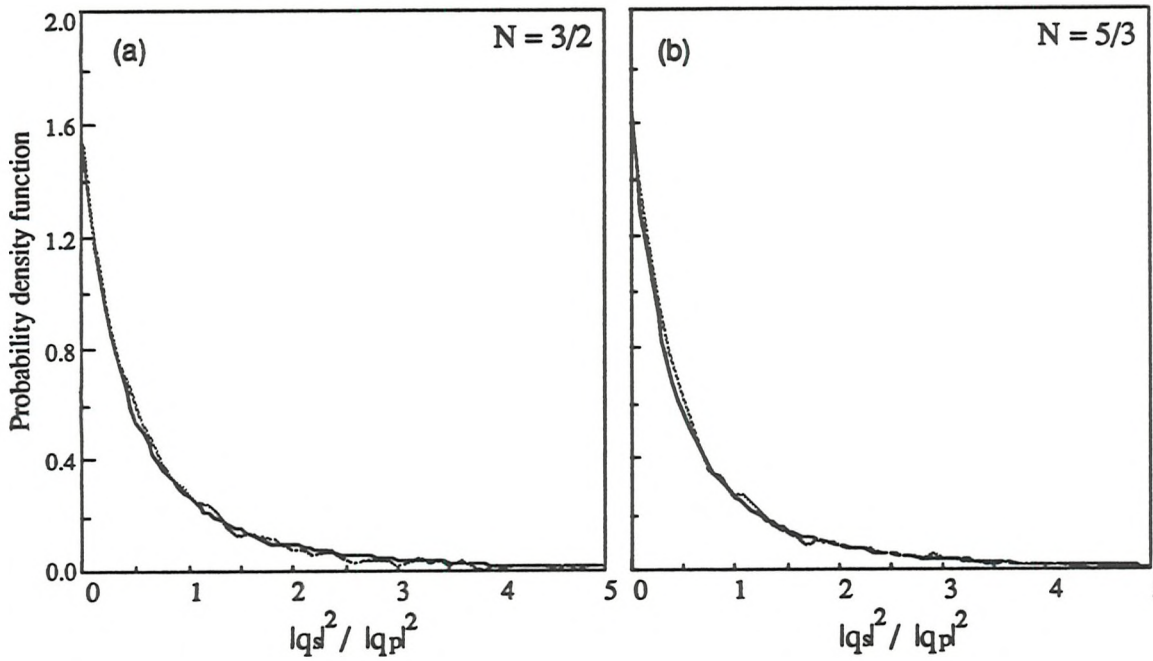

Figure 5.10 The calculated probability density function for the square of the secondary source strength when (a) two secondary sources are made to minimise the sum of square pressures at three well separated points and (b) three secondary sources minimising at five well separated points in a diffuse sound field, each shown as a dashed line. Also shown as a solid line are the Pareto density function for N = 3/2 and N = 5/3.

To test this hypothesis further, the appropriate random transfer impedances were generated in order to mimic the statistical behaviour of three well separated secondary sources seeking to minimise the sum of the square pressures at three well separated points in a diffuse field environment. This arrangement is a representative example of a 'square system' (as is the single channel case) where the number of secondary sources is chosen to equal the number of points of minimisation i.e., L = M where perfect cancellation of the

pressure at all points is always achievable. This simulation was repeated a total of 1,700 times so as to ensure an ensemble of more than 5,000 values of the secondary source strength. The probability density function for the square of the source strength was calculated which indicate a good fit to the F(2,2) probability density function. This apparent agreement, shown below in figure 5.11 is totally in keeping with the original premise since both this square geometry and the single channel case share the same Pareto parameter namely N = 1.

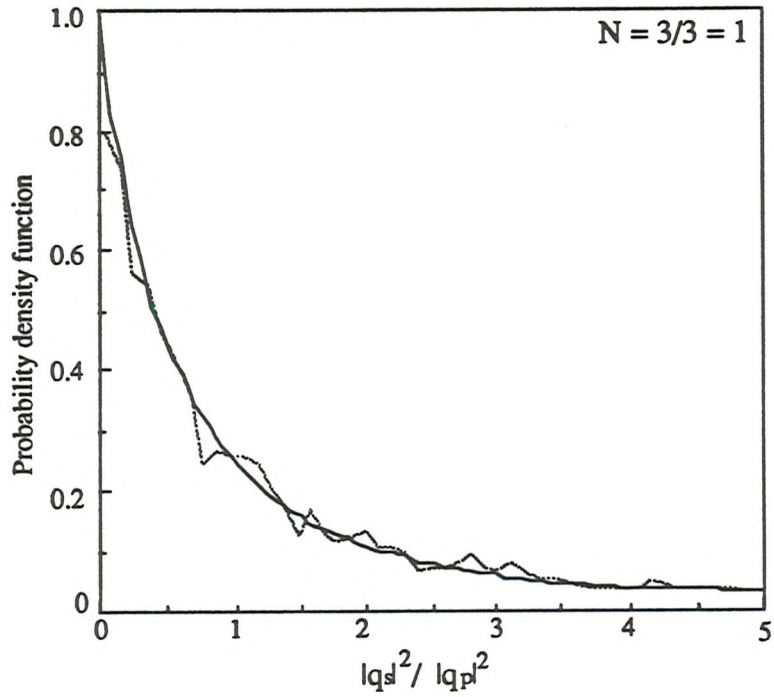

Figure 5.11 The calculated probability density function for the square of the secondary source strength as part of a trio of secondary source strengths required to cancel the pressure at three well separated points (dashed line) together with the F(2,2) probability density function shown as a solid line.

The Pareto probability density function has been shown to provide a good empirical description of the statistical behaviour of the square of the secondary source strength necessary to minimise the sum of the square pressures at a number of well spaced points. What is significant however, is that the sole descriptor of the distribution N, corresponds simply to the number of *independent* points of minimisation *per* secondary source. This of course implies that the susceptibility of each of the secondary source strengths to statistical uncertainty in the diffuse field, depends only on the severity of constraints imposed upon it. Consequently, the expectation of the sum of the squares of the secondary source strength for this higher order system is given by

$$< \sum_{M} |q_{sM}|^2 > = \frac{M^2}{L\text{-}M} |q_p|^2 \qquad (5.56)$$

As the ratio of the number of secondary sources to the number of points of control increases, the variable N correspondingly increases. The form of the Pareto probability density function given by equation (5.52) indicates that the level of excursion exhibited by each of the secondary sources from the mean value decreases as N increases, taking a minimum value of unity in the case of a square system. This is exemplified by the succession of figures 5.9 - 5.11. One interpretation of the parameter N appearing in equation (5.52) therefore, is that it maybe be regarded as a measure of the average constraint imposed on each secondary source.

When N is large for example, the sources have greater scope for distributing their effort over a larger number of points and so the distribution of square source strengths has less tendency to deviate. As a consequence, the secondary source strengths are loosely constrained and the level of sound pressure level reductions at the points of control are therefore variable. When N = 1 however, the source or sources are highly constrained because the perfect cancellation of the pressure is always achieved with no account taken of the effort required and so there is less scope for manoeuvrability. The simple relationship N = L / M (which has been only validated empirically) is clear indication that each source in an array of sources is as equally constrained as if it were acting in isolation to cancel at one point. All of the results presented in Chapter 4 therefore equally apply to this higher order square system.

Perhaps the broadest interpretation of the governing variable N is that it represents the *effective* number of *independent* diffuse field points of minimisation for each secondary source. The notion of fractional points of pressure minimisation is clearly not easily visualised but will be found to a conceptually useful in the next section.

5.5. Employing a single secondary source to minimise the sum of the square pressures at two closely spaced points

Some empirical findings relevant to multi-channel control in the diffuse field have been presented. Simple theoretical analysis and computer simulations were carried out which were only possible by virtue of the assumed independence between transfer impedances evaluated between well separated points. In this section, the problem of minimising the sum of square pressure at two points which are closely spaced compared with the acoustic wavelength is investigated. This problem demands special attention because the independence assumption in this case is no longer valid.

It is now well established that the square of the secondary source strength required to cancel the pressure at a point in a diffuse sound field varies as a Pareto distribution for N = 1. Similarly, one can be reasonably confident that when the same secondary source is driven with the aim of minimising the sum of the squares at two well separated points, the variation of the square of the secondary source strength has now changed to that of a Pareto distribution with N = 2. However, when the control objective is to employ a single secondary source with the goal of minimising the sum of the square pressures at two points which are *close* compared to a wavelength, it is extremely unlikely that the form of the probability density function will change from the Pareto distribution. Assuming that this hypothesis is correct, the number of *effective* points of minimisation N, the Pareto variable, must now lie somewhere between one and two, $1 \leq N \leq 2$.

As the separation distance Δr between the points of minimisation increases from zero to infinity, the number of effective points of minimisation N must vary smoothly from one in the case where $\Delta r = 0$, up to a maximum value of two for the limiting case for $\Delta r \rightarrow \infty$. We now seek to determine the functional dependence of N with the separation distance Δr, $N = N(\Delta r)$. It is instructive to consider the ensemble of independent, unique square pressure evaluated at all points in the diffuse field $|p(\mathbf{r}_1)|^2$ and $|p(\mathbf{r}_2)|^2$ as representing sets. Each of the two sets is constructed from the square of diffuse field pressures which is completely unique to the point at which it is evaluated. Clearly when Δr the separation distance between the two pressures $|\mathbf{r}_1 - \mathbf{r}_2|$ is much larger than the wavelength, then $|p(\mathbf{r}_1)|^2$ and $|p(\mathbf{r}_2)|^2$ are distinct and mutually independent so that their respective sets are non-overlapping as suggested by figure 5.12.

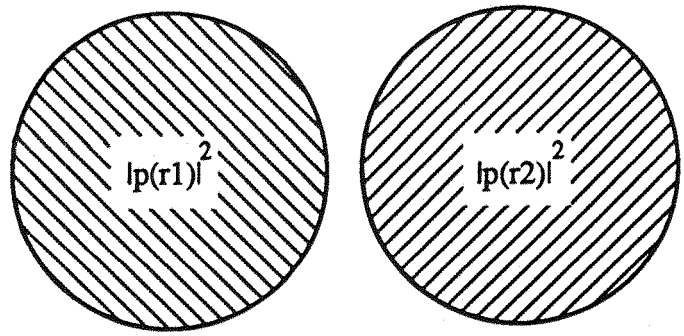

***Figure 5.12** Two independent, non-overlapping sets of square pressures for $\Delta r > \lambda$.*

When Δr is small however, typically a fraction of a wavelength, there will be a component of the square pressure that will be perfectly correlated with the pressure at both points and consequently will not belong exclusively to any one set but will lie in the intersection of the now overlapping sets as indicated in figure 5.13.

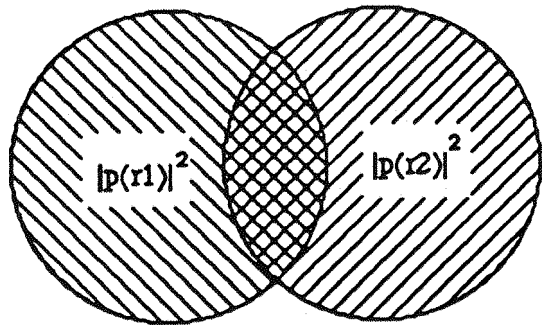

Figure 5.13 Two correlated, overlapping sets of square pressures for $\Delta r < \lambda$.

A rigourous definition of the cost function J_p is now possible aided by the Venn diagram of figure 5.13. The cost function J_p is now formally defined as the sum of the squares of independent points of minimisation. In terms of the sets of square pressures

$$J_p = |p(r_1)|^2 \cup |p(r_2)|^2 \tag{5.57}$$

where $\cup$ simply represents the union of the sets which in physical terms signifies the components of the square pressure which is unique to their respective points r_1 and r_2. Employing a common result in Set theory: If f(A) and f(B) represent the additive sets of A and B then

$$f(A \cup B) = f(A) + f(B) - f(A \cap B) \tag{5.58}$$

The expectation of the cost function $< J_p >$ may now be written as

$$< J_p > = < |p(r_1)|^2 > + < |p(r_2)|^2 > - < |p(r_1)|^2 \cap |p(r_2)|^2 > \tag{5.59}$$

The term $< |p(r_1)|^2 \cap |p(r_2)|^2 >$ simply defines the intersection of the sets, shaded grey, which in physical terms represents that part of the square pressure which is perfectly correlated with the square pressures at both points. From previous work we have seen that the pressure at r_2 which is perfectly correlated with the pressure at r_1 in the three dimensional diffuse field (and *vica-versa* owing to reciprocity) is simply

$$p_c(r_2) = p(r_1)\text{sinc}k\Delta r \tag{5.60}$$

where $r_2 = r_1 + \Delta r$ and the subscript 'c' denotes perfectly correlated. Now given that the spatially sampled diffuse field forms an ensemble of values which are zero mean Gaussian random variables, then it has been shown by, for example Pierce[37] and Lubman[93], that the component of the square pressure $p_c^2(r_2)$ at r_2 which is perfectly correlated with the square

pressure at r_1 varies spatially as $\text{sinc}^2 k\Delta r$. The auto-correlation function of the diffuse field square pressure $\rho_{|p|^2}(\Delta r)$ is therefore given by

$$\rho_{|p|^2}(\Delta r) = \text{sinc}^2 k\Delta r \tag{5.61}$$

From equation (5.59), the expected cost function is now simply

$$< J_p > = < |p(r_1)|^2 > + < |p(r_2)|^2 > - < |p(r_1)|^2 > \text{sinc}^2 k\Delta r \tag{5.62}$$

now noting that $< |p(r_1)|^2 > = < |p(r_2)|^2 > = < |p(r)|^2 >$ yields

$$J_p = < |p(r)|^2 > [\ 2 - \text{sinc}^2 k\Delta r\ ] \tag{5.63}$$

The *effective* number of independent square pressures $< |p(r)|^2 >$ whose minimum is required, N is therefore given by

$$N = 2 - \text{sinc}^2 k\Delta r \tag{5.64}$$

This function has precisely the anticipated properties in that it varies smoothly from two to one as Δr, the separation distance varies from zero in the single channel case to two where the points of minimisation are very far apart.

By way of verification, the square of secondary source strength was calculated according to equation (5.50) with the aim of minimising the sum of the squares of the pressures at ten separation distances Δr ranging from 0.1λ to one wavelength in increments of one tenth of a wavelength. The simulations were performed using the modal model of the diffuse sound field simulated on the computer which has been discussed in chapter 4. For each separation distance, the optimal secondary source strength was calculated a total of 3,000 times and the probability density function $\hat{f}_v(v)$ was evaluated for each ensemble of values. Assuming that $\hat{f}_v(v)$ will eventually tend to the Pareto probability density function with the appropriate value of N as the ensemble size tends to infinity, $f_v(v,N)$, the Pareto variable N appearing in equation (5.52) was chosen to minimise the mean square error $\varepsilon^2(N)$ defined by

$$\varepsilon^2(N) = \int_0^\infty [\ \hat{f}_v(v) - f_v(v,N)\ ]^2\, dv \tag{5.65}$$

The integral was evaluated numerically and the minimisation of the error $\varepsilon^2(N)$ performed on the basis of trial and error. The variation of N, the Pareto variable is shown in figure 5.14 compared with the expected function $2 - \text{sinc}^2 k\Delta r$.

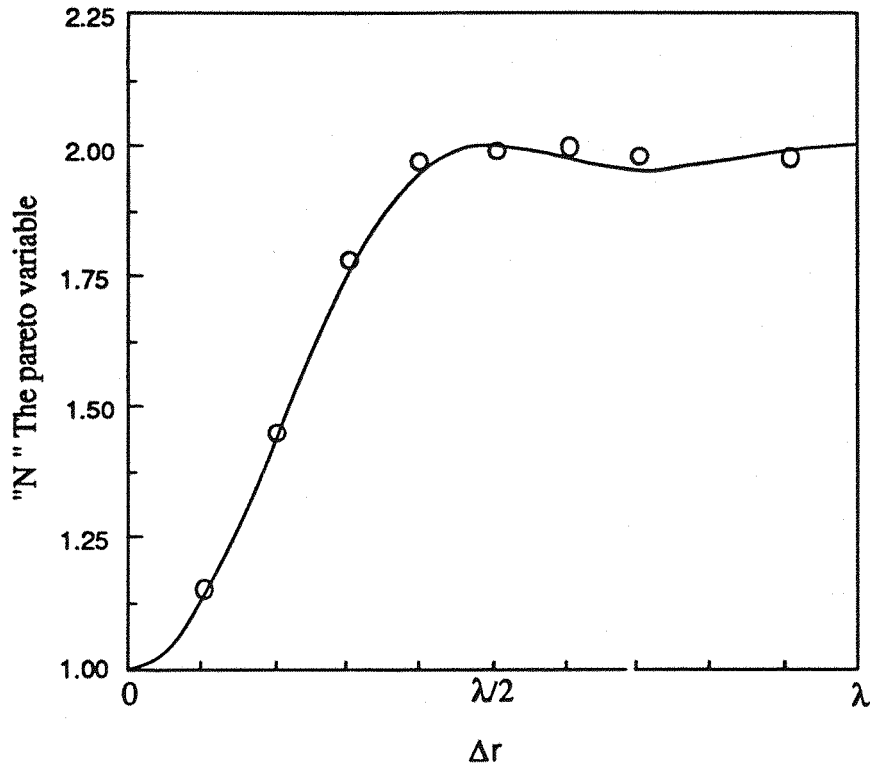

Figure 5.14 The variation of the Pareto variable N which affords a least squares fit to the distribution of simulated values as a function of the separation distance Δr between the points of minimisation. Also shown as a continuous line is the expected function 2 - $sinc^2 k\Delta r$.

The expected function, which has been derived more on the basis of a plausibility argument than formal reasoning, is observed to provide convincing agreement with the simulated data. Some examples of the probability density functions calculated as a function of various Δr are reported in an internal I.S.V.R memorandum[94].

The space averaged zone of quiet formed about the centre of the microphone pair was also investigated. Using the diffuse field model which utilises a modal summation as outlined in chapter 4, the optimal secondary source necessary to minimise the sum of the squares of the pressures at a range of microphone spacings was calculated. For Δr ranging from λ/10 to λ in increments of λ/10, the residual square pressure was evaluated along the line joining the two points of minimisation in increments of λ/50, one and a half wavelengths either side of the geometric centre of the closely spaced microphone pair. For each value of Δr, the residual square pressure was evaluated a total of one hundred times for the same set of one hundred random primary source and secondary source positions and the average taken for each. Figure 5.15 gives two graphical representations of the result obtained from this simulation are shown. One is an isometric plot where a polynomial 'best fit' curve has been used to connect each of the points for the same Δr, the second is a contour plot showing lines of equal square pressure reduction.

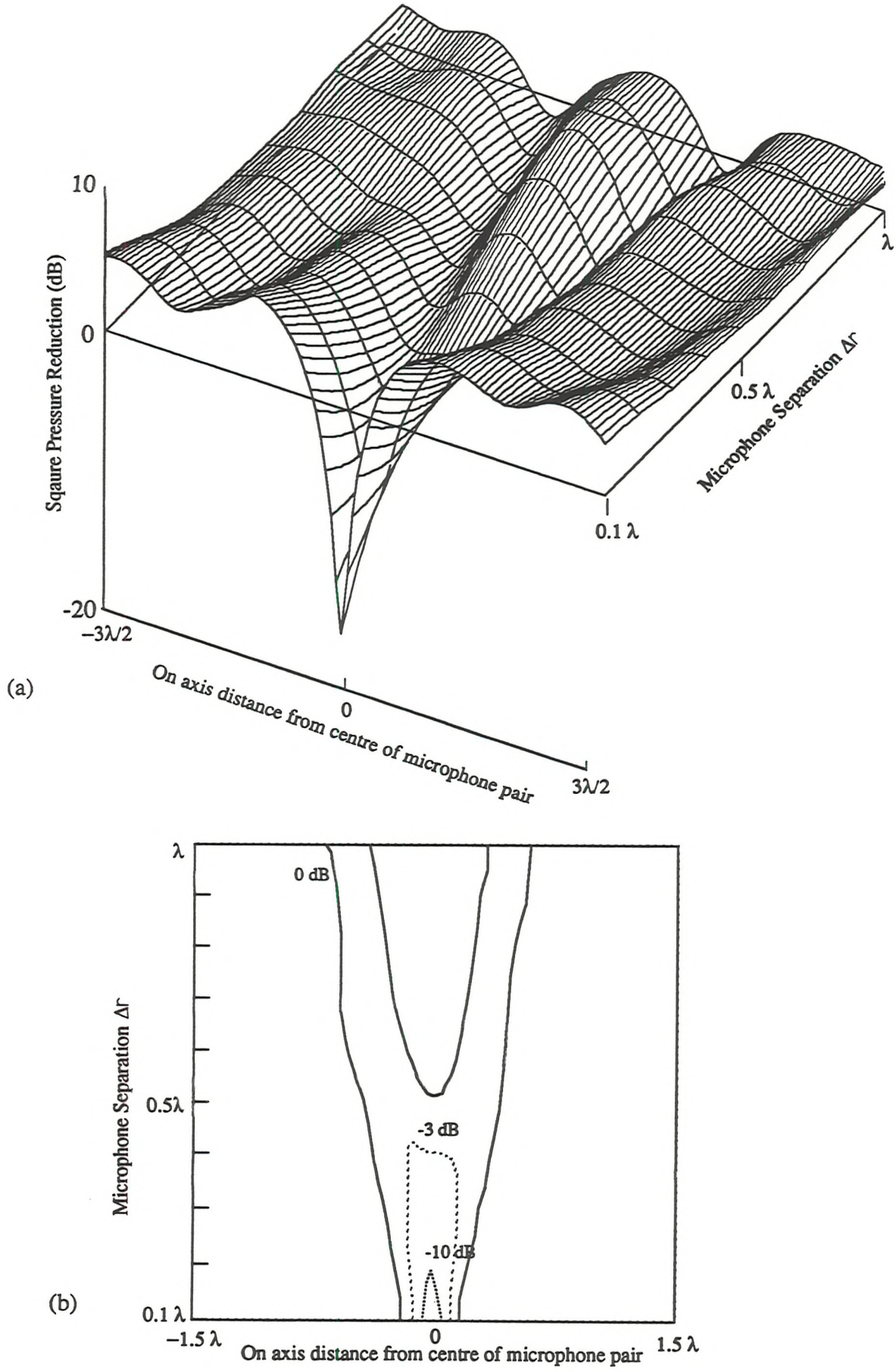

Figure 5.15 The space averaged square pressure profile about two closely spaced points of minimisation in the pure tone diffuse sound field. (a), Isometric plot and (b), showing contours of equal pressure reduction at 0 dB, -3 dB and -10 dB.

The series of curves shown in this figure exhibit the characteristic sin(x)/x type behaviour well away from the points of minimisation as originally predicted by Elliott *et-al*[87]. Near the points of minimisation however, a single unique region of quiet is clearly apparent for error sensor spacings up to about $\Delta r = 0.5\ \lambda$. Above this critical distance, two distinct troughs of quiet begin to emerge which follow the points of minimisation and are at least 3 dB below the primary level. Nevertheless, a 10 dB reduction (which has the been the criterion of quiet in this thesis) is possible for the range of separation distances up to about $0.2\ \lambda$. Most significantly however and which certainly warrants further investigation, is that the spatial extent of attenuation (i.e., any value below 0 dB) remains as a single region for microphone spacings Δr almost exactly equal to one half of a wavelength to within the accuracy of the numerical example and the finite sample size. Above this critical distance however, the 0 dB level only just begins to divide to form two independent zones thereby forcing an increase in the square pressure in the region between.

Microphone separation distances equal to one tenth of a wavelength can be observed to produce a 10 dB zone of quiet nearly equal to $0.1\ \lambda$. Unfortunately, the increase in pressure well away from the control points is still unacceptably high at nearly 6 dB. For a microphone separation distance equal to exactly one half of a wavelength where the respective pressure are perfectly uncorrelated, the zone of pressure reduction remains as a single region peaking at slightly less than 0 dB. The Pareto variable N for this arrangement is 2 since the pressures at two points separated by half a wavelength in the diffuse field are exactly uncorrelated, see figure 5.14. Moving the control microphones still further apart to exactly one wavelength for which the Pareto parameter is also equal to 2, one can see that the spatial extent of reduction is confined to two very small regions which a maximum reduction of less than 2dB. As a direct consequence of constraining the pressure to be a minimum at these two points, the square pressure at the centre of the microphone pair is raised up above the primary square pressure by nearly 4 dB in this case.

The control strategy under consideration here is similar in principle to the pulling apart of a soap bubble. The forces pulling at the bubble can be likened to constraining the square pressure at each of two closely spaced points in the diffuse field to a minimum. The surface tension of the bubble which resists the pulling force and which holds the bubble together, is analogous to the spatial correlation function of the sound field which holds the quiet zone together. Just as a soap bubble retains a similar shape for pulling forces which are less than the critical force necessary to overcome the surface tension of the bubble, the diffuse field quiet zone retains a single trough up to the critical separation distance of about $0.5\ \lambda$. Above these critical values, both the bubble and the diffuse field quiet zone collapse to form two distinct parts.

Some special cases of the square pressure profiles shown isometrically on the preceding page are shown in the figure below for microphone separation distances equal to exactly one tenth, one fifth and one wavelength

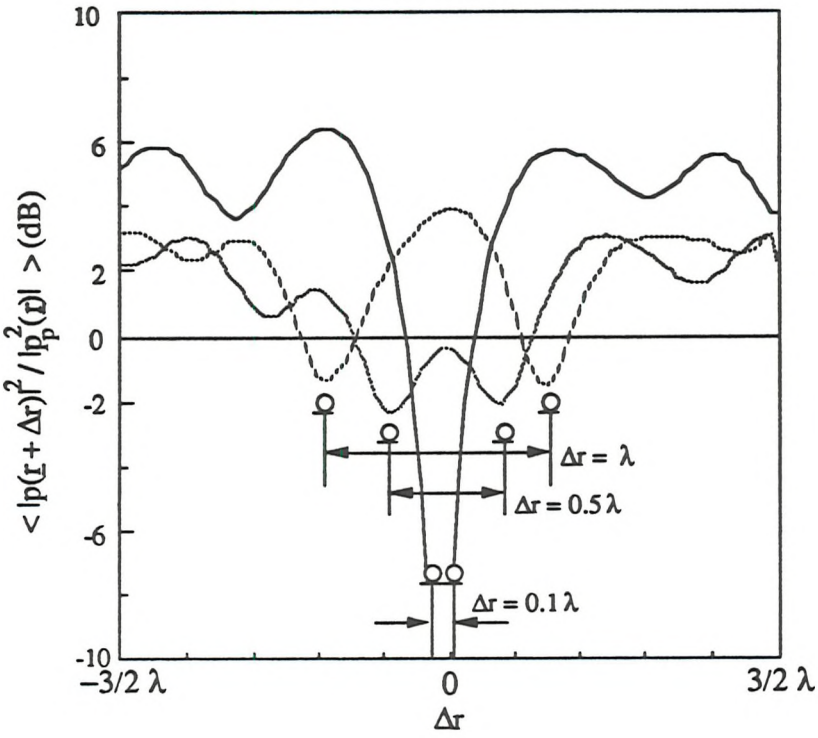

Figure 5.16. The space averaged profiles of the square pressure around the centre of two points of minimisation separated by a distance 0.1 λ, 0.5 λ and 1 λ.

Notice that the increase in the square pressure well away from the points of minimisation are nearly equal for the case where the Pareto variables are both equal to two. The expected increase in the square pressure for these configuration of error microphones is 3 dB where from equation (5.54), the secondary source contribution to the total square pressure is equal to that of the primary source contribution. This prediction is close to the observed simulated increase shown in figure 5.16.

5.6. Discussion and conclusions

In view of the relative success of the results reported in this chapter, the remote unconstrained cancellation of the pressure at a point, discussed at length in the conclusions reached for chapter 4, seems ill-considered. This is because the control schemes investigated here seeks purposefully to restrain the mean square pressure of the diffuse field either by self limiting of the secondary source strength, or by seeking to bring about the point cancellation of the pressure in a manner in which is less prone to statistical

uncertainty and therefore better conditioned. The principal finding of this investigation is the emergence of some upper-bound limit on the size and extent of the region of quiet one is able to engineer in the diffuse sound field. This finding appears to have generally validity over the range of control procedures investigated. In general terms, the size of the diffuse field quiet zone at the 10 dB level has been found to be confined to length scales which are typically one tenth of the acoustic wavelength. This figure will also emerge in the next section when the effect of cancelling the pressure at a point in the near field of a secondary source are investigated

Initial control strategies considered in this chapter involve simple modifications to the cost function. For example, it was demonstrated that placing upper bounds on the maximum secondary source strength only a few times that of the primary source strength, allows for the vast majority of points in the diffuse field to be driven to zero. Moreover, this hard limited control system was shown to restrain the mean square pressure in the diffuse sound field to levels which are not significant compared with the original primary level. The mean and the variance of the hard limited secondary source strength was evaluated as a function of the upper-bound value.

Simple analysis of the so called 'under determined' problem was also shown to prove more advantageous than the elementary unconstrained single channel configuration. While in principal, both can achieve the perfect cancellation of the pressure at a point, employing more independently positioned secondary sources than points of minimisation enables one to impose constraints on the secondary source strengths in addition to the pressure field. Specifically, the redundancy of secondary sources has enabled the pressure at some point to be set to zero under the condition that the sum of the squares of the secondary source strength is a minimum. This secondary source arrangement has an effective source distribution which possesses multiple independent channels to the point of cancellation such that it is able to distributes its effort along the transmission path offering greatest impedance according to a least squares criterion.

With real time computing becoming increasingly faster, one can envisage employing an array of tiny loudspeakers remotely distributed around the enclosure, each constrained to act at the same point. The source strength of each of these transducers would need only to be a disproportionately smaller fraction of the secondary source required than if it were acting alone. It was found that the combined secondary source strength of an array of independently positioned secondary sources is less than that for single source case. However, the implementation of this scheme is clearly costly both in terms of computing time and hardware resources.

Most control configurations currently employed[23,24,25], are over determined and so employ less secondary sources than there are points of minimisation. While this arrangement is useful for low modal density sound fields, such a scheme could be ineffectual depending on the number of independent points per secondary source. Statistical considerations have shown (if only empirically) that it is precisely this ratio which dictates the statistical distribution of the square of each of the secondary source strengths. Perhaps not surprisingly for example, each of the secondary sources in an array of three sources minimising the sum of the square pressures at say five points is as equally liable to a given statistical fluctuation and has the same mean value as say six secondary sources acting at ten points. This was found to be true despite the increased number of transfer impedance paths in the latter arrangement. By way of a summary, the expectation of the square of the total secondary source strength for the under-determined, over-determined and the square system are tabulated below for comparison

	$\sum_i < \lvert q_{s_i} \rvert^2 > / \lvert q_p \rvert^2$
$L > M$	$M^2 / (L - M)$
$L = M$	∞
$L < M$ (for L=1)	$M / (M - L)$

It remains to be shown whether the undetermined result is a general result valid for all values of L. Inspection of the table above indicates a degree of symmetry between the respective results. This suggests that there may be some generalised formula for predicting the expectation for the square of the secondary source strength, and ultimately the increase in potential energy for all multi-channel control schemes whether over determined or under determined. This of course assumes that the Pareto function is the correct choice of probability density function for the over determined arrangement.

In terms of the size and spatial extent of the zone of quiet, complete cancellation of the pressure is possible for ratios of values $L / M \leq 1$ corresponding to the case where the number of secondary sources equals, or out numbers the number of points of cancellation. for these ratios of secondary source to points of minimisation, one can reasonably expect a 10 dB level of reduction which extends in space for at least one tenth of a wavelength. The problem of minimising the sum of the square pressure at two closely spaced points in the diffuse field corresponds to the range $1 < L/M < 1/2$ where of course $L = 1$ in this case.

The extent of the quiet zone for this arrangement is less than 10 dB in most cases but has the advantage of being extended over a broader region.

When one seeks to impose active control within a enclosed sound field which may be tending to 'diffuseness', at least a two to one correspondence between the number of points of minimisation and the number of secondary sources employed is strongly recommended ($N = L/M < 2$). For ratios of L to M less than two, the total effort directed towards controlling the sound field is too thinly spread over the spatially complex wavefield to be very effective. This is particularly true given that the level and confinement of the quiet zone formed by the square system where $L/M = 1$ has already been shown to be poor.

A recent paper by Mioshi and Kaneda[94] have shown that introducing one more secondary source than is absolutely necessary (therefore being under determined) is, in principle, sufficient to circumvent the obvious difficulties imposed by causality considerations and is mentioned for completeness. The author has not been able to fully understand why an additional source should be able to do this but is thought to incorporate a modelling delay into the controller. A scheme of this nature is not realisable in practice but has only been noted here for completeness.

CHAPTER 6

NEAR FIELD ZONES OF QUIET IN THE PURE TONE DIFFUSE SOUND FIELD

6.0. Introduction

Previous investigations in this thesis have suggested that the active attenuation of diffuse field pressures in regions which are remote from the secondary source may cause substantial global pressure increases. For example the previous chapter has indicated that the implementation of a multi-channel control scheme in diffuse fields incurs an average square pressure increase at least equal to 3 dB. This level of increase corresponds to the limiting cases where either the number of secondary sources vastly exceeds the number of control microphones, or visa-versa. When the numbers of sources and control microphones are roughly equal, for which the control configuration starts to approach a square system, the expected increase in pressure well away from the control point is considerably higher than 3 dB.

Active control in diffuse fields using secondary sources remote from the control point is further limited by the fact that the shape of the quiet zone is dictated solely by the functional form of the sound field's spatial cross correlation function. The difficulty here is that the correlation function is, by definition, only an expectation quantity and is therefore susceptible to unpredictable variations between individual measurements. This function is of fundamental importance in describing the inter-dependence between acoustic pressures at neighbouring points and is therefore intrinsically bound up with the large scale characteristics of the wavefield. This property is therefore not amenable to manipulation by the engineer.

In this chapter a control strategy for overcoming these difficulties is discussed which seeks to capitalise on the near field characteristics of the radiation from a secondary loudspeaker. This active control scheme utilises a single secondary loudspeaker in order to drive the acoustic pressure at a point in its immediate geometric near field to zero. This principle is certainly not original and was first proposed by Olson[3] in a historically important paper published in 1953. Although very few acoustic considerations were discussed, the potential of this arrangement was demonstrated by using it to suppress freely propagating plane waves over a frequency range of more than three octaves. Olson was also the first to suggest that a tightly coupled microphone - loudspeaker pair could

have two possible distinct modes of operation: that of an 'electronic sound absorber' and that of a 'sound pressure reducer'. However, no information was provided about how these modes of operation differ in their governing physical principles.

The potential benefits derived from this loudspeaker - microphone configuration are three-fold. First, and perhaps the most significant is the increased ease with which the secondary source is able to couple into the acoustic pressure at the cancellation point thereby ensuring that the energy radiated to the 'far field' is small in relation to that transmitted by the primary source. Second, the shape of the near field quiet zone is, to a large degree, deterministically governed by geometric factors relating to the secondary source near field radiation characteristics. Last, the difficulties imposed by causality considerations when dealing with broadband radiation are to a large degree circumvented. This is because the time delay from the secondary source to the control microphone will be considerable less than the time delay from the primary source.

The transfer impedance which couples the secondary source to the closely spaced point of cancellation now comprises a large directly transmitted near field component which is superimposed on the purely random part arising from wall reflections. The uncertainty arising previously for remote points of cancellation is now largely removed. In this configuration the secondary source strength necessary to bring about the pressure cancellation is now very much less than that of the primary source strength. By the same argument, the sound power output from the 'tightly coupled' system is also small in relation to that of the primary sound power output.

This control methodology has already been applied by Salikudin *et-al*[26] to the exterior of jet aircraft in preliminary experiments aimed at trying to reduce acoustic fatigue. The general philosophy behind this approach is outlined in chapter 1. This work is predominantly experimental however, and is supported by only a limited amount of theoretical discussion. It is hoped that this chapter will go some way to extend the present level of understanding and help clarify some of the physics associated with this control principle.

6.1. Near field zones of quiet

Figure 6.1 shows a baffled circular secondary source $q_s(\omega,y,z)$ within a radius 'a' acting to drive the pressure to zero at some closely spaced point x_0 represented within a cartesian coordinate system.

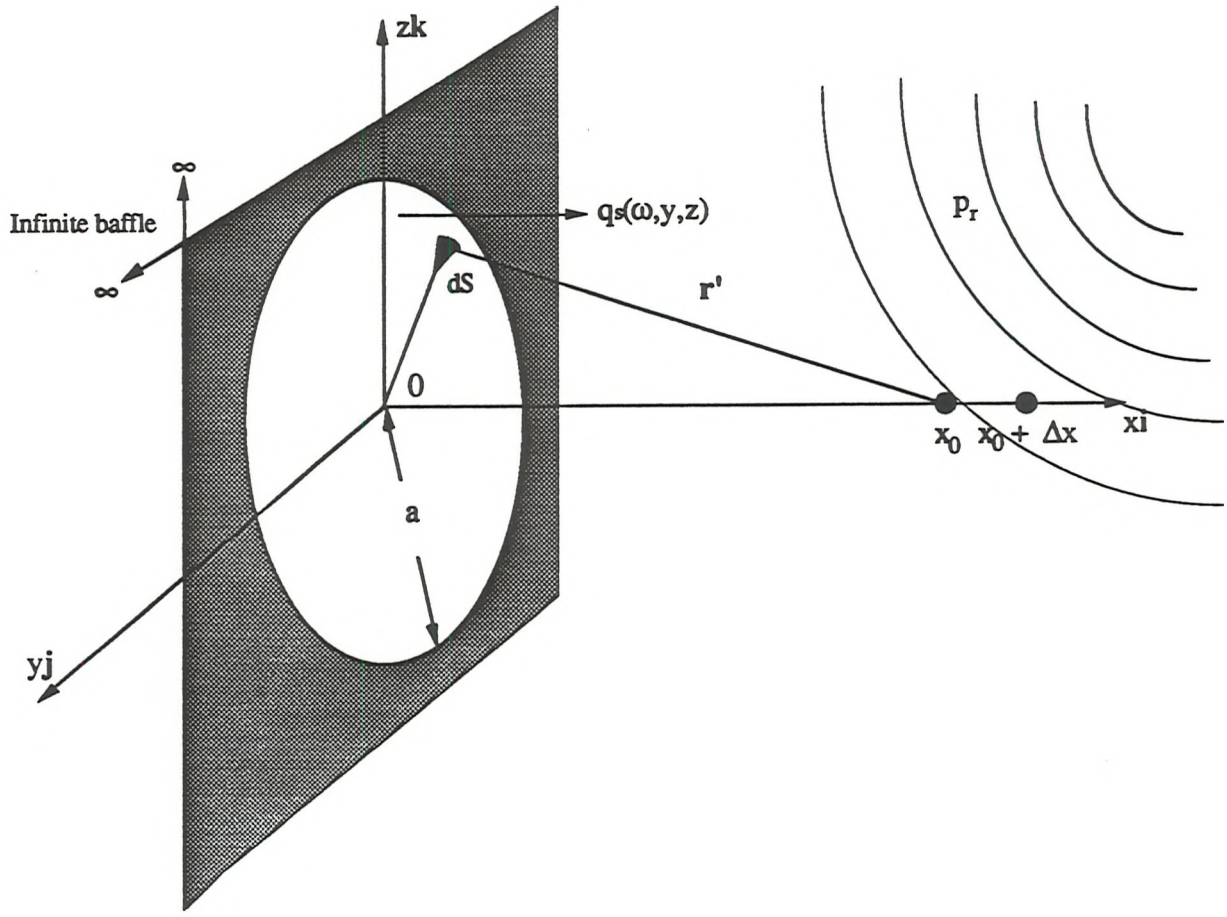

Figure 6.1 A baffled secondary source distribution represented within a Cartesian coordinate system.

Figure 6.1 represents a baffled secondary source radiating within an enclosed space in which there is a diffuse field $p_{pr}(\mathbf{r})$ sustained by a primary source. For the purpose of this analysis it is assumed that the directly transmitted component of acoustic pressure from the primary source everywhere in the near field of the secondary source is negligible. This will be a valid assumption for a large number of real cases for which the primary source distribution is often a large, irregularly shaped vibrating body. Reverberation chamber experiments (which are reported in section 6.5) reveal that the increase in the sound pressure level is not perceptible to the ear well away from a near field point of cancellation for a wide range of microphone separation distances and different loudspeakers. This experimental finding serves to provide experimental justification for this important simplifying assumption.

Resolving the secondary sound field $p_s(\mathbf{r})$ into its directly radiated pressure field $q_s Z_d(\mathbf{r}_s|\mathbf{r})$ and diffuse pressure field $q_s Z_r(\mathbf{r}_s|\mathbf{r})$ yields

$$p_s(\mathbf{r}) = q_s Z_d(\mathbf{r}_s|\mathbf{r}) + q_s Z_r(\mathbf{r}_s|\mathbf{r}) \tag{6.1}$$

where $Z_d(r_s|r)$ is the free space transfer impedance that would be generated by the secondary source in the absence of reflecting surfaces. The diffuse field pressure $q_s Z_r(r_s|r)$ is the pressure transmitted to the field point $\mathbf{r}$ by reflections from the enclosure walls. By superposition the total pressure $p(\mathbf{r})$ at the point of observation may therefore be written as

$$p(\mathbf{r}) = q_s[\, Z_d(r_s|r) + Z_r(r_s|r)\,] + p_{pr}(\mathbf{r}) \tag{6.2}$$

For harmonic sources, the pressure at some point $\mathbf{r}_0$ can always be driven to zero for a secondary source strength q_{so} which is given by

$$q_{so} = -\frac{p_{pr}(r_0)}{Z_d(r_s|r_0)+Z_r(r_s|r_0)} \tag{6.3}$$

For points of cancellation which are close to the secondary source, the configuration in which we are most interested, the acoustic pressure radiated to the near field point of cancellation via wall reflections will in most cases be very small compared to both the primary source diffuse field pressure contribution $p_{pr}(\mathbf{r})$, and the directly radiated secondary source pressure $q_s Z_d(r_s|r_0)$ at the same point. In this tightly coupled configuration the secondary source strength q_{so} is largely insensitive to the secondary source diffuse field impedance $Z_r(r_s|r_0)$. One can therefore closely approximate the total secondary source transfer impedance $Z(r_s|r_0)$ by its corresponding free space impedance value to give

$$q_{so} \approx -\frac{p_{pr}(r_0)}{Z_d(r_s|r_0)} \tag{6.4}$$

It is anticipated that only a small error is incurred as a consequence of this simplification particularly for compact secondary sources. Omitting the secondary source diffuse field pressure enables the total pressure $p(\mathbf{r})$ at some arbitrary point in the enclosure, in most cases, to be closely approximated by

$$p(\mathbf{r}) \approx p_{pr}(\mathbf{r}) - p_{pr}(r_0)\frac{Z_d(r_s|r)}{Z_d(r_s|r_0)} \tag{6.5}$$

Consider some point $\mathbf{r}$ in the vicinity of the point of cancellation $\mathbf{r}_0$ where $\mathbf{r} = \mathbf{r}_0 + \Delta\mathbf{r}$ such that $\Delta\mathbf{r}$ is small compared with the wavelength i.e. $\Delta r < \lambda$. One can therefore write

$$p(r_0 + \Delta r) \approx p_{pr}(r_0 + \Delta r) - p_{pr}(r_0)\frac{Z_d(r_s|r_0 + \Delta r)}{Z_d(r_s|r_0)} \tag{6.6}$$

Consider the modulus of the square of the total pressure $p(r_0 + \Delta r)\, p^*(r_0 + \Delta r)$ which may be expanded to give

$$|p(r_0 + \Delta r)|^2 \approx |p_{pr}(r_0 + \Delta r)|^2 + |p_{pr}(r_0)|^2 \left|\frac{Z_d(r_s|r_0 + \Delta r)}{Z_d(r_s|r_0)}\right|^2$$

$$- p_{pr}(r_0 + \Delta r)p^*_{pr}(r_0)\, \frac{Z^*_d(r_s|r + \Delta r)}{Z^*_d(r_s|r_0)} - p_{pr}(r_0)p^*_{pr}(r_0 + \Delta r)\, \frac{Z_d(r_s|r + \Delta r)}{Z_d(r_s|r_0)} \quad (6.7)$$

The average response of the square pressure in the vicinity of the control point to the cancellation of the pressure at r_0 may be obtained by averaging over all possible square pressure responses at all points in the field keeping the separation distance $|r_s - r_0|$ fixed. Taking the expectation $< |p(r_0 + \Delta r)|^2 >$ over the stochastic part of the equation and noting that

$$< |p_{pr}(r_0)|^2 > = < |p_{pr}(r_0 + \Delta r)|^2 > = < |p_{pr}(r)|^2 > \quad (6.8)$$

together with the defining relation for the cross correlation function

$$< p_{pr}(r_0)p^*_{pr}(r_0 + \Delta r) > = < p_{pr}(r_0 + \Delta r)p^*_{pr}(r_0) > = < |p_{pr}(r)|^2 > \rho(\Delta r) \quad (6.9)$$

yields the simplified expression

$$\frac{< |p(r_0 + \Delta r)|^2 >}{< |p_{pr}(r)|^2 >} \approx 1 - 2\Re\left\{\frac{Z_d(r_s|r_0 + \Delta r)}{Z_d(r_s|r_0)}\right\}\rho(\Delta r) + \left|\frac{Z_d(r_s|r_0 + \Delta r)}{Z_d(r_s|r_0)}\right|^2 \quad (6.10)$$

where $\rho(\Delta r)$ is the three dimensional, pure tone diffuse sound field spatial correlation function which is $(\sin k\Delta r)/k\Delta r$.

It is anticipated that any quiet zone formed according to this control principle will not extend beyond about $\Delta r = 0.1\lambda$ at the -10 dB level (corresponding to a quiet zone $2\Delta r_{0.1}$ equal to one fifth of a wavelength). The change in the spatial correlation function over this interval can be calculated to be approximately 6 %. The corresponding variation in the term $2\Re\{Z_d(r_s|r_0+\Delta r) / Z_d(r_s|r_0)\}$ in equation (6.10) for compact sources according to equation (3.3) however, may be shown to vary like $2kr_0 \cos k\Delta r_0 / (kr_0 + k\Delta r_0)$. Over the same interval therefore, the variation in this function is typically 20 % providing $k|r_s - r_0|$ is small compared to unity. The spatial cross correlation $\rho(\Delta r)$ can therefore be set to unity while incurring only small errors in the region of the quiet zone. This simplification is equivalent to assuming that the diffuse field pressure is, on average, spatially homogeneous throughout the volume of the quiet zone. For Δr less than 0.1λ, one can therefore write

$$\frac{< |p(r_0 + \Delta r)|^2 >}{< |p_{pr}(r)|^2 >} \approx 1 - 2\Re\left\{\frac{Z_d(r_s|r_0 + \Delta r)}{Z_d(r_s|r_0)}\right\} + \left|\frac{Z_d(r_s|r_0 + \Delta r)}{Z_d(r_s|r_0)}\right|^2 \tag{6.11}$$

Further simplification of this expression is possible. Noting that $r_0 = (x_0,y_0,z_0)$ and $r_0 + \Delta r = (x_0+\Delta x, y_0+\Delta y, z_0+\Delta z)$, to first order in Z_d, one obtains the first order Taylor series approximation

$$Z_d(r_s|r_0 + \Delta r) \approx Z_d(r_s|r_0) + \nabla Z_d(r_s|r_0).\Delta r \tag{6.12}$$

for $\Delta r < \lambda/10$

where ∇ is the Gradient operator $\nabla = \frac{\partial}{\partial x}\mathbf{i} + \frac{\partial}{\partial y}\mathbf{j} + \frac{\partial}{\partial z}\mathbf{k}$ and $\Delta r = \Delta x\mathbf{i} + \Delta y\mathbf{j} + \Delta z\mathbf{k}$, where x, y and z are cartesian coordinates and **i**, **j** and **k** are their associated unit vectors. The ratio of free space impedance terms can therefore be approximated by

$$\frac{Z_d(r_s|r_0 + \Delta r)}{Z_d(r_s|r_0)} \approx 1 + \frac{\nabla Z_d(r_s|r_0).\Delta r}{Z_d(r_s|r_0)} \tag{6.13}$$

for $\Delta r < \lambda/10$

Substituting this approximate expression into equation (6.11) yields

$$\frac{< |p(r_0 + \Delta r)|^2 >}{< |p_{pr}(r)|^2 >} \approx 1 - 2\Re\left\{1 + \frac{\nabla Z_d(r_s|r_0).\Delta r}{Z_d(r_s|r_0)}\right\} + \Im^2\left\{\frac{\nabla Z_d(r_s|r_0).\Delta r}{Z_d(r_s|r_0)}\right\} + \Re^2\left\{1 + \frac{\nabla Z_d(r_s|r_0).\Delta r}{Z_d(r_s|r_0)}\right\} \tag{6.14}$$

for $\Delta r < \lambda/10$

Expanding and collecting the terms facilitates the further considerable simplification

$$< |p(r_0 + \Delta r)|^2 > \approx < |p_{pr}(r)|^2 > \left|\frac{\nabla Z_d(r_s|r_0).\Delta r}{Z_d(r_s|r_0)}\right|^2 \tag{6.15}$$

for $\Delta r < \lambda/10$

This surprisingly simple result implies that the pressure near the control point recovers from zero at a rate which is determined by the absolute value of the gradient of the

impedance field in the measurement direction, as a fraction of its absolute value at r_0. It is tempting to look for some geometrical interpretation of this result in terms of the free space transfer impedance function $Z_d(r_s|r_0)$, however none was immediately apparent. Equation (6.15) says that large quiet zones are formed around near field points of null pressure for those sources whose transfer impedance to the point of cancellation is large and unchanging with respect to small deviations from the cancellation position. A large transfer impedance between the secondary source to the chosen point of cancellation is therefore desirable on two accounts. First, it directly influences the shape and therefore the size of the near field quiet zone. But more importantly in practical terms is that the coupling impedance governs the magnitude of the secondary source strength and therefore the energy radiated into the enclosure. This important aspect of the problem is addressed in the next section.

An unfortunate consequence of disregarding the secondary source diffuse field pressure is that one has also removed any facility for incorporating the secondary source contribution to the average square pressure increase $< |p_{sr}(r)|^2 >$ well away from the cancellation point. For most cases, this contribution will be negligible compared with the primary source diffuse field contribution $< |p_{pr}(r)|^2 >$ as will soon become apparent from remote sound pressure level measurements made in a reverberation chamber. Strictly speaking, however, this term should be included.

The diffuse field quiet zone very close to a source of sound is an essentially free field result by virtue of the important approximation $\rho(\Delta r) = 1$ where $p_{pr}(r_0) = p_{pr}(r_0 + \Delta r)$ which says that the primary sound field is homogeneous in the region of the quiet zone. Indeed, one of the reasons why the notion of the diffuse field is so useful conceptually is that many of the properties of a source radiating within it, on average, reduce to their equivalent free field results. Sound power output is an important example[96]. As an immediate consequence of neglecting the dependence on the secondary source diffuse field, the square pressure variation around the near field point of cancellation behaves, on average, as if in a free field environment. In retrospect, this finding is perhaps not surprising since the reverberant, diffuse field will tend to impose small statistical fluctuations on the free field result which when averaged over all space will tend to cancel.

At points of cancellation along the x axis as indicated in figure 6.1, $\Delta y = \Delta z = 0$. In accordance with equation (6.15), the expected axial square pressure variation may now be written as

$$\frac{< |p(x_0+\Delta x, y_0, z_0)|^2 >}{< |p_{pr}(x_0, y_0, z_0)|^2 >} \approx \Delta^2 x \left| \frac{\frac{\partial}{\partial x} Z_d(r_s|r_0)}{Z_d(r_s|r_0)} \right|^2 \qquad (6.16)$$

$$\text{for } \Delta x < \lambda/10$$

Setting equation (6.16) equal to some fraction α say, enables one to solve for the zone of quiet $2\Delta x_\alpha$ for which the average square pressure is a fraction α of the primary source level. The zone of quiet along the axis of the piston motion can be therefore be approximated by

$$2\Delta x_\alpha \approx 2\sqrt{\alpha}\left|\frac{Z_d(r_s|r_0)}{\frac{\partial}{\partial x}Z_d(r_s|r_0)}\right| \tag{6.17}$$

Similarly in the y and z directions

$$2\Delta y_\alpha = 2\sqrt{\alpha}\left|\frac{Z_d(r_s|r_0)}{\frac{\partial}{\partial y}Z_d(r_s|r_0)}\right| \tag{6.18}$$

and

$$2\Delta z_\alpha = 2\sqrt{\alpha}\left|\frac{Z_d(r_s|r_0)}{\frac{\partial}{\partial z}Z_d(r_s|r_0)}\right| \tag{6.19}$$

for small Δx, Δy and Δz. Surfaces of equal pressure reduction around $\mathbf{r}_0$ therefore describe concentric ellipsoids with semi - axes $(\Delta x_\alpha, \Delta y_\alpha, \Delta z_\alpha)$. This analysis is not valid when the gradient of the impedance field is zero, in which event, further terms in the Taylor series expansion of equation (6.12) must be taken.

6.2. Examples of near field quiet zones

It is instructive to consider the behaviour of the quiet zone as described by equation (6.17) for representative examples of real secondary sources which in most cases will be circular loudspeakers. However, as a simple model problem first consider the form of the quiet zone for a point monopole source for which the complex impedance field is simple and can be analytically manipulated. From equation (3.31), the axial free space transfer impedance $Z_d(0|x)$ is given by

$$Z_d(0|x) = jZ_0\frac{e^{-jkx}}{kx} \tag{6.20}$$

where it is assumed that the point secondary source is located at the origin. Performing the differentiation, one can readily show that the derivative evaluated in the radial direction is given by

$$\frac{\partial}{\partial x}Z_d(0|x_0) = jZ_0\frac{e^{-jkx_0}}{kx_0}\left[\frac{-jkx_0 - 1}{x_0}\right] \tag{6.21}$$

The size of the quiet zone is therefore proportional to

$$2\Delta x_{0.1} \sim \left| \frac{Z_d(0|x_0)}{\frac{\partial}{\partial x} Z_d(0|x_0)} \right| = \frac{x_0}{\sqrt{1+(kx_0)^2}} \tag{6.22}$$

From equation (6.17), the size of the quiet zone may be written as

$$2\Delta x_{0.1} \approx 2\sqrt{0.1}\ \frac{x_0}{\sqrt{1+(kx_0)^2}} \tag{6.23}$$

Assuming that the average square pressure contribution from the secondary source remains small, the axial zone of quiet converges to $\sqrt{0.1}\,\lambda / \pi$ for large x_0 which is equal to 0.1007λ or about one tenth of a wavelength to an excellent approximation.

Despite the fact that the transfer impedance and its derivative are both infinite at the secondary source point where $x_0 = 0$, one can verify by inspection that the gradient of the transfer impedance goes to infinity faster with decreasing x_0 than the value itself. The size of the quiet zone therefore becomes increasingly smaller, monotonically tending to zero. In this limit, the form of the quiet zone may be regarded as an infinitesimally small 'pin prick' in the primary sound field as will also become apparent from experimental results. Unfortunately, Olson fails to report the dimensions of the loudspeaker used or the separation distance of the point of cancellation so that verification of his experimental findings with the simple theory developed here is not possible.

Returning now to the form of quiet zones generated by more realistic sources of sound. As a first order approximation to the free space radiation from a real, baffled circular loudspeaker, consider the related analogous model problem of the acoustic radiation from a rigid piston oscillating in an infinite baffle[50]. Surrounding the piston source with a hypothetical baffle of infinite extent ensures against the interference of the forward radiated sound from diffracted waves from the rear of the source. This geometry is indicated in figure 6.1. All points on the source may be regarded as elementary, compact monopole type sources whose sound field radiates spherically out in all directions. The contributions from all the elemental sources at some point r can be integrated to produce the Rayleigh integral given below

$$Z_d(r_s|r) = j\frac{\rho c k}{2\pi S}\int_S \frac{e^{-jk.r'}}{|r'|}\,dS \tag{6.24}$$

The integration is taken over the entire source distribution q_{so} which is assumed to be uniform to give 'piston like' motion, where $\mathbf{r}_s$ now denotes the centre of the piston and $|\mathbf{r}'|$ is the distance from each elemental source to the point of observation at $\mathbf{r}$. It is relatively straightforward to shown that this integral reduces to an exact solution[50] providing the point of observation is 'on axis' such that $\mathbf{r} = (x,0,0)$. Putting the secondary source at the origin of co-ordinates $\mathbf{r}_s = (0,0,0)$ and performing the integration one can show that

$$Z_d(0|x) = \frac{\rho c}{S}\left[e^{-jkx} - e^{-jk\sqrt{x^2 + a^2}} \right] \tag{6.25}$$

where S is the surface area of the piston πa^2. Equation (6.25) indicates that the free space transfer impedance $Z_d(\mathbf{r}_s|\mathbf{r})$ generated by a piston type source in an infinite baffle comprise only those contributions which are on the centre and the circumference of the circular source. Contributions from elemental sources in the disc itself clearly cancel. This simplified model is generally regarded as a reasonable approximation to the acoustic behaviour of real baffled, circular loudspeakers radiating at mid frequencies, see for example the loudspeaker vibration patterns presented in the book by Fahy[83]. This is the frequency range where diffraction effects around the oscillating loudspeaker are small but where the loudspeaker cone remains as a rigid body and has not yet begun to oscillate in its various normal modes of vibration. All points on the cone therefore oscillate with the same phase. The form of equation (6.25) suggests the possibility of using a closely spaced array of appropriately phased point monopole sources in order to simulate an effective secondary source distribution with the desired transfer impedance characteristics. This idea remains to be investigated.

We now seek to determine the variation of the expected value of the 10 dB quiet zone $2\Delta x_{0.1}$ as a function of the microphone separation distance $\mathbf{r}_0$ evaluated for various values of the loudspeaker radius 'a' modelled as a piston in an infinite baffle. This may be determined from equations (6.17) and (6.25) assuming that the increase in the square pressure arising from the secondary source contribution is close to zero and can therefore be neglected. The 'on axis' quiet zone was evaluated in accordance with equation (6.17) for a range of microphone separation distances varying from zero, up to a maximum of one wavelength. A range of loudspeaker radii ranging from near zero (for the case of the elementary point monopole) up to a maximum of one wavelength were also considered. In all cases, the secondary source contribution to the square pressure is assumed to be negligible and has therefore been set equal to zero.

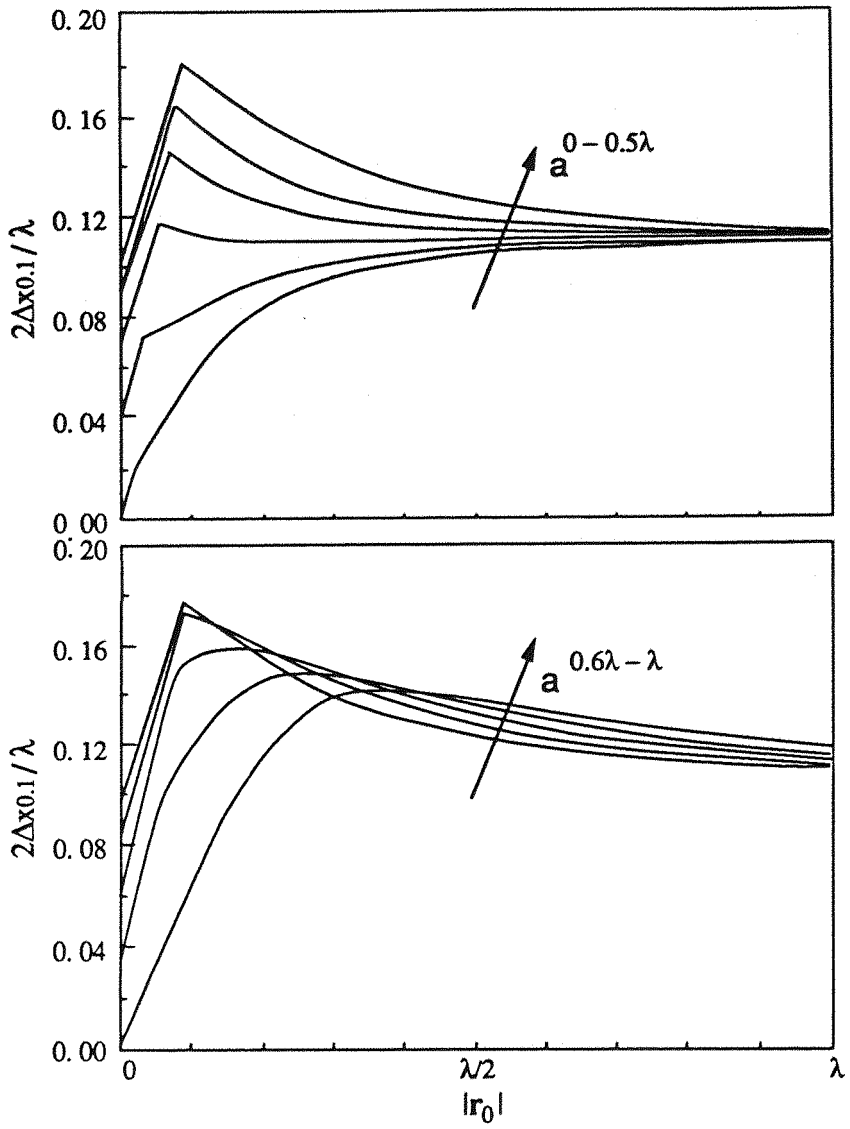

Figure 6.2 The theoretical expectation for the near field zone of quiet shown plotted as a function of the point of cancellation distance and also the loudspeaker radius.

For some values of the loudspeaker radius 'a', there appears to an optimum separation distance r_0 for which the quiet zone takes a maximum value. Figure 6.2 indicates that this usually occurs at separation distances approximately equal to one tenth of a wavelength. This peak in the series of curves corresponds to the critical distance, below which, the 10 dB quiet zone extends into the loudspeaker itself thereby reducing the effective width of the quiet zone. Another equally notable feature of this figure is that the curves asymptote to approximately the same value as the separation distance increases. By inspection, this quiet zone limit is approximately one tenth of a wavelength as observed previously for the behaviour of the quiet zone formed in the vicinity of a point monopole source.

The simplifying assumptions leading to the derivations of the governing equations at these large distances become invalid owing the contribution from a significant level of reflected sound. We have already seen in chapter 5, however, that when the secondary source transfer impedance contribution is dominated by the diffuse field part of the impedance field, but the source strength is reasonably constrained, the zone of quiet limited by the spatial correlation properties of the sound field, is also equal to one tenth of a wavelength. We thus have the interesting observation that the average size of the 10 dB quiet zone appears to remain approximately constant at about one tenth of a wavelength even as the point of cancellation is moved from being close to the secondary source so being determined by the near field, to being very distant so being determined by the diffuse field. The likelihood of deviation from the average value of the quiet zone steadily increases. The crucial difference between the two cases is that the expectation value of the square pressure increase varies from a small fraction of one decibel in the former case, to tens of decibels for the remote case.

The succession of curves plotted for various values of the loudspeaker radius indicate that the largest zone of quiet is achieved by the loudspeaker which is one wavelength in diameter acting to cancel the pressure at a point located at approximately one tenth of a wavelength from its centre. From a practical view point, even at say 500 Hz which may be regarded as being in the mid-frequency range, the loudspeaker diameter is approximately equal to 0.7 m which is already unrealistically large for most practical purposes. In many real applications, the excitation frequency will be fixed and the size and location of the secondary loudspeaker will be dictated by constraints imposed by limited space such as for example, the size of the head rests in vehicles. The only parameter which remains variable to the engineer is therefore the separation distance of the point of cancellation from the secondary source which may be optimised by the use of figure 6.2.

The discussion so far has talked only in terms of the spatial extent of the zone of quiet along the axis in the direction of the piston motion. One may utilise the existing theoretical framework to derive similar results for quiet zones in the orthogonal directions. However, it is worth noting that in these directions the circular piston source has cylindrical symmetry for which the piston free space transfer impedance $Z_d(r_s|r)$ is the identical for all values of the azimuthal angle ϕ (see figure 6.3a) namely

$$Z_d(r_s|r,\phi_1) = Z_d(r_s|r,\phi_2) \tag{6.26}$$

where ϕ_1 and ϕ_2 are arbitrary azimuthal angles. This remark has important implications for the geometry of the quiet zone. A secondary source driven to cancel the pressure at some

some point which is off-axis, will similarly cancel the pressure at an infinite number of points lying on a circle whose origin is on the piston axis passing through the original point of cancellation, see figure 6.3a again assuming that the primary sound field is reasonably uniform over this region. Clearly, when the point of cancellation is closer to the piston axis than some critical distance, the circle of pressure cancellation will form a 'ring' of quiet which will tend to coalesce to produce one unique distinct zone which is symmetric about the piston axis. The spatial extent of this quiet zone in the direction perpendicular to the piston axis will therefore be greater than if it were on axis. Points of cancellation which deviate slightly from the on-axis position are not expected to significantly affect the size of the quiet zone in the axial direction. Similarly, a point monopole secondary source has spherical symmetry so that cancelling the pressure at one point at a given distance from the centre, will cancel the pressure at all points at the same radial distance thereby creating a 'shell' of quiet as suggested by figure 6.3b. A simple sketch indicating these various symmetries for these two source types and the consequences in terms of the quiet zone are given below

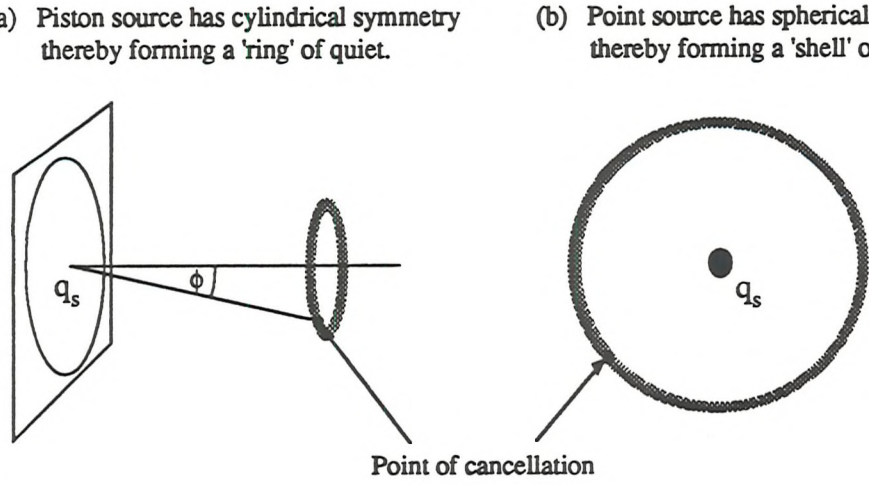

Figure 6.3. A simple sketch indicating the impedance field symmetries of (a), the piston source and (b), the point source and the corresponding effect on the quiet zone.

The size and extent of pressure reductions in these directions remains to be investigated.

6.3. Secondary source strength statistics

The most likely consequence of driving the pressure at some point $\mathbf{r}_0$ to zero which is close to the secondary source at $\mathbf{r}_s$ is that sound power is injected into the medium by the secondary source which will sustain an increase in the acoustic pressure. In the next section this is shown to true on average for the point monopole source. The usual proportionality between the total potential energy in the room to the square of the volume

velocity will no longer be valid in this case. This is because the secondary source is now radiating into an acoustic impedance which differs from the usual diffuse field impedance necessary for these relationships to be valid. In this tightly coupled configuration the secondary source will now 'see' some effective impedance mechanism which forces its pressure at some closely spaced point to zero and it is therefore inevitable that its sound power output will be modified in some sense. The details of this process is addressed in the next section for compact secondary sources. The expectation of the square transfer function $< |H_0|^2 >$ now no longer quantifies the expected value of the added energy in the enclosure but is simply an indication of the average secondary source strength requirements. This quantity is also a good indicator of the degree of acoustic coupling between the loudspeaker and the microphone, which as we have seen in chapter 5, goes to infinity as the point of cancellation is moved outside of the influence of directly transmitted sound. The transfer function H_0 has previously been derived in terms of the primary source and secondary source impedance contributions according to

$$H_0 = \frac{q_{so}}{q_p} = - \frac{Z_T(r_p|r_0)}{Z_d(r_s|r_0) + Z_T(r_s|r_0)} \tag{6.3}$$

It is left to Appendix 6.1 to show that in the case of the diffuse sound field, $< |H_0(<\delta^2>)|^2 >$ is determined from the following integral

$$< |H_0(<\delta^2>)|^2 > = \frac{1}{\pi} \int_0^{\infty} \int_0^{2\pi} \frac{e^{-(r^2 - 2r\cos\theta + 1)/2<\delta^2>}}{r} dr d\theta \tag{6.27}$$

where the term $<\delta^2>$ on which $< |H_0(<\delta^2>)|^2 >$ solely depends is the average of the square of the real part (or imaginary part) of the diffuse field transfer impedance $< \Re^2\{Z_T(r)\} >$ as a fraction of the square impedance radiated directly $|Z_d(r_s|r_0)|^2$. In the present case, $<\delta^2>$ symbolises the relative variance of the diffuse field transfer impedance at the point of cancellation according to equation (6.28) below

$$<\delta^2> = \frac{\sigma_Z^2}{\mu_Z^2} = \frac{< \Re^2\{Z_T(r)\} >}{|Z_d(r_s|r_0)|^2} \tag{6.28}$$

Just as this factor was shown to govern the mean and variance of the minimum sound power output from two closely spaced sources (chapter 3), so it also emerges in this problem as the factor which completely determines the behaviour of $< |H_0(<\delta^2>)|^2 >$.

Unfortunately, equation (6.27) does not lend itself to analytic evaluation. Moreover it would appear from a study of the behaviour of the dummy variable r in the vicinity of $r \approx 0$ in this equation that the mathematical expectation $< |H_0(<\delta^2>)|^2 >$ does not formally exist and is therefore infinite. An unfortunate consequence of this unexpected and surprising result is that one is unable to talk meaningfully and unambiguously about the true mathematical expectation of this well behaved, tightly coupled system. Just as the secondary source strength seeking to minimise the total sound power of a closely spaced point primary source has the potential to become singular, this observation is also true of $|H_0(<\delta^2>)|^2$. The ill-conditioning of this expectation is perhaps more surprising since now the denominator of equation (6.3) comprises two degrees of freedom by virtue of the real and imaginary parts of the impedance field which simultaneously must now go to zero for this to occur.

The cause of this potential singularity occurs when both the in-phase, and quadrature parts of the directly radiated transfer impedance simultaneously destructively interfere with the impedance contributions from subsequent reflections. In the event of this unfortunate (and very unlikely) occurrence, the complex secondary source transfer impedance is zero such that it has no influence at the chosen point of cancellation and is therefore required to be infinitely large. In terms of the integral in equation (6.27), the outcome described here is manifest as a singularity at the origin $r = 0$, by virtue of which the average value of the square of the transfer function $< |H_0(<\delta^2>)|^2 >$ is infinite.

In view of this misleading and ambiguous result, we will now endeavour to use previously established techniques in order to obtain a good estimate for the expectation of the square of the modulus of the transfer function $< |\hat{H}_0|^2 >$. It is shown in Appendix 6.2, that for those source positions for which $\delta^2 < 1$, $< |\hat{H}_0|^2 >$ may be expanded as a polynomial in $<\delta^2>$ of the form

$$< |\hat{H}_0|^2 > \approx 2 <\delta^2> + 4 <\delta^2>^2 + 16 <\delta^2>^3 + 96 <\delta^2>^4 \qquad \text{for } \delta^2 < 1 \tag{6.29}$$

where $<\delta^2> = < \Re^2\{Z_t(r)\} > / |Z_d(r_s|r_0)|^2$. Thus, $< |\hat{H}_0|^2 >$ is a highly non-linear function of the impedance variance $<\delta^2>$. This function is plotted below and compared with the expectation value obtained from a 15,000 point ensemble of values generated from computer simulations. The real and imaginary parts of the impedance terms appearing in equation (6.3) were arbitrarily assigned an independent, normally distributed random variable with a pre-determined variance $<\delta^2>$ taken from a random number generator. The

process was repeated 15,000 times for a range of values of $<\delta^2>$, $<|\hat{H}_o|^2$ evaluated, and the sample mean calculated for each value of $<\delta^2>$. Also shown is the linearised approximation $<|\hat{H}_o|^2> \approx 2<\delta^2>$ representing the predicted mean when the diffuse field secondary source transfer impedance is neglected. This approximation is used to calculate the secondary source sound power output in the next section.

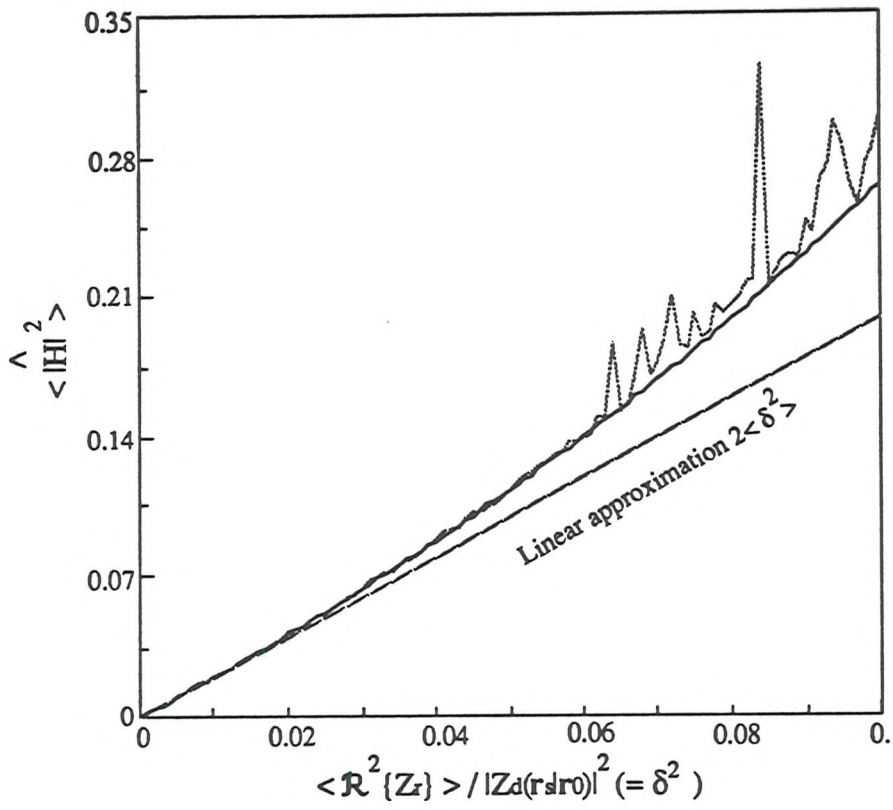

Figure 6.4. The estimate of the square of the modulus of the optimal transfer function for driving a closely spaced point pressure to zero derived as a series expansion (solid line) together with the mean value obtained from computer simulations (dashed line). Also shown is the linearised approximation taking the first term only.

Good agreement between the estimated average square transfer function $<|\hat{H}_o|^2>$ and the computer simulated ensemble mean is apparent for $<\delta^2>$ over the entire range of values. For values of $<\delta^2>$ greater than 0.05 the inherent ill-conditioning of the system, which compelled one to take the series expansion in the first place, begins to emerge as sudden departures from the theoretical curve. Deviation from the expected value occurs whenever a given ensemble of values (for a given $<\delta^2>$) violates the simplifying assumptions. This will of course become increasingly frequent as the relative variance $<\delta^2>$ of the impedance coupling the source to the point of cancellation increases. Note also that taking the series expansion of $<|\hat{H}_o|^2>$ to the leading linear term also provides a reasonable approximation to the observed, simulated mean. This finding should be borne in mind for

the next section when the sound power output of a point monopole secondary source is derived.

For small $<\delta^2>$ where the coupling mechanism between the secondary source and the point of cancellation is predominantly via directly radiated sound, $< |\hat{H}_0|^2 >$ is small in relation to unity. In this configuration, there is small likelihood that the secondary source will experience difficulties in coupling into the near field point of cancellation. This is because the secondary impedance term is contrived to contain a large free field component. The corresponding primary impedance term however, comprises only a reverberant contribution which is of course subject to uncertain statistical fluctuation from point to point in the diffuse wave field. This helps to explain why the parameter $<\delta^2>$ is so important since it is this term which exactly characterises the likelihood of departure of the complex transfer impedance from its mean value. As a general guide-line, one should aim to locate the error microphone sufficiently close to the secondary source such that the ratio of reflected sound to directly transmitted sound is less than about 0.1. In this configuration, the system is tightly coupled and the probability of departure from this assumption is small.

By way of illustration, consider again the special case of a point monopole source. The square of the modulus of the free space transfer impedance is determined from equation (3.31) to give

$$|Z_d(r_s|r_0)|^2 = \frac{Z_0^2}{(k\Delta r)^2} \tag{6.30}$$

where $\Delta r = |r_s - r_0|$. From equation (6.28), the ratio of impedance terms $<\delta^2>$ is therefore equal to

$$<\delta^2> = \frac{< \Re^2\{Z_r(r)\} >}{Z_0^2} (k\Delta r)^2 \tag{6.31}$$

Recalling equation (3.51), one can write

$$<\delta^2> = \frac{(k\Delta r)^2}{\pi M_{0.5}(\omega)} \tag{6.32}$$

At frequencies greater than the Schröder frequency, the relative variance of the diffuse field transfer field transfer impedance is very much less than unity. For example, at a frequency equal to the Schröder frequency where $M_{0.5}(\omega) = 3$ and for a cancellation distance equal to one tenth of a wavelength, $<\delta^2>$ may be calculated to be equal 0.05, from which the corresponding value of $< |\hat{H}_0|^2 >$ according to figure 6.4 is 0.1 which is small compared to unity. For small kr_0 therefore, taking the leading term in equation (6.29), the average

secondary source strength may be shown to be proportional to the distance from the point of cancellation thus

$$\sqrt{< |q_{so}|^2 >} \approx \sqrt{\frac{2}{\pi M_{0.5}(\omega)}}\, k\Delta r\ |q_p| \qquad (6.33)$$

for $k\Delta r << \lambda$

6.4. The sound power output of a point monopole source in driving a closely spaced point pressure to zero

The considerable insight into the mechanisms of active noise control shown by Olson in his now classic paper 'Electronic Sound Absorber' has already been mentioned. In the paper written as far back as 1953, it was postulated that a secondary source could be used in one of two possible modes of operation: that of a 'Sound pressure reducer' and a 'Electronic Sound Absorber'. The purpose of this section is to provide further evidence that in the diffuse sound field, these possible modes of operation are distinct and exclusive inasmuch that a loudspeaker functioning to drive a point pressure to zero must necessarily radiated sound power into a room. It is strongly suspected that the same principle also holds for other non-diffuse sound fields. We now consider the sound power output of a point monopole source driven to cancel the pressure at a closely spaced point in a diffuse sound field.

Consider a point monopole source of sound acting to drive the acoustic pressure at some closely spaced point to zero. As usual, consider the total acoustic pressure $p(\mathbf{r})$ as comprising the superposition of directly radiated sound and scattered sound. However, consider only those points of observation $\mathbf{r}$ and points of cancellation $\mathbf{r}_0$ for which the diffuse field due to the secondary sound field is negligible in comparison to the diffuse field contribution from the primary source. This simplifying assumption has been validated in the previous section where a linearised power series approximation to the expectation $< |\hat{H}_0|^2 >$ was found to be adequate for small $k|\mathbf{r}_s - \mathbf{r}_0|$. Neglecting the secondary source diffuse field pressure, to a good level of accuracy, the total pressure may be represented by

$$p(\mathbf{r}) \approx q_{sj} Z_0 \frac{e^{-jkr}}{kr} + p_{pr}(\mathbf{r}) \qquad (6.34)$$

where $\mathbf{r}_s = 0$. The pressure at some point $\mathbf{r}_0$ (also assumed to be small compared with the wavelength), may therefore be driven to zero $p(\mathbf{r}_0) = 0$ for a secondary source strength q_{so} which is given by

$$q_{so} = j p_{pr}(\mathbf{r}_0) \frac{kr_0}{Z_0} e^{jkr_0} \qquad (6.35)$$

so that

$$p(r) \approx -p_{pr}(r_0)\frac{r_0}{r}e^{-jk(r-r_0)} + p_{pr}(r) \tag{6.36}$$

The sound power output from the secondary source W_s as a consequence of performing the point pressure cancellation may be derived from

$$W_s = \tfrac{1}{2}\Re\{\lim_{r\to 0} p(r)\, q_{so}^*\} \tag{6.37}$$

where the sound power output for this infinitesimal point source distribution, assumed to be at the origin of coordinates $r = 0$, is evaluated from the product of the complex source strength and the acoustic pressure at the source point. On substitution of the terms one obtains

$$W_s = \tfrac{1}{2}\Re\{\lim_{r\to 0}(-p_{pr}(r_0)\frac{r_0}{r}e^{-jk(r-r_0)} + p_{pr}(r))(-jp_{pr}(r_0)\frac{kr_0}{Z_0}e^{-jkr_0})\} \tag{6.38}$$

$$= |p_r(r_0)|^2 \lim_{r\to 0}\frac{k^2r_0^2}{2Z_0}\frac{\sin kr}{kr} - \tfrac{1}{2}\Re\{\lim_{r\to 0} p_{pr}^*(r_0)\, p_{pr}(r)\frac{kr_0}{Z_0}je^{-jkr_0}\} \tag{6.39}$$

Taking the expectation only affects the stochastic part of the equation as indicated below

$$\langle W_s\rangle = \langle |p_r(r_0)|^2\rangle \frac{k^2r_0^2}{2Z_0} - \tfrac{1}{2}\Re\{\lim_{r\to 0}\langle\{p_{pr}^*(r_0)\, p_{pr}(r)\frac{kr_0}{Z_0}j\,e^{-jkr_0}\}\rangle \tag{6.40}$$

Note that

$$\langle\{p_{pr}^*(r_0)\, p_{pr}(r)\frac{kr_0}{Z_0}j\,e^{-jkr_0}\}\rangle = \langle\{p_{pr}^*(r_0)\, p_{pr}(r)\rangle\frac{kr_0}{Z_0}j\,e^{-jkr_0} \tag{6.41}$$

and also the result $\langle p_r^*(r_0)\, p_r(r)\rangle = \langle |p_r(r)|^2\rangle \operatorname{sinc} k|r_0 - r|$ which is real and further that $\langle |p_r(r_0)|^2\rangle = \langle |p_r(r)|^2\rangle$. These results may be combined to produce the following expression for the space averaged secondary source sound power output $\langle W_s\rangle$

$$\langle W_s\rangle = \langle |p_r(r)|^2\rangle \lim_{r\to 0}\{\frac{(kr_0)^2}{2Z_0} - \frac{kr_0}{2Z_0}\operatorname{sinc} k|r_0 - r|\sin kr_0\} \tag{6.42}$$

$$\langle W_s\rangle = \langle |p_r(r)|^2\rangle \left\{\frac{(kr_0)^2 - \sin^2 kr_0}{2Z_0}\right\} \tag{6.43}$$

Equation (6.43) can be conveniently normalised with respect to the primary source free space sound power output W_p, which is also equal to the space averaged diffuse field sound power output given by equation (3.45)

$$W_p = \tfrac{1}{2} |q_p|^2 Z_0 \qquad (3.45)$$

Further noting that $< |p_r(r)|^2 > = |q_p|^2 < |Z_{pr}(r)|^2 >$ gives

$$\frac{< W_s >}{W_p} = \frac{< |Z_{pr}(r)|^2 >}{Z_0^2} \{ (kr_0)^2 - \sin^2 kr_0 \} \qquad (6.44)$$

This ratio of square impedance terms in equation (3.51) is now familiar and is equal to

$$\frac{< |Z_{pr}(r)|^2 >}{Z_0^2} = \frac{2}{3\pi}\left[\frac{f_{sch}}{f}\right]^3 = \frac{2}{\pi M_{0.5}(\omega)} \qquad (6.45)$$

which upon substitution into equation (6.41) yields

$$\frac{< W_s >}{W_p} \approx \frac{2}{3\pi}\left[\frac{f_{sch}}{f}\right]^3 \{ (kr_0)^2 - \sin^2 kr_0 \} \qquad (6.46)$$

Since we are only concerned with the range of separation distances in the region of r_0 for which $r_0 << \lambda$, the following small angle approximation $\sin^2 x \approx x^2 - x^4/3$ may be applied to give

$$\frac{< W_s >}{W_p} \approx \frac{2^5 \pi^3}{9} \left[\frac{f_{sch}}{f}\right]^3 \left[\frac{r_0}{\lambda}\right]^4 \qquad (6.47)$$

for $r_0 << \lambda$

Equation (6.47) shows that on average, a secondary source driven to cancel the pressure at a closely spaced point to zero cannot absorb any energy since $< W_s >$ is always positive. This follows directly from equation (6.41) by virtue of the basic identity $x \geq \sin x$. This finding is roughly consistent with Olson's original hypothesis which says that a 'Sound pressure reducer' and a 'Sound power absorber' are independent secondary source configurations; namely that a sound pressure reducer cannot absorb any sound power and visa - versa. Whilst this is a valid generalisation for all practical purposes, strictly speaking this is not entirely correct. Specifically, in chapter 3 it was shown that the minimum square pressure in the vicinity of a perfectly absorbing point monopole source is approximately 3 dB *below* the primary source level signifying a sound pressure reduction. It is interesting to contrast the modes of operation for the case of a point monopole secondary source. By driving a point pressure very close to the source to zero, the extent of the quiet zone is

negligible. However, even though the point secondary source is infinitesimal, as an absorber of sound it has an effective area of absorption equal to λ^2 / π. This is despite the fact that the source can only match itself to the acoustic pressure at a single point in the field which can be explained in terms of diffraction of the incident wavefield.

The sound power radiated by a secondary source acting as a near field 'pressure reducer' is only small for separation distances which are very close to the secondary source compared with the acoustic wavelength. This follows from the constant of proportionality in equation (6.47), $2^5\pi^3/9$ which can be calculated to be approximately 110. The sound power radiated by a secondary source in this rôle is therefore small in comparison to the original primary source level. For example, a point of cancellation which is say, one tenth of a wavelength from a compact source radiating at a frequency equal to the Schröder frequency, is sufficiently well coupled to ensure that the sound power radiated into the enclosure by the secondary source as a fraction of the primary contribution is about 0.01 corresponding to an increase in the total potential in the enclosure of about 0.01 dB. From figure 6.2, the corresponding 10 dB quiet zone for a point monopole source in this configuration is nearly one tenth of the acoustic wavelength.

As the cancellation point is brought closer to the point secondary source, the size of the quiet zone tends to zero and is identically zero in the limit where $r_0 = 0$. The sound power output from the secondary source is likewise zero. This is consistent with the underlying philosophy behind active control whereby in general, the degree of reduction attained is broadly in line with the level of pressure increase caused elsewhere. Most significantly, the level of secondary source sound power output radiated into the enclosure is extremely sensitive to the separation distance of the cancellation point of which a fourth power dependence has been ascertained. It is interesting to note that if the secondary source sound power output had been assumed to be proportional to $|q_{so}|^2$, then the predicted dependence would have been on the square of the microphone separation distance according to equations (6.29) and (6.32).

This idealised model is believed to provide a reasonable description of the energetic processes that govern a real system which utilises a finite size loudspeaker. As already shown in the previous section, the diameters of typical loudspeaker operating at reasonably high frequencies is a small fraction of the acoustic wavelength so that the compactness assumption $ka < 1$ remains valid even for real loudspeakers. Appreciable departure from this model is therefore not anticipated in practice.

6.5. Experimental determination of the quiet zone in the near field of a secondary loudspeaker in a reverberation chamber

Ultimately, theoretical analyses are only meaningful when considered in the light of corresponding experimental results. The aim of this section therefore is to present some experimental findings relating to the zone of quiet measured around a control microphone in the near field of a secondary loudspeaker at which the pressure is driven to zero in a reverberation chamber.

An attempt to validate the predictions of the near field quiet zones made in section 6.3 was carried out within an non-rectangular 13.3 m^3 reverberant enclosure excited by a harmonically driven loudspeaker as a primary source. By adjusting the quantity of sound absorbing foam in the enclosure, the reverberation time was arranged to be approximately 0.4 s corresponding to a Schröder frequency of about 330 Hz. The pressure at a microphone close to, and on axis of a secondary loudspeaker was set to zero by adjusting the relative gain and phase between the two outputs of a variable phase oscillator through which the primary and secondary loudspeakers were driven. The frequency was chosen to be 572 Hz (such that $\lambda = 0.6$m), well above the Schröder frequency for the room.

For each control configuration investigated, corresponding to a given loudspeaker diameter and microphone - source separation distance, the primary source position was randomly positioned at ten different locations. At each primary source position the acoustic pressure about the point of cancellation was measured over a distance equal to one wavelength with the aid of a small computer controlled trolley which was made to support a measurement microphone. The trolley was made to run along a track down which were drawn regularly spaced alternating black and white strips of tape. The measurement position of the trolley was determined by a light sensitive switch mounted on the front of the trolley which was made to send the appropriate control signal to the microcomputer depending upon the received brightness level reflected from the strips. With the aid of some electronic logic and a microcomputer, the trolley was made to traverse along the axis of the loudspeaker stopping at each of the regularly spaced measurement positions.

On arrival at each of the measurement stations identified by a black strip separated 1 cm apart, the trolley was made to stop and a measurement of the acoustic pressure was made which was then sent to the microcomputer via an A / D converter for subsequent processing. One complete traverse of the trolley corresponding to sixty measurement positions was made before and after control and the ratio evaluated for each primary source position. Complete automation of the measurement process meant that it was possible to make a total of eighteen sets of ten averages corresponding to three loudspeaker diameters

for each of six cancellation positions. The location of the points of cancellation were varied from the position of the loudspeaker cone itself where $\Delta r = 0$, up to a maximum separation distance equal to one fifth of the acoustic wavelength in regular increments of 0.05λ (equal to 3 cm at 572 Hz). A schematic representation of the experimental arrangement is shown below.

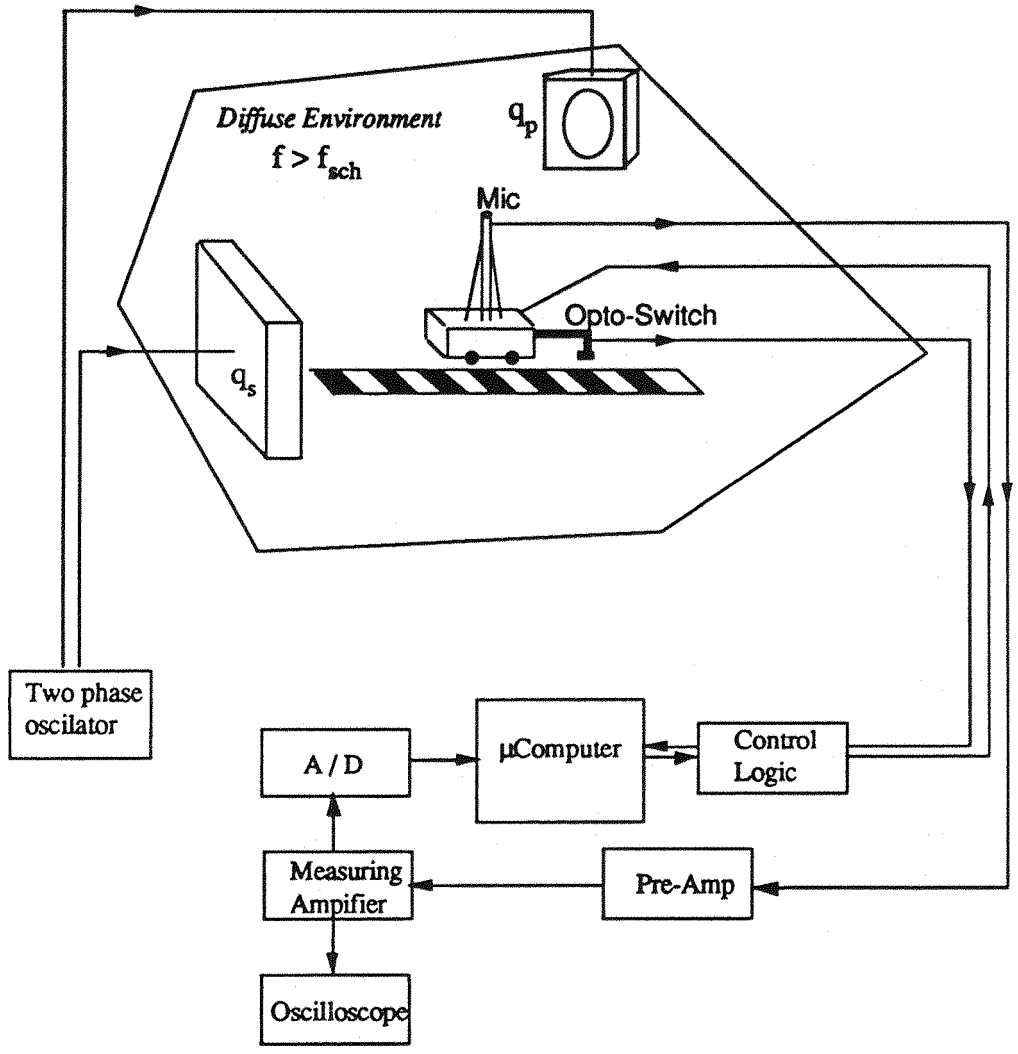

Figure 6.5 A schematic representation of the experimental arrangement employed in measuring the near field zone of quiet in a reverberation chamber driven above the Schröder frequency.

Before commencing near field measurements in the reverberation chamber, the opportunity was taken to measure the zone of quiet formed well away from the influence of directly transmitted sound as described at length in chapter 4. The relative gain and phase of the secondary loudspeaker was adjusted with respect to the primary source so as to form a pressure null at a randomly positioned microphone located many wavelengths from both loudspeakers. The sound pressure level was recorded one and a half wavelengths about the point of cancellation along some randomly chosen axis relative to the room. This was

achieved by a single traverse of the measurement microphone supported by the computer controlled trolley orientated through the point of cancellation. Performing the measurement procedure both before and after control enabled the sound pressure level ratio to be determined. The average from fifty such measurement ratios corresponding to fifty random primary source, secondary source and point of cancellation positions is shown below in figure 6.6 together with the theoretical curve of equation (4.25). For this set of fifty measurement averages, good agreement is established for $< |p_s|^2 > \approx 3.8 < |p_p|^2 >$.

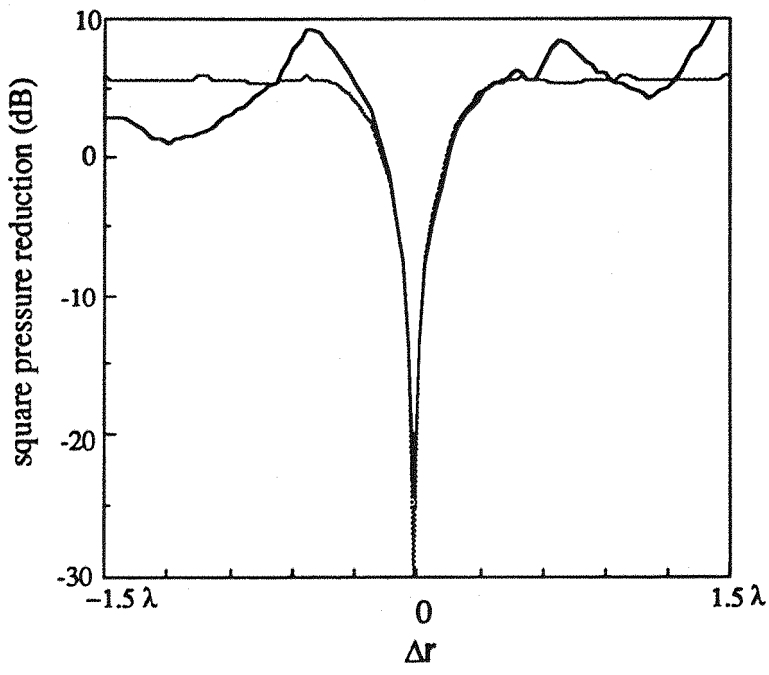

Figure 6.6 The average variation from 50 measurements of the ratio of square pressures before and after the cancellation of the pressure at point remote from sources of sound in a reverberation chamber at a frequency of (solid line). Also shown is the theoretical curve 3.8[1 - $sinc^2 k\Delta r$] (dashed line).

The 10 dB zone of quiet for this set of measurements can be observed to be approximately one tenth of the acoustic wavelength. This experimental finding is roughly consistent with the 10 dB quiet zone obtained from computer simulations described in chapter 4. In both cases however, this localised region of quiet appears to be at the expense of a four fold increase in the average square pressure globally.

The experiment was repeated at the lower frequency of 343 Hz which is close to the Schröder frequency for the enclosure and is therefore on the borderline of 'diffuseness'. The square pressure was monitored along some randomly chosen axis orientated through the point of cancellation which was repeated fifty times for a different set of fifty primary source, secondary source and cancellation point positions. Owing to the increased wavelength at this lower frequency, the variation of the square pressure was only measured one half of a

wavelength either side of the point of cancellation. The averaged result from fifty such measurements is shown below in figure 6.7. For this set of averages, the theoretical curve provides a good fit to the experimental curve for $< |p_s|^2 > \approx 2.0 < |p_p|^2 > [1 - \text{sinc}^2 k\Delta r]$.

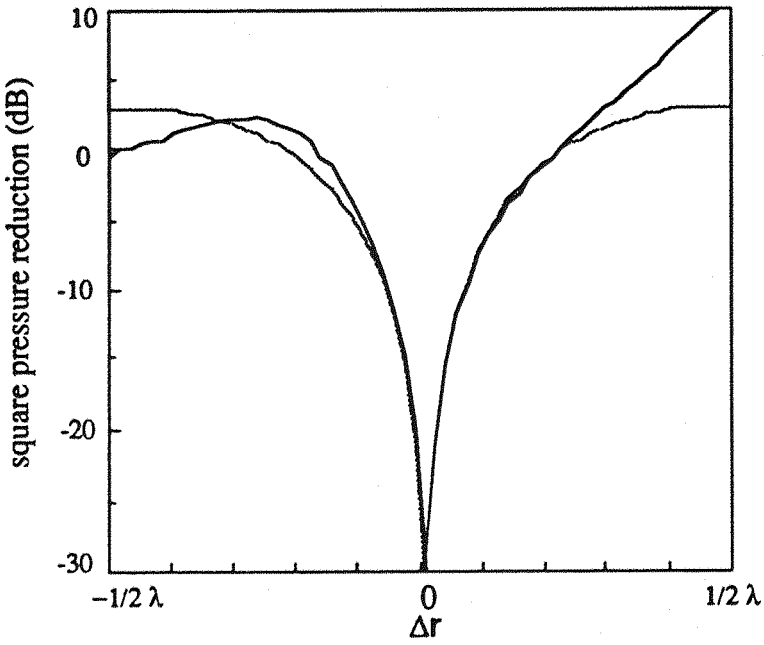

Figure 6.7 The results of fifty measurement averages of the square pressure ratio for another set of random source positions evaluated at the lower frequency of 343 Hz between plus and minus one half of a wavelength.

For this set of fifty measurement averages, fortuitous positioning of the sources and point of cancellations positions has produced a 10 dB quiet zone which is approximately one eighth of the acoustic wavelength corresponding to about 12 cm at 343 Hz.

Having established the size of the typical zone of quiet one can expect from the remote cancellation of the acoustic pressure at a point experimentally, it remains to be shown that the near field contribution from the secondary source can improve on this uncertain arrangement which is known to produce large global pressure increases. As representative examples of typical loudspeakers, three were selected whose radii in descending order of diameter were chosen to be 0.11 m, 0.055 m and a third loudspeaker whose cone was enclosed by a rigid plastic funnel with a 1 cm aperture. The purpose of the latter arrangement was to produce a source of sound whose source distribution was concentrated into a very small volume in an attempt to mimic the acoustic behaviour of a point monopole. Thus, it was hoped that the funnelled source would behave as an oscillating slug of air although leakage of sound radiated from the sides was anticipated.

Each of the three loudspeakers were systematically driven so as to null the pressure at six on-axis microphone positions ranging from the centre of the loudspeaker

cone itself, up to a maximum of one fifth of the acoustic wavelength at regular increments of 0.05 λ. The frequency was again set to 572 Hz and the near field quiet zone was measured along the loudspeaker axis a total of ten times corresponding to ten random primary source positions. For the sake of consistency, the set of ten primary source positions in the enclosure were kept the same for each configuration tested. The variation in the pressure measurements close to the point of cancellation between successive measurements was found to be sufficiently small so as to indicate that an average result comprising of only ten independent measurements would be sufficient to characterise the representative behaviour of each configuration. This contrasts the previous example where the zone of quiet was controlled remotely from the point of cancellation where it was found that one set of fifty averages was found to behave very differently from another.

Some examples of the results obtained from this measurement procedure are shown below. Firstly, consider the cancellation of the pressure at a point on the surface of the source itself such that $|\mathbf{r}_s - \mathbf{r}_0| = 0$. According to figure 6.2, one can expect a quiet zone which is of infinitesimal extent for the limiting case of a point monopole although this should increase to about 0.07λ for the medium size loudspeaker (a = 0.092λ) and still further to about 0.1λ for the largest loudspeaker (a = 0.19λ). The results for this set of loudspeaker-control microphone combinations are shown below. The experimental results are shown as a solid line while the corresponding theoretical results are shown as a dashed line.

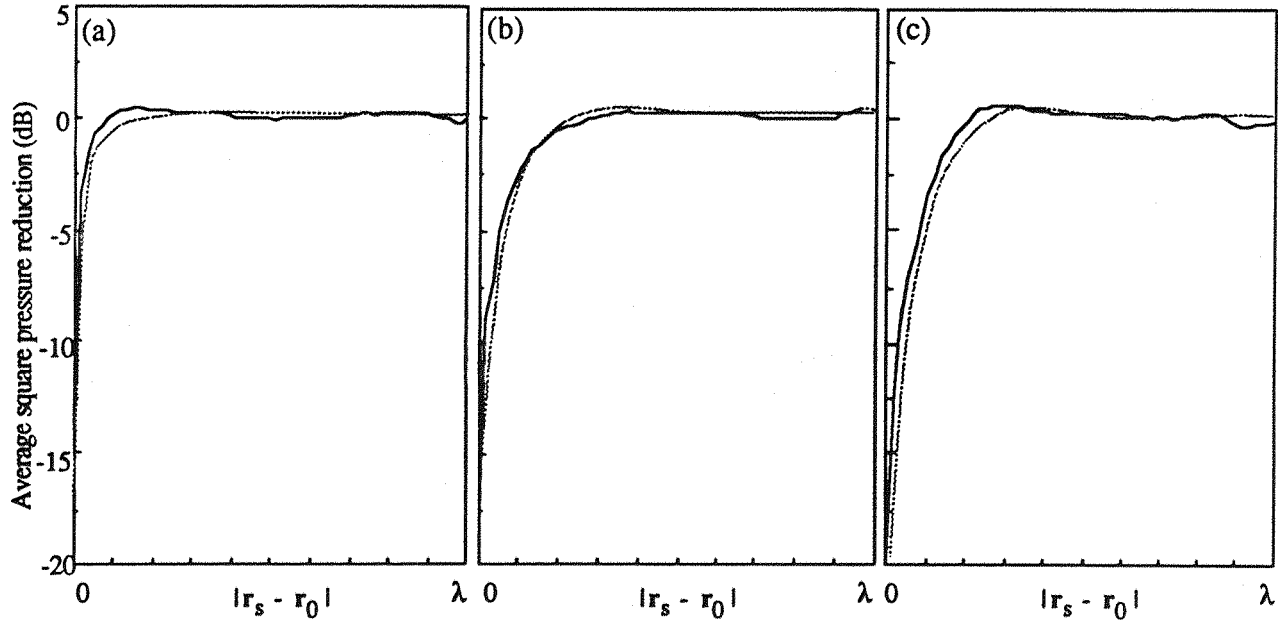

Figure 6.8 The square pressure ratio formed from the average of ten measurements around the point of cancellation on the surface of a secondary loudspeaker of radius (a) 1 cm, (b) 0.055 m, (c) 0.11m

The average result obtained from ten secondary source positions shown above indicate good agreement with the theory. More important is that general trends in the behaviour of the near field quiet zones are correctly predicted. Wholly consistent with the theory, the quiet zone formed near the funnelled source is observed to be negligible. Moreover, the fact that any region of quiet is formed which is of finite extent can be attributed to the finite volume of the source and to a lesser degree, leakage of sound from the sides of the funnel. In the limiting case of a hypothetical point source, the impedance field is known to be strongly divergent very close to the source whose strength decays inversely as distance from its centre.

The most significant feature of this series of results is that the increase in the square pressure well away from the point of cancellation is small in contrast to the case where the point of cancellation is remote from the secondary source, which may be many decibels. This is true even for the largest loudspeaker where the remote square pressure increase is only a fraction of one decibel. In this respect, it would appear that this strategy is capable of producing something for nearly nothing inasmuch as one is able to selectively impose regions of quiet in the diffuse sound field while leaving the global sound field largely unchanged. Unfortunately, it soon becomes clear that as the point of cancellation is moved away from the source, the size of the quiet zone increases only at the expense of an expected increase in the square pressure far from the source as indicated by the increased secondary source sound power output given in equation (6.47).

As a technical aside, it is worth recording the difficulty experienced trying to reduce the pressure at a microphone very close to loudspeakers to levels of more than about 15 dB. This is almost certainly attributable to the large pressure gradient, and therefore the non-uniformity of pressure across the finite diaphragm of the control microphone at these positions thereby introducing inaccuracies owing to the non-zero pressure integrated over the diaphragm. Close to the funnelled source for example, a 15 dB variation in the square pressure was measured over a distance of 3 cm corresponding to an average change of 5 dB over the 1 cm diaphragm of the control microphone. A minimum of -15 dB in the square pressure level at this position therefore corresponds to the average square pressure over a 1 cm region. This is an additional reason why one should choose to cancel the pressure at a point in the sound field where the rate of transfer impedance with distance is small.

Figure 6.9 show three plots of the experimentally determined square pressure profile about a point of cancellation one tenth of a wavelength from the centre of the three secondary loudspeakers averaged over ten measurements.

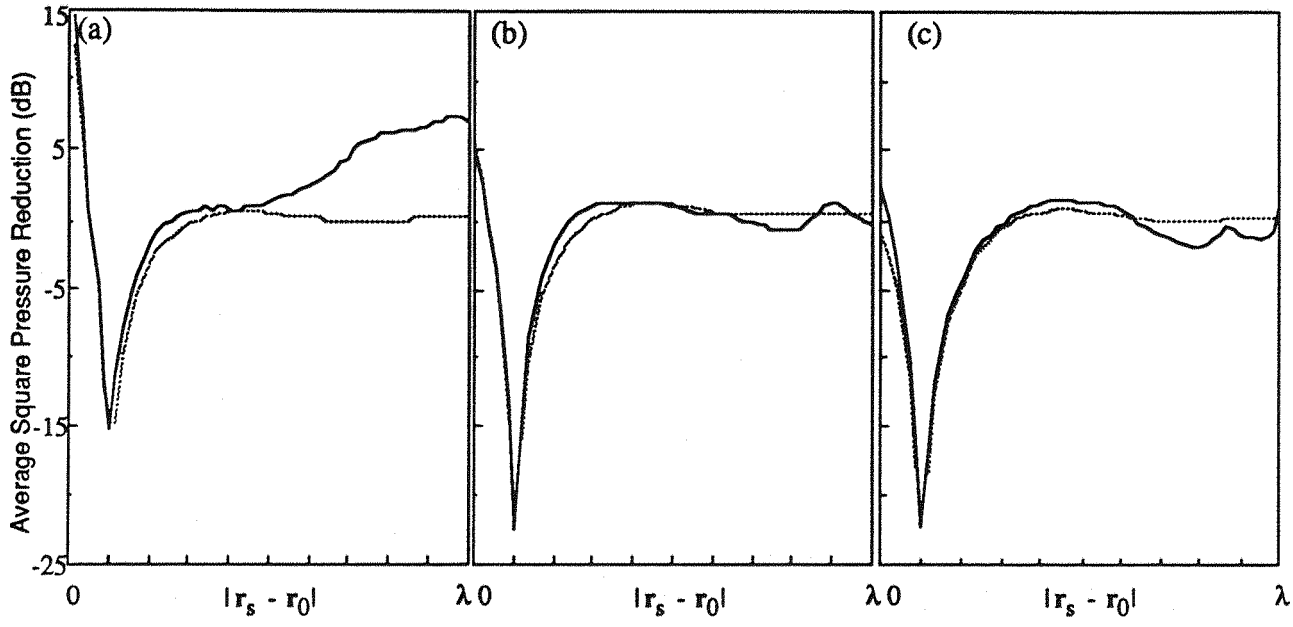

Figure 6.9 The square pressure ratio formed from the average of ten measurements around the point of cancellation at an 'on axis' point one tenth of a wavelength from the cone of a secondary loudspeaker of radius (a) 1 cm, (b) 0.055 m, (c) 0.11 m.

Again the simple theory appears to provide satisfactory description of the series of results obtained experimentally although perhaps less convincingly for the quiet zone formed around the funnelled source. This is almost certainly due to sound radiated from the sides of the funnel whose contribution to the total acoustic pressure is now significant and perhaps non-linear owing to the increased volume velocity required to perform the point cancellation. For the two remaining loudspeakers, good agreement between the theory and experiment is obtained.

The 10 dB quiet zone formed around the middle size loudspeaker shown in figure 6.9b can be seen to be slightly less than one tenth of a wavelength while the zone of quiet formed around the largest size loudspeaker is slightly more as indicated in figure 6.9c. Moving the point of cancellation away from the surface of the source can be seen to have the effect of producing a substantial increase in the average square pressure between the source and the point of cancellation. This is due to the near field contribution from the secondary loudspeaker which progressively diminishes as the size of loudspeaker increases. In practice, one should take steps to ensure that the listener's ear cannot enter this region where the increase in the square pressure can be typically as high as 15 dB. Nevertheless, the average square pressure increase well away from the point of cancellation

still remains small for these finite size loudspeakers. Moreover, there are small regions far from the point of cancellation which have also undergone a reduction in the pressure although this is probably more fortuitous than by design.

As further vindication of the underlying philosophy behind this control scheme, the results obtained from the cancellation of the pressure at a point exactly one quarter of a wavelength from the centre of the secondary loudspeaker is shown in the last series of figures below

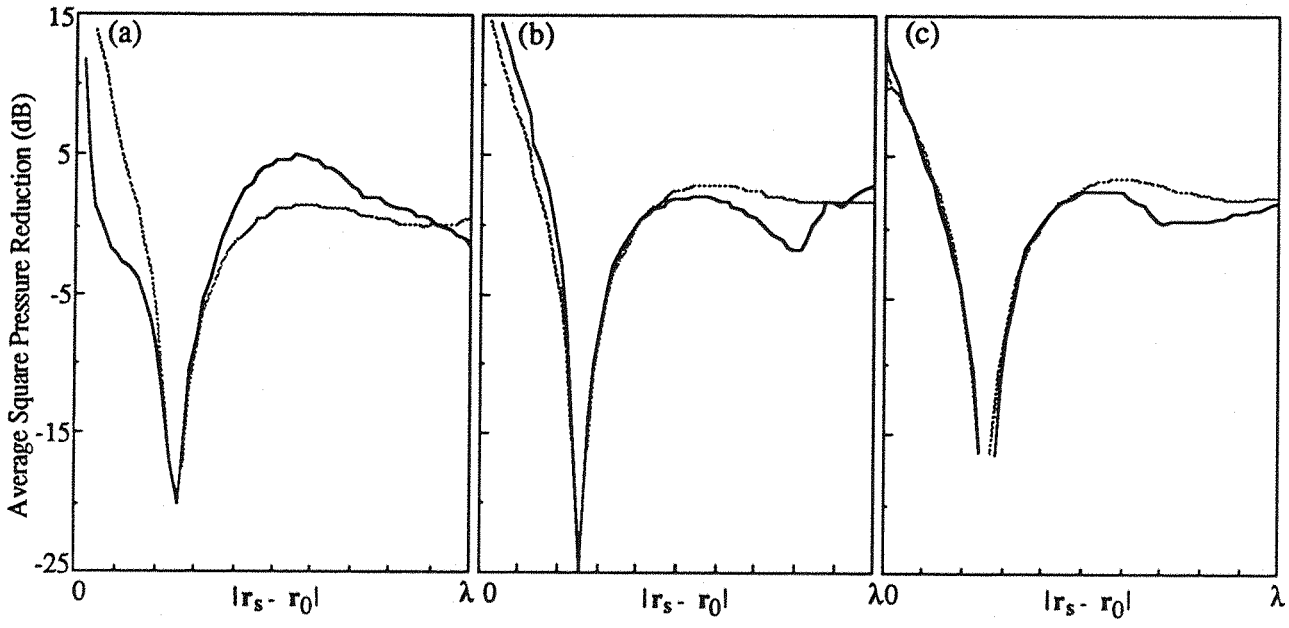

Figure 6.10 The square pressure ratio formed from the average of ten measurements around the point of cancellation at an 'on axis' point one quarter of a wavelength from the cone of a secondary loudspeaker of radius (a) 1 cm, (b) 0.055 m, (c) 0.11 m.

The predicted result obtained between the theory and experiment for this combination of funnelled source and cancellation position now fail to agree to any reasonable degree. However, good agreement is obtained for the remaining two loudspeakers. Consistent with the theory, the size of the quiet zone continues to increase with increasing loudspeaker size and cancellation position. For the largest loudspeaker seeking to cancel the pressure at the furthest distance which is a quarter of a wavelength for this set of measurements, is able to produce a quiet zone nearly equal to one eighth of a wavelength. The effect on the square pressure well away from the control point still remains less than 2 dB.

6.6. Discussion and conclusion

Undoubtedly, the size and shape of the diffuse field quiet zone benefits appreciably from the large, highly correlated, deterministic secondary source near field pressure contribution before being scattered by the walls of the enclosure. However what is most significant, is that the form of the quiet zone benefits twice over from this large near field contribution to the pressure at the point of cancellation. First and most unexpectedly, the size of the quiet zone depends proportionately on the magnitude of the transfer impedance at this point and secondly, the near field impedance contribution as a ratio of the reverberant contribution governs the energy radiated by the secondary source into the enclosure.

Simple expressions have been developed which seek to describe the size and shape of the zone of quiet formed around a point of cancellation in the near field of a secondary loudspeaker. Unfortunately, no unified analysis has been possible which encompasses both the two extreme cases which have had to be considered separately in this thesis. At one extreme where the point of cancellation is close to the source, the direct field completely dominates the reflected sound field so that a free field analysis for the quiet zone becomes appropriate. At the other extreme where the point of cancellation is far from the sources, the direct fields are negligible compared with the reverberant contribution so that one can talk entirely of random quantities in order to derive expressions for the quiet zones and related statistics. However, in the intermediate region where the total pressure contributions is roughly shared between the free field and reverberant contribution, the form of the quiet zone is indeterminate. Although most likely at these positions, the form of the quiet zone will comprise some unspecified combination of the two.

One of the features of this control strategy which makes it most appealing as a viable technique for high frequency, reverberant sound fields is that it is tightly coupled and therefore the level and spatial extent of the pressure reductions does not depart significantly from one position in the sound field to another. From a practical viewpoint, this offers the considerable advantage that each source can be adjusted independently to cancel the pressure at their respective microphone. One can envisage installing an array of identical systems operating at high frequencies in order to produce a localised quiet zone about the ears of the seated passengers while simultaneously radiating at low frequencies in order to suppress individual modes of the enclosure. One practical complication might be the changing acoustic space due to the moving head of the passenger. However, this could in principle be removed by an adaptive controller which responds rapidly to the changing acoustic space. One may of course argue that the presence of a near spherical rigid body which is large compared with the wavelength will destroy the diffuseness of the sound field

thereby violating the underlying diffuse field assumptions. This problem should provide an interesting area of research which is probably better tackled experimentally.

Another interesting area of research which remains to be investigated is that of high frequency broadband control at a point in an enclosed space. This problem has been neglected here mainly because of its complexity and also not wanting to obscure the underlying physics. The control configuration advocated here is ideally suited to broadband control which is probably the motivation behind Olson's experimental arrangement. Causality considerations are largely overcome since the pressure at the point of cancellation will respond almost instantaneously to the action of the secondary source while the primary pressure takes the entire propagation time from an infinite number of image sources to reach the point of cancellation.

The results reported in this chapter also goes some way to clarifying the relationship between the two possible modes of operation of a secondary source vaguely alluded to in Olson's paper. The work of chapter 3 has already shown that a source of sound can absorb energy in a diffuse sound field which has been shown to effect a small area of pressure reduction in the vicinity of the source. However, in this chapter the converse problem has been contemplated where the sound power output of a point secondary source which acts to produce a point of null pressure close to the source has been derived. A simple analysis has established the sensitivity of the sound power output from compact sources to the separation distance of the point of cancellation of which a fourth power dependence has been ascertained.

In summary therefore, the cancellation of the pressure in the near field of a secondary loudspeaker acts to produce zones of quiet which are broadly in line with those attained when the point of cancellation is remote from the sources. However, the advantage of this this control geometry is that it adds a high degree of determinism into what would otherwise be an ill-conditioned and uncertain arrangement. Moreover, the levels of square pressure produced far from the point of cancellation are reduced from typically 6 dB in the case of the former arrangement to negligible fractions of 1 dB for some combinations of loudspeaker diameter and microphone separation distances.

APPENDIX 6

Appendix 6.1. A formal calculation of the space averaged squared transfer function $< |H_o|^2 >$

Consider the transfer function H_o defined in equation (6.3)

$$H_o = - \frac{Z_r(r_p|r_0)}{Z_d(r_s|r_0) + Z_r(r_s|r_0)} \qquad \text{(A6.1)}$$

where $Z_r(r_p|r_0)$ and $Z_r(r_p|r_0)$ are the diffuse field transfer impedances whose real and imaginary parts are independent and normally distributed random variables. In terms or more concise notation, $|H_o|^2$ can be written as

$$|H_o|^2 = \frac{Z}{(1 + x)^2+y^2} \qquad \text{(A6.2)}$$

where $Z = |Z_r(r_p|r_0)|^2 / |Z_d(r_s|r_0)|^2$, $x = \Re\{Z_r(r_s|r_0) / |Z_d(r_s|r_0)\}|$ and $y = \Im\{Z_r(r_s|r_0) / |Z_d(r_s|r_0)|$. For well separated primary and secondary sources, the expectation $< |H_o|^2 >$ is given by the product of the independent factors

$$< |H_o|^2 > = < Z > < \frac{1}{(1 + x)^2+y^2} > \qquad \text{(A6.3)}$$

It has been shown previously that Z is a Chi squared random variable with two degrees of freedom whose mean value may be determined from equation (6.28) to give

$$< Z > = \frac{< |Z_r(r_p|r_0)|^2 >}{|Z_d(r_s|r_0)|^2} = 2< \delta^2 > \qquad \text{(A6.4)}$$

The mean of the second factor may be determined by recalling that (x+1) and y in equation (A6.3) are normally distributed random variables whose variance are equal to $< \delta^2 >$ and whose mean values are equal to unity and zero respectively. Putting $x_1 = x+1$, one can write

$$f_{X1}(x1) = \frac{1}{\sqrt{2\pi<\delta^2>}} e^{-(x_1 -1)^2/2< \delta^2 >} : \qquad \forall\, x_1 \qquad \text{(A6.5)}$$

$$f_Y(y) = \frac{1}{\sqrt{2\pi<\delta^2>}} e^{-y^2/2< \delta^2 >} : \qquad \forall\, y \qquad \text{(A6.6)}$$

In terms of the current notation, we require the expectation value $< g(x_1,y) >$ where $g(x_1,y)$ is the function

$$g(x_1,y) = \frac{1}{x_1^2 + y^2} \tag{A6.7}$$

A well known result is that the expectation of some multi-variable function $g(x_1,y)$ is determined from[63]

$$< g(x_1,y) > = \int_{-\infty}^{\infty}\int_{-\infty}^{\infty} g(x_1,y)\, f_{x1,y}(x_1,y)\, dx_1 dy \tag{A6.8}$$

where $f_{x1,y}(x_1,y)$ is the joint probability density function between the random variables x1 and y which is simply the product of their respective density functions by virtue of their mutual independence which can be assumed for well separated sources. One can therefore write

$$< g(x_1,y > = \frac{1}{2\pi<\delta^2>} \int_{-\infty}^{\infty}\int_{-\infty}^{\infty} \frac{\exp[-(x_1^2 + y^2 - 2x_1 + 1)/2<\delta^2>]}{x_1^2 + y^2}\, dx_1 dy \tag{A6.9}$$

This double integral may be simplified by the change of variable $x_1 = r\cos\theta$, $y = r\sin\theta$ which may be substituted into equation (A6.9) and combined with equations (A6.3) and (A6.4) to produce

$$< |H_o(<\delta^2>)|^2 > = \frac{1}{\pi} \int_0^{\infty}\int_0^{2\pi} \frac{e^{-}(r^2 - 2r\cos\theta + 1)/2<\delta^2>}{r}\, dr d\theta \tag{A6.10}$$

Appendix 6.2. A power series approximation to the space averaged squared transfer function $< |H_o|^2 >$

Equation (6.3) may be re-written as

$$H_o = - \frac{Z_r(r_p|r_0)}{Z_d(r_s|r_0)} \left(1 + \frac{Z_r(r_s|r_0)}{Z_d(r_s|r_0)}\right)^{-1} \tag{A6.11}$$

from which the expectation of the square of the transfer function may be derived according to

$$< |H_o|^2 > = < \left|\frac{Z_r(r_p|r_0)}{Z_d(r_s|r_0)}\right|^2 > < \left[\left(1 + \frac{\Re\{Z_r(r_s|r_0)\}}{|Z_d(r_s|r_0)|}\right)^2 + \left(\frac{\Im\{Z_r(r_s|r_0)\}}{|Z_d(r_s|r_0)|}\right)^2 \right]^{-1} > \tag{A6.12}$$

The expectation of the first factor in this equation is just $2<\delta^2>$ according to equation (3.21). The considerably more complicated second factor may be more concisely represented by the function $g(x,y) = ((1+x)^2 + y^2)^{-1}$. The variables x and y are respectively the normalised real part and normalised imaginary part of the diffuse field impedance. Both x and y are therefore mutually uncorrelated, zero mean random variables whose relative variances are equal according to $<x^2> = <y^2> = <\delta^2>$.

The expectation $< g(x,y) >$ has previously been shown to be infinite. An identical procedure to that proposed in chapter 3 for overcoming the singularities in the expression relating to the problem of diffuse field sound power minimisation is now employed. One can immediately see that g(x,y) goes to infinity when (x+1) and y are *simultaneously* zero. An estimate for the expectation $< g(x,y) >$ is now sought based on behaviour of the function $((1+x)^2 + y^2)^{-1}$ for which $|x+1| < 1$ and $|y| < 1$. It is believed that this condition is sufficiently un-restrictive to enable one to derive a mean value which is representative of the average behaviour of the vast majority of possible out-comes. This will be particularly true when $< \delta^2 >$ is very much less than unity such as is the case for compact sources seeking to cancel the pressure at a very closely spaced point.

A good approximation to the first order behaviour of f(x,y) for those commonly occurring cases where $|x+1| < 1$ and $|y| < 1$ may be obtained by expanding the function as a two dimensional power series centred about the origin (0,0). A power series representation of the function about x = 0 and y = 0 (Maclaurin series) in x and y is given by

$$g(x,y) = g(0,0) + x\frac{\partial g}{\partial x}\Big|_{(0,0)} + y\frac{\partial g}{\partial y}\Big|_{(0,0)}$$

$$+ \frac{1}{2!}\left\{ x^2\frac{\partial^2 g}{\partial x^2}\Big|_{(0,0)} + 2xy\frac{\partial^2 g}{\partial x \partial y}\Big|_{(0,0)} + y^2\frac{\partial^2 g}{\partial y^2}\Big|_{(0,0)} \right\}$$

$$+ \cdots \frac{1}{n!}\left\{ x^n\frac{\partial^n g}{\partial x^n}\Big|_{(0,0)} + \binom{n}{1} x^{n-1}y\frac{\partial^n g}{\partial x^{n-1}\partial y}\Big|_{(0,0)} + \cdots \binom{n}{n} y^n\frac{\partial^n g}{\partial y^n}\Big|_{(0,0)} \right\} \qquad \text{(A6.13)}$$

Strictly speaking the order of the power series n should be taken to infinity to ensure an exact representation of the desired function g(x,y). However, in practice only a few terms are required in order to provide a good approximation to the function providing x and y are simultaneously small. For the function under consideration here, a program capable of symbolic differentiation was used to generate all the necessary partial derivatives in x and y

in order to evaluated the power series expansion of the function to sixth order. The derivatives were evaluated at the origin (0,0) and substituted into equation (6.31) to produce

$$g(x,y) \approx 1 - 2x + (3x^2 - y^2) + (-4x^3 + 4xy^2) + (5x^4 - 10x^2y^2 + y^4) +$$

$$(-6x^5 + 20x^3y^2 - 6xy^4) + (7x^6 - 35x^4y^2 + 21x^2y^4 - y^6) \qquad \text{(A6.14)}$$

Recall that x and y are independent, Gaussian random variables where all odd moments are equal to zero. Further note that the moments of x and y are equal, so that taking the expectation $< >$, one can shown that to sixth order

$$< g(x,y) > \approx 1 + 2< x^2 > + 6< x^4 > - 10< x^2 >^2 + 6< x^6 > - 14< x^4 >< x^2 > \qquad \text{(A6.15)}$$

where $< x^2 >$, $< x^4 >$ and $< x^6 >$ symbolise the second moment (variance), the fourth moment (Kurtosis) and the sixth moment of the Gaussian distribution. Since the Gaussian distribution is completely specified by its mean μ and standard deviation $<\delta^2>^{1/2}$, all higher moments may be written in terms of these principal moments. According to standard texts[63], if x is a Gaussian random variable, then the r^{th} moment namely μ_r may be derived from $<\delta^2>$ via

$$\mu_r = \frac{r!\ <\delta^2>^{r/2}}{(r/2)!\ 2^{r/2}} \qquad \text{(A6.16)}$$

where r is even. Note that $\mu_r = 0$ for odd r. One can therefore write

$$< x^2 > = <\delta^2>,\ < x^4 > = 3<\delta^2>^2 \text{ and } < x^6 > = 15<\delta^2>^3 \qquad \text{(A6.17)}$$

Providing $<\delta^2>$ is small compared with unity, the function g(x,y) may be closely approximated by

$$< g(x,y) > = 1 + 2<\delta^2> + 8<\delta^2>^2 + 48<\delta^2>^3 \qquad \text{(A6.18)}$$

Returning to equation (A6.12) for $< |H_o|^2 >$ and noting that $< |Z_r(r_p|r_0)|^2 > / |Z_d(r_s|r_0)|^2 = 2<\delta^2>$ enables the expectation of the square of the transfer function to be written completely in terms of a power series expansion in the relative variance $<\delta^2>$ of the transfer impedance written below

$$< |\hat{H}_o|^2 > \approx 2 <\delta^2> + 4 <\delta^2>^2 + 16 <\delta^2>^3 + 96 <\delta^2>^4 \qquad \text{(A6.19)}$$

for $|x+1|,\ |y| < 1$

CHAPTER 7

CONCLUSIONS AND SUGGESTIONS FOR FURTHER WORK

7.0. General remarks

It is hoped that the work described in the preceding pages has gone some way to revealing the potential and the limitations of active control technology to produce reductions of the acoustic pressure in high frequency enclosed sound fields. As an objective assessment of the contribution to this field, it is first necessary to put this work into a proper perspective amongst the more conventional main stream type of research which deals almost exclusively with low modal density sound fields. It is unlikely that one would choose to install an active control system with the sole purpose of controlling high frequency sound. With this in mind, the investigation has been undertaken with the understanding that in reality, high frequency active control would probably only be carried out as an added benefit over and above the main objective, namely the suppression of low frequency sound, where active control is already known to be considerably more effective. One can conceive of a practical controller which contains perhaps a separate dedicated micro-processor which is independently programmed with the task of performing high frequency active control. Constraints imposed by cost, size and weight would necessitate that the high frequency controller utilise the same array of loudspeakers and error microphones at all frequencies whose positions in the enclosure would be heavily biased by those source and microphone locations which gave maximum observability and controllability at low frequencies. Those factors which govern the level of reductions at high frequencies would therefore come only as a secondary consideration.

The ineffectiveness of the active control of high frequency enclosed sound fields derives from its spatial complexity. Paradoxically however, it is precisely this spatial disorder which enables one to accurately describe the statistical behaviour of a large number of similar, independent diffuse field measurements. One can no longer make definite statements relating to the outcome of a single experiment, but only generalisations regarding the average behaviour of a large number of similar experiments. It turns out that above some critical frequency, which is particular to each enclosure, the statistical properties of the high frequency enclosed sound field are well defined. Perhaps one of the most important contributions of this thesis is the bringing

together of simple optimisation techniques and elementary statistical methods for determining the absolute performance limits, in an average sense, of active control in diffuse fields. To the author's knowledge, this is the first time active noise control has been treated from a such a probabilistic view point although it is difficult to envisage how else one could tackle this problem theoretically.

7.1. Conclusions

It is recognised early on in this thesis that sound fields in which there is a 'random' relationship between acoustic pressure measurements made at different field points will lessen the performance of active control. In practice, randomness appears as either unsteady fluctuations in the temporal characteristics of the signal such as jet noise, or spatial randomness which occurs by virtue of the seemingly random interference from a large number of acoustic modes in the enclosure even for harmonic sources. The most complex active noise control problem from the point of view of analysis is the situation whereby a broadband source of sound is radiating into a large three dimensional enclosure. Measurements of the acoustic pressure would therefore be random functions of both time and space. For ease of analysis, the temporal and spatial aspects of this more general problem are treated independently in this thesis.

Chapter 2 focuses on the temporal aspects of active noise control. Well established time domain techniques are applied with the aim of determining the causally constrained minimum sound power output from a pair of sources situated within an infinite duct. At the expense of over simplification, the difficulties arising from complicated spatial pressure variations in the room are essentially removed by considering only sound propagation in one dimension in the absence of reflections. The difference between the levels of reduction obtained for sound fields excited at a single frequency, and the reductions obtained for random broadband noise, is determined by the degree of predictability associated with each signal. Just as the name suggests, predictability is that property of a signal which enables it to be pre-determined on the basis of a knowledge of all its past values. It would appear intuitively correct that the predictability of the signal, as defined in some systematic fashion, somehow bears a simple relationship to the bandwidth of the signal. In chapter 2 a reciprocal relationship between the two quantities is proposed.

The time domain theory developed in the first part of chapter 2 for free space radiation is extended to include reflections. The most elementary kind of reverberation is considered in the form of a single reflecting surface. It is recognised that the level of

reduction physically achievable in the acoustic pressure for some arbitrary broadband signal is bounded somewhere between the level of reduction obtainable for pure tone signals and the corresponding level obtainable for Gaussian white noise signals. The steady state level of reduction for each limiting class of signal is therefore evaluated as a function of the reflection coefficient. It is shown that the level of reduction is more dependent on the level of reverberation in the space (as governed by the reflection coefficient) than the bandwidth of the signal for *this* geometry. The amount of sound power reduction obtainable for white noise signals, even in this reverberant space, is found to be never less than about 50 % of the corresponding average value obtained for pure tones.

Analysis has shown that for broadband primary signals, the emphasis of the control mechanism is towards sound power absorption whereas for narrow band signals, the mechanism of energy reduction is roughly shared between sound power absorption and primary source loading. In the simple acoustic space investigated, the difference in sound power reduction levels for the two signals types at any given value of the reflection coefficient, is found to be never less than 3 dB. The active control of broadband noise is therefore possible in principle for simple reverberant spaces although no mention is given to practical considerations such as, for example, the filter length or how might realise such an optimal filter in practice. A discussion concerned with practical details is thought to be outside the scope of interest of this thesis and is extensively dealt with in the literature, particularly for simple duct borne noise.

The work described in chapter 2 is very much a digression from the main emphasis of this thesis which has been predominantly concerned with the active control of diffuse sound fields. A discussion of the various interpretations of diffuseness is given at the start of chapter 3 for which even today there is not complete general agreement. This thesis has chosen to adopt the probabilistic definition of diffuseness which says that the pressure at any point in space has an equal *probability* of energy arriving from all elemental solid angle. This contrasts the more restrictive, idealised definitions of diffuseness, some of which envisage the sound field inside of a sphere generated by an infinite number of incoherent point sources on the sphere surface. The pressure at the centre of the hypothetical sphere *is* regarded as being perfectly diffuse, and points slightly away from the centre are regarded as being substantially diffuse. One can immediately see that the two points of view are fundamentally different inasmuch that the first talks in terms of likelihoods while the second talks in terms of a definite state of diffuseness at some pre-determined point in space.

The idealised concept of a diffuse sound field is extremely important in that it identifies the asymptotic form of sound field to which all enclosed sound fields converge as the frequency is increased. In considering active noise control in diffuse sound fields, one is identifying the upper bound frequency limit on the active control of sound in enclosed spaces which in many respects, signifies the worst possible case. Although in essence a physical, non-realisable idealisation, the diffuse sound field is characteristic of the acoustic behaviour of a large number of real sound fields which quite often, are irregularly shaped, posses inhomogeneous absorption properties and in general, contain a large number of randomly shaped scattering objects. For example, inside some vehicles and aeroplanes where active control has already been applied, the Schröder frequency has been experimentally estimated to be between 100 Hz and 200 Hz. Even at frequencies well below the Schröder frequency, this type of low modal density sound field is more appropriately described by statistical methods to which the diffuse sound field is a useful idealisation.

In all of the work presented in this thesis concerned with active control in diffuse sound fields, a feedfoward controller has been assumed. This type of controller is presumed to have access to some control signal which is perfectly coherent with the primary source whose radiation can therefore be predicted perfectly. The levels of reduction predicted by these results in no way refer to inadequacies of the controller, but serve to identify the absolute performance limits on the active control of diffuse fields which are dictated solely by the unique spatial characteristics of this type of sound field.

Chapter 3 has considered the possibilities for the global attenuation of diffuse field pressures using compact sources. By virtue of the vast number of contributing modes which conspire to produce the state of diffuseness, reductions in the pressure can only be accomplished globally if ones's secondary source is able to couple into all the modes simultaneously. This is precisely what happens when two point monopole sources are closely situated in an enclosed space. The scenario outlined here therefore provides the basis of a convenient model problem which readily lends itself to simple analysis in terms of optimisation techniques and elementary statistical theory. Using the diffuse field statistical theory set out by Schröder, the minimum sound power output of two closely spaced sources has been deduced together with the secondary source strength requirements. Converse to the problem in chapter 2, the analysis is restricted to single frequencies thereby removing the obvious complications arising from causality considerations.

This exercise has served to locate the first and second order moments of the secondary source strength and the total minimum sound power output from the source pair. An attempt to determine the statistical behaviour of the diffuse field variables in the conventional manner, via a specification of the mean and variance, was shown to be impossible. These moments were found not to exist inasmuch as the integrals from which they are derived fail to converge. In physical terms, this complication arises from the very small probability of obtaining very large values, whose product will tend to dominate, say, the much larger probability of obtaining commonly occurring values. This finding raises the important fundamental question about what information statistical moments are meant to convey. In a large number of cases (although not all), a formal assessment of the expectation value is an inappropriate estimator of statistical behaviour which says more about the ill-conditioning of the actual integral from which the expectation value is derived than the first order behaviour of the random variable itself.

In the light of this fundamental difficulty, a pragmatic solution was sought. It was decided to take the expectation over an ensemble of values comprising only those results obtained at source positions for which the sound power flowing from the secondary source into the medium directly, is less than the power radiated into the medium via wall reflections. While it is acknowledged that this criterion is essentially ad-hoc, the new ensemble is believed to be more representative of the occurrences observed in reality, furthermore, helps to simplify the analysis at the same time. All of the various moments associated with the random distribution are now gauranteed to converge to meaningful and consistent expressions.

The same approach has been used to deduce the maximum sound power absorption for an elementary point monopole source in a diffuse sound field. The efficiency with which sources of sound are able to extract energy from a given sound field is fully characterised by their cross sectional areas of absorption. For an optimally absorbing point monopole source in a diffuse sound field, this area takes the form of the surface of a sphere which has been shown to vary according to the square of the acoustic wavelength. This additional area of active absorption evaluated at typical values of the Schröder frequency compared with the existing area of passive absorption is clearly small. For example, inside a medium size room of about 100 m^3 evenly lined with typical sound absorbent tiles excited at the Schröder frequency, the optimal absorption of sound has been shown to provide only about a 10 % level of reduction in the total potential energy. This control strategy is therefore not advocated at high frequencies. Extrapolating this result down to low frequencies, although it is not strictly

valid, indicates that the optimal absorption of sound is very effective. This is the frequency region for which the modal overlap factor is less than unity and so the modal responses of the enclosure are non-overlapping. The sound field now comprises distinct, isolated resonances for which active control has been shown to be most effective. However, the relative variance associated with the maximum sound power absorption at low frequencies has been show to be large at low frequencies so that the mean value is therefore not particularly meaningful.

Global control in diffuse sound fields is generally acknowledged to be an unrealistic objective for most commonly occuring noise sources. Chapter 4 has therefore considered the possibilities for localised active control. The simplest control strategy possible has been investigated which involves using a remotely positioned secondary source in order to drive the acoustic pressure at a point to zero. Statistical approaches have been adopted in order to deduce expressions for the space averaged quiet zone, the statistical behaviour of the secondary source strength and the resulting increase in the potential energy. Unlike low modal density sound fields, the space averaged zone of quiet created about a point of null pressure in the diffuse field limit has been shown to converge to a well defined expression as a function of the spatial correlation function.

The study undertaken in chapter 4, which uses elementary statistical techniques, has been most useful in highlighting the ill-conditioning of a controller seeking to apply active control to diffuse fields. This arises from the spatial random behaviour intrinsic to this type of sound field. More specifically, the difficulty lies in the form of the probability density function for describing the distribution of diffuse field complex transfer impedances evaluated between two well spaced points. Outside the influence of directly transmitted sound, all of the principal indicators of central location such as the mean, mode and medium are exactly equal to zero. Thus, on average, a remotely positioned secondary source is poorly coupled to the primary pressure at the desired point of cancellation. This property is explicitly revealed in results obtained from computer simulations of the total diffuse field potential energy. A single source allowed to radiated freely in a diffuse field environment has been found to sustain a level of potential energy in the room as it moves from point to point in the enclosure which is normally distributed and subject to a normalised variance which is considerable less than unity (varying approximately as the inverse of the modal overlap factor). On the introduction of a secondary source into the enclosure for the purpose of driving the pressure at some random remotely positioned point to zero, the normalised mean of the combined potential energies from 15,000 computer simulations has been found to be

approximately equal to ten indicating a substantial average increase. Formally however, the predicted space averaged potential increase is equal to infinity. While this study has been enlightening from the point of view of gaining insight into diffuse field pressure cancellation, this is not an approach one would be advised to implement in practice. Better behaved control schemes are investigated in chapter 5.

The work of Olson *et-al* has featured largely in this thesis. Despite being widely acknowledged as an important work in active noise control, it is perhaps surprising to realise that in nearly forty years, nobody has sought to provide a more rigourous theoretical basis by which to understand these ideas even though a comparatively large amount of experimentation has been performed. The investigation reported in chapter 6 represents just such an initial attempt. The considerable advantage in controlling the sound field close to the secondary source is that the total secondary acoustic pressure is dominated by the near field of the source superimposed on which, the diffuse field contribution can be neglected. The diffuse, reverberant field therefore only appears as a small random fluctuation on the deterministic near field of the source which tends to average to zero as the average over all source positions is evaluated. In this closely spaced configuration, one has managed to circumvent the fundamental restrictions imposed by the random, diffuse field as discussed at length in chapter 4 so that the analysis only involves free field terms. Moreover, because the acoustic coupling between the secondary source to the desired point of cancellation is now much greater compared to the acoustic coupling from the primary source, the ratio of secondary source strength to primary source strength is therefore small compared to unity. Using this technique, one is now able to engineer reductions in the sound pressure level in a diffuse field environment which are of the same spatial extent as that obtained from a remotely positioned control secondary source, if not greater, but now the global increases in the sound pressure level are now restricted, in most cases, to a fraction of one dB.

The two results which more than any exemplify the extent to which active control may be applied to diffuse fields are the values for the zone of quiet around a point of null pressure, defined at the 10 dB level of reduction, and the cross sectional area of absorption for a perfectly absorbing point monopole source. The former result characterises the scope for cancelling diffuse field pressures. Both theory and experiment have indicated that for sensibly behaved values of the secondary source strength, say, of the order of the primary source strength, the size of the diffuse field quiet zone is limited to approximately one tenth of a wavelength. This value reflects both the correlation structure of the diffuse field and to perhaps

to a greater extent, the statistical inter-dependence between the primary and secondary diffuse pressure fields as governed by the inter-relations between their source strengths. It was found to be not uncommon to measure, both from results obtained from computer simulations and experimentation, increases in the sound pressure level well away from the control point is typically ~~equal to~~ 10 dB.

Alternatively, if one chooses to adopt a global strategy so as, for example, to maximise the sound power absorption of a secondary source, the efficiency with which this can be achieved is fully characterised by the cross sectional area of absorption which is approximately given by square of the wavelength divided by pi. This value must of course be compared with the existing effective area of passive absorption for a given enclosure, in order to asses the level of reductions in the steady state level of potential energy which ultimately may be achieved.

7.3 Suggestions for further work

Active control is widely perceived as a possible solution to low frequency noise control problems. However, the precise area of applicability still remains to be identified as manifest by the diversity of approaches and situations currently been studied. Given the infancy of the technology and understanding of active noise control at the present time, it is unlikely that very much research will be undertaken in the near future specialising in frequencies greater than about 300 Hz. This is despite the fact that there is clearly a large amount of work remaining in this area of research as indicated in the thesis.

It is envisaged that the development of high frequency active noise control in the long term will evolve on two fronts. The first concerns technological advancements in the form of real time dedicated digital signal processors. The fundamental task of these devices will be to compute the optimal secondary source strengths required to minimise the signals received by an array of strategically placed microphones according to some optimal criterion. Presently, the upper working frequency limit, set by the maximum sampling rate, and the number of secondary sources and error microphones is limited by computing speed. The second area for potential advance concerns increasingly sophisticated experiments aimed at optimising the source strength, or strength source array for determining the largest size quite zone while least affecting the global sound field, where chapter 6 is an initial attempt investigating single channel control schemes

The application of active control to the idealised diffuse field provides a fruitful area of research where new results can be obtained relatively easily. It is probably fair to suggest that in a large number of cases these findings are of academic interest only and are not particularly relevant to real life implementations. It is believed that high frequency active control can be advanced furthest by adopting a more experimental approach although the necessity of a thorough understanding of the underlying physical principles is recognised. Undoubtedly, active control at high frequencies will be restricted to local control which involves creating zones of quiet around the head of a listener whose movements must inevitably be restricted. This might be, for example, the seated passenger of an aeroplane or the driver of an automobile. It is in this objective where most effort should be directed.

Whilst the results derived in this thesis provide general guidelines relating to the principle of localised diffuse field control, the analyses are necessarily simplistic, neglecting important considerations such as the effect of the listener's head on the sound field which will tend to act as a large diffracting body. The moving head will cause the sound field to be in a constant state of change which will therefore require an adaptive control scheme which constantly adjusts itself to the changing acoustic response of the enclosure. Each control unit will require two control points, one for each ear. This raises the important issue concerning the psycho-acoustic impression given to the recipient of the device as the perceived phase change accompanying the pressure cancellation may appear unnatural. This is an important departure from the main thrust of active noise control research which to the author's knowledge, has never been investigated.

Some of the ideas suggested by Olson would also benefit from further investigation. In particular, the notion that active methods may be used to enhance the efficiency of passive absorption of acoustic energy should also be explored further. The control strategy suggested by Olson involves driving the pressure at a point to zero in the near field of a secondary source with the aim of establishing a large pressure gradient between the source and the point of null pressure. Chapter 6 has shown that for very compact sources, pressure gradients of up to 5 dB cm^{-1} are readily obtainable for which, following from the momentum equation, the particle velocity is correspondingly large. It was suggested by Olson that a resistive screen in the form of sound absorbent foam in the region of this increased particle velocity would be highly efficient as a passive absorber of sound. While this control arrangement will undoubtedly be efficient in absorbing the energy radiated by the secondary source, it

remains to demonstrated either experimentally, or theoretically whether this scheme will be efficient in absorbing incident primary energy.

Another interesting area for future research would be to use the same probabilistic treatment used in chapter 3 to investigate high frequency active noise control to study the active absorption of sound at low frequencies whose effectiveness is considerably greater. It is anticipated that the expression for the area of absorption for an optimally absorbing point monopole source derived for the high frequency limit, is also a good estimate to the average area of active absorption afforded at low frequencies. A probabilistic approach would enable one to investigate the variance associated with the maximum sound power absorption obtained between successive measurements as the secondary source position is varied. This is believed to vary inversely as the modal overlap factor, although formal verification obtained from computer simulations would be valuable and revealing. This approach would also enable such effects as the influence of enclosure boundaries on the sound absorbing capabilities to be studied, although it is anticipated that the optimal absorption of sound power is statistically independent of the proximity of enclosure walls.

The last control principle worthy of note, which is attracting growing attention, involves shaking the intermediary structure through which noise is known to be transmitted. This technique is appropriate, for example, the structure borne noise radiated into an aircraft fuselage which is thought to predominate over air-borne transmission paths. Consider, for example, the case when two large, highly damped rooms are separated by an elastic panel capable of vibration. Noise on one side of the room will be transmitted to the adjoining room via structural vibration of the partition. It is conceivable that although the acoustic field in each of the enclosures may contain many thousands of significantly contributing acoustic modes, acoustic energy is only transmitted between them via the energy carried by only a few structural modes of the plate. In this case, a more appropriate control strategy would be to apply vibration control to the plate directly, with the objective of minimising the potential energy radiated to the other side of the room. This approach is already beginning to yield promising results[97,98] although there still remains a large amount of work to be performed. A particularly interesting aspect of this work is the complicated structural - acoustical interactions which arise from the use of double partitions when active control is applied in the air space in between.

So far we have only considered short term objectives for active control, say, over the next ten years. In the long term however, it is inevitable that active control will

attain a new level of sophistication, particularly for controlling unwanted structural vibrations. Active control in the future will combine very fast, real time, parallel signal processing capabilities, together with the new generation of distributed type transducers such as the piezo ceramic, or magneto-strictive devices to form intelligent, or 'smart structures'. These high stress transducers are able to provide large in-plane forcing over a wide frequency range so that when bonded to a structure, they are able to modify its structural characteristics in response to changing external stimuli which could be either acoustical or mechanical in origin. Furthermore, the problem often encountered with modal spillover are lessened due to the distributed nature of these types of transducers whereas the more conventional type of shakers, which act at a point, tend to excite a uniform wavenumber response thereby exciting many modes over and above the desired modes required for optimal control. Some authors[99] are already beginning to study the use of this new technology for active control in for example, applications in space vehicles, commercial aircraft design and automotive applications and in many other examples where weight is an important consideration.

8. SUMMARY OF IMPORTANT RESULTS

Case	Variable	Mean	Normalised standard deviation σ / μ	Comments
Single point monopole source in a room.	$\|p(r)\|^2$	$\frac{\rho^2 \omega c_0}{8\pi\zeta V}$	$\sqrt{\frac{1}{M_N(\omega)}}$	Mean value assumes constant modal damping model
Cancellation of the pressure at a point using a remote secondary source	$\|q_{so}\|$	$\frac{\pi}{2}\|q_p\|$	∞ ($\approx 10\|q_p\|$ †)	$\|q_{so}\|_{med} = \|q_p\|$ and $\|q_{so}\|_{mode} = \frac{1}{\sqrt{3}}\|q_p\|$
	$2\Delta r_{0.1}$	0 ($\lambda/10$†)	?	Mean value of 10 dB quiet zone formally zero but $\lambda/10$ from a large but finite number of computer simulations
	E_{pres}	∞ ($\approx 10 \langle E_{pp} \rangle$†)	∞ ($\approx 175 \langle E_{pp} \rangle$†)	Values in brackets refer to the results obtained from 15,000 computer simulations
Minimising the total sound output from two closely spaced point sources	$\hat{q}_{so}$	$-q_p \text{sinc} k\Delta r$	$\sqrt{\frac{1}{M_N(\omega)}}\sqrt{1-\text{sinc}^2 k\Delta r}$	Approximate expressions based on well 'behaved' values, see main text.

Case	Variable	Mean	Normalised standard deviation σ / μ	Comments
	$\hat{W}_{min}$	$W_p(1 - \mathrm{sinc}^2 k\Delta r)(1 - M_N(\omega)^{-1})$	$\sqrt{\frac{1}{M_N(\omega)}}\sqrt{1-\mathrm{sinc}^4 k\Delta r}$	
The minimum diffuse field sound power output	$\hat{W}'_{so}$	$-\langle \lvert I_r(\mathbf{r})\rvert \rangle \frac{\lambda^2}{\pi}$	$\sqrt{\frac{1}{M_N(\omega)}}$	
Cancellation of the pressure at a point situated in the near field of a point secondary source	$2\Delta r_{0.1}$	$\sqrt{0.1}\,\lambda / \pi$	?	Mean value refers asymptotic limit, see main text
	$\lvert q_{so}\rvert$	$\sqrt{\frac{2}{\pi M_{0.5}(\omega)}}\, k\Delta r \lvert q_p\rvert$	?	an approximate expression for small Δr
	$\hat{W}_s$	$W_p \frac{2^5\pi^3}{9}\left[\frac{f_{sch}}{f}\right]^3\left[\frac{r_0}{\lambda}\right]^4$	?	for small Δr for a secondary source at the origin

† = the average result obtained in practice from a large, but finite number of computer simulations (see main text for details)

REFERENCES

1. **Lueg. P. 1933.** Process of silencing sound oscillations. US Patent No 2,043,416.

2. **Swanson. D.C.** 1988. Active attenuation of acoustic noise: past, present, and future. Submitted to the American Society of Heating, Refrigeration and Air conditioning Engineering.

3. **Olson. H.F, May. E.G.** 1953. Electronic sound absorber, *Journal of the Acoustical Society of America*, **25**(6), 1130 - 1136.

4. **Doyle. C.** 1988. Vogue magazine (British edition). July, Volume 152, 150 - 154.

5. **Jessel. M.J.M.** 1967. Procede electroacoustque d'absorption des sons et bruits genants dans des zones etendues. Brevet d'Invension (French patent) No 1 494 967. Filed Aug 4, 1966. Patented: Aug 7, 1967.

6. **Guicking. D.** 1988. Active noise and Vibration Control Reference Bibliography. 3rd edition. Drittes Physikalisces Institut. University of Gottenburg.

7. **Jessel. M.J.M, Mangiante. G.** 1972. Active sound absorbers in an air duct. *Journal of Sound and Vibration* **23**, 383 - 390.

8. **Swinbanks. M.A.** 1973. The active control of sound propagation in long ducts. *Journal of Sound and Vibration* **27**, 411 - 436.

9. **Leventhall. H.G, Eghtesadi. Kh.** 1979. Active attenuation of noise: Dipole and monopole systems. Internoise 79, Warsaw, Poland. Proceedings 175 - 180.

10. **Curtis. A.R.D, Nelson. P.A, Elliott. S.J, Bullmore, A.J.** 1987. Active suppression suppression of acoustic resonances. *Journal of the Acoustical Society of America*, 81, 624 - 631.

11. **Swinbanks. M.A.** 1982. The active control of low frequency sound in a gas turbine compressor turbine compressor installation. Internoise, San Francisco Proceedings 423 - 426.

12. **Bullmore. A.J, Nelson. P.A, Curtis. A.R.D, Elliott. S.J.** 1987. The active minimisation of harmonic enclosed sound fields. Part II: A computer simulation. *Journal of Sound and Vibration* **117**, 15 - 33.

13. **Nelson. P.A, Curtis. A.R.D, Elliott. S.J, Bullmore. A.J.** 1987. The active minimisation of harmonic enclosed sound fields. Part I: Theory. *Journal of Sound and Vibration* **117**, 1 - 13.

14. **Elliott. S.J, Curtis. A.R.D, Bullmore. A.J, Nelson. P.A.** 1987. The active minimisation of harmonic enclosed sound fields. Part III: Experimental verification. *Journal of Sound and Vibration* **117**, 35 - 58.

15. **Kempton. A.J.** 1976. The ambiguity of acoustic sources - a possibility for active control. *Journal of Sound and Vibration* **48**, 475 - 483.

16. **Ffowcs Williams. J.E.** 1978. The theoretical modelling of noise sources. Proceedings of the Indian Academy of sciences 1C 57 - 72.

17. **Keith. S.E, Scholaert, H.S.B.** 1981. A study of the performance of an Olson type Active Noise Controller and the possibility of the reduction of cabin noise. University of Toronto, Institute for Aerospace Sciences (UTIAS). Technical note No. 228.

18. **Berge. T.S.** 1983. Active noise cancellation of low frequency sound inside vehicle cabs. Internoise 83. Edinburgh. Proceedings 457 - 460.

19. **Brewer. P.A, Leventhall. H.G.** 1985. Active attenuation in small enclosures. Proceedings of the Institute of Acoustics (IOA), 7 113 - 114.

20. **Chaplin. G.B.B.** 1980. The cancellation of repetitive noise and vibration. Internoise 80, Miami, Proceedings 699 - 702.

21. **Elliott. S.J, Stothers. I.M, P. A. Nelson.** 1988. The active control of engine noise inside cars. Internoise 88, Avignion, France. 987 - 990.

22. **Ross. C.F.** 1981. A demonstration of active control of broadband sound. *Journal of Sound and Vibration* **74**, 411 - 417.

23. **Elliott. S.J, Nelson. P.A, Stothers. I.M, Boucher. C.C.** 1989. Preliminary results of in-flight experiments on the active control of propeller-induced cabin noise *Journal of Sound and Vibration* **128**(2), 355-357.

24. **Dorling. C.M, Eatwell. G.P, Hutchins. S.M, Ross. C.F, Sutcliff. S.G.C.** 1989. A demonstration of active noise control reduction in an aircraft cabin. *Journal of Sound and Vibration* **128**(2), 358-360.

25. **Simpson. M.A, Luong. T.M, Swinbanks. M.A, Russell. M.A, Leventhall. H.G.** 1989. Full scale demonstration tests of cabin noise reduction using active noise. Internoise 89, Newport Beach California, U. S. A. Proceedings 459 - 462.

26. **Salikuddin. M, Ahuja. K.K.** 1989. Application of localised active control to reduce propeller noise transmitted through fuselage surface. *Journal of Sound and Vibration* **133**(3), 467-481.

27. **Ffowcs Williams. J.E.** 1984. Anti-Sound. Review lecture. Proceedings of the Royal. Society. London. 395, 63 - 88.

28. **Warneka. G.E.** 1982. Active attenuation of noise: The state of the art. Noise control engineering May - June.

29. **Lindqvist. E.** 1983. Active sound reduction: a study of its recent developments and some future possibilities, Chalmers school of technology, Gotenborg, Sweden.

30. **Olson. H.F.** 1956. Electronic control of noise, Vibration and reverberation. *Journal of the Acoustical Society of America*, **28**(5) 966-972.

31. **Elliott. S.J, Nelson. P.A.** 1985. Algorithm for multi-channel LMS adaptive filtering. Electronic letters 21, 979 - 981.

32. **Ross. C.F.** 1980. Active control of sound, Ph.D thesis, University of Cambridge.

33. **Wiener. N.** 1949. Extrapolation, interpolation and smoothing and stationary time series. John Wiley.

34. **Bozic. M.** 1979. Digital and Kalman filtering. Edward Arnold.

35. **Nelson. P.A, Hammond. J.K, Joseph. P, Elliott. S.J.** 1990. Active control of stationary random sound fields. *Journal of the Acoustical Society of America.* (in press).

36. **Joplin. P.M, Nelson. P. A.** 1990. Active control of low frequency random sound in enclosures. *Journal of the Acoustical Society of America* (In press).

37. **Pierce. A.R.** 1981. Acoustics: An introduction to its physical principles and applications. McGraw Hill.

38. **Nelson. P.A, Elliott. S.J.** 1989. M.Sc Course notes. I. S. V. R, University of Southampton.

39. **Nelson. P.A, Elliott. S.J.** 1989. Active minimisation of acoustic fields. Journal de Mechanique theoretique et applique, special issue supplement to Vol 6(7).

40. **Nelson. P.A, Curtis. A.R.D, Elliott. S.J, Bullmore. A.J.** 1987. The minimum power output of free field point sources and the active control of sound. *Journal of Sound and Vibration* **116** 1987, 397 - 414.

41. **Elliott. S.J, Nelson. P.A.** 1986. The implications of causality in active control. Internoise 86, Cambridge MA. proc 583 - 588.

42. **Hildebrand. P.** 1965. Methods of applied mathematics. Prentice Hall.

43. **Lanning. J.H, Battin. R.H.** 1965. Random processes in automatic control, McGraw Hill - Control system Engineering.

44. **Papoulis. A.** 1977. Signal analysis, International students edition. McGraw Hill.

45. **Bendat. J, Piersol. M.** 1986. Random data 2nd edition. Analysis, measurement procedures. John Wiley.

46. **Fahy. F.J.** 1988. Sound intensity. Elsever.

47. **Joseph. P, Nelson. P.A, Elliott. S.J.** 1987. Causality, filtering and prediction in active noise control. I.O.A. Autumn conference, Portsmouth. 295 - 238.

48. **Wylie C.R, Barrett. L.C.** 1977. Advanced engineering mathematics, International students edition. McGraw Hill.

49. **Roure. A.** 1985. Self adaptive broadband active sound control system. *Journal of Sound and Vibration* **101**(2), 429 - 441.

50. **Kinsler. L.E, Frey. A.R.** 1967. Fundamentals of acoustics 2nd edition. John Wiley.

51. **Bullmore. A.J.** 1988. The active minimisation of harmonic sound fields with particular reference to propeller induced cabin noise. Ph.D thesis, university of Southampton.

52. **Chu. W.T.** 1981. Comments on the the coherent and incoherent nature of reverberant sound fields. *Journal of the Acoustical Society of America*, **69**(6), 1710 - 1715.

53. **Beranek. L.L.** 1971. Noise and Vibration control. McGraw Hill.

54. **Balanchandran. C.G, Robinson. D.W.** 1967. Diffusion of the decaying sound field. Acustica 19, 245 - 257.

55. **ASTM E90-55.** Recommended practice for laboratory measurement of the airborne sound transmission loss of building floors and walls.

56. **American standard acoustical technology.** 1960. A.N.S 1.1 - 1960.

57. **Doak. P.E.** 1959. Fluctuations of the sound pressure levels in rooms. *Acustica*, **9**(1), 1 - 9.

58. **Schroeder. M.R, Kutruff. K.H.** 1962. On frequency response curves in rooms. Comparison of experimental, theoretical and , Monte-Carlo results for the average frequency spacing between them. *Journal of the Acoustical Society of America*, **34** 1819 - 1823.

59. **Schroeder. M.R.** 1954. Die statistischen parameter der frequenzkurven von grossen ruamen. Acustica 4, 594 - 600.

60. **Wente. E.C.** 1935. The characteristics of sound transmission irregularity in rooms. *Journal of the Acoustical Society of America*, **7**, 123 - 126.

61. **Bolt. R.H, Roop, R.W.** 1950. Frequency response fluctuations in rooms. *Journal of the Acoustical Society of America*, **22**, 280.

62. **Ebeling. K.J.** 1984. Statistical properties of random wave fields. Chapter 4, "Physical Acoustics; principles and methods", **XVII.**

63. **Mood. A.M, Graybill. F.A, Boes. D.C.** 1974. Introduction to the theory of statistics 3rd edition. McGraw Hill (international students edition).

64. **Skudrzyk. E.** 1971. The foundations of acoustics. Springer Verlag.

65. **Morse. P.M.** 1936. Vibration and sound 2nd edition. McGraw Hill.

66. **Sepmeyer. L.W.** 1965. Computer frequency and angular distribution of the normal modes of vibration in a rectangular room. *Journal of the Acoustical Society of America*, **37**, 414 - 420.

67. **Bodlund. K.** 1976. A new quantity of comparitive measurement concerning the diffusion of stationary sound fields. *Journal of Sound and Vibration* **44**, 191-207.

68. **Cook. R.J, Waterhouse. R.V, Berendt. R.D, Edelman. S, Thompson. M.C.** 1955. Measurement of correlation functions in reverberant sound fields. *Journal of the Acoustical Society of America*, **27**, 1072.

69. **Chien. C.F, Soroka. W.W.** 1976. Spatial cross correlation of acoustic pressure in steady and decaying reverberant sound fields. *Journal of Sound and Vibration* **48**(2), 235 - 242.

70. **Morrow. C.T.** 1971. Point to point correlation of sound pressures in reverberant chambers. *Journal of Sound and Vibration* **16**, 28 - 42

71. **Baxter. S.M, Morfey. C.L.** 1986. Angular distribution analysis in acoustics. Springer Verlag, Lecture notes in engineering 17.

72. **Levine. H.** 1980. On source radiation. *Journal of the Acoustical Society of America*, **68**, 1199 - 1205.

73. **Waterhouse. R.V.** 1968. Statistical properties of reverberant sound fields. *Journal of the Acoustical Society of America*, **43** 1436.

74. **Waterhouse. R.V.** 1963. Radiation impedance of a source near reflectors. 1963. *Journal of the Acoustical Society of America*, **35**(8) 1144 - 1151.

75. **Lyon. R.H.** 1969. Statistical analysis of power injections and responses in structures and rooms. *Journal of the Acoustical Society of America*, **45**(3) 545-565.

76. **Jacobsen. F.** 1979. The diffuse sound field. The acoustics laboratory, Technical university of Denmark. Report No 27.

77. **Davy. J.L.** 1981. The relative variance of the transmission function of a reverberation room. *Journal of Sound and Vibration* 1976 **77**(4), 455 - 479.

78. **Maling. G.C.** 1973. Guidelines for determination of average sound power radiated by a discrete frequency source in a reverberation room. *Journal of the Acoustical Society of America*, **53**(4) 1064 - 1069.

79. **Allen. J. B, Berkley. D. A.** 1979. Image model method of simulating small room acoustics. *Journal of the Acoustical Society of America*, **65**(4) 943 - 950.

80. **Hough. S.P.** 1988. Some implications of causality in the active control of sound. Ph.D thesis, University of Southampton.

81. **Nelson. P.A, Hammond. J.K, Joseph. P, Elliott. S.J.** 1989. The calculation of causally constrained optima in the active control of sound. I.S.V.R. Technical report No 145.

82. **Nelson. P.A, Curtis. A.R.D, Elliott. S.J.** 1986. On the active absorption of sound. Internoise 86, Cambridge. MA. Proceedings 601 - 606.

83. **Fahy. F.J.** 1987. Sound and structural vibration. Academic press.

84. **Shaw. E.A.G.** 1988. Diffuse field response, receiver impedance and the acoustical reciprocity principle. Letter to the editor of the *Journal of the Acoustical Society of America*, **84**(6) 2284 - 2287.

85. **Gradshteyn. J.S, Ryzhik. J.M.** 1965. Table of integrals, series and products. Academic press.

86. **Elliott. S.J, Nelson. P.A.** 1984. Models for describing active noise control in ducts. I.S.V.R Technical report No 127.

87. **Elliott. S.J, Joseph. P, Bullmore. A.J, Nelson. P.A.** 1988. Active cancellation at a point in a pure tone diffuse sound field. **120**(1) 183 - 187.

88. **Sargent. C.** 1990. Sunday times, Motoring section, 4th February.

89. **Koyasu. M, Yamashita. M.** 1971. Evaluation of the degree of the diffuseness in reverberation chambers by spatial correlation techniques. *Journal of the Acoustical Society of Japan.* **27**, 132 - 143.

90. **Oppenheim. A.V, Schafer. R.N.** 1985. Digital signal processing. Prentice Hall.

91. **Trinder. M.C.J, Nelson. P.A.** 1983. Active noise control in finite length ducts. *Journal of Sound and Vibration* **89**(1), 95 - 105.

92. **Elliott S.J. Joseph. P. Nelson P.A.** 1988. Active control in diffuse sound fields. Proceedings of the Institute of Acoustics, Cambridge.

93. **Lubman. D.** 1971. Spatial averaging in a diffuse field. *Journal of the Acoustical Society of America*, **16**, 43 - 58.

94. **Joseph. P.** 1988. I.S.V.R, internal Memorandum No 645. Active noise control in high frequency enclosed sound fields.

95. **Myoshi. M, Kaneda. Y.** 1988. Active noise control in a reverberant three dimensional sound field, Internoise 88, 983 - 986.

96. **Maling. G.C.** 1967. Calculation of acoustics power radiated by a point monopole in a reverberation chamber. *Journal of the Acoustical Society of America*, **42**(4), 859 - 865, 1967.

97. **Fuller. C.R.** 1990. Active control of sound transmission/radiation from elastic plates by vibration inputs. I. Analysis. *Journal of Sound and Vibration* **136**(1), 1 - 15.

98. **Thomas. D.R, Nelson. P.A, Elliott. S.J.** 1990. The active control of the transmission of sound. Proc of the Institute of acoustics 605 - 612.

99. **Fuller. C.R, Rogers. C.A, Robertshaw. H.H.** 1989. Active structural acoustic control with smart structures. Paper submitted to the S.P.I.E conference 1170 on Fiber Optics smart structures and skins II, Boston, MA.